



Phd THESIS

UPC – program on Environmental Engineering

**Microbial fuel cells running on high strength
animal wastewater - Nitrogen removal strategies and
microbial community characterization.**

Ana Sotres Fernández

Supervised by

Dr. Marc Viñas Canals and Dr. August Bonmatí Blasi

Barcelona, May 2015

GIROUnitat mixta IRTA-UPC
IRTA
Torre Marimon
08140 Caldes de Montbui
Tel. 93 467 40 40
www.irta.cat

GIRO
integral manage
of organic wast



El Dr. Marc VIÑAS CANALS i el Dr. August BONMATÍ BLASI del GIRO unitat mixta IRTA-UPC,

CERTIFIQUEM:

Que Ana Sotres Fernández ha realitzat sota la nostra direcció el treball titulat “*Microbial fuel cell running on high strength animal wastewater – Nitrogen removal strategies and microbial community characterization*”, presentat en aquesta memòria, i que constitueix la seva Tesi Doctoral per optar al Grau de Doctor per la Universitat Politècnica de Catalunya.

I perquè es tingui coneixement i consti als efectes oportuns, presentem al Programa de Doctorat d'Enginyeria Ambiental de l'Institut de Recerca en Ciència i Tecnologia de la Sostenibilitat, l'esmentada Tesi Doctoral, signant el present certificat a

Caldes de Montbui, Barcelona, Maig 2015

Dr. Marc Viñas Canals

Dr. August Bonmatí Blasi

*A mis padres,
Rosa y Gabriel*

A Gustavo

"It's always seems impossible until it's done."

Nelson Mandela

"Queda prohibido llorar sin aprender, olvidar el ayer, no pensar que mañana puede ser todo mejo, algo mejor, mucho mejor."

Once varas

Agradecimientos

Parecía que no iba a llegar nunca este momento, pero al final...ha llegado!. Ya son unos cuantos años, y muy intensos, en los que he vivido buenos y malos momentos, estancias, congresos, viajes, despedidas, e incluso una mudanza de laboratorio. Y ahora por fin, es cuando toca respirar hondo, echar la vista atrás y agradecer a todas aquellas personas, que de una u otra manera han intervenido a que este trabajo haya salido adelante, o simplemente han estado ahí haciendo el día a día mas agradable.

En primer lugar quisiera dar las gracias a las dos personas a las que mas me gustaría que agradara este trabajo, a mis directores. A Marc Viñas por haberme dado la oportunidad de entrar a formar parte del GIRO y empezar a hacer la tesis en el mundo de las “microbial fuel cells”, muchas gracias por esta oportunidad!. A August Bonmatí, por muchas cosas, pero sobre todo por toda la ayuda brindada y disponibilidad en el trabajo, por los ánimos, sobre todo en la recta final que no ha sido fácil, y por escucharme siempre que lo he necesitado. Sin tu ayuda no hubiese podido terminar esta tesis, así que mil gracias!.

A toda la gente del GIRO. Xavier, Francesc, Miriam, Joan, Victor, Jordi, Edu, Maycoll, Vicente, Josep. A Laura Burgos, por las horas que pasamos juntas compartiendo despacho y laboratorio. A Miriam Cerrillo, muchísimas gracias por haberme ayudado tanto en los últimos meses de laboratorio y por aportar esa dosis de calma y serenidad que a mí me faltan. A Belén y Eva, me alegro que el traslado a Torre Marimón me haya servido para conoceros un poquito más, y compartir aunque sea charlas en el pasillo y a la hora de comer, son las pequeñas cosas que amenizan el día a día. A Laura Tey, por todo el tiempo que hemos compartido en el laboratorio, en el despacho, por todas las charlas, desahogos, risas y por tu amistad en general. Laura Burgos, Laura Tey y Rim, nunca olvidaré el viaje a Túnez!

A los que ya se han ido, Jordi, Ángela y Rim. Y a mi clan favorito, Anna, Laia y Salva, por ser tan buenos compañeros de trabajo y estar siempre dispuestos a echar una mano en lo que haga falta. Ha sido un placer haber compartido despacho y laboratorio con vosotros. Gracias también por los buenos ratos que hemos vivido y vivimos fuera del trabajo.

A Antonio, me alegra mucho haberte conocido. La pesadilla de tener que preparar a la vez un visado para ir a Australia tuvo su recompensa.

I would like to thank Professor Korneel Rabaey for giving me the opportunity to stay two months at LabMET (University of Ghent). And thanks to Joachim Desloover for learning from him during my stay at LabMET.

I would like to thank Dr. Stefano Freguia for giving me the opportunity to stay six months at AWMC (University of Brisbane). Thanks to all the Aussie people who made my stay in Australia as awesome (Jinghsi, Ilje, Shao, Tomas, Rob, Apra, Julia, Ludo, TingTing, Elena, Babet, Guillermo, Sergi). I am especially grateful to Elisa, thank you for sharing together the long hours and hard moments at the lab, and also thank you for all the fun and all the talks.

A mis amigos, porque aunque últimamente os he tenido muy descuidados, sé que puedo contar con vosotros. A mi grupo de Gijón, las de toda la vida. A Ángela y Cris, porque no hay nada que me ponga mas contenta que cuando estamos las tres juntas. A Celia, porque nunca he conocido a nadie como tú!. A todos los que he tenido la suerte de conocer en Barcelona.

Quiero dar las gracias a mi familia, en especial a mis padres, a mi hermano y a Silvia, por todo el cariño y la ayuda incondicional que me habéis dado siempre. Simplemente gracias por estar ahí, y demostrarme siempre vuestro apoyo.

Gracias a Gustavo...en este caso un simple gracias se queda corto para todo lo que tendría que agradecerte. Te han salpicado todos mis problemas, agobios y estreses, sobre todo estos últimos meses, y sin embargo has tenido una paciencia envidiable. Gracias por hacerme las cosas más fáciles, por cuidarme, por intentar entender que era eso que me agobiaba tanto y por hacerme reir cada día. Y sobre todo, gracias por creer más en mí más que yo misma.

A todos muchas gracias!!

Table of contents

Index of figures	
Index of tables	
Glossary	I
List of abbreviations	III
Summary	V
Resumen	VI
Resum	IX
General Introduction	1
1.1. Electricity generation from microorganisms and microbial fuel cell concept	3
1.2. Bioelectrochemical systems principles	5
1.3. Exploring electrochemically active microorganisms	12
1.3.1. Mechanisms involved in the interaction between bacteria and anodes	13
1.4. MFCs for high strength wastewater treatment	18
1.4.1. Management and processing of livestock wastes	18
1.4.2. Nitrogen removal and recovery in microbial fuel cells.....	19
1.4.2.1. Nitrogen removal.....	19
1.4.2.2. Nitrogen recovery.....	22
1.5. References	23
Objectives and Thesis outline	29
2.1. Objectives	31
2.2. Research chronology and scope	33
2.3. Thesis outline	34
Materials and Methods	37
3.1. Reactors designs	39
3.1.1. Small scale two-chambered MFC	39
3.1.2. Medium scale two-chambered MFC	40

3.1.3. Stripping-BES system.....	41
3.2. Influent and inocula	42
3.2.1. Experiments performed with the small scale/batch two-chambered MFC.....	42
3.2.1.1. Influent.....	42
3.2.1.2. Inocula.....	43
3.2.2. Experiments with the medium scale/continuous two-chambered MFC.....	43
3.2.2.1. Influent.....	43
3.3. Analytical techniques.....	45
3.3.1. pH measurement.....	45
3.3.2. Total and volatile solids	45
3.3.3. Chemical Oxygen Demand	46
3.3.4. Ammonium nitrogen.....	46
3.3.5. Total Kjeldahl nitrogen.....	47
3.3.6. Anions and cations measurements	47
3.3.7. Methane dissolved measurement	47
3.4. Electrochemical techniques	48
3.4.1. Electrochemical monitoring	48
3.4.2. Polarization curves.....	50
3.5. Scanning electron microscopy	50
3.6. Microbial community analysis by molecular biology techniques	51
3.6.1. Nucleic acid extraction and Polymerase Chain Reaction	52
3.6.2. Denaturing Gradient Gel Electrophoresis	53
3.6.3. Sequencing and statistical data analysis.....	54
3.6.4. Quantitative real time polymerase chain reaction.....	54
3.6.5. Pyrosequencing and data.....	55
3.6.7. Diversity indices measurement.....	56
3.7. References.....	56
 Screening of different inocula to start-up a microbial fuel cells (MFCs)	 59
Abstract.....	61
4.1. Introduction.....	61
4.2. Material and methods	62

4.2.1. MFC reactors.....	62
4.2.2. Inocula	62
4.2.3. Voltage monitoring.....	63
4.2.4. Microbial community analysis	63
4.3. Results.....	64
4.3.1. Electrochemical results.....	64
4.3.2. Microbiological characterization.....	65
4.4. Conclusions	67
4.5. References.....	68

Microbial community dynamics in two-chambered microbial fuel cells: effect of different ion exchange membrane.....69

Abstract.....	71
5.1. Introduction.....	71
5.2. Materials and methods.....	74
5.2.1. MFC reactors.....	74
5.2.2. Inoculum.....	74
5.2.3. Electrochemical characterization	74
5.2.4. Scanning Electron Microscopy.....	75
5.2.5. Denaturing gradient gel electrophoresis molecular profiling	76
5.2.6. Quantitative PCR assay.....	77
5.3. Results and discussion	78
5.3.1. Electrochemical activity	78
5.3.2. Microbial community analysis	82
5.4. Conclusions	89
5.5. References.....	89

Microbial community dynamics in a continuous microbial fuel cell fed with synthetic wastewater and pig slurry.....95

Abstract.....	97
6.1. Introduction.....	97
6.2. Materials and methods.....	99

6.2.1. MFC configuration	99
6.2.2. MFC operation	100
6.2.4. Anode community characterization	101
6.2.4.1 Biofilm morphology.....	101
6.2.4.2. DNA extraction and PCR amplification	102
6.2.4.3. DGGE molecular profiling.....	102
6.2.4.4. 454-pyrotag sequencing of massive 16S rRNA gene libraries pyrosequencing	103
6.2.4.5. Analysis of pyrosequencing data	103
6.3. Results and discussion	104
6.3.1. MFC performance	104
6.3.1.1. Synthetic-fed MFC performance	104
6.3.1.2. Pig slurry-fed MFC performance	106
6.3.1.3. Synthetic-fed MFC performance after the addition of BES inhibitor.....	107
6.3.2. Biofilm morphology.....	109
6.3.3. Microbial community dynamics.....	111
6.3.3.1. Microbial population adaptation over time and under different operational conditions	111
6.3.3.2. Effect of different substrates feed.....	115
6.3.3.3. Effect of BES inhibitor.....	115
6.3.4. Richness and diversity of bacteria phylotypes	116
6.3.4.1. Microbial population adaptation overtime and under different operational conditions	116
6.3.4.2. Effect of different substrates feed.....	118
6.3.4.3. Effect of BES inhibitor.....	118
6.3.5 Comparative analysis of microbial communities	119
6.3.5.1. Microbial population adaptation overtime and under different operational conditions	122
6.3.5.2. Effect of BES inhibitor.....	124
6.3.6. Eubacteria community composition	125
6.3.6.1. Microbial population adaptation overtime and under different operational conditions	125
6.3.6.2. Effect of different substrates feed.....	127
6.3.6.3. Effect of BES inhibitor.....	129
6.3.7. Arhaea community composition	133

6.3.7.1. Microbial population adaptation overtime and under different operational conditions	133
6.3.7.2. Effect of different substrates feed.....	134
6.3.7.3. Effect of BES inhibitor	134
6.4. Conclusions	135
6.5. References.....	136
Nitrogen recovery from pig slurry in a two-chambered bioelectrochemical system	139
Abstract.....	141
7.2. Introduction.....	141
7.2. Material and methods	143
7.2.1. Experimental set-up	143
7.2.2. Batch experiments.....	144
7.2.3. Continuous experiments	144
7.2.4. Medium composition	145
7.2.5. Electrochemical characterization	145
7.2.6. Chemical analysis and calculations.....	146
7.2.7. Microbial community analysis	147
7.3. Results and discussion	148
7.3.1. Ammonia recovery in batch experiments	148
7.3.2. Ammonia recovery in a continuously fed BES	150
7.3.2.1. Influence of organic and nitrogen loading rate	150
7.3.2.2. Stripping experiments in MFC mode.....	151
7.3.2.3. Stripping experiments in MEC mode	152
7.3.2. Microbial community analysis	155
7.4. Conclusions	160
7.5. References.....	161
Nitrogen removal in a two-chambered microbial fuel cell- Establishment of a nitrifying-denitrifying microbial community on an intermittent aerated cathode. .	165
Abstract.....	167
8.1. Introduction.....	167
8.2. Materials and Methods.....	170

8.2.1. Experimental set-up.....	170
8.2.2. MFC operation.....	170
8.2.3. Denitrification batch assays.....	171
8.2.4. Electrochemical analysis.....	172
8.2.5. Chemical analysis and calculations.....	172
8.2.6. Microbial community analysis.....	173
8.2.6.1. Denaturing gradient gel electrophoresis.....	173
8.2.6.2. Quantitative PCR assay.....	174
8.2.6.3. Pyrosequencing and data analysis.....	175
8.2.6.4. Nucleotide Sequence Accession Numbers.....	176
8.3. Results and discussion.....	176
8.3.1. Nitrogen dynamics in the continuous aerated cathode period.....	176
8.3.1.1. MFC operation and nitrogen dynamics.....	176
8.3.1.2. Microbial community assessment.....	177
8.3.2. Denitrification batch assays.....	180
8.3.2.1. Microbial community assessment.....	182
8.3.3. Nitrogen dynamics during the intermittent aerated cathode periods.....	183
8.3.3.1. MFC operation and nitrogen dynamics.....	183
8.3.3.2. Microbial community assessment.....	186
8.4. Conclusions.....	188
8.5. References.....	189
General conclusions.....	193
9.1. General conclusions.....	195
9.2. Further research.....	199
Annexed Information.....	201
10.1. Annex: Research stays.....	203
Curriculum Vitae.....	209

Index of figures

Figure 1.1. (a) The number of publications on MFCs from the year 1990 to 2015, and (b) the country-wise distribution in MFC research. The data is based on the number of publications mentioning "microbial fuel cell or bioelectrochemical system" in Scopus database (February 2015).	4
Figure 1.2. Timeline outlining of the major achievements of bioelectrochemical systems (BES).	5
Figure 1.3. Scheme of (a) microbial fuel cell (MFC) and (b) microbial electrolysis cell (MEC).	7
Figure 1.4. Components involved in the electron transfer chain from the cells to the anode in MFCs using ARB microorganisms (<i>Geobacter</i> species) (Drawn with modifications after Lovley et al., 2004).	13
Figure 1.5. Schematic diagram of proposed electron-transfer mechanisms (Drawn with modifications after Borole et al., 2011).	14
Figure 1.6. Representative scheme of the ammonia removal and recovery in a standard two-chambered BES equipped with a CEM. Ammonium can be transported through the membrane (1) either passively via diffusion of ammonia (1a) or actively via migration in the form of ammonium (1b). Ammonia can be removed from the cathode by stripping (1c). Ammonium can be biologically nitrified by oxygen and denitrified by microorganisms at the cathode (2a), or in solution (2b). The dashed lines represent no bioelectrochemical processes. The ammonium can be recirculate into an external nitrifying reactor, and then the nitrate is reduced to nitrogen gas in the cathode chamber (3) (Redrafted with modifications after Arredondo et al., 2015).	20
Figure 2.1. Graphical abstract of the main goals purposed for this thesis.	32
Figure 3.1. a) MFC schematic overview of all reactor components, and b) materials used in the construction of the MFC (Plexiglas frame, rubber and the electrodes).	39
Figure 3.2. Picture of the MFCs (10 mL/chamber).	39
Figure 3.3. Small two-chambered MFCs experimental set-up and data acquisition unit (Mod. 34970A, Agilent Technologies, Loveland, CO, USA) used for recording the voltage.	40
Figure 3.4. A picture of one of the MFC from different perspectives.¡Error! Marcador no definido.	
Figure 3.5. Picture of the experimental set-up with the stripping-absorption unit coupled to the cathode chamber.	42

Figure 3.6. Liquid fraction of pig slurry sampling at the Sat Caseta d'en Grau farm (Calldetenes, Catalonia).	44
Figure 3.7. Biofilm sampling from the MFC fed with synthetic medium. The graphite granules sample was taken from the anode to inoculate anode material/chamber in MFC fed with liquid fraction of pig slurry.	45
Figure 3.8. Schematic overview of the molecular techniques used to analyse the microbial community developed on the MFC anode and cathode under different experimental conditions.	51
Figure 4.1. Picture of the reactors where the three inocula were sampled.	62
Figure 4.2. Current density produced in MFCs inoculated with three different inocula.	64
Figure 4.3. DGGE 16SE rRNA profile for the total Eubacteria community. 1: initial inocula sample and, 2, 3, 4: electricity production peak number, and richness values.	65
Figure 4.4. Principal component analysis (PCA) 2D-plot from digitalized DGGE profiles.	66
Figure 5.1. Voltage produced in MFCs working with an external resistance of 1000 Ω after three consecutive substrate loads and depending on the ion exchange membrane used: CMI (-·), AMI (-), and N-117 (··).	78
Figure 5.2. Effect of current density on the power density depending on the type of membrane used: CMI (●), AMI (○), and N-117 (▼).	79
Figure 5.3. Results obtained through SEM and EDS concerning the CMI-7000 anode and cathode side respectively.	80
Figure 5.4. Results obtained through SEM and EDS concerning the AMI-7000 anode and cathode side respectively.	81
Figure 5.5. Results obtained through SEM and EDS concerning the N-117 anode and cathode side respectively.	81
Figure 5.6. (a) DGGE profiles on eubacterial 16S rDNA amplified from samples obtained in MFCs. (b) Principal component analysis (PCA) 2D-plot from digitalized DGGE profiles. DA: initial inoculum. 1, 2, and 3: electricity production peak number.	82
Figure 5.7. DGGE profiles on archaeal 16S rDNA amplified from samples obtained in MFCs. DA: initial inoculum. 1, 2, and 3: electricity production peak number.	83
Figure 5.8. DGGE profile 16S rDNA for the total archaea community. D.A: initial inoculums; Nafion-B: biofilm of the MFC equipped with Nafion; Nafion-S: supernatant of the MFC (Nafion); CMI-B:biofilm of the MFC (CMI-Ultrex™); CMI-S:	

supernatant of the MFC (CMI-Ultrex™). AMI-B: biofilm of the MFC (AMI-Ultrex™); AMI-S: supernatant of the MFC (AMI-Ultrex™).84

Figure 5.9. qPCR results for 16S rRNA (in black) and mcrA (in gray) genes, for the initial inoculum and for the three different MFCs equipped with the three tested membranes and ratio mcrA/16SE genes. D.A: initial inoculum; AMI-B: biofilm of the MFC (AMI-Ultrex™); AMI-S: supernatant of the MFC (AMI-Ultrex™); CMI-B:biofilm of the MFC (CMI-Ultrex™); CMI-S: supernatant of the MFC (CMI-Ultrex™);N117-B: biofilm of the MFC equipped with Nafion; N117-S: supernatant of the MFC (Nafion).84

Figure 5.10. DGGE profile 16S rRNA for the total eubacteria community. Nafion-B: biofilm of the MFC equipped with Nafion N-117; Nafion-S: supernatant of the MFC (Nafion N-117); CMI-B: biofilm of the MFC (Ultrex CMI-7000); CMI-S: supernatant of the MFC (Ultrex CMI-7000). AMI-B: biofilm of the MFC (Ultrex AMI-7000); AMI-S: supernatant of the MFC (Ultrex AMI-7000).88

Figure 6.1. The structure of the CoM of methanogens and the BES-Inh. analog.98

Figure 6.2. Schematic diagram of both two chambered MFCs, and the biofilm samples collected from the anode compartments.....100

Figure 6.3. Evolution of voltage during the synthetic-fed MFC performance (R_{ext} 500 Ω).104

Figure 6.4. Polarization curves and power density curves (a) and (b) of synthetic fed-MFC; (c) and (d) of pig slurry-fed MFC; (e) and (f) of synthetic fed-MFC operated with different BES-Inh. concentrations.105

Figure 6.5. Evolution of voltage during the pig slurry-fed MFC performance (R_{ext} 500-100 Ω). This MFC was inoculated with a biomass taken from the synthetic-fed MFC (B_2 MFC_{sw}) after 45 weeks of operation.....106

Figure 6.6. Evolution of voltage during the synthetic-fed MFC performance (R_{ext} 500 Ω), when BES-Inh. was added to the medium.107

Figure 6.7. SEM images for anode biofilms; a-d) anode biofilm adhering onto granular graphite in the MFC_{sw}, and e-h) anode biofilm onto carbon felt in the MFC_{ps}. The squares in the figures on the right indicate the SEM images for both controls (granular graphite and carbon felt). The arrow indicates a typical rod cell with a long appendage-like filament.110

Figure6.8. Diagram of the samples taken and compared in the present work.111

Figure 6.9. DGGE of PCR-amplified 16S rRNA gene fragments (V_3 - V_5 regions) of Eubacterial communities (a) from In.AD: initial inoculum, and B_1 MFC_{sw} / B_2 MFC_{sw}: biofilm samples from the synthetic wastewater-fed MFC, and (b) from PS: pig slurry, and B_1 MFC_{ps} / B_2 MFC_{ps}: biofilm samples from the pig slurry-fed MFC.112

Figure 6.10. DGGE of PCR-amplified 16S rRNA gene fragments (V_3 - V_5 regions) of Archaeal and Eubacterial communities before (B_2 MFC_{sw}) and after (B_3 MFC_{sw-BES}) the addition of BES-Inh.....115

Figure 6.11. Rarefaction curves of a) eubacterial and b) archaeal number of operational taxonomic units (OTUs) obtained from the 454-pyrosequencing results, for the different samples (B_1 MFC_{SW}, B_2 MFC_{SW}, B_1 MFC_{PS} and B_2 MFC_{PS}) in relation to the initially inoculated biomass (In.AD) and the liquid fraction of pig slurry (PS) using as feed. The OTUs were defined by 3% distances using MOTHUR software..... 119

Figure 6.12. Correspondence analysis (CA) of bacterial communities from In.AD, B_1 MFC_{SW}, B_2 MFC_{SW}, B_3 MFC_{SW-BES}, PS, B_1 MFC_{PS} and B_2 MFC_{PS} samples, based on pyrosequencing of archaea 16S rRNA gene based on, a) OTUs matrix, b) family level taxonomy..... 120

Figure 6.13. Correspondence analysis (CA) of Archaeal communities from AD, S MFC-I, S MFC-II, S MFC(BES), PS, PS MFC-I and PS MFC-II samples, based on 454-pyrosequencing of archaea 16S rRNA gene, based on family level taxonomy.... 121

Figure 6.14. Overlap of the three bacterial communities: a) from the initial inoculum (In.AD) and the synthetic-fed MFC (B_1 MFC_{SW} and B_2 MFC_{SW}), b) from the liquid fraction of pig slurry (PS) and pig slurry-fed MFC (B_1 MFC_{PS} and B_2 MFC_{PS}), based on OTU (3% distance), and the taxonomic identities of the shared OTUs at family level. The total number of OTUs in each sample is shown between parentheses..... 123

Figure 6.15. Overlap of the four bacterial communities for B_2 MFC_{SW}, PS, B_1 MFC_{PS} and B_2 MFC_{PS}, based on OTU (3% distance), and the taxonomic identities of the shared OTUs at family level. The total number of OTUs in each sample is shown between parentheses. 124

Figure 6.16. Overlap bacterial communities from the synthetic-fed MFC before (B_2 MFC_{SW}) and after (B_3 MFC_{SW-BES}) BES addition, based on OTU (3% distance), and the taxonomic identities of the shared OTUs at family level. The total number of OTUs in each sample is shown between parentheses. 125

Figure 6.17. Taxonomic classification of 454-pyrosequencing of 16S rRNA gene from Eubacterial communities of a) In.AD, B_1 MFC_{SW}, B_2 MFC_{SW}, and b) PS, B_1 MFC_{PS}, B_2 MFC_{PS} at phylum, class and order levels. Groups making up less than 1% of the total number of sequences per sample were classified as "others". 126

Figure 6.18. Taxonomic classification of 454-pyrosequencing of 16S rRNA gene from eubacterial communities of In.AD, B_1 MFC_{SW}, B_2 MFC_{SW}, PS, B_1 MFC_{PS} and B_2 MFC_{PS} at a family level. Groups making up less than 1% of the total number of sequences per sample were classified as "others". 128

Figure 6.19. Taxonomic classification of 454-pyrosequencing of 16srRNA from eubacterial communities of B_2 MFC_{SW} and B_3 MFC_{SW-BES} at a class and family level. In the box above the phyla classification level. Groups making up less than 1% of the total number of sequences per sample were classified as "others". 129

Figure 6.20. Taxonomic classification of 454-pyrosequencing data from archaeal communities of In.AD, B_1 MFC_{SW}, B_2 MFC_{SW}, B_3 MFC_{SW-BES}, PS, B_1 MFC_{PS} and B_2 MFC_{PS} at a family and genus level. Groups making up less than 1% of the total number of sequences per sample were classified as "others". 135

Figure 7.1. Scheme of the BES coupled with the stripping/absorption unit.	144
Figure 7.2. Ammonia transported through the CEM at the abiotic two-chambered cell at different working voltages and passive diffusion in batch mode. (a and b) cell fed with synthetic wastewater and buffer phosphate and NaCl as catholyte, (c and d) cell fed with liquid fraction of pig slurry and buffer phosphate and NaCl as catholyte. The significance of the differences between values is represented in lowercase.	149
Figure 7.3. Cations concentration at the cathode, at the beginning (0 h) and at the end (56 h) of the abiotic batch experiment, in passive diffusion (P.D.) and 0.6V. (a) cathode fed with phosphate buffer, and b) cathode fed with sodium chloride.	149
Figure 7.4. Polarization curves of continuously-fed MFC with liquid fraction of pig slurry at different OLR and NLR.	150
Figure 7.5. Voltage evolution and COD influent through the different periods of the continuous fed MFC experiment.	152
Figure 7.6. Nitrogen flux ($\text{g N d}^{-1} \text{m}^{-2}$), a) for the five assays carried out on the MFC under different organic ($\text{g COD L}^{-1} \text{d}^{-1}$) and nitrogen ($\text{g N-NH}_4^+ \text{L}^{-1} \text{d}^{-1}$) loading rates.	154
Figure 7.7. Taxonomic classification of pyrosequencing from Eubacterial community of MFC and MEC mode. At the family (bar chart), and phylum (pie chart) levels. (Note: relative abundance was defined as the number of sequences affiliated with that taxon divided by the total number of sequences per sample. Phylogenetic groups with relative abundance lower than 1% were categorized as "others").	156
Figure 7.8. Taxonomic classification of pyrosequencing from Archaeal community of MFC and MEC mode. At the family and order levels. (Note: relative abundance was defined as the number of sequences affiliated with that taxon divided by the total number of sequences per sample. Phylogenetic groups with relative abundance lower than 1% were categorized as "others").	159
Figure 7.9. Comparison of the phyla and family candidate division between Greengenes and RDP (50% and 80% threshold) databases: a) comparison for the Eubacterial community, and b) for the Archaeal community under MEC operational mode.	160
Figure 8.1. Nitrification-Denitrification pathway.	169
Figure 8.2. Voltage and nitrogen evolution over time during continuous aeration cathode (P. 1) (data shows 3 samples periods).	177
Figure 8.3. (a) Total eubacterial community DGGE profile in the anode biofilm-electrode and in the biomass located in the supernatant aerated cathode chamber. (b) 16S rRNA, nosZ and amoA genes for both compartments.	178

Figure 8.4. Taxonomic assignment of 16SrRNA based-pyrosequencing assessment of bacterial community at the aerated cathode chamber during the different periods: (a) continuous aerated cathode - P. 1 - (phylum (i), class (ii), order (iii) and family (iv) level); (b) intermittent aerated period – P. 2.2 - (family level) ; and (c) during the intermittent aerated period + acetate – P. 2.3- (family level). Note: Phylogenetic groups with relative abundance lower that 1% were categorized as “others”.	179
Figure 8.5. N-NO ₃ ⁻ removal in the denitrification batch assays using cathode effluent from MFC cathode chamber and different biomass sources after 7 days. In brackets, nitrate removal percentage.	181
Figure 8.6. (a) DGGE 16SrDNA (V ₃ -V ₅ region) of the total eubacteria microbial community from the different batch assays and (*) sample from MFC cathode chamber. (b) Principal Component Analysis (PCA) 2D-Plot from DGGE profiles. In brackets, the percentage of nitrate removal after 7d of incubation in the denitrification batch assays.	181
Figure 8.7. Nitrogen dynamics (N-NO ₃ ⁻ , N-NO ₂ ⁻ and N-NH ₄ ⁺) in the cathode during the intermittent aerated periods. (a) Short intermittent aerated cycles (P. 2.1), and (b) Long intermittent aerated cycles with addition of acetate (P. 2.3).	185
Figure 8.8. Abundances of the 16S rRNA and two functional genes (amoA and nosZ) according to the last point of four periods studied. The number of copies for these genes (a) functional genes (amoA and nosZ) and (b) 16S rRNA and nosZ at aerated cathode, after two non-aerated cathode periods and non-aerated period with acetate pulses. Standard errors of the mean (n=3) are indicated.	187
Figure 10.1. Pictures of the electrochemical cell used during the experiments.	203
Figure 10.2. Diagram of the reactors setup and pictures of the materials used.	206
Figure 10.3. Picture of the reactors used during the experiments.	206
Figure 10.4. Current progress profile.	207

Index of tables

Table 1.1. MFCs reactors based on different classification criteria.....	8
Table 1.2. Some electrogenic microbes for MFCs and their extracellular electron transfer mechanisms.	15
Table 1.3. Some microorganisms capable of current production in pure cultures without and with mediator additions.....	17
Table 1.4. Nitrogen removing mechanisms performed in BES.	21
Table 3.1. Conditions used for the measurement for the quantification of the methane produced.....	48
Table 3.2. Primers used for DGGE-PCR for eubacteria and archaea community. ...	52
Table 3.3. PCR reaction conditions.	52
Table 3.4. Detailed PCR conditions per program performed for 16S rRNA eubacterial and archeal populations.	53
Table 3.5. Primers and conditions used for qPCR for the functional genes.	54
Table 3.6. PCR reaction mix for Qpcr (SybrGreen).	55
Table 4.1. Characteristics of the sequenced bands from Eubacterial 16S rRNA gene based-DGGE from Figure 4.3.	67
Table 5.1. Maximum voltage (V_{max}), maximum power density (P_{max}), and internal resistance (Ω_{int}) obtained for the three reactors through a polarization curve test (Figure 5.2).	80
Table 5.2. Characteristics of the sequenced bands from Eubacterial 16S rRNA gene based-DGGE from samples obtained in the MFCs. DA: initial inoculum. 1, 2, and 3: electricity production peak number (Figure 5.6).	86
Table 5.3. Characteristics of the bands from the 16S rRNA DGGE eubacteria gel from the following samples: D.A: initial inocula; Nafion-B: biofilm of the MFC equipped with Nafion N-117; Nafion-S: supernatant of the MFC (Nafion N-117); CMI-B: biofilm of the MFC (Ultrex CMI-7000); CMI-S: supernatant of the MFC (Ultrex CMI-7000). AMI-B: biofilm of the MFC (Ultrex AMI-7000); AMI-S: supernatant of the MFC (Ultrex AMI-7000) (Figure 5.10).....	87
Table 5.4. Characteristics of the bands from the 16S rRNA DGGE archaea gel from the following samples: D.A: initial inoculums; Nafion-B: biofilm of the MFC equipped with Nafion N-117; Nafion-S: supernatant of the MFC (Nafion N-117); CMI-B: biofilm of the MFC (Ultrex CMI-7000); CMI-S: supernatant of the MFC (Ultrex CMI-7000). AMI-B: biofilm of the MFC (Ultrex AMI-7000); AMI-S: supernatant of the MFC (Ultrex AMI-7000) (Figure 5.8).	88

Table 6.1. Overview of the operational conditions during experiments with synthetic and pig slurry feeding.	101
Table 6.2. Electrochemical parameters obtained from the polarization curves for the synthetic wastewater and pig slurry feed MFC, and for the synthetic feed MFC before and after the addition of BES inhibitor.	108
Table 6.3. Closest match for bands excited from the 16S rRNA DGGE Eubacterial gel from the MFC _{sw} (Figure 6.9a).	113
Table 6.4. Closest match for bands excited from the 16S rRNA DGGE Eubacterial gel from the MFC _{PS} (Figure 6.9b).	114
Table 6.5. Closest match for bands excited from the 16S rRNA DGGE Eubacterial gel from the MFC _{sw} before and after BES addition (Figure 6.10).	114
Table 6.6. N° of sequences, and OTUs, estimated richness (S_{obs} and Chao1), diversity indices (Shannon and $1/Simpson$) and sample coverage values for Eubacterial operational taxonomic units (OTUs), calculated with MOTHUR at the 3% distance level.	117
Table 6.7. N° of sequences, and OTUs, estimated richness (S_{obs} and Chao1), diversity indices (Shannon and $1/Simpson$) and sample coverage values for Archaeal operational taxonomic units (OTUs), calculated with MOTHUR at the 3% distance level.	117
Table 6.8. Changes in relative abundances of the bacteria genera.	131
Table 7.1. Operational conditions and results obtained in the continuous experiment working with pig slurry and the stripping/absorption unit coupled with the BES (MFC mode).	151
Table 7.2. Operational conditions and results obtained in the continuous experiment working with pig slurry and the stripping/absorption unit coupled with the BES (MEC mode).	153
Table 7.3. pH of the cathode and nitrogen recovered (%) in the absorption column during the continuous experiment working with pig slurry and the stripping/absorption unit coupled with the BES (MFC and MEC mode).	154
Table 7.4. Eubacterial microbial community enriched in MFC and MEC mode (percentage of total 16S rRNA reads).	157
Table 7.5. Archaeal microbial community enriched in MFC and MEC mode (percentage of total 16S rRNA reads).	158
Table 8.1. Set up and operational characteristics of the anode and cathode chambers.	171

Table 8.2. Characteristics of the bands excised and sequenced from Eubacterial 16S rRNA gene based-DGGE (Figure 8.6) from samples obtained in denitrification batch experiments.....	183
Table 8.3. Effect of the intermittent aerated periods on the nitrate removal efficiency at cathode chamber.	186
Table 10.1. Experimental plan made to carry out experiments.	205

Glossary

Anode: electrode of an electrochemical device that accepts electrons from an electrochemical reaction.

Anion exchange membrane (AEM): type of membrane that is selectively permeable to anions.

Bioelectrochemical system (BES): an electrochemical system in which electrochemically active microorganisms catalyse the anode and/or the cathode reaction.

Biofilm: multilayered aggregation of microorganisms.

Cation exchange membrane (CEM): type of membrane that is selectively permeable to cations.

Cathode: electrode of an electrochemical device that donates electrons to an electrochemical reaction.

Chemical oxygen demand (COD): measure used to indicate the amount of organic material in wastewater. It is expressed in mg O₂/l, which is the amount of oxygen needed to oxidize the entire organic material to carbon dioxide.

Coulombic efficiency (%): amount of coulombs captured in electrical current generation relative to the maximum possible assuming complete oxidation of the substrate.

Current density (A m⁻²): measured current (*I*, in A) produced or applied to an MEC normalized to the project surface area of an electrode.

Diffusion: transport of chemical species by gradient of concentration.

Electrochemically active microorganisms: microorganisms that are capable of either donating electrons to or accepting electrons from an electrode.

Extracellular electron transfer (EET): mechanism by which electrochemically active microorganisms donate electrons to or accept electrons from an electrode.

Gibbs free energy: maximum amount of useful work that can be obtained from a reaction (expressed in J/mol).

Hydraulic retention time (HRT): the average residence time of water applied to a continuous-flow system: $HRT = V/Q$, in which *V* is the system volume and *Q* is the continuous flow rate.

Methanogenesis: microbial production of methane.

Microbial fuel cell (MFC): bioelectrochemical system that is capable of converting the chemical energy of dissolved organic materials directly into electrical energy.

Microbial electrolysis cell (MEC): bioelectrochemical system that is capable of generating a product (e.g. hydrogen) from dissolved organic materials and that drives the reactions with an electrical energy input.

Migration: transport of chemical species caused by an electric field.

Nanowire: an electrically conductive appendage produced by a bacterium that is proposed to conduct electrons from the cell to surfaces such as metal oxides or electrodes.

Open circuit voltage (OCV): voltage that can be measured after some time in the absence of current.

Polarization curve: cell potential response versus current intensity, performed varying the external resistance from a very high load to very small load. Infinite load corresponds to OCV.

Power density (W m^{-2}): power (P , in W) produced by or applied to a BES normalized to the surface area of an electrode.

Syntrophy: nutritional association among species, which live off the products of other species.

Shuttles mediators: redox compounds which act as electron carriers from the microorganism to the electrode. These molecules can be added to the BES or can be produced and excreted by specific microorganisms.

List of abbreviations

AD	<u>A</u> naerobic <u>d</u> igestion
AOB	<u>A</u> mmonia <u>o</u> xidizing <u>b</u> acteria
AmoA	<u>A</u> mmonia <u>m</u> onooxygenase
ARB	<u>A</u> node <u>r</u> espiring <u>b</u> acteria
16S rRNA	Small subunit of the ribosomal RNA
BES	<u>B</u> ioelectrochemical <u>s</u> ystem
2-BES	2-bromoethanesulfonate
BLAST	<u>B</u> asic <u>l</u> ocal <u>a</u> lignment search <u>t</u> ool
CA	<u>C</u> orrespondence <u>a</u> nalysis
CE	<u>C</u> oulombic <u>e</u> fficiency (%)
CEM	<u>C</u> ation <u>e</u> xchange <u>m</u> embrane
COD	<u>C</u> hemical <u>o</u> xxygen <u>d</u> emand ($\text{g} \cdot \text{L}^{-1}$)
DET	<u>d</u> irect <u>e</u> lectron <u>t</u> ransfer
DGGE	<u>D</u> enaturing <u>G</u> radient <u>G</u> el <u>E</u> lectrophoresis
EAB	<u>E</u> lectroactive <u>b</u> acteria
ECM	<u>E</u> xtracellular <u>m</u> atrix
EET	<u>E</u> xtracellular <u>e</u> lectron <u>t</u> ransfer
EDTA	<u>E</u> thylenediaminetetraacetic <u>a</u> cid
emf	<u>E</u> lectromotive <u>f</u> orce
HRT	<u>H</u> ydraulic <u>r</u> etention <u>t</u> ime (h)
IET	<u>I</u> ndirect <u>e</u> lectron <u>t</u> ransfer
IEM	<u>I</u> on <u>e</u> xchange <u>m</u> embrane
CEM	<u>C</u> ation <u>e</u> xchange <u>m</u> embrane
NAD⁺	<u>O</u> xidized form of nicotinamide <u>a</u> denine <u>d</u> inucleotide
NADH	<u>R</u> educed form of nicotinamide <u>a</u> denine <u>d</u> inucleotide
NADPH	<u>N</u> icotinamide <u>a</u> denine <u>d</u> inucleotide <u>p</u> hosphate
MEC	<u>M</u> icrobial <u>e</u> lectrolysis <u>c</u> ell
MFC	<u>M</u> icrobial <u>f</u> uel <u>c</u> ell
NAV	<u>N</u> et <u>a</u> nodic <u>v</u> olumen
NCV	<u>N</u> et cathodic <u>v</u> olume
NGS	<u>N</u> ext <u>g</u> eneration <u>s</u> equencing

<i>nar</i>	<u>N</u> itrate <u>r</u> eductase gene
<i>nir</i>	<u>N</u> itrite <u>r</u> eductase gene
NDN	<u>N</u> itrification- <u>d</u> enitrification
NLR	<u>N</u> itrogen <u>l</u> oading <u>r</u> ate ($\text{g} \cdot \text{L}^{-1} \text{d}^{-1}$)
N-NH₄⁺	Amonium [$\text{mg N-NH}_4^+ \cdot \text{L}^{-1}$]
N-NO₂⁻	Nitrite [$\text{mg N-NO}_2^- \cdot \text{L}^{-1}$]
N-NO₃⁻	Nitrate [$\text{mg N-NO}_3^- \cdot \text{L}^{-1}$]
<i>nor</i>	<u>N</u> itric <u>o</u> xide <u>r</u> eductase gene
<i>nosZ</i>	<u>N</u> itrous <u>o</u> xide <u>r</u> eductase gene
N-TKN	Total Kjeldahl nitrogen [$\text{mg N-TKN} \cdot \text{L}^{-1}$]
<i>nxr</i>	<u>N</u> itrite <u>o</u> xidoreductase gene
OCV	<u>O</u> pen <u>c</u> ircuit <u>v</u> oltage
OLR	<u>O</u> rganic <u>l</u> oading <u>r</u> ate ($\text{g} \cdot \text{L}^{-1} \text{d}^{-1}$)
OM	<u>O</u> uter <u>m</u> embrane
OTU	<u>O</u> perational <u>t</u> axonomic <u>u</u> nit
PCR	<u>P</u> olymerase <u>c</u> hain <u>r</u> eaction
PEM	<u>P</u> roton <u>e</u> xchange <u>m</u> embrane
(q)PCR	(<u>Q</u> uantitative) <u>p</u> olymerase <u>c</u> hain <u>r</u> eaction
QIIME	<u>Q</u> uantitative <u>i</u> nsights <u>i</u> nto <u>m</u> icrobial <u>e</u> cology
RDP	<u>R</u> ibosomal <u>d</u> atabase <u>p</u> roject
SEM	<u>S</u> canning <u>e</u> lectron <u>m</u> icroscope/ <u>m</u> icroscopy
SNDN	<u>S</u> imultaneous <u>n</u> itrification- <u>d</u> enitrification
TSS	Total <u>s</u> suspended <u>s</u> olids [mg or $\text{g TSS} \cdot \text{L}^{-1}$]
VSS	<u>V</u> olatile <u>s</u> suspended <u>s</u> olids [mg or $\text{g VSS} \cdot \text{L}^{-1}$]
WW	<u>W</u> astewater

Summary

A microbial fuel cell (MFC) is a bioelectrochemical system (BES) capable of converting the chemical energy contained in the chemical bonds of a substrate into electrical energy by means of electrochemical reactions catalyzed by microorganisms. The amount of energy to be gained by bacteria capable of transferring electrons to an anode is significantly higher compared to other alternative electron acceptors. Exoelectrogenic microbial populations tend to be selectively enriched on the anode electrode, being essential for the performance improvement of the MFC in terms of electricity production from organic matter oxidation. MFC technology arises as an attractive alternative for the treatment of high strength animal wastewater, such as pig slurries, to potentially improve energetic valorisation of organic wastes, concomitantly to carbon and nitrogen content reduction or recovery.

The first part of the thesis (Chapters 4, 5 and 6) focuses on the study of microbial populations harboured on the anode electrode of MFCs. The effect of different ion exchange membrane materials and different inoculum sources over the microbial population was studied in discontinuously fed MFCs. A detailed study of the microbial community dynamics and composition onto the anode biofilms, under different feeding conditions (synthetic wastewater and the liquid fraction of pig slurry), was then studied in continuously fed MFC. A highly diverse microbial community is shown to be present under these different scenarios and, its final composition is being dependent on the factors studied.

The second part of the thesis is focused on understanding the nitrogen dynamics in a two-chambered MFC, and the possible strategies available to remove or recover it. First of all, the diffusion/migration of ammonia nitrogen through the cation exchange membrane was studied in batch essays under different operational conditions (Chapter 7). The results obtained showed that the diffusion/migration of ammonia nitrogen is dependent on the voltage applied and, when using pig slurry, ammonia migration reaches values close to 50%.

These results suggested that the use of MFC technology could be a good strategy to deal with the nitrogen excess in this kind of substrates. Two different processes for MFC nitrogen recovery and removal were developed. First, a physicochemical-based process for nitrogen recovery was developed coupling a stripping-absorption unit to the cathode chamber (Chapter 7). Results showed the

stripping/absorption-BES system is a feasible technology to recover ammonia from pig slurries.

Second, a nitrogen removal strategy by means of biological processes was studied using synthetic high strength wastewater as feed (Chapter 8). In this case, the ammonia nitrogen migrating from the anode to the cathode, was removed applying intermittent aeration cycles in the cathode chamber of the MFC where a concomitant nitrifying-denitrifying microbial community being established.

The feasibility to recover/remove nitrogen from high strength animal wastewater, such as pig slurries, using different MFC strategies has been demonstrated at lab scale. Hence, it can be considered as a potential technology for scaling up the treatment of high strength (organic and nitrogen) wastewaters, so as to accomplish the requirements needed for agricultural uses. Likewise, the knowledge acquired about the biofilm developed on the anode reveals itself as a key point for the resilience of BES at different environmental conditions and for further developments.

Resumen

Una celda de combustible microbiana (MFC), es un tipo de sistema bioelectroquímico (BES) capaz de convertir la energía contenida en los compuestos químicos en energía eléctrica mediante reacciones electroquímicas catalizadas por microorganismos. La cantidad de energía ganada por las bacterias que son capaces de transferir electrones a un ánodo, es significativamente mayor comparada con otros aceptores de electrones alternativos. Las poblaciones de microorganismos exoelectrogénicos tienden a enriquecerse selectivamente en los electrodos del compartimento anódico, siendo esenciales para la mejora del rendimiento de las MFCs en términos de producción de electricidad a partir de la oxidación de la materia orgánica. La tecnología de las MFCs se plantea como una alternativa para el tratamiento de aguas residuales de alta carga de origen animal, como por ejemplo los purines, para mejorar potencialmente su valorización energética, vinculada a la reducción o recuperación del contenido de carbono y nitrógeno.

La primera parte de esta tesis (Capítulos 4, 5 y 6) está centrada en el estudio de las poblaciones microbianas hospedadas en los electrodos de las MFCs. Se estudió el efecto de diferentes tipos de materiales de membranas de intercambio iónico, así como inóculos de diferente naturaleza, sobre las poblaciones de microorganismos en MFCs operando en discontinuo. Posteriormente, se realizó un estudio más detallado de la dinámica y la composición microbiana establecida sobre el biofilm del ánodo, bajo diferentes condiciones de alimentación (agua residual sintética y la fracción líquida de purín porcino), en MFCs operadas en modo continuo. Bajo estas condiciones de estudio, se mostró una elevada diversidad de la comunidad microbiana, siendo la composición final dependiente de los factores estudiados.

La segunda parte de la tesis está centrada en el estudio de la dinámica del nitrógeno en MFCs de doble compartimento, y el desarrollo de posibles estrategias para eliminarlo o recuperarlo. Primero, se estudió la difusión/migración del amonio a través de una membrana de intercambio catiónico, en experimentos en discontinuo bajo diferentes condiciones de operación (Capítulo 7). Los resultados obtenidos mostraron que la difusión/migración del amonio es función del voltaje aplicado, y cuando se usan purines, la migración de amonio llega a valores cercanos al 50%.

Estos resultados sugirieron que el uso de la tecnología de las MFCs podría ser una buena estrategia para tratar el exceso de nitrógeno de esta clase de residuos orgánicos. Se desarrollaron dos procesos diferentes de recuperación y eliminación de nitrógeno. Primero, se desarrolló un proceso fisicoquímico para la recuperación de nitrógeno acoplado a una unidad de stripping/absorción al compartimento catódico (Capítulo 7). Los resultados mostraron que este sistema de BES-stripping/absorción se puede considerar como una tecnología factible para llevar a cabo la recuperación del nitrógeno de los purines.

En segundo lugar, se estudió una estrategia de eliminación de nitrógeno mediante procesos biológicos, utilizado en este caso agua residual sintética de alta carga (Capítulo 8). En este caso, el amonio que migró desde el ánodo al cátodo, fue eliminado aplicando ciclos intermitentes de aireación en el compartimento catódico de la MFC, lo que provoca el establecimiento de una población nitrificante-desnitrificante.

La viabilidad para recuperar/eliminar nitrógeno de aguas residuales de alta carga de origen animal, como purines, mediante MFCs ha sido demostrada a escala de laboratorio utilizando diferentes estrategias. Por lo tanto, se puede considerar, que es una tecnología potencialmente aplicable en el tratamiento de aguas residuales de alta carga (carbono y nitrógeno), así como para lograr los requerimientos necesarios para uso agrícola. Igualmente, el conocimiento adquirido sobre el desarrollo del biofilm en el ánodo, revela que es un factor clave para la adaptabilidad de BES en diferentes condiciones medioambientales y para futuros desarrollos.

Resum

Una cel·la de combustible microbiana (MFC) és un sistema bioelectroquímic (BES) capaç de convertir l'energia química continguda en els enllaços químics d'un substrat, en energia elèctrica mitjançant reaccions electroquímiques catalitzades per microorganismes. La quantitat d'energia que poden guanyar els bacteris capaços de transferir electrons a un ànode és significativament superior a la guanyada quan s'utilitzen altres acceptors d'electrons alternatius. Les poblacions de microorganismes exoelectrogènics tendeixen a enriquir-se selectivament a l'elèctrode anòdic, essent essencials per a la millora en l'operació de la MFC en quant a producció d'electricitat procedent de la oxidació de la matèria orgànica. La tecnologia de les MFCs es mostra com una alternativa atractiva per al tractament d'aigües residuals animals d'alta càrrega, com els purins de porc, per a la potencial millora de la valorització energètica, així com la reducció i recuperació del contingut de carboni i nitrogen.

La primera part d'aquesta tesi (Capítols 4, 5 i 6) es centra en l'estudi de les poblacions microbianes presents a l'elèctrode anòdic de les MFCs. Es va estudiar l'efecte de l'ús de diferents materials en les membranes d'intercanvi iònic, així com de inòculs de diferents procedències, sobre la població microbiana en MFC operades en discontinu. Així mateix, es va realitzar un estudi en detall de la dinàmica i la composició de la comunitat bacteriana establerta al biofilm de l'ànode de MFCs operades en continu amb diferents condicions d'alimentació (aigua residual sintètica i la fracció líquida de purins de porc). En aquestes condicions, es mostra una elevada diversitat de la comunitat bacteriana, amb composicions finals diferents en funció dels factors estudiats.

La segona part de la tesi es centra en entendre la dinàmica del nitrogen en MFCs de doble compartiment, i desenvolupar possibles estratègies per a eliminar-lo o recuperar-lo. En primer lloc, la difusió/migració del nitrogen amoniacal a través de una membrana d'intercanvi catiònic en experiments en discontinu amb diferents condicions d'operació (Capítol 7). Els resultats obtinguts mostren que la difusió/migració del nitrogen amoniacal depèn del voltatge aplicat i, quan s'utilitzen purins de porc, la migració de l'amoni arriba a valors propers al 50%.

Aquests resultats suggereixen que l'ús de la tecnologia de les MFCs podria ser una bona estratègia per a tractar l'excés de nitrogen d'aquest tipus de substrats. Es van desenvolupar dos processos diferents per a la recuperació i eliminació del

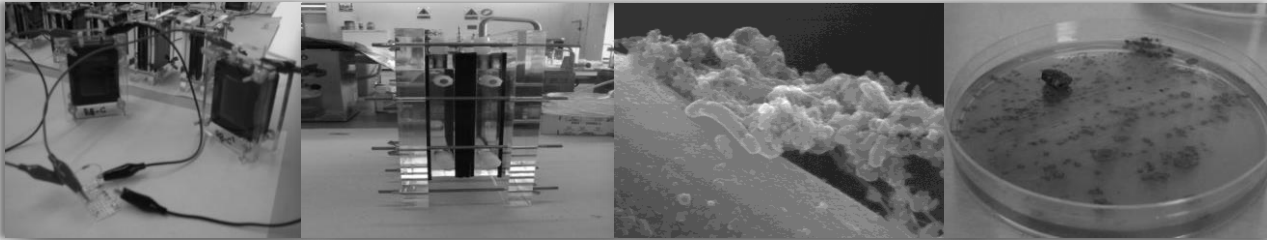
nitrogen en MFCs. En primer lloc, es va desenvolupar un procés fisicoquímic per a la recuperació del nitrogen, acoblant una unitat de stripping/absorció al compartiment catòdic (Capítol 7). Els resultats mostren que el sistema BES-stripping/absorció és una tecnologia viable per a recuperar el nitrogen amoniacal dels purins de porc.

En segon lloc, es va estudiar una estratègia d'eliminació de nitrogen mitjançant processos biològics utilitzant com a substrat aigua residual sintètica d'alta càrrega (Capítol 8). En aquest cas, el nitrogen amoniacal que migra de l'ànode al càtode, va ser eliminat aplicant cicles intermitents d'aireació al compartiment catòdic de la MFC, afavorint-hi l'establiment d'una comunitat microbiana nitrificant-desnitrificant.

La viabilitat de recuperar/eliminar nitrogen d'aigües residuals animals d'alta càrrega, com purins de porc, mitjançant MFCs, ha estat demostrada a escala laboratori utilitzant diferents estratègies. Per tant, pot ser considerada com una tecnologia per al tractament d'aigües residuals d'alta càrrega (orgànica i amoniacal) a gran escala, així com per a complir amb els requeriments específics per a usos agrícoles. Així mateix, el coneixement adquirit sobre el desenvolupament del biofilm a l'ànode indica que es un factor clau per a la resiliència dels BES sotmesos a diferents condicions ambientals, així com per a desenvolupaments futurs.

Chapter 1

General Introduction



In this chapter, an introduction about general fundamentals of bioelectrochemical systems (BES), developments and current status are presented. Special attention was given to the implementation of BES for wastewater treatment and nitrogen removal and recovery.

General introduction

1.1. Electricity generation from microorganisms and microbial fuel cell concept

The origin of the microbial fuel cell development was attributed a century ago to Potter in 1911 (Ieropoulos, 2005), when it was discovered that electrical energy could be produced by from living cultures of *Escherichia coli* and *Saccharomyces* by using platinum electrodes (Potter, 1911). But the interest of the scientific community really started in 1980s, when it was discovered that the current density and the power output could be enhanced by the addition of electron mediators. Although the MFC concept was demonstrated from early nineties and even the MFC technology for wastewater treatment was already presented in 1991 (Habermann et al., 1991), the interest in these systems has blossomed in the last twenty years and nowadays is considered to be a promising sustainable technology to achieve new challenges. **Figure 1.1a** shows the 'Scopus' search with keyword "microbial fuel cell" or "bioelectrochemical system" between 1996-2014, as can be seen there is a roughly 100-fold increase in the number of publications during this period. In addition, the research activities in this topic has been spread to many different countries, covering up to 60 countries, being nowadays the 20 more important topics (**Figure 1.1b**), being Spain located in the top ten.

MFC technology has been studied in depth in the past decade, their interest have already gained attention as an interdisciplinary research field which integrates for instance microbiology, electrochemistry, material science, energy and engineering. Microbial oxidation processes in bioanodes is a shared principle in all BES, but with the utilization of the electrons in the cathode to carry out the reduction reactions arises new possibilities and challenges (Wang et al., 2013). **Figure 1.2** shows a summary of some important achievements of MFC developed to date.

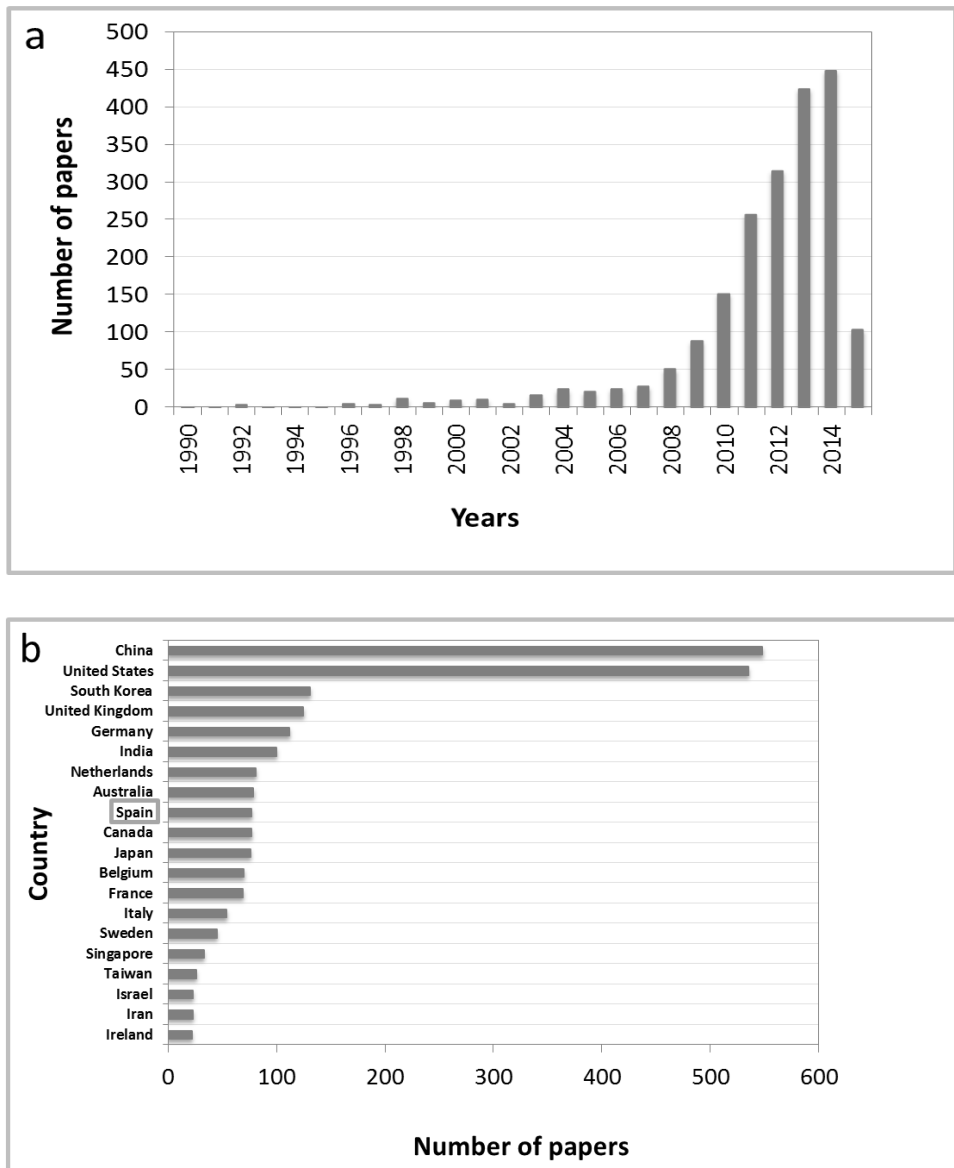


Figure 1.1. (a) The number of publications on MFCs from the year 1990 to 2015, and **(b)** the country-wise distribution in MFC research. The data is based on the number of publications mentioning "microbial fuel cell or bioelectrochemical system" in Scopus database (February 2015).

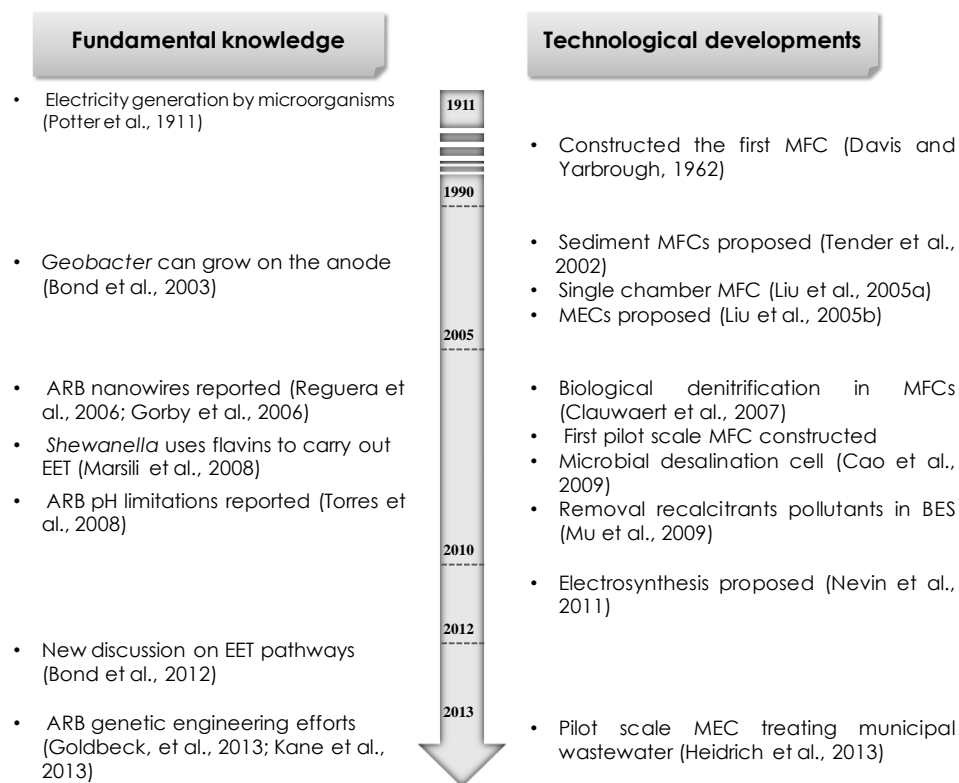


Figure 1.2. Timeline outlining of the major achievements of bioelectrochemical systems (BES).

1.2. Bioelectrochemical systems principles

A bioelectrochemical system (BES) is a bioreactor that converts chemical energy contained in the chemical bonds of organic and some inorganic compounds (Ngunye et al., 2015) directly into electricity (Logan and Regan 2006a; Du et al., 2007). A BES can be distinguished from other type of fuel cells by the fact that at least one of the two reactions that take place in the anodic or cathodic compartment uses microorganisms as catalysts through the exoelectrogenic-based metabolic activity. There are two types of BES according to the way of use electricity. A microbial fuel cell (MFC), which is a bioelectrochemical system capable of converting the chemical energy of dissolved organic materials directly into electrical energy without additional current (**Figure 3a**), and a microbial electrolysis cell (MEC), when an external electrical energy input is needed to overcome a thermodynamically unfavorable redox reaction to produce value added products such as hydrogen, methane, H_2O_2 , VFA or alcohols (Zaybak et al., 2013) (**Figure 3b**) (Rozenal et al., 2008a).

A standard BES (**Figure 1.3**) consists in two compartments, anodic and cathodic, separated by a proton exchange membrane (PEM). The electrodes in each compartment are connected by an external resistance. Microbial populations in the anodic chamber oxidize the *organic/inorganic* substrates and generate electrons and protons. The electrons produced are transferred to the anode by means of different mechanisms (**section 1.3.1**), and then the electrons flow through an external circuit to the cathode chamber. Simultaneously, the protons migrate through the membrane from anode to the cathode to maintain electroneutrality conditions, where they combine with the transferred electrons reducing the electron acceptor, typically oxygen, producing water (Logan and Regan, 2006a).

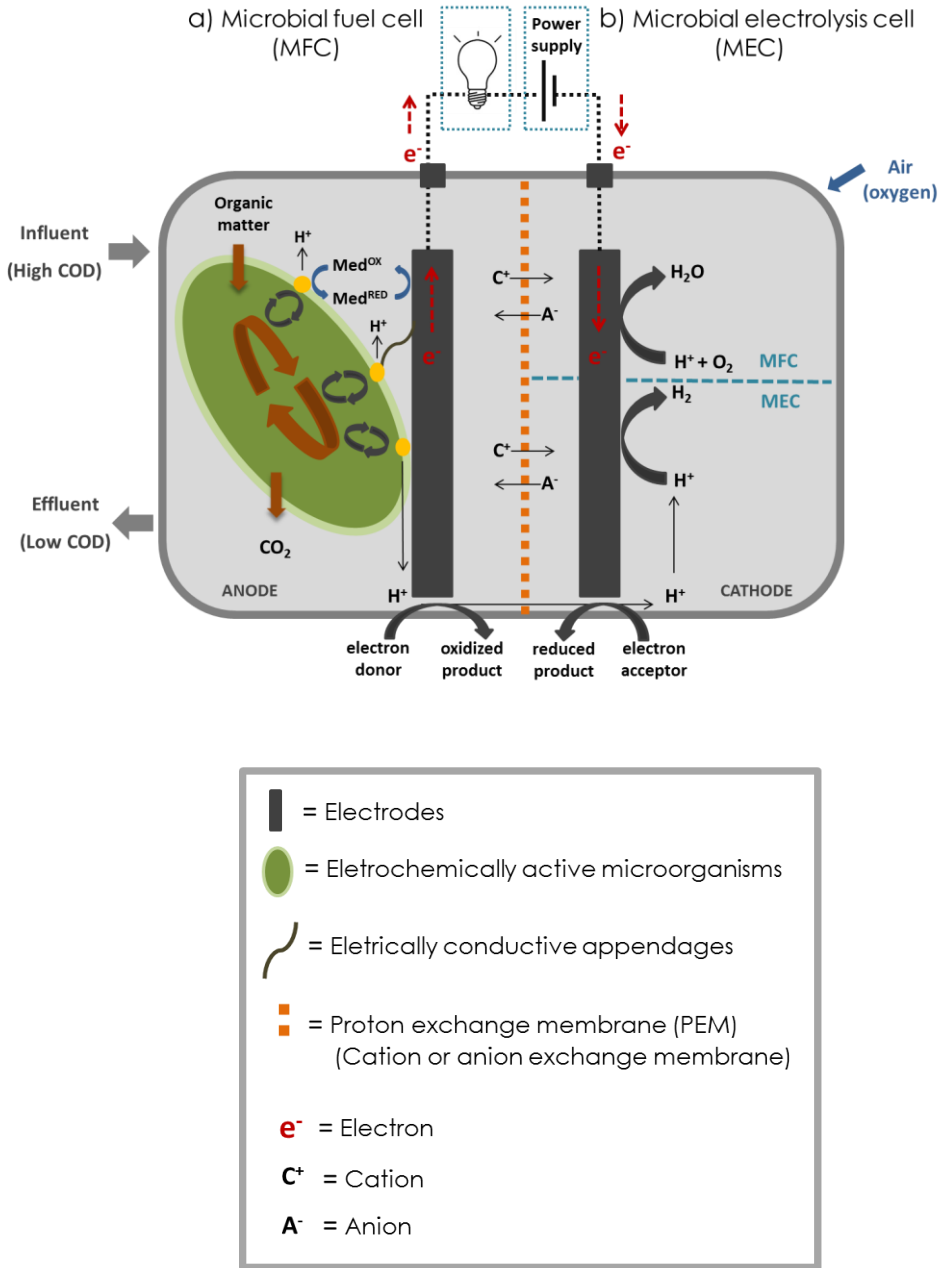


Figure 1.3. Scheme of (a) microbial fuel cell (MFC) and (b) microbial electrolysis cell (MEC).

Although the most typical MFC is a two-chamber MFC configuration, described above, different MFC configurations have been described so far (Du et al., 2007). Reactor design can be varied on different classification criteria, such as MFC configuration, reactor structure, separator, flow type and cathode type (**Table 1.1**).

Table 1.1. MFCs reactors based on different classification criteria.

MFC reactor design				
MFC configuration	Reactor structure	Separator	Flow type	Cathode type
<ul style="list-style-type: none"> single-chambered 	<ul style="list-style-type: none"> flat-plate disc 	<ul style="list-style-type: none"> salt bridge membrane-less 	<ul style="list-style-type: none"> batch continuous flow 	<ul style="list-style-type: none"> air cathode biocathode
<ul style="list-style-type: none"> two-chambered 	<ul style="list-style-type: none"> tubular 	<ul style="list-style-type: none"> anion exchange membrane 		<ul style="list-style-type: none"> chemical cathode
<ul style="list-style-type: none"> multi-chambered 	<ul style="list-style-type: none"> concentric cylinders 	<ul style="list-style-type: none"> anion exchange membrane 		
<ul style="list-style-type: none"> roll type-chamber 		<ul style="list-style-type: none"> cation exchange membrane 		

Likewise, different types of materials, specially anode, cathode and membrane materials, have been widely studied in order to increase MFC performance while reducing investment and operating costs. Anodic materials must be highly conductive, non-corrosive, with high specific surface area able to fix the biofilm, and chemically stable in the reactor solution (Logan et al., 2006b). The typical anodes materials that comply these characteristics are made of graphite, which is available in many forms, such a graphite felts, graphite paper, graphite granules, and graphite foam, or carbon, such as carbon paper, carbon cloth, and reticulated vitreous carbon (Bond and Lovley 2003; Chaudhuri and Lovley 2003; Rabaey et al., 2005). In recent years, different techniques to modify the electrodes surfaces are investigated to improve a more rapid start-up of bioelectrochemical processes and to increase the current generation (Flexer et al., 2013; Tang et al., 2011).

Cathode materials also affect MFC performance, and depending on the application different materials are used. The same electrodes materials used for the anode can be used for the cathode, but the major difference is the need to use a catalyst. Oxygen is the most sustainable electron acceptor and the most commonly used in MFC operation.

Regarding the membrane, the majority of MFC designs require the separation of the anode and the cathode compartment. There are different types of membranes (anion, cation and bipolar membranes), which are selective for the different ions.

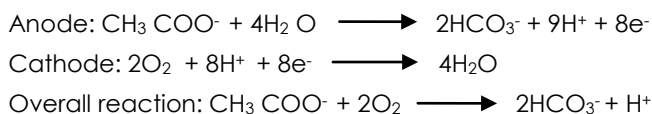
1.2.1. Fundamentals of voltage generation.

As aforementioned in **section 1.2. (Figure 1.3)**, in a standard MFC the electrodes in each compartment are connected by an external circuit, and as a result of this electrical connection between both electrodes, the electrons can flow from the anode to the cathode. This difference of voltage between both compartments is the electromotive force (*emf*), E_{emf} (V), and it can be calculated with the Gibbs free energy, according to:

$$\text{(Equation 1.1)} \quad emf = -\Delta G/nF$$

with *emf* being the electromotive force (V), ΔG the Gibbs free energy of the reaction (J/mol), *n* the amount of electrons involved in the reaction (mol), and *F* is Faraday's constant (96485.3 C/mol).

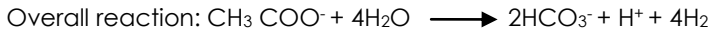
When the Gibbs free energy of the overall reaction is negative and the *emf* is positive, electrical energy can be produced, and accordingly the BES is operated as a MFC. For example, when acetate is the electron donor, ($[\text{CH}_3\text{COO}^-] = [\text{HCO}_3^-] = 10 \text{ Mm}$, pH 7, 298.15 K, $p_{\text{O}_2} = 0.2 \text{ bar}$), the reactions occurring in each electrode can be expressed as:



with an overall cell electromotive force of $E_{emf} = E_{cathode} - E_{anode} = 1.1\text{V}$
($\Delta G = -847,60 \text{ kJ/mol}$; $emf = 1.1\text{V}$)

Contrary when the Gibbs free energy is positive and *emf* is negative, electrical energy needs to be invested, and the BES system is operated as MEC. For example if acetate is used as the organic substrate and hydrogen is produced in the cathode. With this conditions: $[\text{CH}_3\text{COO}^-] = [\text{HCO}_3^-] = 10 \text{ Mm}$, pH 7, 298.15 K, $p_{\text{H}_2} = 1 \text{ bar}$, the half reactions produced are:

General introduction



with an overall cell electromotive force of $E_{emf} = E_{cathode} - E_{anode} = -0.12\text{V}$
($\Delta G = 93,14 \text{ kJ/mol}$; $emf = -0.12\text{V}$)

Hence, the value of *emf* indicates the maximum cell voltage that can be generated in a MFC, and the minimum cell voltage required to drive a MEC, but in practice the produced energy is less than the theoretical one (in MFC mode) and the required energy is more than the theoretical (in MEC mode).

As aforementioned, electricity is generated in a MFC when the overall reaction is thermodynamically favorable, thus there is a potential difference between the cathode and the anode (E_{emf}) (equation 1.2):

$$\text{(Equation 1.2)} \quad E_{emf} = E_{cathode} - E_{anode}$$

The cell *emf* is a thermodynamic value that does not take into account internal losses or overpotentials. The open circuit voltage (OCV), is the highest voltage produced in a MFC, which is measured with the circuit disconnected (infinite resistance, zero current). Although the OCV should be approach the total cell potential (*emf*), in practice is lower due to potential losses. The maximum electromotive force attainable in a MFC is theoretically in the order of 1.1V (Rozendal et al., 2008a), however due to the potential losses, the *emf* falls below 0.6V under operating conditions (Logan et al., 2006b).

1.2.2. Factors determining the performance of microbial fuel cells.

The power that can be generated in a MFC is dependent on several biological and electrochemical parameters. Thereby, there are some critical points to consider with respect to losses in MFC systems:

1. Substrate conversion rate

The bacterial conversion rates depend on the substrate nature, the amount and structure of microbial populations, the organic loading rate, the mixing and mass transfer, bacterial kinetics and other environmental conditions, such as temperature.

2. Overpotentials at the anode

As mentioned before, the electricity produced mainly depends on the electrode, surface, materials and its electrochemical characteristics, the microbial community and their mechanisms of electron transfer from the microbial cells to the electrode, and the availability of electron shuttles (chemical redox mediators). It is well known that some microorganisms are able to produce electron mediators (**section 1.3.1**), but besides it has been found that for instance humic acids, which are naturally present in environmental samples, could act as well as redox mediators in MFC (Gerritse et al., 2004; Milleken and May, 2007).

3. Overpotentials at the cathode

Similar to the losses observed at the anode, the cathode has also potential losses. In many cases oxygen reduction at the cathode is one of the factors determining maximum power output of the MFC. The electron transfer rate at the cathode can be improved by sparging pure oxygen (Rabaey et al., 2003) or by adding potassium ferrocyanide solution (Rabaey et al., 2004; Rabaey et al., 2003).

4. Proton supply into the cathode compartment

In a standard two-chambered MFC, the proton transport into the cathode compartment mainly depends on the type of IEM used. The market of IEM is very extensive, although the first studies used Nafion™ (Dupont; <http://www.dupont.com>), a type of cation exchange membrane (CEM), and good results were achieved (Bond and Lovley, 2003). This membrane has a high selectivity towards protons, however it has been reported that Nafion membrane is very sensitive to the presence of ammonium, as the sulfonic acid groups of the membrane rapidly bind with the ammonia present in the anolyte. Hence, this membrane could display a low stability and trap free nitrogen (Rabaey et al., 2005). Another type of CEM, with lower selectivity but higher stability are Ultrex CMI membranes (Membranes International; <http://www.membranesinternational.com>), and alternatively, anion exchange membranes (AEMs) and ultrafiltration membranes have been proposed as feasible alternatives (Kim et al., 2007).

5. Internal resistance of the MFC

Internal resistance is described to be dependent of several factors, such as the resistance of the electrolyte between the electrodes and by the membrane

resistance, the distance between the electrodes (anode and cathode), and also proton migration to the cathode compartment (Rabaey and Verstraete, 2005).

1.3. Exploring electrochemically active microorganisms

Those microorganisms that are able to oxidize the organic matter available and further are capable of either donating electrons to or accepting electrons from an insoluble anode or electrode as the terminal electron acceptor in anaerobic conditions are called electrochemically active microorganisms¹.

¹Microorganisms capable of interacting with electrodes has received different appellations so far, including: **anodophiles**, **exoelectrogens**, **electrogenic microorganisms**, **electroactive bacteria (EAB)**, **anode-respiring bacteria (ARB)**, and **electrochemically active bacteria**. The same terminology used for other forms of anaerobic respiration such a sulphate/Fe(III)-reducing microorganisms, may be used for microorganisms that donate electrons to the anode (**electrode-reducing microorganisms**), or accept electrons from electrodes (**electrode-oxidizing microorganisms**).

Since this lack of standardization can leads to confusion, it will be used throughout the text electrochemically active bacteria to refer to microorganisms that interact with electrodes of microbial fuel cells.

Bacteria gain more energy by reducing terminal acceptors at a more positive potential when the bacteria have metabolic pathways capable of capturing the energy available (Kumar et al., 2012). The model microorganisms used to carry out the first studies about this type of respiration were *Shewanella oneidensis* MR-1 and *Geobacter sulfurreducens*, which belong to dissimilatory metal reducing microorganisms. It has been described that these microorganisms produce energy in form of ATP during the dissimilatory reduction of metal oxides under anaerobic conditions in soils and sediments at environmental conditions. The electrons are transferred to the final insoluble acceptor such as Fe₂O₃ by a direct contact of mineral oxides and conductive proteins encountered on the external membrane of these microorganisms (Nealson and Saffarini, 1994). The anode on MFCs acts as the final electron acceptor just like the solid mineral oxides. In **Figure 1.4** an electron transfer chain in electrochemically active microorganisms is proposed, where the electrons go from electron carriers in the intracellular matrix to the electron acceptor (anode) (Lovley et al., 2004).

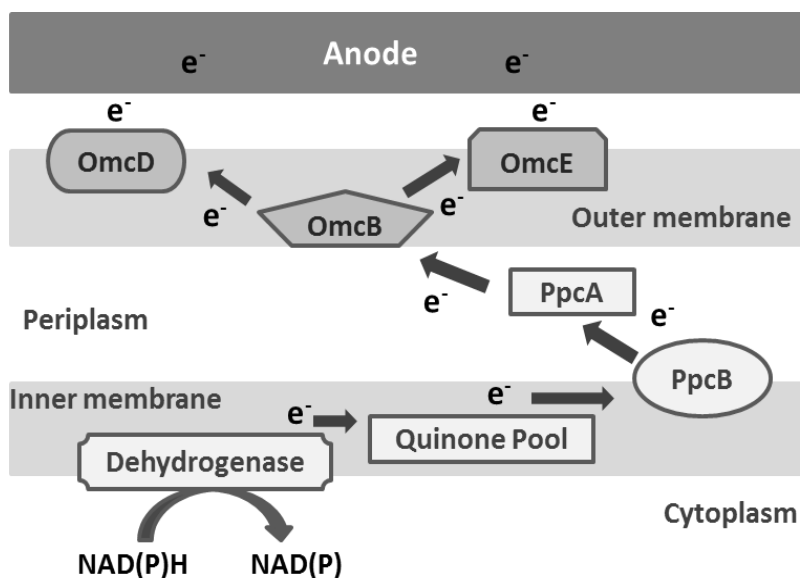


Figure 1.4. Components involved in the electron transfer chain from the cells to the anode in MFCs using ARB microorganisms (*Geobacter* species) (Drawn with modifications after Lovley et al., 2004).

1.3.1. Mechanisms involved in the interaction between bacteria and anodes

All the interest in MFC research till some years ago has been mainly focused on increase power output, or to select materials to develop economically feasible systems. However, the interest in understanding microbial community roles and electron transfer mechanisms has increased exponentially in the last ten years.

As aforementioned, the findings of microorganisms with the ability to transport electrons extracellularly was first reported by Potter in 1911, and during long time these capacity was attributed only to the dissimilatory metal-reducers bacteria. But in the last years, the investigations of the microbial communities enriched in BES have revealed the presence of high diversity linked to the anode biofilm and in the extracellular electron transfers (EET) mechanisms. Such high diversity settled up on the anode surface is crucial to the establishment of stable synthrophies by means different pathways (Kumar et al., 2012).

In **Figure 1.5** are depicted different EET mechanisms proposed so far, which can be divided in two main groups; i) namely direct electron transfer (DET) and ii) indirect electron transfer (IET). DET is based on the physical contact between the microbial outer membrane (OM) proteins, such as c-type cytochromes (Holmes et al., 2006), or a membrane organelle, such as conductive nanowires² or pili (Gorby

et al., 2006; Malvankar et al., 2011), and the anode electrode surface. Contrary, in IET, direct contact between the microbes and the electrode surface is not required, and in this case soluble electron shuttles or electron mediator compounds are involved in this process. In some cases, mediators are externally supplied and moreover, some microorganisms are able to produce and excrete their own mediators. Mediators in an oxidized state can be reduced by capturing the electrons from the membrane, then can diffuse in and out of the membrane and transport the electrons to the anode and become oxidized again. A range of electron mediators produced by bacterial have been reported so far, such as melanin, phenazines (Rabaey et al., 2005), flavins and quinones (Freguia et al., 2009). The last indirect mechanism proposed is the formation of an extracellular matrix (ECM). In this matrix not only the monolayer of cells are responsible for electricity generation, since in this multilayer conductive biofilm the bacteria cell to cell communication is carried out through nanowires networking and mediators with the last step carried out by DET (Borole et al., 2011; Strycharz-Glaven et al., 2011).

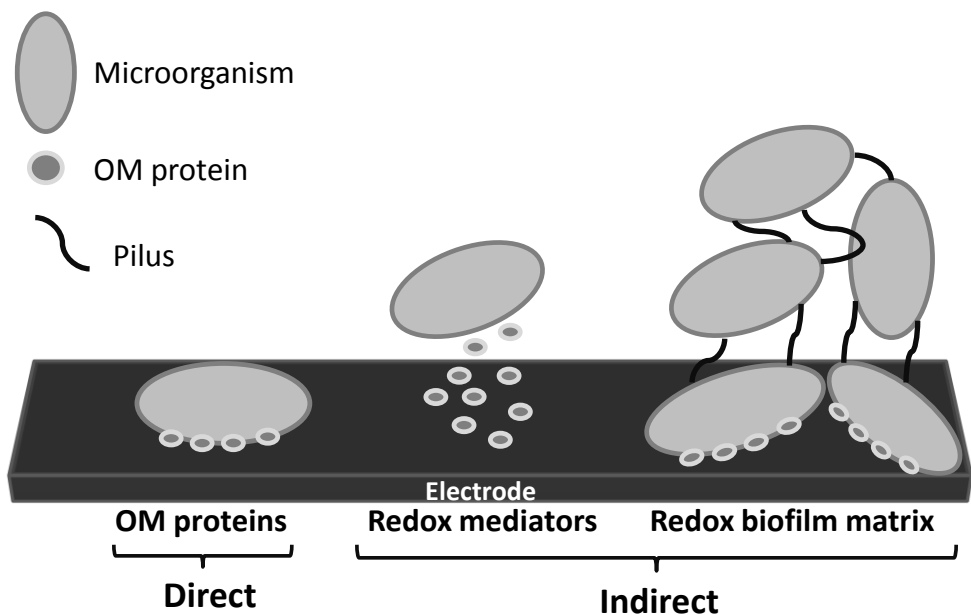


Figure 1.5. Schematic diagram of proposed electron-transfer mechanisms (Drawn with modifications after Borole et al., 2011).

²**Nanowire**, is a term appeared in microbiology literature as “bacterial or microbial nanowires”, and it was reported first time by Reguera et al., 2005. Electrical conductivity measurements have been reported across the diameter of sheared pilus-like filaments from mineral reducing bacteria, mainly *Geobacter* and *Shewanella* sp. Although later, conductive unknown pilus-like filaments have also been described in other non-mineral reducing bacteria as *Synechocystis*, *Pelotomaculum thermopropionicum* alone and in coculture with *Methanothermobacter thermoautotrophicus* (Gorby et al., 2006).

Although there are still many microbes to be characterized, **Table 1.2** shows some examples of well-known anodophilic bacteria in MFCs and their EET.

Table 1.2. Some electrogenic microbes for MFCs and their extracellular electron transfer mechanisms.

Microbes	Mechanism	Reference
<i>Aeromonas hydrophila</i>	DET	Pham et al., 2003
<i>Geobacter metallireducens</i>	DET	Min et al., 2005
<i>Rhodospirillum rubrum</i>	DET	Chaudhuri and Lovley 2003
<i>Shewanella putrefaciens</i>	DET	Kim et al., 1999
<i>Actinobacillus succinogenes</i>	IET	Park and Zeikus 1999; Park and Zeikus 2000
<i>Alcaligenes faecalis</i>	IET	Rabaey et al., 2004
<i>Enterococcus gallinarum</i>	IET	Rabaey et al., 2004
<i>Proteus vulgaris</i>	IET	Thurston et al., 1985
<i>Shewanella oneidensis</i>	IET	Ringeisen et al., 2006

1.3.2. Microbial anode communities

The formation of a biofilm on the anode surface is essential for the efficient transfer of electrons in a MFC (Franks, et al., 2010). Microbial fuel cells can be operated in pure and mixed cultures. Pure cultures are essential to study the mechanisms of EET and the capability of strains to produce electricity (Park et al., 2001). So far, strains described as capable to produce electricity in pure cultures belongs mainly to *Proteobacteria* (α , β , γ , and ϵ -*Proteobacteria*), and also *Firmicutes* and *Actinobacteria* phylum (**Table 1.3**). As we can observe in **Table 1.3**, most of these strains belong to *Proteobacteria* phylum, until Bond and Lovley 2005, reported a strain belong to *Acidobacteria* phylum (*Geothrix fermentans*) as the first isolate outside of the *Proteobacteria* phylum able to oxidize organic compounds linked to electrode reduction. And regarding *Firmicutes* phylum, *Clostridium butyricum* was described as the first Gram-positive bacterium that produces electrical current in a MFC.

In contrast, mixed cultures are more sustainable and resilient when complex substrates such a wastewater are used, due to the possibility of metabolize a large range of organic compounds.

The interest of studying the anode microbial communities has tremendously grown in the last years, so the information about which are the predominant populations is very extensive, and sometimes it makes a difficult task to compare the results from different types of systems.

Different factors can directly determine the microbial community composition, such as inoculum, MFC configuration, substrate used and its concentration. Thus the diversity of the electrochemically active bacteria in MFCs is much greater than those model iron reducing bacteria such as *Geobacter* or *Shewanella*. But regardless of these factors that can determine the anode microbial community, most of works reported that the predominant phyla found on the anode are *Proteobacteria*, *Firmicutes*, *Actinobacteria*, *Bacteroidetes*, *Deferribacteres* and some yeast. Some of these phyla have been found abundant in bioanodes even though no strains have been shown to product current in pure cultures.

Archaeal populations are also present in MFC anodes. To date, no pure culture is known to produce current, but active methanogenesis has been observed in some MFCs reactors (He et al., 2005), suggesting that they might play a role in the electrons transfer process via syntrophic interactions.

Table 1.3. Some microorganisms capable of current production in pure cultures without and with mediator additions.

Pure culture	Phylum/Class	Substrate	Electrode type	Current (mA)	Power (mW m ⁻²)	Reference
<i>Shewanella putrefaciens</i> ^a	γ - proteobacteria	lactate	woven graphite	0.031	0.19	Kim et al., 2002
<i>Geobacter sulfurreducens</i> ^a	δ - proteobacteria	acetate	graphite	0.40	13	Bond and Lovley, 2003
<i>Rhodospirillum rubrum</i> ^a	β - proteobacteria	glucose	graphite	0.2	8	Chaudhuri and Lovley, 2003
<i>Clostridium butyricum</i> ^a	Firmicutes	glucose	graphite felt	0.22	n.a.	Park et al., 2001
<i>Corynebacterium sp.</i> ^a	Firmicutes	glucose	carbon felt	n.a.	7.3	Liu et al., 2010
<i>Proteus vulgaris</i> ^b	γ - proteobacteria	glucose	glassy carbon	0.7	85	Choi et al., 2003
<i>Pseudomonas aeruginosa</i> ^b	γ - proteobacteria	glucose	plain graphite	0.1	88	Rabaey et al., 2005
<i>Escherichia coli</i> ^b	γ - proteobacteria	lactate	woven graphite	3.3	1.2	Park and Zeikus 2003
<i>Geotrix fermentans</i> ^b	Acidobacteria	acetate	graphite	0.08	n.a.	Bond and Lovley 2005
<i>Corynebacterium sp.</i> ^b	Firmicutes	glucose	carbon felt	n.a.	41.8	Liu et al., 2010

^amicroorganisms capable of current production in pure culture without mediator addition

^bmicroorganisms capable of current production in pure culture with mediator addition

n.a. data not available

1.4. MFCs for high strength wastewater treatment

MFCs are deemed a promising sustainable technology with operational and functional advantages over the technologies currently used for generating energy from organic matter (Rabaey and Verstraete 2005). Some of these advantages are that the direct conversion of substrate energy to electricity enables high conversion efficiency and these systems can operate efficiently at ambient and low temperatures. For those reasons, MFC technology is considered a possible alternative for generating electricity and accomplishes wastewater treatment simultaneously, thus may offset the operational costs of wastewater treatment plant (Lu et al., 2009).

Industrial, agricultural, and domestic wastewater produced by the human activity contain dissolved organics that require removal before discharge into the environment (Angenent et al., 2004). Wastewaters are recognized as a renewable resource for the production of electricity, fuels and chemicals. To date, there are several technologies to extract this energy from wastewaters, being the more mature anaerobic digestion (AD), which is established as a commercial scale. Treatment strategies based on anaerobic digestion (AD) allows the energetic valorization of swine manure, being codigestion approaches (mixture of manure with other organic waste) applicable in order to increase the biogas yield. In relation to nitrogen management, there is a dichotomy between strategies based on transferring nitrogen to the atmosphere (N_2) through biological nitrification-denitrification (NDN), and strategies that focus on the nitrogen recovery by means of producing of struvite or concentrated nitrogen streams that are potentially reusable in agricultural areas with nutrient shortages: stripping-absorption (Bonmati and Flotats, 2003a; Laurení et al., 2013), thermal concentration (Bonmati and Flotats, 2003b), struvite precipitation (Cerrillo et al., 2015).

1.4.1. Management and processing of livestock wastes

Intensive pig breeding has experienced a rapid growth in the last decade, and in this context Spain is the European Union's second-largest pig producer, just behind Germany, with 19% of the total production. In this regard, pig manure has resulted in nitrate concentrations exceeding EU norms in many aquifers.

Nitrogen is considered one of the key nutrients for improving agricultural production but it is also a contaminant when it is release in excess into the environment. Commons forms of nitrogen present in wastewater are ammonia (NH_3), and nitrate (NO_3^-) which can be reduced to nitrite (NO_2^-), and. All forms may cause health and environmental threat.

Yearly nitrogen generation by livestock farming corresponds to an average charge of 74 kgN/ha. In principle, the reuse of pig slurry as fertilizer is the most appropriate option, although requirements and transportation costs should be considered in order to identify the most advantages management strategy. If the production of animal slurries in a given region is higher than the fertilizing requirements of the implanted crops there is an excess in the availability of nutrients, and hence some problem arise caused by this nutrients surplus (Burton and Turner, 2003; Ghafari et al., 2008). Excessive nitrogen surpluses, the difference between inputs and removals by crops, can pose a threat to the environment, leading to pollution of water, air and soil.

1.4.2. Nitrogen removal and recovery in microbial fuel cells

Concerning these environmental problems described above and the stricter discharge regulation, new challenges, such as BES for nitrogen removal and recovery are required. As it is well-known, BESs are able to combine energy production and nitrogen removal and/or recover, thus they can be considered an interesting opportunity for the improvement of pig slurry management.

Firstly, in a standard two-chambered BES, Rozendal et al., 2008b and Kim et al. 2008 reported that the ammonium ion can pass through the anolyte into the catholyte across cation exchange membrane via either current-driven migration or diffusion. Then, the ammonium can be removed and/or recovered through biological or physicochemical processes.

1.4.2.1. Nitrogen removal

Focusing on nitrogen removal, it is mainly carry out by using biological processes such as nitrification and denitrification. To date, two processes are reported: i) nitrification and bioelectrochemical denitrification (NDN), and ii) simultaneous nitrification and bioelectrochemical denitrification (SNDN). These processes are detailed in **Figure 1.6**.

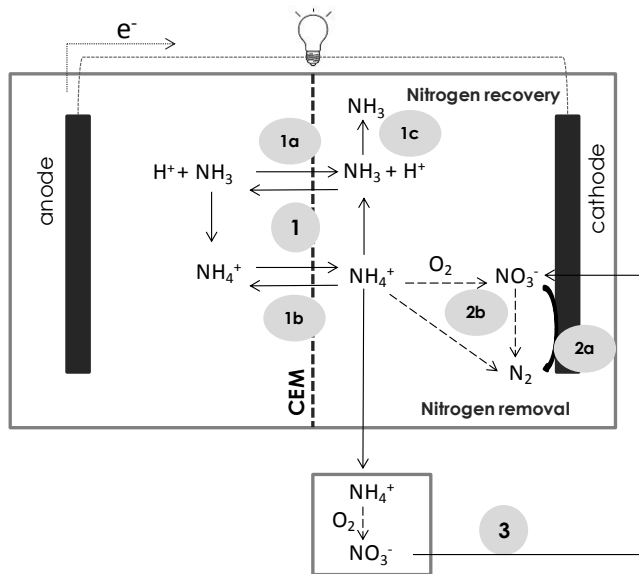


Figure 1.6. Representative scheme of the ammonia removal and recovery in a standard two- chambered BES equipped with a CEM. Ammonium can be transported through the membrane (1) either passively via diffusion of ammonia (1a) or actively via migration in the form of ammonium (1b). Ammonia can be removed from the cathode by stripping (1c). Ammonium can be biologically nitrified by oxygen and denitrified by microorganisms at the cathode (2a), or in solution (2b). The dashed lines represent no bioelectrochemical processes. The ammonium can be recirculate into an external nitrifying reactor, and then the nitrate is reduced to nitrogen gas in the cathode chamber (3) (Redrafted with modifications after Arredondo et al., 2015).

Gregory et al. (2004) reported for the first time that electrodes may serve on the cathode as a direct electron donor for anaerobic respiration, and using nitrate as the electron acceptor in a pure culture of *Geobacter metalireducens*. Just one year later, Park et al., 2005, also observed that nitrate could be biologically reduced using electrons from the cathode in the absence of organic substances. In this case the experiments were carried with a mixed culture under an applied electric current. Those findings opened a new alternative demonstrating the feasibility of a bioelectrochemical denitrification in BES. After these studies, Clauwaert et al., 2007 performed for the first time the simultaneous removal of an organic substrate (in a bio anode), power production and complete denitrification (in a bio cathode), using two separate liquid streams, without relying on H_2 formation or an external added power. Later, nitrification and subsequent bioelectrochemical denitrification in a second step with the same liquid stream was described by Viridis et al., 2008. In this system an external nitrifying bioreactor

was needed to oxidize the ammonia from the anode effluent to nitrate, and then the nitrate was reduced to nitrogen gas in the cathode chamber. Afterwards, different reactor design were performed, and in this way Xie et al., 2011 designed a couple MFC system, one with dual aerobic biocathodes and the other with dual anaerobic biocathodes to separate nitrification and denitrification respectively. This system was scaled up then, consisting in a 50 L novel denitrifying MFC with an oxic-anoxic two stages-based biocathode (Liang et al., 2013).

This MFC system was simplified later, contained also a dual aerobic and anoxic cathode, but in the same MFC to each side of the anode with different configurations (Zhang and He, 2012a and 2012b). All these systems needed an oxygen supply to the aerobic cathode, hence Zhang et al., 2013, constructed a new design consisted in a MFC with a cathode exposed to the air for nitrification coupled with another MFC with anoxic denitrification cathode.

The bioelectrochemical denitrification can be carry out in the cathode chamber of a MFC without previous nitrification, in case of treating groundwater with high content in nitrates (Puig et al., 2012).

To date, there have been fewer studies reported in regard to SNDN. The first study in which a simultaneous nitrification and denitrification was accomplished was reported by Viridis et al., 2010; Viridis et al., 2011, where the loop configuration described in Viridis et al., 2008 was modified integrating the aerobic process into the cathode and therefore dispensing with the external nitrifying bioreactor.

An overview of different nitrogen removing processes and the nitrogen removal rates achieved in BES are summarized in **Table 1.4**.

Table 1.4. Nitrogen removing mechanisms performed in BES.

Nitrogen removing	Removal rate (Kg m⁻³ d⁻¹)	MFC system design	Reference
NDN	0.051	Two-chambered MFC, plus an external nitrifying bioreactor	Viridis et al., 2008
NDN	0.013	Two MFCs with aerobic an anaerobic cathodes	Xie et al., 2011
NDN	0.003 0.013	Tubular MFC with dual cathodes	Zhang and He 2012a Zhang and He 2012b
NDN	n.a.	MFC with a cathode exposed to the air coupled with another MFC with anoxic cathode	Zhang et al., 2013
SND	0.1 0.024	Two-chambered MFC with aerobic process integrated into the cathode	Viridis et al., 2010 Viridis et al., 2011

n.a. data not available

1.4.2.2. Nitrogen recovery

Nitrogen recovery in BES is mainly focus on ammonia recover via ammonium migration driven by electricity generation. As aforementioned, ammonium ion can diffuse from the anode to the cathode compartment throughout the cation exchange membrane (Rozendal et al., 2008b) via either diffusion or current-driven migration (Kuntke et al., 2011; Villano et al., 2013). Then, due to the pH increase in the cathode chamber, the ammonium is transformed into volatile ammonia, which can be removed from the cathode compartment by NH₃ stripping with a suitable gas stream (**Figure 1.6**). Kuntke et al. (2012) successfully recovered ammonia from urine following this stripping strategy in a MFC system. After this study, Desloover et al. (2012) developed an electrochemical cell in which a stripping unit was coupled to the cathode chamber achieving a successful ammonia recovery from both synthetic wastewater and digestate. Later, Wu and Modin, 2013 achieved to recover ammonia in a MEC with simultaneous hydrogen production, from reject wastewater with high concentration of ammonium (~1000 mg/L) and low amount of organic compounds.

Despite many advances have been accomplished regarding the nitrogen removal and recovery in BES so far, there are many influence factors such as oxygen, pH, C/N ratio, microbial community composition, reactor design, materials and electricity generation for instance, which affect BES performance and therefore nitrogen removal/recover efficiency. Further studies are needed regarding the anode microbial community, especially when real organic wastes are used as fed. In these cases, it is expected that microorganisms that are able to metabolize these complex compounds present in real substrates will also be components of the anode microbial community. These microbial populations may not have capacity for electrons transfer to the anode, but their metabolism is key to powering MFCs, and thus for the overall MFC performance.

Finally, all these key aspects should be taken into account for improving efficiencies reducing costs to move from bench scale towards scaling-up in the future.

1.5. References

- Angenent, L.T., Karim, K., Al-Dahhan, M.H., Wrenn, B.A., Domínguez-Espinosa, R., 2004. Production of bioenergy and biochemicals from industrial and agricultural wastewater. *Trends Biotechnol.* 22(9), 477-485.
- Arredondoe, M. R., Kuntke, P., Jeremiasse, A.W., Sleutels, T.H.J.A, Buisman, C.J.N., Heijne, A.T., 2015. Bioelectrochemical systems for nitrogen removal and recovery from wastewater. *Environ. Sci.: Water Res. Technol.* 1, 22-33.
- Bond, D.R., Lovley, D.R., 2003. Electricity production by *Geobacter sulfurreducens* attached to electrodes. *Appl. Environ. Microbiol.* 69, 1548-1555.
- Bond, D.R. and Lovley, D.R., 2005. Evidence for involvement of an electron shuttle in electricity generation by *Geothrix fermentans*. *Appl. Environ. Microbiol.* 71, 2186-2189.
- Bond, D.R., Strycharz-Glaven, S.M., Tender, L.M., Torres, C.I., 2012. On electron transport through *Geobacter* biofilms. *ChemSusChem.* 5, 1099-1105.
- Bonmati, A., Flotats, X., 2003a. Air stripping of ammonia from pig slurry: characterization and feasibility as a pre- or post-treatment. *Waste Manag.* 23, 261-272.
- Bonmati, A., Flotats, X., 2003b. Pig slurry concentration by vacuum evaporation: influence of previous mesophilic anaerobic digestion process. *J. Air Waste Manag.* 53, 21-31.
- Borole, A.P., Reguera, G., Ringeisen, B., Wang, Z-W., Feng, Y., Kim, B.H., 2011. Electroactive biofilms: Current status and future research needs. *Energy Environ. Sci.* 4, 4813-4834.
- Burton, C.H., Turner, C., 2013. *Manure Management: Treatment Strategies for Sustainable Agriculture*. 2nd ed. Silsoe Research Institute, Wrest Park, Silsoe, Bedford, UK.
- Cao, X., Huang, X., Liang, P., Xiao, K., Zhou, Y., Zhang, X., Logan, B.E., 2009. A New Method for Water Desalination Using Microbial Desalination Cells. *Environ. Sci. Technol.* 43, 7148-7152.
- Cerrillo, M., Palatsi, J., Comas, J., Vicens, J., Bonmati, A., 2015. Struvite precipitation as a technology to be integrated in a manure anaerobic digestion treatment plant – removal efficiency, crystal characterization and agricultural assessment. *J. Chem. Technol. Biotechnol.* 90(6), 1135-1143.
- Clauwaert, P., Rabeay, K., Aelterman, P., De Schampelaire, L., Pham, T.H., Boeckx, P., Boon, N., Verstrate, W., 2007. Biological Denitrification in Microbial Fuel Cells. *Environ. Sci. Technol.* 41, 3354-3360.
- Chaudhuri, S.K., Lovley, D.R., 2003. Electricity generation by direct oxidation of glucose in mediatorless microbial fuel cells. *Nat. Biotechnol.* 21, 1229-1232.
- Choi, Y., Kim, N., Kim, S., Jung, S., 2003. Dynamics behaviors of redox mediators within the hydrophobic layers as an important factor for effective microbial fuel cell operation. *B. Kor. Chem. Soc.* 24, 437-440.
- Davis, J.B., Yarbrough, H.F., 1962. Preliminary experiments on a microbial fuel cell. *Science.* 137, 615-616.
- Desloover, J., Woldeyohannis, A.A., Vestraete, W., Boon, N., Rabaey, K., 2012. Electrochemical resource recovery from digestate to prevent ammonia toxicity during anaerobic digestion. *Environ. Sci. Technol.* 46(21), 12209-12216.

- Du, Z., Li, H. Gu, T., 2007. A state of the art review on microbial fuel cells: a promising technology for wastewater treatment and bioenergy. *Biotechnol. Adv.* 25, 464-482.
- Franks, A.E., Malvankar N., Nevin, K.P., 2010. Bacterial biofilms: the powerhouse of a microbial fuel cell. *Biofuels*. 1, 589-604.
- Flexer, V., Marque, M., Donose, B.C., Virdis, B., Keller, J., 2013. Plasma treatment of electrodes significantly enhances the development of anodic electrochemically active biofilms. *Electrochim. Acta*. 108, 566-574.
- Freguia, S., Masuda, M., Tsujimura, S., Kano, K., 2009. *Lactococcus lactis* catalyses electricity generation at microbial fuel cell anodes via excretion of a soluble quinone. *Bioelectrochem.* 76, 14-18.
- Gerritse, J., Saakes, M., Stams, A., Johannes, M., 2004. Biofuel cell for processing organic waste in an environmentally friendly manner. Patent. (Nederlandse Organisatie voor Toegepast – Natuurwetenschappelijk Onderzoek TNO, The Netherlands). PCT Int.
- Ghafari, S., Hasan, M., Aroua, M.K., 2008. Bio-electrochemical removal of nitrate from water and wastewater – A review. *Biores. Technol.* 99(10), 365-3974.
- Goldbeck, C.P., Jensen, H.M., TerAvest, M.A., Beedle, N., Appling, Y., Hepler, M., Cambray, G., Mutalik, V., Angenent, L.T., Ajo-Franklin, C.M., 2013. Turning promoter strengths for improved synthesis and function of electron conduits in *Escherichia coli*. *ACS Synth. Biol.* 2, 150-159.
- Gorby, Y.A., Yanina, S., McLean, J.S., Rosso, K.M., Moyles, D., Dohnalkova, A., Beveridge, T.J., Chang, I.S., Kim, B.H., Kim, K.S., Culley, D.E., Reed, S.B., Romine, M.F., Saffarini, D.A., Hill, E.A., Shi, L., Elias, D.A., Kennedy, D.W., Pinchuk, G., Watanabe, K., Ishii, S., Logan, B., Nealson, K.H., Fredrickson, J.K., 2006. Electrically conductive bacterial nanowires produced by *Shewanella oneidensis* strain MR-1 and other microorganisms. *Proc. Natl. Acad. Sci.* 103(30), 11358-11363.
- Gregory, K.B., Bond, D.R., Lovley, D.R., 2004. Graphite electrodes as electron donors for anaerobic respiration. *Enviro. Microbiol.* 6(6), 596-604.
- Habermann, W., Pommer, E.H., 1991. Biological fuel cells with sulphide storage capacity. *Appl. Microbiol. Biotechnol.* 35, 128-133.
- He, Z., Minteer, S.D., Angenent, L.T., 2005. Electricity generation from artificial wastewater using an upflow microbial fuel cell. *Environ. Sci. Technol.* 39, 5262-5267.
- Heidrich, E.S., Dolfig, J., Scott, K., Edwards, S.R., Jones, C., Curtis, T.P., 2013. Production of hydrogen from domestic wastewater in a pilot-scale microbial electrolysis cell. *Appl. Microbiol. Biotechnol.* 97, 6979-6989.
- Holmes, D.E., Chaudhuri, S.K., Nevin, K.P., Metha, T., Methe, B.A., Liu, A., Ward, J.E., Woodard, T.L., Webster, J., Lovley, D.R., 2006. Microarray and genetic analysis of electron transfer to electrodes in *Geobacter sulfurreducens*. *Environ. Microbiol.* 8(10), 1805-1815.
- Ieropoulos, I.A., Greenman, J., Melhuish, C., Hart, J., 2005. Comparative study of three types of microbial fuel cell. *Enzyme Microb. Technol.* 37, 238-245.
- Kim, B.H., Kim, H.J., Hyun, M.S., Park, D.H., 1999. Direct electron reaction of Fe(III)-reducing bacterium, *Shewanella putrifaciens*. *J. Microbiol. Biotechnol.* 9, 127-131.

- Kim, H.J., Park, H.S., Hyun, M.S., Chang, I.S., Kim, M., Kim, B.H., 2002. A mediator-less microbial fuel cell using a metal reducing bacterium, *Shewanella putrefaciens*. *Enzyme Microb. Technol.* 30(2), 145-152.
- Kim, J.R., Cheng, S., Oh, S.E., Logan, B.E., 2007. Power generation using different cation, anion, and ultrafiltration membranes in microbial fuel cells. *Environ. Sci. Technol.* 4, 1004-1009.
- Kim, J.R., Zuo, Y., Regan, J.M., Logan, B.E., 2008. Analysis of ammonia loss mechanisms in microbial fuel cells treating animal wastewater. *Biotechnol. Bioeng.* 99, 1120-1127.
- Kumar, A., Katuri, K., Lens, P., Leech, D., 2012. Does bioelectrochemical cell configuration and anode potential affect biofilm response?. *Biochem. Soc. Trans.* 40(6), 1308-1314.
- Kuntke, P., Geleji, M., Bruning, H., Zeeman, G., Hamelers, H.V.M. Buisman, C.J.N., 2011. Effects of ammonium concentration and charge exchange on ammonium recovery from high strength wastewater using a microbial fuel cell. *Bioresour. Technol.* 102, 4376-4382.
- Kuntke, P., Smiech, K.M., Bruning, H., Zeeman, G., Saakes, M., Sleutels, T.H., Hamelers, H.V., Buisman C.J., 2012. Ammonium recovery and energy production from urine by a microbial fuel cell. *Water Res.* 46(8), 2627-2635.
- Laureni, M., Palatsi, J., Llovera, M., Bonmati, A., 2013. Influence of pig slurry characteristics on ammonia stripping efficiencies and quality of the recovered ammonium-sulfate solution. *J. Chem. Technol. Biotechnol.* 88(9), 1654-1662.
- Liang, P., Wei, J., Li, M. Huang, X., 2013. Scaling up a novel denitrifying microbial fuel cell with an oxic-anoxic two stage biocathode. *Front. Environ. Sci. Eng.* 7(6), 913-919.
- Liu, H., Grof, S., Logan, B.E., 2005a. Electrochemically assisted microbial production of hydrogen from acetate. *Environ. Sci. Technol.* 39, 4317-4320.
- Liu, H., Cheng, S., Logan, B.E., 2005. Production of electricity from acetate or butyrate using a single-chamber microbial fuel cell. *Environ. Sci. Technol.* 39, 658-662.
- Liu, M., Yuan, Y., Zhang, L., Zhuang, L., Zhou, S. Ni, J., 2010. Bioelectricity generation by a Gram-positive *Corynebacterium* sp. strain MFC03 under alkaline condition in microbial fuel cells. *Bioresour. Technol.* 101, 1807-1811.
- Logan, B.E., Regan, J.M., 2006a. Microbial fuel cells – challenges and applications. *Environ. Sci. Technol.* 40, 5172-5180.
- Logan, B.E., Hamelers, B., Rozendal, R., Schröder, U., Keller, J., Freguia, S., Aelterman, P., Verstraete, W., Rabaey, K., 2006b. Microbial fuel cells: Methodology and technology. *Environ. Sci. Technol.* 40(17), 5181-5192.
- Lovley, D.R., Holmes, D.E., Nevin, K.P., 2004. Dissimilatory Fe(III) and Mn(IV) reduction. *Adv. Microb. Physiol.* 49, 219-286.
- Lu, N., Zhou, S.G., Zhuang, L., Zhanga, J.T., Ni, J.R., 2009. Electricity generation from starch wastewater using microbial fuel cell technology. *Biochem. Eng. J.* 43, 246-251.
- Malvankar, N.S., Vargas, M., Nevin, K.p., Franks, A.E., Leang, C., Kim, B.C., Inoue, K., Mester, T., Covalla, S.F., Johnson, J.P., Rotello, V.M., Tuominen, M.T., Lovley, D.R., 2011. Tunable metallic-like conductivity in microbial nanowire networks. *Nat. Nanotechnol.* 6, 573-579.

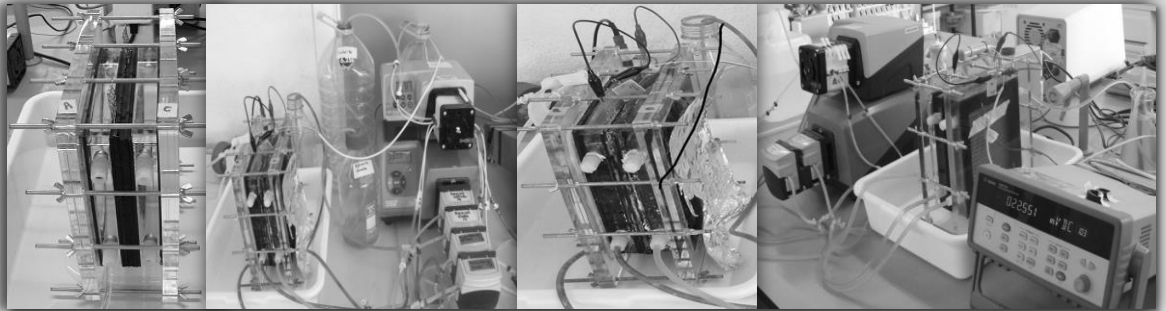
- Marsili, E., Baron, D.B., Shikhae, I.D., Coursolle, D., Gralnick, J.A., Bond, D.R., 2008. Shewanella secretes flavins that mediate extracellular electron transfer. *Proc. Natl. Acad. Sci. USA.* 105, 3968-3973.
- Milliken, C.E., May, H.D., 2007. Sustained generation of electricity by the spore-forming, Gram-positive, *Desulfitobacterium hafniense* strain DCB2. *Appl. Microbiol. Biotechnol.* 73, 1180-1189.
- Min, B., Cheng, S., Longan B.E., 2005. Electricity generation using membrane and salt bridge microbial fuel cells. *Water Res.* 39, 1675-1686.
- Mu, Y., Rozendal, R.A., Rabaey, K., Keller, J., 2009. Nitrobenzene removal in bioelectrochemical systems. *Environ. Sci. Technol.* 43, 8690-8695.
- Nealson, K.H., Saffarini, D.A., 1994. Iron and Manganese in Anaerobic Respiration: Environmental Significance, Physiology, and Regulation. *Annu. Rev. Microbiol.* 48, 311-343.
- Nevin, K.P., Hensley, S.A., Franks, A.E., Summers, Z.M., Ou, J.H., Woodard, T.L., Snoeyenbos-West O.L., Lovley, D.R., 2011. Electrosynthesis of organic compounds from carbon dioxide catalyzed by a diversity of acetogenic microorganisms. *Appl. Environ. Microbiol.* 77, 2882-2886.
- Nguyen, T.T., Luong, T.T., Tran, P.H., Bui, H.T., Nguyen, H.Q., Dinh, H.T., Kim, B.H., Pham, H.T., 2015. A lithotrophic microbial fuel cell operated with pseudomonads-dominated iron-oxidizing bacteria enriched at the anode. *Microb. Biotechnol.* DOI: 10.1111/1751-7915.12267.
- Park, D.H., Zeikus, J.G., 2000. Electricity generation in microbial fuel cells using neutral red as an electronophore. *Appl. Environ. Microbiol.* 66, 1292-1297.
- Park, H.S., Kim, B.H., Kim, H.S., Kim, H.I., Kim, G.T., Kim, M., Chang, I.S., Park, Y.K., Chang, H.I., 2001. A novel electrochemically active and Fe(III)-reducing bacterium phylogenetically related to *Clostridium butyricum* isolated from a microbial cell. *Anaerobe.* 7, 297.
- Park, D.H., Zeikus, J.G., 1999. Utilization of electrically reduced neutral red by *Actinobacillus succinogenes*: physiological function of neutral red in membrane-driven fumarate reduction and energy conservation. *J. Bacteriol.* 181, 2403-2410.
- Park, D.H., Zeikus, J.G., 2003. Improved fuel cell and electrode designs for producing electricity from microbial degradation. *Biotechnol. Bioenerg.* 81, 348-355.
- Potter, M.C., 1911. Electrical effects accompanying the decomposition of organic compounds. *Proc. R. Soc. Lond. B. Biol. Sci.* 84, 260-276.
- Puig, S., Coma, Desloover, J., Boon, N., Colprim, J., Balaguer, M.D., 2012. Autotrophic denitrification in microbial fuel cells treating low ionic strength waters. *Environ. Sci. Technol.* 46, 2309-2315.
- Pham, C.A., Jung, S.J., Phung, N.T., Lee, J., Chang, I.S., Kim, B.H., Yi, H., Chun, J., 2003. A novel electrochemically active and Fe(III)-reducing bacterium phylogenetically related to *Aeromonas hydrophila*, isolated from a microbial fuel cell. *FEMS Microbiol. Lett.* 223, 129-134
- Rabaey, K., Lissens, G., Siciliano, S.D., Verstraete, W., 2003. A microbial fuel cell capable of converting glucose to electricity at high rate and efficiency. *Biotechnol. Lett.* 25(18), 1531-1535.

- Rabaey, K., Boon, N., Siciliano, S.D., Verhaege, M., Verstraete, W., 2004. Biofuel cells select for microbial consortia that self-mediate electron transfer. *Appl. Environ. Microbiol.* 70, 5373-5382.
- Rabaey K., Verstrate, W., 2005. Microbial fuel cells: novel biotechnology for energy generation. *Trends in Biotechnology.* 23, 291-298.
- Rabaey, K., Boon, N., Hofte, M., Verstraete, W., 2005. Microbial phenazine production enhances electron transfer in biofuel cells. *Environ. Sci. Technol.* 39, 3401-3408.
- Reguera, G., Nevin, K.P., Nicoll J.S., Covalla, S.F., Woodard, T.L., Lovley, D.R., 2006. Biofilm and nanowire production leads to increased current in *Geobacter sulfurreducens* fuel cells. *Appl. Environ. Microbiol.* 72, 7345-7348.
- Ringeisen, B.R., Henderson, E., Wu, P.K., Pietron, J., Ray, R., Little, B., Biffinger, J.C., Jones-Meehan, J.M., 2006. High power density from a miniature microbial fuel cell using *Shewanella oneidensis* DSP10. *Environ. Sci. Technol.* 40, 2629-2634.
- Rozendal, R.A., Hamelers, H.V., Rabaey, K., Keller, J., Buisman, C.J., 2008a. Towards practical implementation of bioelectrochemical wastewater treatment. *Trends Biotechnol.* 26(8), 450-459.
- Rozendal, R.A., Sleutels, T., Hamelers, H.V.M., Buisman, C.J.N., 2008b. Effect of the type of ion exchange membrane on performance, ion transport, and pH in biocatalyzed electrolysis of wastewater. *Water Sci. Technol.* 57, 1757-1762.
- Strycharz-Glaven, S.M., Snider, R.M., Guiseppi-Eliec, A., M.Tender, L., 2011. On the electrical conductivity of microbial nanowires and biofilms. *Energy Environ. Sci.* 4, 4366-4379.
- Tang, X., Guo, K., Li, H, Du, Z., Tian, J., 2011. Electrochemical treatment of graphite to enhance electron transfer from bacteria to electrodes. *Bioresour. Technol.* 102(3), 3558-3560.
- Tender, L.M., Reimers, C.E., Stecher, H.A., Holmes, D.E., Bond, D.R., Lowy, D.A., Pilobello, K, Fertig, S.J., Lovley, D.R., 2000. Harnessing microbially generated power on the seafloor. *Nat. Biotechnol.* 20, 821-825.
- Torres, C.I., Marcus, A.K., Rittmann, B.E., 2008. Proton transport inside the biofilm limits electrical current generation by anode-respiring bacteria. *Biotechnol. Bioenergy.* 100, 872-881.
- Thurston, C.F., Bennetto, H.P., Delaney, G.M., Mason, J.R., Roller, S.D., Stirling, J.L., 1985. Glucose metabolism in a microbial fuel cell. Stoichiometry of product formation in a thionine-mediated *Proteus vulgaris* fuel cell and its relation to Coulombic yields. *J. Gen. Microbiol.* 131, 1393-1401.
- Villano, M., Scardala, S., Aulenta, F., Majone, M., 2013. Carbon and nitrogen removal and enhanced methane production in a microbial electrolysis cell. *Bioresour. Technol.* 130, 366-371.
- Viridis, B., Rabaey, K., Rozendal, R.A., Yuan, Z., Keller, J., 2010. Simultaneous nitrification, denitrification and carbon removal in microbial fuel cells. *Water Res.* 44, 2970-2980.
- Viridis, B., Rabaey, K., Yuan, Z., Keller, J., 2008. Microbial fuel cells for simultaneous carbon and nitrogen removal. *Water Res.* 42, 3013-3024.

- Viridis, B., Read, S.T., Rabaey, K., Rozendal, R.A., Yuan, Z., Keller J., 2011. Biofilm stratification during simultaneous nitrification and denitrification (SND) at a biocathode. *Bioresour. Technol.* 102, 334-341.
- Wang, H., Ren, Z.J., 2013. A comprehensive review of microbial electrochemical systems as a platform technology. *Biotechnol. Advan.* 31, 1796-1807.
- Wu, X., Modin, O., 2013. Ammonium recovery from reject waster combined with hydrogen production in a bioelectrochemical reactor. *Bioresour. Technol.* 146, 530-536.
- Xie, S., Liang, P., Chen, Y., Xia, X., Huang, X., 2011. Simultaneous carbon and nitrogen removal using an oxic/anoxic-biocathode microbial fuel cells coupled system. *Bioresour. Technol.* 102, 348-354.
- Zhang, F., Ge, Z., Grimaud, J., Hurst, J., He, Z., 2013. Long-term performance of liter-scale microbial fuel cells installed in a municipal wastewater treatment facility. *Environ. Sci. Technol.* 47, 4941-4948.
- Zhang, F., He, Z., 2012a. Integrated organic and nitrogen removal with electricity generation in a tubular dual-cathode microbial fuel cell. *Process Biotechnol.* 47, 2146-2151.
- Zhang, F., He, Z., 2012b. Simultaneous nitrification and denitrification with electricity generation in dual-cathode microbial fuel cells. *J. Chem. Technol. Biotechnol.* 87, 153-159.
- Zaybak, Z., Pisciotta, J.M., Tokash, J.C., Logan, B.E., 2013. Enhanced start-up of anaerobic facultatively autotrophic biocathodes in bioelectrochemical systems. *J. Biotechnol.* 168(4), 478-485.

Chapter 2

Objectives and Thesis outline



The objectives of the thesis, the research chronology and the thesis outline are presented.

2.1. Objectives

The general objective of the present PhD thesis is to study nitrogen removal/recovery strategies in a bioelectrochemical system (BES) fed with high strength animal wastewater, such as pig slurries, and to study the selective enrichment of microbial populations in the anode. To achieve that goal, the following specific objectives have been set (**Figure 2.1**):

1. To assess the effect of different membrane materials and microbial inocula in the performance of two-chambered MFCs (10 mL/chamber), in order to select the inoculum and the materials to scale up to the two-chambered MFCs (~250mL/chamber) (**Chapters 4 and 5**).
2. To assess the diversity and dynamics of the microbial community on the biofilms attached onto the anode of the MFCs (~250mL/chamber) using different feeding substrates (synthetic wastewater and the liquid fraction of pig slurry) and under different operational conditions (**Chapter 6**).
3. To investigate nitrogen diffusion and migration from the anode to the cathode, of a two-chambered MFC (**Chapter 7**).
4. To develop a physicochemical strategy to recover the nitrogen migrated to the cathode chamber (**Chapter 7**).
5. To work out a biological strategy to remove the nitrogen migrated to the cathode chamber (**Chapter 8**).

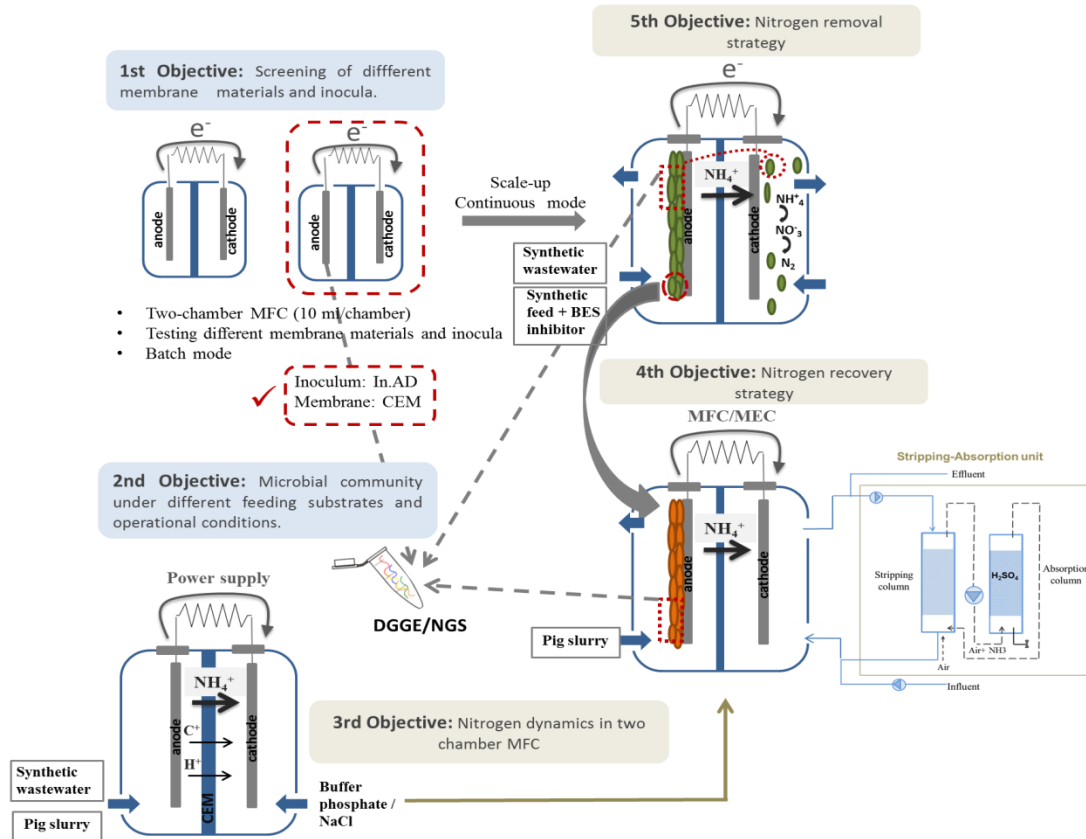


Figure 2.1. Graphical abstract of the main goals proposed for this thesis.

2.2. Research chronology and scope

The activities of this PhD thesis were carried out within the framework of Spanish Ministry of Science and Innovation projects (MICINN project CTM2009-12632 and INIA project RTA2012-00096-00-00). Development of the research work started at GIRO CT (Integral management of organic waste, Technological Centre) and later on at IRTA in GIRO, Joint Research Unit IRTA-UPC group, within the context of the doctoral program on "Environmental Engineering" at Universitat Politècnica de Catalunya, Barcelona TECH (UPC), and under the supervision of Dr. August Bonmatí Blasi and Dr. Marc Viñas Canals.

Anaerobic digestion (AD) of organic wastes, co-digestion, mathematical modelling of the AD process, together with nitrification and denitrification processes of pig slurries are the principal research lines of the GIRO group. This PhD Thesis has opened a new research line, aiming to develop a MFC/BES technology for the treatment of high strength wastewater, such as pig slurries, focusing in electricity production from organic matter and its simultaneous nitrogen reduction.

In the context of the present PhD Thesis, I had also the privilege to gain an internship during two months in the Laboratory of Microbial Ecology and Technology (LabMET) (Ghent, Belgium 08/2012 – 09/2012), under the supervision of Prof. Korneel Rabaey. This stay was financed by a Ministry of Education (ECD/3628/2011) Grant program. This group of research is globally renowned as a pioneer in bioelectrochemical systems, and has nowadays several active projects in the scope of microbial electrocatalysis. I had also the possibility to enjoy a second research stay at the University of Queensland's Advanced Water Management Centre (AWMC) (Brisbane, Australia, 09/2013 – 02/2014), under the supervision of Dr. Stefano Freguia. This Centre is renowned internationally for its excellent and innovative water technologies and management techniques; the field of bioelectrochemical systems being one of its most outstanding research lines. This stay lasted 6 months and was financially supported by AGAUR (Government of Catalonia) within the framework of is Grants for Research Stay Abroad program (BE-DGR 2012) ECO/1225/2012.

The present PhD thesis is the first one to be completed in this line of research of bioelectrochemical systems at GIRO, Joint research unit IRTA-UPC.

2.3. Thesis outline

The main scope of the present dissertation is to characterize nitrogen fate and electrochemical performance in bioelectrochemical systems fed with high strength animal wastewater (synthetic media and pig slurry). Moreover, the microbial community harboured in these BESs has also been studied.

This PhD thesis is divided into nine chapters.

Chapter 1: General introduction

This chapter provides a general introduction regarding the main topics of the Thesis. Firstly, a literature review of the background and state of the art of bioelectrochemical system developments is provided. Secondly, basic concepts of this technology, and a summary of the microbial ecology of anodic microbial communities described so far, and the application of this technology on nitrogen removal/recovery strategies, are presented.

Chapter 2: Objectives and thesis outline

Objectives of the present study, research chronology and scope of the thesis, and the outline of the thesis, are presented in this chapter.

Chapter 3: Materials and Methods

The configuration of bioelectrochemical systems as well as its operational conditions, and the analytical, electrochemical and molecular biology techniques used to perform the experiments are described in detail in this chapter.

Chapter 4: Screening of different inocula to start-up a microbial fuel cell

In this chapter, small sized two-chambered MFCs were used to test microbial inocula from different origins using cation exchange membranes (CEM), assessing their effects over its general performance, and over microbial community changes upon the anodic chamber.

Chapter 5: Microbial community dynamics in two-chambered microbial fuel cells: effect of different ion exchange membranes

Similarly to chapter 4, the effect of three different membrane materials was evaluated in small sized two-chambered MFCs. The inoculum used was the one showing the best results in Chapter 4.

Based on the results obtained in these two previous chapters, a particular type of membrane and inoculum was selected to build up a medium sized two-chambered MFC in order to accomplish the following purposes of the thesis.

Chapter 6: Microbial community dynamics in continuous microbial fuel cells fed with synthetic wastewater and pig slurry.

In this chapter, microbial community dynamics together with their anodic biofilm composition in a MFC fed with synthetic wastewater and fed with pig slurry was studied. Additionally, in the present chapter, the effect of 2-Bromo etano sulphonate (BES-Inh.) as methanogenic inhibitor for the entire microbial community (Eubacteria and Archaea) was also studied.

Chapter 7: Nitrogen recovery from pig slurry in two-chambered bioelectrochemical system

In this chapter, preliminary batch experiments using both synthetic wastewater and the liquid fraction of pig slurry, testing with different voltages applied were carried out. In a second stage, the feasibility of nitrogen recovery using a stripping unit coupled to the cathode compartment of a two-chambered BES was studied. Finally, the microbial community attached onto the anode electrode, both under MFC and MEC modes was assessed.

Chapter 8: Nitrogen removal in a two-chambered microbial fuel cell- Establishment of a nitrifying-denitrifying microbial community on an intermittent aerated cathode

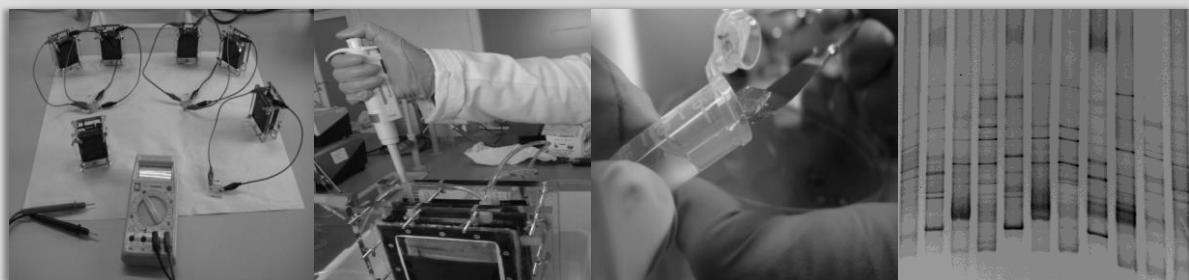
The purpose of this chapter was to enhance the nitrification-denitrification process at the cathode chamber of a BES, and its feasibility for processing high strength wastewaters. These experiments were carried out in a MFC harbouring current-producing microbial biomass both in the anode and cathode chambers.

Chapter 9: General conclusions and suggestions for further research

The general conclusions of this work are compiled in this last chapter. Furthermore, some recommendations for further investigations in this research topic are proposed.

Chapter 3

Materials and Methods



This chapter details the experimental set-ups used for the experiments carry out in this thesis. The adopted multidisciplinary methodological approach for the analysis of the experimental data is also described. This was based such on the analytical and electrochemical characterization for the MFCs performances, and on the characterization of the microbial communities by means of molecular biology approaches.

3.1. Reactors designs

This section describes the materials used and the experimental set-up for all the experiments performed. The operational conditions and experimental procedures adopted in each experiment are described in detail in each chapter.

3.1.1. Small scale two-chambered MFC

Two Plexiglas flat plates (88 × 65 mm) (NCBE, University of Reading, UK) were bolted together forming both compartments 10 mL each (anode and cathode), and rubber sheet were inserted between each of the frames to ensure sealing (**Figure 3.1a and b**) (**Chapters 4 and 5**). An ion exchange membrane (IEM) was placed between both compartments. Electrodes (anode and cathode) were made of fibre tissue joined to graphite rod to facilitate connection between copper wire and the external resistance (1000 Ω) (**Figure 3.1b and Figure 3.2**).

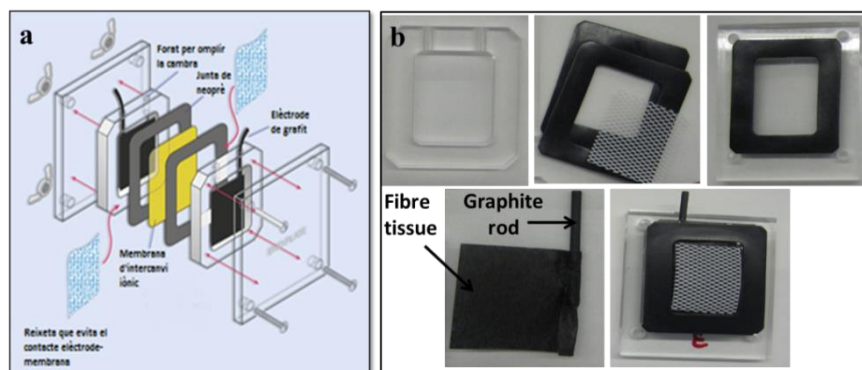


Figure 3.1. **a)** MFC schematic overview of all reactor components, and **b)** materials used in the construction of the MFC (Plexiglas frame, rubber and the electrodes).

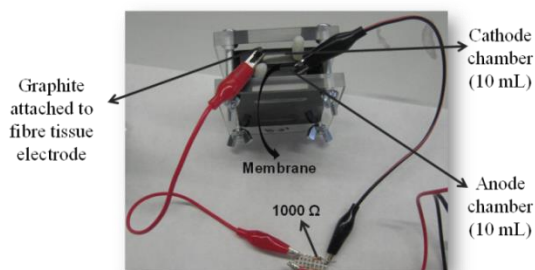


Figure 3.2. Picture of the MFCs (10 mL/chamber).

Three different IEM materials were used: Nafion N-117 (DuPont Co., Wilmington, DE, USA) as PEM, Ultrex CMI-7000 (Membranes International Inc., Ringwood, NJ, USA)

as CEM; and Ultrex AMI-7000 (Membranes International Inc.), with a surface area exposed of 12 cm² to either compartment.

Experiments were carried out per duplicate (**Figure 3.3**) and performed at room temperature (23°C±2).

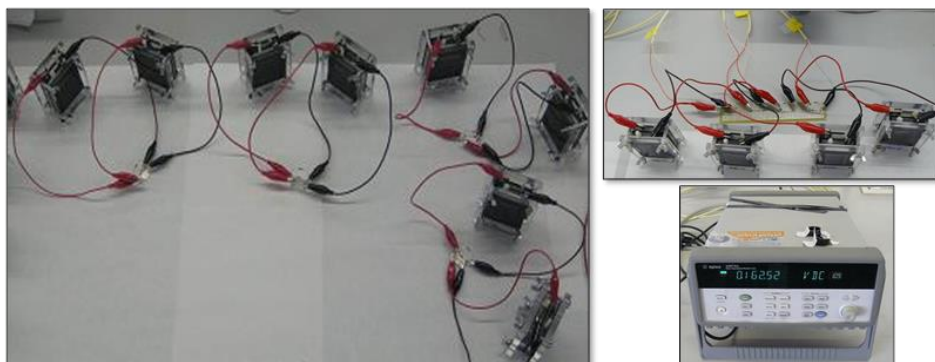


Figure 3.3. Small two-chambered MFCs experimental set-up and data acquisition unit (Mod. 34970A, Agilent Technologies, Loveland, CO, USA) used for recording the voltage.

3.1.2. Medium scale two-chambered MFC

A second type of MFC was used in this thesis (**Chapters 6, 7 and 8**). Materials used and configuration was similar to the small scale MFC.

Methacrylate plates and frames were used with internal dimensions of 0.14 x 0.12 x 0.02 m³ (**Figure 3.4**). A cation exchange membrane (CEM) (14x12 cm) (Ultrex CMI-7000, Membranes International Inc., Ringwood, NJ, USA) was used for all the experiments carried out in medium scale MFC. Two different anode electrodes were used: granular graphite with a diameter ranging from 2 to 6 mm (El Carb 100, Graphite Sales, Inc., U.S.) (MFC fed with synthetic medium), and Carbon felt, 3.18 mm thick, 99.0% (Cymit Química, S.L.) (MFC fed with liquid fraction of pig slurry). As cathode electrode stainless mesh were employed. Copper wires were used to connect the electrodes to an external resistance ranged between 100 – 1000 Ω.

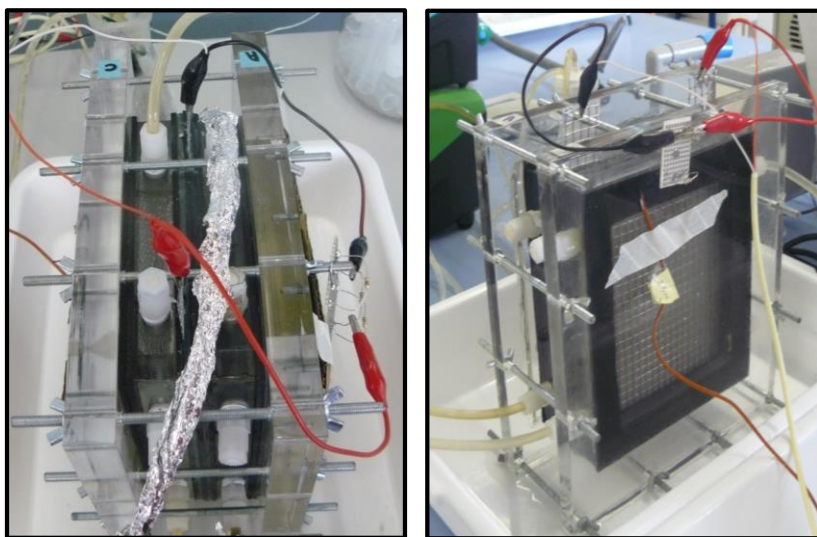


Figure 3.4. A picture of one of the MFC from different perspectives.

3.1.3. Stripping-BES system

A stripping-absorption unit was used in the stripping experiments with liquid fraction of pig slurry (**Chapter 7**). The BES system was the two-chambered MFC unit described previously (operating with pig slurry and using carbon felt as anode electrode), in which a stripping-absorption unit was coupled to the cathode chamber, following a modified model based on the previously one reported by Desloover et al., 2012 (**Figure 3.5**). BES system was operated under MFC and MEC mode during these experiments, and the operational conditions are described further in **Chapter 7**.

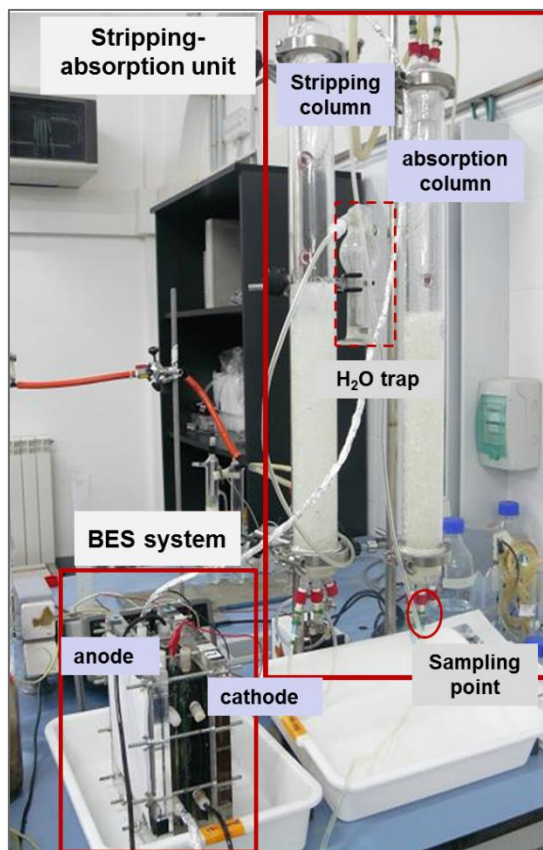


Figure 3.5. Picture of the experimental set-up with the stripping-absorption unit coupled to the cathode chamber.

3.2. Influent and inocula

The media (influent) and the inocula used varied depending on the experiment performed. Thus, the media and inocula are described below for each experiment:

3.2.1. Experiments performed with the small scale/batch two-chambered MFC

3.2.1.1. Influent

Synthetic wastewater

The anodic chamber was filled with 8 mL of a mineral medium previously autoclaved (120°C , 21 minutes), 1 mL of inoculum, and 1 mL of a sodium acetate solution (2.95 g L⁻¹) being the final acetate concentration in the anodic chamber of 0.1 M. The mineral medium was prepared according to Kennes et al., 1996,

containing (per liter of distilled water): 4.5 g KH_2PO_4 , 0.5 g K_2HPO_4 , 2 g NH_4Cl , 0.1 g $\text{MgSO}_4 \cdot 7\text{H}_2\text{O}$, 1 mL of a trace mineral solution and 1 mL of a vitamin solution. The cathodic chamber was filled up with 10 mL of a chemical solution containing (per litre): 16.5 g $\text{K}_3\text{Fe}(\text{CN})_6$ as final electron acceptor and 4.5 g KH_2PO_4 + 0.5 g K_2HPO_4 as phosphate buffer (**Chapters 4 and 5**).

3.2.1.2. Inocula

The MFC anodic chamber was inoculated with different inocula depending on the experiment carried out. For the experiments carried out in **Chapter 4**, 1 mL of inocula from the three different sources were used, i) inoculum from constructed wetlands working with urban wastewater, ii) inoculum from a two-chambered MFC operating with cow manure, and iii) inoculum from a bench-scale mesophilic methanogenic reactor fed with slaughterhouse waste. This third inoculum was used for all the experiments carried out in **Chapter 5**.

3.2.2. Experiments with the medium scale/continuous two-chambered MFC

3.2.2.1. Influent

Synthetic wastewater

The anode compartment, used for the experiments in **Chapters 6 and 7**, was fed with autoclaved growth medium containing (per liter of tap water): CaCl_2 , 0.0147 g; KH_2PO_4 , 3 g; Na_2HPO_4 , 6 g; MgSO_4 , 0.246 g; and 1 mL L^{-1} trace elements solution as described in Lu et al. (2006). Additionally, CH_3COONa was added as carbon source, ranged between 0.46 – 2.91 g L^{-1} , and NH_4Cl was added as a nitrogen source, ranged between 0.26 – 3.82 g L^{-1} , depending on the experimental set-up. Particular feeding conditions are described in more detail in each corresponding chapter. The solution to the cathode chamber contained KH_2PO_4 , 3 g L^{-1} and Na_2HPO_4 , 6 g L^{-1} .

Methanogenesis inhibitor

2- bromoethanesulfonate (BES-Inh.) was used as inhibitor to study its effect on MFC performance (**Chapter 6**). Concentration ranged between 0.16 mM and 10 mM as it was defined in He et al., 2005; Chae et al., 2010 and Zhuang et al., 2012.

Inoculation with mesophilic methanogenic biomass from reactor fed with slaughterhouse waste was used for the small scale MFCs, and it was also used for the two-chambered MFC fed with synthetic medium.

Pig slurry

The liquid fraction of pig slurry used as feed for the experiments carried out in **Chapters 6** and **7**, was collected from the pig farm Caseta d'en Grau (Calldetenes, Catalonia) and it was centrifuged before using (4991 g during 10 minutes) (**Figure 3.6**). The composition was the following: pH, 7.72; COD_t (mg O₂ Kg⁻¹), 6908; COD_s (mg O₂ Kg⁻¹), 3462; N-NH₄⁺ (mg N-NH₄⁺- N L⁻¹), 858.15; Kjeldahl-N (mg N L⁻¹), 1068.47; TSS (%), 0.78; VSS (%), 0.42 and conductivity (mS cm⁻¹), 7.73. In order to procure the desired concentrations for the different assays, specific dilutions were carried out and are explained in more detail in the corresponding chapter (**Chapter 6** and **7**). The cathode feed consisted of either buffer phosphate (KH₂PO₄, 3 g L⁻¹ and Na₂HPO₄ 6 g L⁻¹) or sodium chloride (NaCl, 0.1 g L⁻¹), depending on the experiment performed.



Figure 3.6. Liquid fraction of pig slurry sampling at the Sat Caseta d'en Grau farm (Calldetenes, Catalonia).

The MFC fed with liquid fraction of pig slurry was inoculated with the biofilm of the MFC fed with synthetic medium after one year of operation. **Figure 3.7** shows the procedure of sampling the biofilm from synthetic fed MFC.

MFC fed with synthetic medium**MFC fed with liquid fraction of pig slurry**

Figure 3.7. Biofilm sampling from the MFC fed with synthetic medium. The graphite granules sample was taken from the anode to inoculate anode material/chamber in MFC fed with liquid fraction of pig slurry.

3.3. Analytical techniques

3.3.1. pH measurement

The pH from bulk solution (anode and cathode) was tested in each experiment using a pH electrode CRISON 2000.

3.3.2. Total and volatile solids

The total and volatile solids (TS, VS) were determined according to standard methods (APHA, AWA, WEF, 2005). A well homogenized sample is dried in a muffle at 105°C during 24-48 hours till constant weight, obtaining the total solids (TS). TS content is expressed as follows:

(Equation 3.1)

$$TS(\%) = 100 - \frac{W_w - W_d}{W_w - T} \cdot 100$$

Then the sample is placed in the muffle at 550°C and is weighed. The weight difference between the TS and the ashes is the volatile solids (VS) content, and is calculated using the following equation:

$$\text{(Equation 3.2)} \quad VS(\%) = \frac{W_d - W_a}{W_d - T} \cdot 100$$

Where, W_d denotes sample dry weight (g), W_w denotes sample's wet weight (g), W_a denotes sample's ashes weight (g), and T is the weight of the capsule used to contain the sample (g).

3.3.3. Chemical Oxygen Demand

Chemical oxygen demand (COD) was analyzed by oxidation with 1.5 mL of digestion reagent (potassium dichromate, 0.5 N, mercury sulfate and sulfuric acid 95-97%) and 1.5 mL of catalyst (silver sulfate 1%, and sulfuric acid 95-97%) and is digested at 150°C for 2 h in a digester (Hach Lange LT 200), according to an optimized method APHA-AWWA-WPCF Standard Method 5220 (Noguero et al., 2012). The change in dichromate concentration was measured colorimetrically (spectrophotometer Hach Lange DR 2800). For the soluble COD measurement the samples were previously filtered through a 0.45 µm pore diameter Nylon syringe filter (Scharlau, S.L.).

3.3.4. Ammonium nitrogen

Ammonium nitrogen ($N-NH_4^+$) was determined according to standard methods (APHA, AWA, WEF, 2005) and analysed by Büchi B-324 distiller, and autotitrator Metrohm 702 SM. This analysis is based on the transformation of ammonium ion (NH_4^+) into ammonia (NH_3), when a base as sodium hydroxide (NaOH) is present. The ammonia (NH_3) is distilled and is recovered again as ammonium (NH_4^+), in a known volume of boric acid (known concentration), obtaining ammonium borate, and this process allows quantifying the ammonium in the initial sample following the Equation 3.3:

$$\text{(Equation 3.3)} \quad N - NH_4 \text{ (mg} \cdot KgWw) = \frac{(V1 - V0) \cdot 1000 \cdot N \cdot 14 \cdot D}{Ww}$$

where, V_1 is HCl consumed volume in sample titration (mL), V_0 is HCl consumed volume in control titration (mL), N is the normality of the HCl, D denotes dilution factor (volume of extraction solution/volume of sample distilled), and W_w is sample wet weight (g).

3.3.5. Total Kjeldahl nitrogen

The organic nitrogen's content expressed as total Kjeldahl nitrogen (NKT) was determined according to standard methods (APHA, AWA, WEF, 2005), using 0.25 – 0.50 g dried and milled sample. The sample was digested at 150°C - 30', 250°C - 10', or 360°C - 240' using 10 mL of H₂SO₄ (96%) per 0.5 g of sample, in a 300 mL glass Kjeldahl tubes using a block digester Büchi K-437. Before the the acid digestion, a catalyst (Kjeltab®) was added. After the acid digestion, a Büchi Distillation Unit B-324 was used for sample distillation with an excess of NaOH solution (35%). The condensate was collected in a glass flask containing 100 mL of boric acid (4%). The solution was titrated with HCl to determine nitrogen's content. TKN was calculated using Equation 3.4:

$$\text{(Equation 3.4)} \quad TKN(\%) = \frac{(V_1 - V_0) \cdot N \cdot 1.4}{W_{db}}$$

where, V_1 is volume of HCl consumed (mL) in sample titration, V_0 is volume of HCl consumed (mL) in control titration, N is the normality of the HCl used in determination, and W_{db} is sample weight in dry basis (g).

3.3.6. Anions and cations measurements

Anions and cations concentration were quantified in liquid samples by ion chromatography (Metrohm 861 Advanced Compact IC), using a Metrohm Metrosep A Supp 4 column and pre-column Metrosep A Supp 4/5 Guard. The eluent for cations samples consisted of: 4 mmol C₄H₆O₆/L (tartaric acid) and 0.75 mmol pyridine-2,6-dicarboxylic acid/L, and the eluent for anions samples consisted of: 1.8 mmol NaCO₃/L and 1.7 mmol NaHCO₃/L eluent, after filtering through a 0.2 µm pore diameter PTFE syringe filter (VWR International, LLC.).

3.3.7. Methane dissolved measurement

The concentration of methane dissolved in the liquid phase, was determined sampling first 2 mL from the anode compartment and introduced in a 5 mL vacuum tube (Vacutianer ®). After the time required to reach liquid/gas equilibrium, CH₄ in the headspace was determine by means of gas chromatography equipped with a TCD detector (mod. VARIAN CP-3800), following the conditions described in **Table 3.1**.

Table 3.1. Conditions used for the measurement for the quantification of the methane produced.

Condition	Determination of biogas
Column type	Empacada Hayesep® Q (80/100 mesh)
Injector temperature (°C)	180
Oven temperature (°C)	90
Detector temperature (°C)	180
Detector type	TCD (Thermal conductivity)
Carrier gas	Heli
Carrier gas flux (ml/min)	45
Split	OFF
Injection volume (µl)	200

The moles of methane were obtained at normal conditions (1 atm, 25°C), and the concentration of dissolved methane at the liquid phase, was calculated from the methane percentage in the tube headspace using (Equation 3.5):

$$(Equation 3.5) \quad [CH_4] \text{ in the liquid (mg/l)} = \frac{CH_4 \text{ (gas)} \cdot V_{\text{gas}} \cdot PM_{CH_4}}{Vm_{CH_4} \cdot V_{\text{liq}}}$$

where $CH_4 \text{ (gas)}$, is the gas percentage in the vacuum tube headspace, V_{gas} is the volume of the tube headspace, PM_{CH_4} is the molecular weight of methane, Vm_{CH_4} is the molar volume of methane and V_{liq} is the volume of the liquid at the vacuum tube.

3.4. Electrochemical techniques

3.4.1. Electrochemical monitoring

Voltage between anode and cathode were measured and recorded every 10-20 minutes in a data acquisition unit (Mod. 34970A, Agilent Technologies, Loveland, CO, USA). Current density is calculated using Ohm’s law (equation 3.6) and accordingly power is calculated with equation 3.7 or equation 3.8:

$$(Equation 3.6) \quad I = E_{\text{cell}}/R$$

(Equation 3.7)
$$P = I \cdot E_{cell}$$

(Equation 3.8)
$$P = E^2_{cell} / R_{ext}$$

where, I stands for current density (A), P stands for power (W), E_{cell} is the difference between the measured cell voltage (V) and R_{ext} the external resistance (Ω). Besides, the power output is usually normalized to the projected electrode (anode) surface area ($W \cdot m^{-2}$), or the reactor volume ($W \cdot m^{-3}$), in order to compare the power output of different systems. Thus, power density is calculated as follows (equation 3.9):

(Equation 3.9)
$$P_{an} = E^2_{cell} / A_{an} \cdot R_{ext}$$

where, P_{an} stands for power density ($W \cdot m^{-2}$), A_{an} is the electrode surface area (m^2), and R_{ext} the external resistance (Ω). Similarly, if it is normalized to the reactor volume, power density is expressed as $W \cdot m^{-3}$.

Moreover there are other ways to evaluate the overall performance of MFC, as coulombic efficiency (CE), defined as the ratio of total electronic charges transferred to the anode from the substrate, to maximum possible charges if all substrate removal produced current (Logan et al., 2006). It is calculated as follows (equation 3.10):

(Equation 3.10)
$$CE = \frac{\int_{t_0}^t I(t) dt}{F \cdot b \cdot \Delta S \cdot V}$$

where, t is the time (s), F is the Faraday's constant (96485 C/mol-e⁻), b is the stoichiometric number of electrons produced per mol of substrate (e.g. 8mol e⁻/mol acetate), ΔS is the substrate consumption (mol/L) and V the liquid volume (L). For a mixed substrate, CE can be calculated based on COD consumption ($b = 4 \text{ mol-e}^- / \text{mol O}_2$).

Some experiments were carried out under MEC mode (**Chapter 7**). To supply the required voltage and those cases a power station (PS23032 Diotronic, S.A.) was used.

3.4.2. Polarization curves

Polarization curves (P versus I) is used to characterize current as a function of voltage (P versus I). They were used to estimate the enrichment of the exoelectrogenic community and calculate the maximum value of P . The system was left during one hour in open circuit to achieve stable voltage, then the circuit was closed and the external resistance was gradually decreased from 30000 to 1.2 Ω . Upon the connexion of each resistance, the system was left for stabilization during 30 min before recording the voltage data. The open system voltage (OCV) measured for an MFC is the maximum voltage that can be obtained with the system, and is only achieved under a condition where there is infinite resistance.

Polarization curves can be also used to calculate internal resistance. The two methods to evaluate the internal resistance of an MFC in this work were:

- *Polarization slope method*: in a plot of current versus measured voltage, the slope is R_{int} .
- *Power density peak*: the maximum power occurred at the point where the internal resistance was equal to the external resistance.

3.5. Scanning electron microscopy

Both IEMs precipitates and graphite and carbon felt samples were analysed by means of a Scanning Electron Microscope (SEM) (mod. Quanta 200, FEI Co., Hillsboro, OR, USA). IEMs precipitates at the end of the experimental phase were operated at 15 kV and high vacuum. The samples were mounted on stubs using double-stick tape and coated with carbon. The surface of the samples on the slides was observed through secondary electrons (SE) and back-scattered electrons (BSE) imaging, and X-ray energy dispersive spectroscopy (EDS). Surface IEMs measurements were performed at the Nanometric Unitin Scientific and Technological Centers of the University of Barcelona (CCiTUB) (chapter 4). And graphite and carbon felt samples from the anodic compartment and graphite and carbon felt (as a control) were also analysed by SEM (mod. Hitachi S-4100FE), in order to determinate the biofilm morphology (chapter 5). In this case, the samples were immersed in 2% glutaraldehyde buffer at pH 7.4. Next, the fixed samples were dried and sputter-coated with a graphite layer, and images were captured digitally.

3.6. Microbial community analysis by molecular biology techniques

Anode, cathode and supernatant were sampled, depending on the requirement for each experiment and culture-independent molecular techniques were applied in order to analyse the microbial communities harboured at the studied system. A schematic overview of the molecular techniques used in this work is represented in **Figure 3.8**.

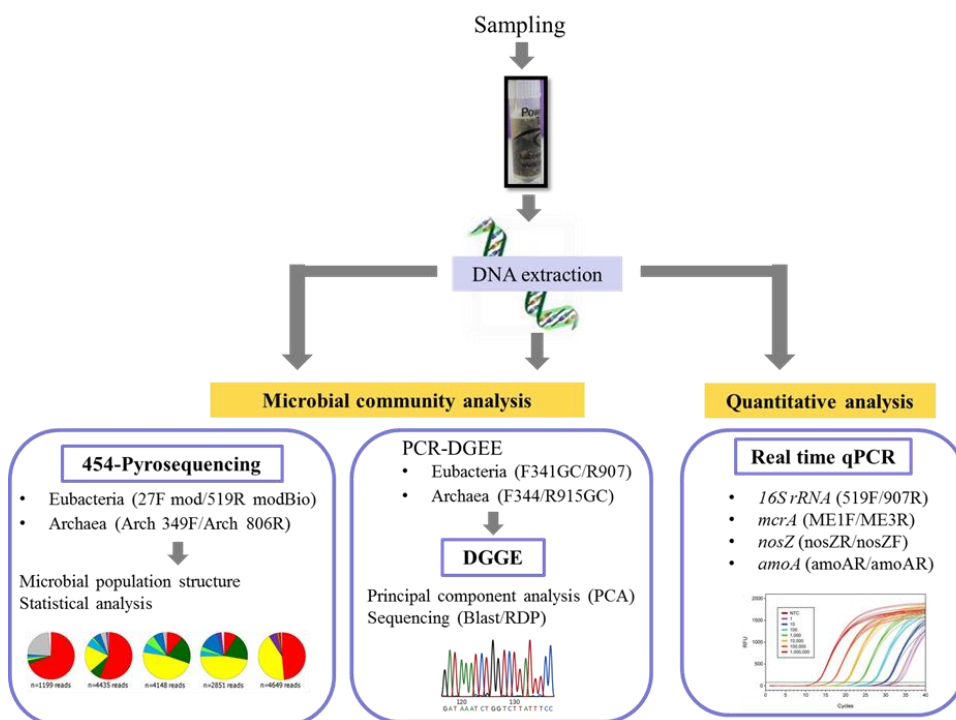


Figure 3.8. Schematic overview of the molecular techniques used to analyse the microbial community developed on the MFC anode and cathode under different experimental conditions.

3.6.1. Nucleic acid extraction and Polymerase Chain Reaction

Nucleic acid extraction was directly extracted in triplicate from samples using the PowerSoil® DNA Isolation Kit (MoBio Laboratories Inc., Carlsbad, CA, USA) according to the provided protocol. Universal eubacterial and archaeal primers were used to amplify the hypervariable V3-V5 region from the *16S rRNA* gene by the polymerase chain reaction (PCR), as previously reported by Yu and Morrison 2004. For archaeal population a NESTED-PCR approach was previously performed (Palatsi et al., 2010) by using specific primers pairs. All the primers used are described in **Table 3.2**. PCR reactions were carried out in a Mastercycler (Eppendorf, Hamburg, Germany) and each reaction mix (25 µL mix/reaction) contained the following reagents described in **Table 3.3**. A description of the PCR programs carried out is summarized in **Table 3.4**.

Table 3.2. Primers used for DGGE-PCR for eubacteria and archaea community.

Primers	Sequence (5'-3')	Bases	PCR type	Reference
16F341-GC1	CCT ACG GGA GGC AGC AG	17	PCR-DGGE	Viñas et al., 2005
16R907	CCG TCA ATT CCT TTR AGT TT	20	PCR-DGGE	Viñas et al., 2005
-D-Arch-0025-α-S-17	CTGGTTGATCCTGCCAG	17	PCR-DGGE	Vertriani et al 1999
S-Univ-1517-α-A-21	ACGGCTACCTTGTTACGACTT	21	PCR-DGGE	Vertriani et al 1999
Arch_F344	ACGGGYGCAGCAGGCGCGA	19	PCR-DGGE	Casamayor et al., 2002
Arch_R915 GC ²	CTGCTCCCCCGCCAATTCCT	20	PCR-DGGE	Casamayor et al., 2002

¹ GC clamp: 5'-CGCCCGCCGCGCCCGCGCCCGTCCCGCCGCCCCCGCCCG-3'.

² GC clamp: 5'-GCCCGGGGCGCGCCCGGGCGGGGCGGGGGCACGGGGGG-3'.

Table 3.3. PCR reaction conditions

Component	Volume (µl)	Final concentration
Nucleases free water	17.375	
Buffer solution (10x) (20 mM Mg ²⁺)	2.5	1X (2 mM)
DNTPs (2.5 mM)	2	200 µM
Primer F (10 µM)	1.25	0.5 µM
Primer R (10 µM)	1.25	0.5 µM
TaqDNA polymerase (10 U/ µl)	0.125	2.5 U

Table 3.4. Detailed PCR conditions per program performed for 16S rRNA eubacterial and archeal populations.

	Primers	Denaturation		Annealing		Extension		Cycles	Final extension	
ArchNestcd	ArchF0344/R915CG	94°	30"	63°	30"	72°	45"	25	72°	7'
Arch	ArchF0025/R1517	94°	30"	56°	30"	72°	45"	30	72°	7'
Eubact	16SEF341GC/R907	94°	1'	55°	1'	72°	45"	30	72°	10'
Band 16A	ArchF0344/R915	94°	30"	63°	30"	72°	45"	30	72°	5'
Band 16E	16SF341/R907	94°	30"	55°	0"	72°	45"	30	72°	10'
Seq	16SR907 (Eub) ArchR915 (Arch)	96°	10"	55°	5"	72°	4'	25		

3.6.2. Denaturing Gradient Gel Electrophoresis

Sequence-specific separation by denaturing gradient gel electrophoresis (DGGE) (Muyzer et al., 1993) was performed using PCR products obtained by the amplification of the V3-V5 variable region of the 16S rRNA gene described in the previous section (2.5.1). These PCR amplicons (20 µL) were loaded in an 8% (w/v) polyacrylamide gel (0.75 mm thick) with a increasing chemical denaturing gradient ranging from 30% to 70% (100% denaturant stock solution contained 7 M urea and 40% (w/v) of formamide). The electrophoresis coursed at 100 V for 16 h at 60°C in a 1x TAE buffer solution (40 mM Tris, 20 mM sodium acetate, 1 mM EDTA, pH 7.4). The gel ran in a DGGE-4001 system (CBS Scientific Company Inc., Del Mar, CA, USA). The gel was stained with 15 mL of 1x TAE buffer solution containing 3 µL of SYBR® Gold 10,000x (Molecular Probes, Eugene, OR, USA) in darkness for 45 min, and scanned with a transilluminator (GeneFlash, Synoptics Ltd., Cambridge, UK). Predominant DGGE bands were excised with a sterile filter tip, suspended in 50 µL of molecular biology grade water, and stored at 4°C overnight. The resuspended DNA-bands were subsequently reamplified by PCR as described above in Table 4 and, in some cases, sequenced using the ABI Prism Big Dye Terminator Cycle-Sequencing Reaction Kit v. 3.1 and an ABI 3700 DNA sequencer (both Perkin-Elmer Applied Biosystems, Waltham, MA, USA), according to the manufacturer's instructions at Macrogen (Macogren, the Netherlands).

3.6.3. Sequencing and statistical data analysis

Sequences were edited by using the BioEdit software package v.7.0.9 (Ibis Biosciences, Carlsbad, CA, USA) and aligned with the NCBI genomic database using the BLAST search alignment tool and checked by RDP (Ribosomal Data Project) database. And DGGE profiles were digitized and parameterized by using the image analysis program Gene Tools (Syngene) and a covariance-based Principal Component Analysis (PCA) based on the position and relative intensity of the bands present on the DGGE profiles previously digitalized was carried out. The MS Excel application StatistiXL v.1.4 (Broadway, Nedlands, Australia) and XLSTAT (Addinsoft, Paris, France) was used for this purpose.

3.6.4. Quantitative real time polymerase chain reaction

The quantitative analysis of individuals (assuming the correspondence one gene sequence per one cell) belonging to the Eubacteria and Archaea domain was completed using different primer set for *16S rRNA*, *mcrA*, *nosZ* and *amoA* genes, purified by HPLC and described in **Table 3.5**.

Table 3.5. Primers and conditions used for qPCR for the functional genes.

Gene	Primers	Sequence (5'-3')	PCR conditions
<i>16S rRNA</i>	519F	GCCAGCAGCCGCGGTAAT	Primer conc: 200 nM Annealing: 50°
	907R	CCGTCAATTCCTTTGAGTT	
<i>nosZ</i>	NosZF	CGYTGTTCMTCGACAGCCAG	Primer conc: 200 nM Annealing: 56°
	NosZR	CAKRTGCAKSGCRTGGCAGAA	
<i>amoA</i>	<i>amoAF</i>	GGGGTTTCTACTGGTGGT	Primer conc: 200 nM Annealing: 54°
	<i>amoAR</i>	CCCCTCKGSAAGCCTTCTTC	
<i>mcrA</i>	<i>mcrAR</i>	GCMATGCARATHGGWATGTC	Primer conc: 400 nM Annealing: 54°
	<i>mcrAF</i>	TGTGTGAASCCKACDCCACC	

Quantitative-PCR reaction (qPCR) was performed using Brilliant II SYBR Green qPCR Master Mix (Stratagene, La Jolla, CA, USA) in a Real-Time PCR System Mx3000P (Stratagene). The amplification reaction was performed with the Brilliant SYBR Green QPCR Master Mix (Agilent Technologies, USA according to the details provided by the manufacturer, with the following PCR conditions described in **Table 3.5**, and each reaction was performed according the characteristics described in **Table 3.6**.

Table 3.6. PCR reaction mix for Qpcr (SybrGreen).

Component	Volume (μ l)	Concentration
Nucleases free water	1.3	
Ready reaction mix	2.5	
Primer F (10 μ M)	0.1	200 nM
Primer R (10 μ M)	0.1	200 nM
Refence ROX	0.5	30 nM

The standard curves were performed with the following reference genes: *16S rRNA* gene from *Desulfovibrio vulgaris ssp. vulgaris* ATCC 29579, and *mcrA* gene fragment obtained from *Methanosarcina barkeri* DSM 800, both inserted in a TOPO TA vector (Invitrogen Ltd., Paisley, UK), and a custom-made *amoA* synthetic gBlock™ gene fragment (IDT, IA, Coralville, USA) from *Nitrosomonas europaea* ATCC 19718, and a set of *amoAF/amoAR* primers (Shimomura et al 2012). Per assay, eight non-zero concentrations were used in the generation of standard curves using triplicate serial 10-fold dilutions of plasmid DNA (ranging from 10^8 to 10^0 copies per reaction). Reference genes concentrations were determined by NanoDrop 1000 (Thermo Scientific).

Melting curve analysis to check specificity of PCR reaction and to detect the presence of primer dimers was performed after the final extension by increasing the temperature from 55 to 95°C at heating rates of 0.5°C each 10 s. Image capture was performed at 82°C to exclude fluorescence from the amplification of primer dimers. The qPCR efficiencies of amplification were greater than 98%. All results were processed by MxPro QPCR Software (Stratagene).

3.6.5. Pyrosequencing and data

Tag encoded sequencing of 16SrDNA massive gene libraries was performed by 454-pyrosequencing at Molecular Research DNA (Shallowater, Texas, USA). The primer set for the eubacterial analysis population is described in Table X. For the amplification 2 μ l of each DNA was used and reaction was carried out in 50 μ l which contained 0.4 mM of fusion primers, 0.1 mM of dNTPs, 2.5 U of Taq ADN polymerase (Qiagen) and 5 μ l of reaction buffer (Qiagen). The PCR amplification operated with the following protocol: 30 s at 95 °C, followed by 30 cycles at 94 °C for 30 s, annealing at 55 °C for 30 s, extension at 72 °C for 10 min and the PCR was carried out in a thermocycler GeneAmp_PCRsystem 9700 (Applied Biosystems).

The obtained DNA reads were compiled in FASTq files for further bioinformatic processing. Trimming of the *16S rRNA* barcoded sequences into libraries was carried out using QIIME software version 1.8.0 (Caporaso et al., 2010). Quality filtering of the reads was performed at Q25, prior to the grouping into Operational

Taxonomic Units (OTUs) at a 97% sequence homology cutoff. The following steps were performed using QIIME: Denoising using Denoiser (Reeder and Knight, 2010). Reference sequences for each OTU (OTU picking up) were obtained via the first method of UCLUST algorithm (Edgar, R.C., 2010). For sequence alignment was used PyNAST (Caporaso et al., 2010b) and Chimera detection was used ChimeraSlayer (Haas et al., 2011). OTUs were then taxonomically classified using BLASTn against GreenGenes database and compiled into each taxonomic level (DeSantis, Hugenholtz et al. 2006).

3.6.7. Diversity indices measurement

Mothur software version 1.33.3 was used to calculate alpha diversity by means the microbial diversity indices. The following indices and formulas are used in this work:

S number of taxa, **n** number of individuals.

Simpson:
$$D = \frac{1}{\sum_{i=1}^S P_i^2}$$

Shannon-Wiener: $H = - \sum_i \frac{n_i}{n} \ln \frac{n_i}{n}$, where n_i is the number of sequences of a particular OUT and n_t is the total number of sequences.

Chao-1: $Chao1 = \frac{s+F_1(F_1-1)}{2(F_2+1)}$, where F_1 is the number of singleton species and F_2 the number of doubleton species.

3.7. References

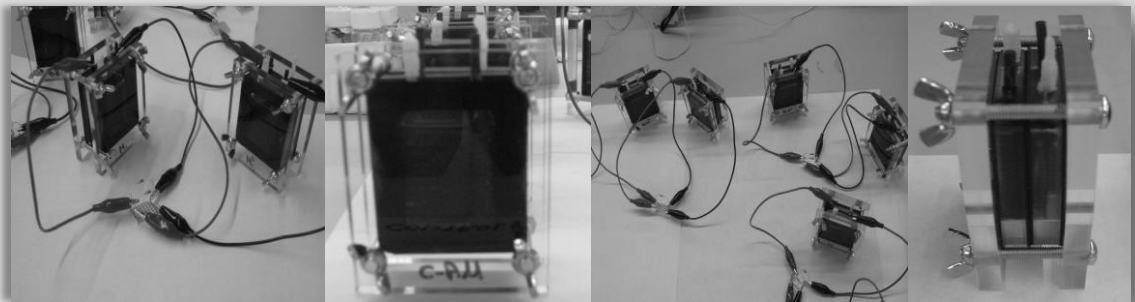
- APHA, AWA, WEF., 2005. Standard methods for the examination of water and waste water, 21th ed. American Public Health Association/American Water Works Association/Water Environment Federation, Washington, DC, USA.
- Vetriani, C., Jannasch, H.W., MacGregor, B.J., Stahl, D.A., Reysenbach, A.L., 1999. Population structure and phylogenetic characterization of marine benthic archaea in deep-sea sediments. *Appl. Environ. Microbiol.* 65, 4375–4384.
- Caporaso, J. G., J. Kuczynski, J. Stombaugh, K. Bittinger, F.D. Bushman, E.K. Costello, N. Fierer, A. Gonzalez-Pena, J.K. Goodrich, J.I. Gordon, G.A. Huttley, S.T. Kelley, D. Knights, J.E. Koenig, R.E. Ley, C.A. Lozupone, D. McDonald, B.D. Muegge, M. Pirrung, J. Reeder, J.R. Sevinsky, P.J. Turnbaugh, W.A. Walters, J. Widmann, T. Yatsunencko, J. Zaneveld, R. Knight., 2010. QIIME allows analysis of high-throughput community sequencing data, *Nature Methods.* 7, 335-336.

- Caporaso, J.G., K. Bittinger, F.D. Bushman, T.Z. DeSantis, G.L. Andersen, R. Knight., 2019. PyNASt: A flexible tool for aligning sequences to a template alignment, *Bioinformatics*. 26, 266-267.
- Chae, K-J., Choi, M-J., Kim, K-Y., Ajayi, F. F., Park, W., Kim C-W., Kim, I. S., 2010. Methanogenesis control by employing various environmental stress conditions in two-chambered microbial fuel cells. *Bioresource Technology*. 101, 5350-5357.
- DeSantis, T. Z., P. Hugenholtz, et al., 2006. Greengenes, a chimera-checked 16S rRNA gene database and workbench compatible with ARB. *Appl Environ Microbiol* 72(7), 5069-5072.
- Desloover, J., Woldeyohannis, A.A., Vestraete, W., Boon, N. and Rabaey, K., 2012. Electrochemical resource recovery from digestate to prevent ammonia toxicity during anaerobic digestion. *Environ. Sci. and Technol.* 46(21), 12209-12216.
- Haas, B.J., D. Gevers, A.M., Earl, M. Feldgarden, D.V. Ward, G. Giannoukos., 2011. Chimeric 16S rRNA sequence formation and detection in Sanger and 454-pyrosequenced PCR amplicons, *Gen. Res.* 21, 494-504.
- He, Z., Minter, S.D., Angenent, L.T., 2005. Electricity generation from artificial wastewater using an upflow microbial fuel cell. *Environmental Science and Technology*. 39, 5262-5267.
- Kennes, C., Cox, H.H.J., Harder, W., 1996. Design and performance of biofilters for the removal of alkylbenzene vapors. *Chem Technol Biotechnol.* 66, 300-304.
- Logan, B.E., Regan, J.M., 2006. Electricity-producing bacterial communities in microbial fuel cells. *Trends in Biotechnology*. 14, 512-518.
- Lu, H., Oehmen, A., Virdis, B., Keller, J., Yuan, Z., 2006. Obtaining highly enriched cultures of *Candidatus Accumulibacter* phosphates through alternating carbon sources. *Water Research*. 40(20), 3838-3848.
- Muyzer, G., DeWaal, E.C., Uitterlinden, A.G., 1993. Profiling of complex microbial populations by denaturing gradient gel electrophoresis analysis of polymerase chain reaction-amplified genes coding for 16S rRNA. *Appl. Environ. Microbiol.* 59, 695-700.
- Noguerol, J., Rodríguez-Abalde, A., Romero, E., Flotats, X., 2012. Determination of Chemical Oxygen Demand in Heterogeneous Solid or Semisolid Samples Using a Novel Method Combining Solid Dilutions as a Preparation Step Followed by Optimized Closed Reflux and Colorimetric Measurement. *Analytical Chemistry*. 84, 5548–5555.
- Palatsi, J., Illa, J., Prenafeta-Boldú, F.X., Laureni, M., Fernandez, B., Angelidaki, I., Flotats, X., 2010. Long-chain fatty acids inhibition and adaptation process in anaerobic thermophilic digestion: Batch tests, microbial community structure and mathematical modelling. *Bioresour. Technol.* 101, 2243-2251.
- Reeder, J., R. Knight., 2010. Rapidly denoising pyrosequencing amplicon reads by exploiting rank-abundance distributions. *Nature Methods*. 7, 668-669.
- Shimomura, Y., Morimoto, S., Takada Hoshino, Y., Uchida, Y., Akiyama, H., Hayatsu, M., 2012. Comparison among amoA primers suited for quantification and diversity analyses of ammonia-oxidizing bacteria in soil. *Microbes Environ.* 27, 94-98.

- Zhuang, L., Chen, Q., Zhou, S., Yuan, Y., Yuan, H., 2012. Methanogenesis control using 2-bromoethanesulfonate for enhanced power recovery from sewage sludge in air-cathode microbial fuel cells. *International Journal of Electrochemical Science*. 7, 6512-6523.
- Vetriani, C., Jannasch, H.W., MacGregor, B.J., Stahl, D.A., Reysenbach, A.L., 1999. Population structure and phylogenetic characterization of marine benthic archaea in deep-sea sediments. *Appl. Environ. Microbiol.* 65, 4375–4384.
- Viñas, M., Sabaté, J. Espuny, M.J., Solanas, A.M., 2005. Bacterial community dynamics and PAHs degradation during bioremediation of a heavily creosote-contaminated soil. *Applied Environmental Microbiology*. 71, 7008-7018.
- Yu, Z., Morrison, M., 2004. Comparisons of different hypervariable regions of *rrs* genes for use in fingerprinting of microbial communities by PCR-denaturing gradient gel electrophoresis. *Appl. Environ. Microbiol.* 70, 4800-4806.

Chapter 4

Screening of different inocula to start-up a microbial fuel cells (MFCs)



Sotres, A., Bonmatí, A., Viñas, M. (2010)

IX Meta conference, 9 – 10 December, Bilbao (Spain): [oral presentation](#)

Abstract

Microbial fuel cell (MFC) is a bioelectrochemical system that is capable of converting the chemical energy of dissolved organic compounds directly into electrical energy. In these systems the microorganisms acts as a catalyst for the electrochemical oxidation of the organic/inorganic materials, and the electrode is referred as a bianode. These exoelectrogenic microbes are able to transfer electrons released during the oxidation process to an electron acceptor (electrode), promoting a flow of electrons that can be harnessed in the form of electricity current. In this study a two chambered microbial fuel cells were used to test different inocula sources in order to study the influence of inoculums source on the established microbial community composition and dynamics in the anodic compartment over time.

Significant changes were detected in the diversity of the microbial community in MFC reactors comparing with the initial inocula, which could demonstrate the existence of an enrichment process in the microbial community at the anode compartment.

4.1. Introduction

A microbial fuel cell (MFC) is a bioelectrochemical reactor that, through metabolic activity, converts the chemical energy of biodegradable organic components into electricity (Kim et al., 2007; Pham et al., 2006).

Certain microorganisms are able to produce electric current, transferring electrons from an electron donor (organic/inorganic reduced compounds) to a final acceptor, thanks to the electrochemical potential existing between them. The biological strategies for transferring electrons to the anode can be both by direct contact, and by using electron shuttles (Logan, 2009). The electrons that are captured in the anode are transferred through an external electrical circuit to the cathodic chamber, where they reduce the final electron acceptor, typically oxygen.

The interest of the microbial community involved in all these processes taking place in the anodic compartment is growing intensively in the last years. The knowledge of these microbial communities is fundamental for understanding the ecology of the anodophilic populations, as for the competitive and/or exchange electron mechanisms among microorganisms and the anode, and/or among microorganisms, fact that would allow to designing strategies to improve the electron transference process (Logan, 2007). Hereby, one of the key parameters

for the development of this technology is the study of microbial populations involved in these processes.

The aim of this study was to analyse the microbial community composition in three different types of inocula, such in the initial inoculum as in the biofilm adapted to an anode compartment of a MFC, in order to select an enriched inoculum in exoelectrogenic bacteria to scale-up the MFC for further experiments.

4.2. Material and methods

4.2.1. MFC reactors

The MFC reactors used in this study consisted of a two-chambered cell constructed with two Plexiglas flat plates (88 x 65 mm) bolted together. These two chambers were separated by a cation exchange membrane (CEM), Ultrex CMI-7000 (Membrane International Inc.). The experiments were performed at room temperature in duplicate.

The anodic chamber was filled with 8 mL of a mineral medium, 1 mL of inoculum, and 1 mL of a sodium acetate solution (2.95 g L⁻¹). The micronutrients medium was prepared as described elsewhere (Kennes et al., 1996).

The experiments were carried out in batch mode, and the anodic chamber was fed with acetate solution. Periodicaly, when de intensity of the cell decreased to zero, 1 mL of anolyte was replaced by a 1 mL pulse of acetate solution 2.95 g L⁻¹ in mineral medium. The cathodic cahmber was filled with 10 mL of a chemical solution containing (per litre): 16.5 g K₃ Fe(CN)₆ as final electron acceptor and 4.5 g KH₂PO₄ + 0.5 g K₂HPO₄ as phosphate buffer.

4.2.2. Inocula

The MFC anodic chamber was inoculated with three different types of inocula from different bioreactors: i) constructed Wetlands working with urban wastewater (In. WET), ii) digestate from a bench-scale mesophilic methanogenic continuously stirred reactor fed with slaughterhouse waste (with high nitrogen load) (In. AD), iii) inoculum from a MFC working with cattle manure (In. CM) (**Figure 4.1**).



Figure 4.1. Picture of the reactors where the three inocula were sampled.

4.2.3. Voltage monitoring

The voltage was recorded every 10 minutes using a data acquisition unit (Mod. 34970A, Agilent Technologies, Loveland, CO, USA). The current density (I) was then calculated according to Ohm's law, and the power density was calculated as described in material and methods (**Chapter 3, section 3.4.1**).

4.2.4. Microbial community analysis

Nucleic acids were extracted from the initial inocula and from the samples obtained from the anodic compartment, following a physical-chemical extraction protocol of bead-beating using the PowerSoil® DNA Isolation Kit (MoBio Laboratories Inc., Carlsbad, CA, USA). To obtain DNA amplicons for further analysis of the total bacteria community by Denaturing Gradient Gel Electrophoresis (DGGE), a PCR was performed with F341-GC and R907 primers for Eubacterial community. PCR reactions were carried out in a Thermocycler Mastercycler (Eppendorf).

A DGGE-4001 system (CBS Scientific Company Inc., Del Mar, CA, USA) was used to perform a DGGE analysis as described previously (Muyzer et al., 1993). In brief, PCR amplicons samples were loaded onto 8% (w/v) polyacrylamide gel (0.75 mm thick) in 1X TAE buffer solution (40 mM Tris, 20 mM sodium acetate, 1 mM EDTA, pH 7.4). The polyacrylamide gels were made with a denaturing gradient ranging from 30% to 70%. Overnight electrophoresis was performed for 16 h at 60 °C and 100 V, and subsequently the gels were soaked in darkness for 45 min in 15 mL of a 1x TAE buffer solution containing 3 µL of SYBR® Gold 10,000x (Molecular Probes, Eugene, OR, USA). Afterwards, images of the gels were scanned under blue light by means of a blue converter plate (UV Products Ltd., Cambridge, UK) and a transilluminator (GeneFlash, Synoptics Ltd., Cambridge, UK). For sequence analysis purpose, the desired DGGE band fragments were cut out and reamplified by PCR and sequenced using the ABI PRISM Big Dye Terminator Cycle Sequencing Kit (version 3.1 Applied Biosystems, Foster City, CA). The sequencing reaction conditions were: initial denaturing at 96°C/1 minute, followed of 25 cycles of: 96°C/10 seconds, 55°C/5 seconds, 60°C/4 minutes. The sequence reaction was read in an automatic capillary sequencer ABI PRISM 3700 (PE Applied Biosystems, Foster City, CA). Sequences were processed using the BioEdit software package v.7.0.9 (Ibis Biosciences, Carlsbad, CA, USA) and aligned with the BLAST basic local alignment search tool (NCBI, Bethesda, MD, USA) and the Naïve Bayesian Classifier tool of RDP (Ribosomal Database Project) v.10 (East Lansing, MI, USA) for the taxonomic assignment.

Changes on the microbial community structure were analysed by covariance-based Principal Component Analysis (PCA) based on the position and relative intensity of the bands present on the DGGE profiles previously digitalized. The MS Excel application StatistiXL v.1.4 (Broadway, Nedlands, Australia) was used for this purpose.

The range-weighted richness (Rr) was derivated from the DGGE patterns of anodic biofilm overtime and calculated as equation 4.1:

$$(Equation 4.1) \quad Rr = N^2 \times Dg$$

where, N is the total number of bands in the pattern (lane) and D_g is the denaturing gradient between the first and the last band of the pattern (Marzorati et al., 2008).

4.3. Results

4.3.1. Electrochemical results

The voltage monitoring of the different MFC reactors showed different behaviors depending on the initial inoculums origin. The higher current density during three feeding cycles was obtained with the In. AD (**Figure 4.2**), obtaining similar results to the ones described in the literature for MFC of this volume (Sun et al., 2008).

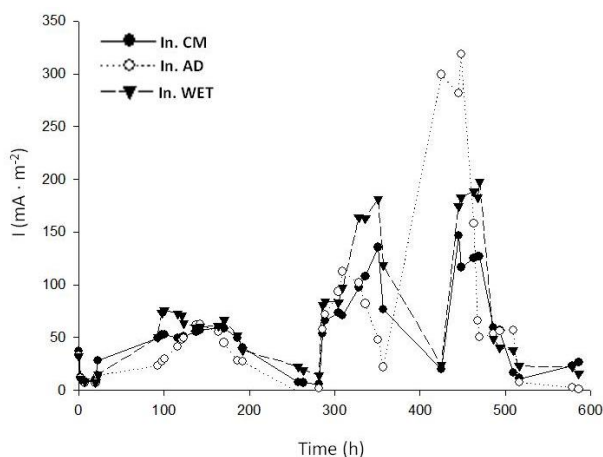


Figure 4.2. Current density produced in MFCs inoculated with three different inocula.

As **Figure 4.2** shows, the current density is increasing throughout the feeding cycles, showing an adaptation of the microbial communities to the anodic compartment.

4.3.2. Microbiological characterization

The profile obtained for the Eubacteria community (**Figure 4.3**), showed different bands pattern from the initial sample and the anodic samples at different times of electricity production. Besides, a gradual population shift through the electricity production processes is also observed. This fact shows an adaptation process of the microbial population in the anodic chamber. Besides, DGGE profile pattern in the anodic compartment is clearly different from the three inocula tested (**Figure 4.3**).

The range-weighted richness index (Rr) can be used to estimate the diversity of microbial communities. The Rr was calculated for the DGGE pattern of each sample to characterise the diversity and shifting of the bacterial anodic communities. The In. AD₁ showed the highest number of species with a Rr = 65, compared with a Rr of 34 for the In. CM₁, and just Rr of 8 for the In. Wet₁. The species richness increased in the anode biofilm over time in the MFC inoculated with In. AD₁, with a final Rr value of 90 (In. AD₄) after 10 acetate feeding cycles (two months), in the case of the MFC inoculated with In. CM, the Rr reached a value of 73 (In. CM₄). In both cases these values correspond to high range-weight richness according to Marzorati et al., 2008. Contrary, the species richness was very low for the MFC inoculated with In. WET (Rr = 5).

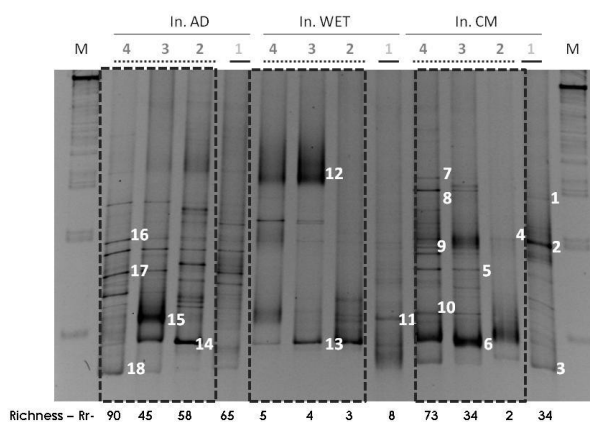


Figure 4.3. DGGE 16S rRNA profile for the total Eubacteria community. 1: initial inocula sample and, 2, 3, 4: electricity production peak number, and richness values.

Principal component analysis (PCA) of the DGGE profile (**Figure 4.4**) shows a cluster formed by the three initial inocula (In. AD₁, In. CM₁, In. WET₁), and confirmed that the population structure changed with the first peaks of voltage production. At the same time, the community structure also suffered a shift at the different times of electricity production through time.

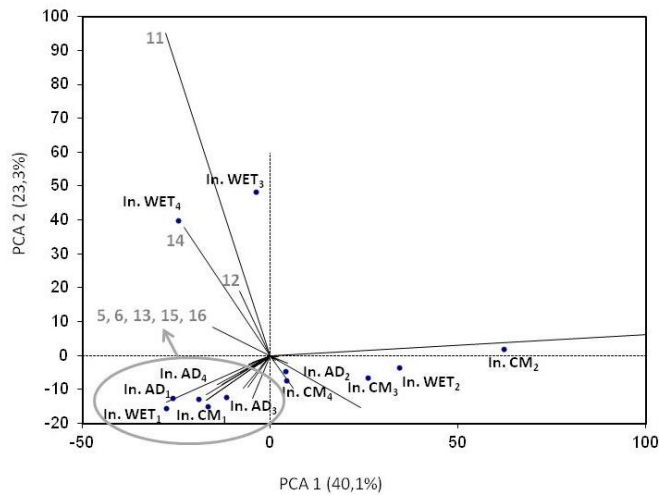


Figure 4.4. Principal component analysis (PCA) 2D-plot from digitalized DGGE profiles.

Predominant sequences belonging to the *Bacteroidetes* group have been found, mainly in the In. CM (**Table 4.1**). β -*proteobacteria* are good represented in the three MFC, in correlation with recent studies that reveal the high diversity of this group in MFC (Lefebvre et al., 2010), and that may have an important role in anode biofilm. Within this group, sequences belonging to the *Alcaligenaceae* and *Hydrogenophilaceae* family are found, and bands 13/14 (**Figure 4.3**) related to the *Comamonadaceae* family stand out.

Table 4.1. Characteristics of the sequenced bands from Eubacterial 16S rRNA gene based-DGGE from **Figure 4.3**.

Band	Length (bp)	Reference species strain or uncultivated microorganism (environmental source)	H (%)	Phylogenetic group (RDP)
1	272	Uncultured Bacteroidetes bacterium clone (HM443058)	98	Bacteroidaceae (Bacteroidetes)
2=4	513	Uncultured Bacteroidetes bacterium clone (AB547643)	100	Bacteroidaceae (Bacteroidetes)
3	471	<i>Spirochaeta</i> sp (AF357916)	99	Spirochaetaceae (Spirochaetes)
5	310	Uncultured Bacteroidetes bacterium clone (GQ979690)	98	Bacteroidetes
6	263	<i>Pseudomonas stutzeri</i> (HQ130335)	98	Pseudomonadaceae (Gammaproteobacteria)
7=8	490	Uncultured bacterium clone (DQ443965)	98	Porphyromonadaceae (Bacteroidetes)
10	370	<i>Achromobacter xylosoxidans</i> (HM641131)	97	Alcaligenaceae (Betaproteobacteria)
11	430	<i>Thiobacillus thioparus</i> (HM535226)	99	Hydrogenophilaceae (Betaproteobacteria)
12	487	<i>Arcobacter cryaerophilus</i> (EF064151)	99	Campylobacteraceae (Epsilonproteobacteria)
13	474	<i>Comamonas testasteroni</i> (GQ140333)	100	Comamonadaceae (Betaproteobacteria)
14	470	<i>Comamonas kerstersii</i> (NR_025530)	99	Comamonadaceae (Betaproteobacteria)
15	474	<i>Alcaligenes faecalis</i> (HM597239)	100	Alcaligenaceae (Betaproteobacteria)
16	418	Uncultured bacterium partial 16S rRNA gene (AM982611)	97	Bacteroidetes
17	488	Uncultured Bacteroidetes bacterium (EU586217)	99	Bacteroidetes
18	472	<i>Spirochaeta</i> sp (AY800103)	93	Spirochaetaceae (Spirochaetes)

4.4. Conclusions

The performance of the reactors equipped with the cation exchange membrane (CMI-7000) but inoculated with different inoculum, showed that the source of the inoculum determine the current density obtained. On the other hand, the start of the production of electricity is linked to a population shift for the three inoculums.

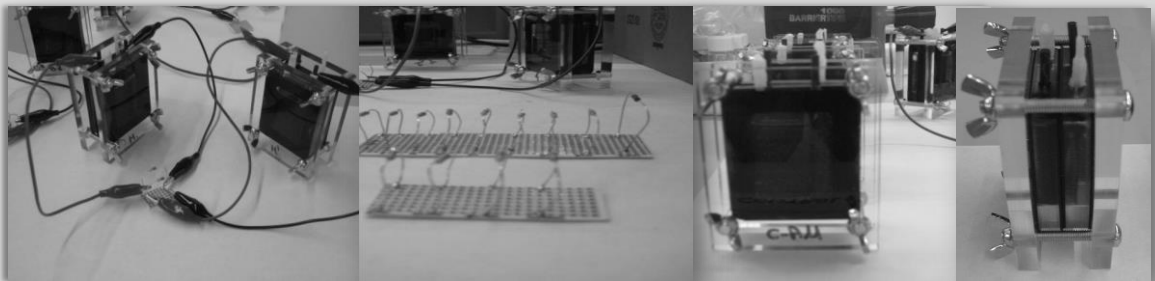
Based on our results, the In. AD could be considered as a good inoculum for the start-up of a MFC, due to its high species richness and the microbial composition found in it belonging to taxonomic groups previously described in MFC.

4.5. References

- Deremil, B., Scherer, P., 2008. The roles of acetotrophic and hydrogenotrophic methanotrophic methanogens during anaerobic conversion of biomass to methane: a review. *Environ. Sci. Biotechnol.* 7, 173-190.
- Kennes, C., Cox, H.H.J., Harder, W., 1996. Design and performance of biofilters for the removal of alkylbenzene vapors. *Chem. Technol. Biotechnol.* 66, 300-304.
- Kim, B.H., Chang, I.S., Gadd, G.M., 2007. Challenges in microbial fuel cell development and operation. *Appl. Microbiol. Biotechnol.* 76, 485-494.
- Lefebvre, O., Ha Nguyen, T.T., Al-Mamun, A., Chang, I.S., Ng H.Y., 2010. T-RFLP reveals high β -Proteobacteria diversity in microbial fuel cells enriched with domestic wastewater. *Journal of Appl. Microbiol.* 109, 839-850.
- Logan, B.E., 2007. *Microbial Fuel Cells*. Wiley-Interscience. John Wiley & Sons, Inc. New Jersey. ISBN: 978-0-470-23948-3.
- Logan, B.E., 2009. Exoelectrogenic bacteria that power microbial fuel cells. *Microbiology*. 7, 375-381.
- Marzorati, M., Wittebolle, L., Boon, N., Daffonchio, D., Verstraete, W., 2008. How to get more out of molecular fingerprints: practical tools for microbial ecology. *Environ. Microbiol.* 10, 1571-1581.
- Pham, T.H., Rabaey, K., Aelterman, P., Clauwaert, P., De Schamphelaire, L., Boon, N., Verstraete, W., 2006. Microbial Fuel Cells in relation to conventional anaerobic digestion technology. *Eng. Life Science*. 6(3), 285-292.
- Sun, Y.J., Zuo, J.E., Cui, L.T., Dang, Y., 2008. Analysis of microbial diversity in microbial fuel cells under different wastewater. *China Environmental Science*. 28(12), 1068-1073.
- Viñas, M., Sabaté, J., Espuny, M.J., Solanas, A.M., 2005. Bacterial community dynamics and PAHs degradation during bioremediation of a heavily creosote-contaminated soil. *Appl. Environ. Microbiol.* 71, 7008-7018.

Chapter 5

Microbial community dynamics in two-chambered microbial fuel cells: effect of different ion exchange membrane



Sotres, A., Díaz-Marcos, J., Guivernau, M., Illa, J., Magrí, A., Prenafeta-Boldú, F.X., Bonmatí, A., Viñas, M. (2014)
Journal Chemical Technology and Biotechnology DOI 10.1002/jctb.4465

Abstract

The utilization of different Ion Exchange Membranes (IEM) in bioelectrochemical systems, such as, cationic, anionic and bipolar membranes, for different purposes is a common practice. However little is known on the effects of the different membrane materials on the anodic microbial community diversity. In the present study the effect of two cationic and one anionic exchange membranes (Nafion N-117, Ultrex CMI-7000 and AMI-7000 respectively) on the microbial communities has been assessed. Microbial community dynamics were analysed by means of 16SrDNA-DGGE (eubacteria and archaea) and qPCR (16SrRNA and *mcrA* genes) approaches. Archaea microbial populations were highly abundant in all MFC reactors being above 5% of total microbial populations both in the anode material biofilm and suspended cells. Eubacteria-DGGE results showed a similar population shift over time, being predominant *Bacteroidetes* and β -*proteobacteria* populations, conversely, changes in microbial diversity of archaea were dependent on the type of membrane used. Methanogenic archaea, phylotypes belonging to *Methanosarcina* genus were predominant (15-17% of total microbial community) in MFC equipped with Nafion-117. Coincidentally, this MFC, showed the highest current production, suggesting that both anodophilic eubacteria and methanogenic archaea populations might play an important role in MFC performance.

5.1. Introduction

A microbial fuel cell (MFC) is a bioelectrochemical system (BES) designed for the direct production of electricity using microorganisms as catalysts. This biotechnology represents a promising approach for the valorisation of wastewaters and organic waste as a renewable energy source (Oh et al., 2010; Pant et al., 2010). In a MFC, the chemical energy available in organic substrates is directly harvested in an external circuit as free flowing electrons. The efficiency of this process is, therefore, potentially higher than that of other bioconversions such as methane and hydrogen fermentations (Pham et al., 2006).

Many different MFC configurations have been assayed (Logan et al., 2006), but the designs based on a double chamber are rather common (Logan et al., 2006; Bond and Lovley, 2002; Kim et al., 2007; Park et al., 2000; Rozendal et al., 2008). A conventional two-chambered MFC is formed by an anaerobic anodic and an aerobic cathodic chambers separated by an ion exchange membrane (IEM). The main function of the membrane is to keep the soluble components of

both compartments apart, while allowing the permeation of protons from the anodic to the cathodic chamber. The ionic balance is then closed by the flow of electrons from the anode to cathode through an external circuit.

Microorganisms from the anodic chamber act as catalysts by oxidizing organic substrates and transferring the released electrons to the external circuit. This transfer can be achieved by means of different strategies: (i) directly via the physical contact with the anode (cell adhesion or through nanowires); (ii) mediated through exogenous redox chemical mediators, or microbial secondary metabolites (chemical shuttles); and (iii) mediated through microbial primary metabolites formed during anaerobic respiration or fermentation (Schröder et al., 2007). The protons produced during the biological oxidation in the anodic chamber migrate to the cathodic chamber through the IEM, where they usually combine with oxygen and electrons to form water. Alternatively, chemicals such as ferricyanide have been used as final electron acceptor (Logan et al., 2006; Park et al., 2000).

As aforementioned, the IEM is a critical element in two-chambered MFCs as it maintains separation between the electron donor and acceptor while facilitating the flux of protons from the anodic to the cathodic compartments. In addition, the migration of larger ionic species and organic molecules and, especially, the diffusion of oxygen (or other electrolytes) from the cathodic to the anodic compartments, which would impair the overall process efficiency, is also prevented. Different membrane materials with specific physicochemical properties have already been assayed. Nafion, a sulfonated tetrafluoroethylene copolymer, has widely been used as proton exchange membrane (PEM) due to its high selectivity towards protons (Rabaey et al., 2005). However, its relatively high price has prompted the use of less specific but structurally stronger cation exchange membranes (CEMs) (Kim et al., 2007). The use of PEMs and CEMs may still result in the migration of positive charges (cationic species) other than protons, resulting in an increased pH in the cathodic chamber and a decreased MFC performance (Rozenal et al., 2006). Alternatively, anion exchange membranes (AEMs) and ultrafiltration membranes have been proposed as feasible alternatives (Kim et al., 2007). Therefore, the utilization of both PEM and AEMs is an issue of growing up interest on bioelectrochemical research (Hamelers et al., 2010; Dhar et al., 2013).

The microbial ecology in the anodic chamber of a MFC may be significantly different from a methanogenic reactor albeit both are running anaerobically. On this regard, it is interesting to study the microbial community structure concerning the presence of exoelectrogenic microorganisms (Chung et al., 2009; Jung et al.,

2007; Wrighton et al., 2008), either suspended in the liquid bulk or attached in the biofilm (Beecroft et al., 2012).

So far, there are two well-known bacterial genera which present exoelectrogenic activity in pure culture, i.e., *Shewanella* (Ringeisen et al., 2006) and *Geobacter* (Richter et al., 2008). However, the power density achieved in most of the experiments working with pure cultures turn out to be lower than those collected in mixed cultures (Nevin et al., 2008). These results reinforce the idea that increased electricity generation could be attributed to synergistic interactions within the microbial community. Namely, there could be microorganisms that do not exchange directly electrons with the electrode, but could be setting interactions between other members of the microbial community and be playing a crucial role in the operation of a MFC.

Recent studies have reported presence of archaeal cells attached to the biofilm in the anode of MFCs (Chung et al., 2009; Abrevaya et al., 2011; Higgins et al., 2013), suggesting that they might play a role in the electron transfer process. Franks *et al.*, have suggested that the development of biofilms with exoelectrogenic activity may be due to syntrophic interactions between eubacteria and methanogenic archaea. Yet, conversely to the biomass of anaerobic digesters, little is known on the syntrophic interactions between bacterial and archaeal populations in BES, concerning their distribution and role in the anode of a MFC in relation to operational and design reactor parameters.

The aim of this research was to evaluate the effect of three different materials (Nafion N-117, Ultrex CMI-7000, and Ultrex AMI-7000) as IEM in the performance of two-chambered MFCs. Nafion N-117 has been widely used with good results on MFCs performance, however it is an expensive material when scaling-up of bioreactors is needed. Therefore, it is interesting to test other alternative membrane materials (cation and anion exchange membrane more economically, and compare their performances on electricity productions and its potential effects on microbial community dynamics and structure. The effect of the membrane physicochemical properties on the anodic microbial community structure, both in the biofilm and supernatant cells, was also assessed by culture-independent molecular methods. In this work we also study the interactions between eubacteria and archaea in order to gain new insights into the microbial processes that potentially could govern the electron transfer in the anodic compartment.

5.2. Materials and methods

5.2.1. MFC reactors

Two-chambered MFC reactors consisted of two Plexiglas flat plates (88 × 65 mm) bolted together were used in this research. These external plates were framed so that they formed two chambers separated by an IEM fitted using neoprene gaskets (NCBE, University of Reading, UK). Both the anode and the cathode electrodes were made of carbon fibre tissue and were connected to an external resistance of 1000 Ω through an electric circuit. The IEM had an effective surface area of 12 cm² exposed to either compartment. Three different IEM materials were investigated: Nafion N-117 (DuPont Co., Wilmington, DE, USA) as PEM, Ultrex CMI-7000 (Membranes International Inc., Ringwood, NJ, USA) as CEM; and Ultrex AMI-7000 (Membranes International Inc.) as AEM. Experiments were performed at room temperature and by duplicate. Thus, a total of six MFC reactors were set-up and operated in parallel.

The anodic chamber was filled with 8 mL of a mineral medium, 1 mL of inoculum, and 1 mL of a sodium acetate solution (2.95 g/L) being 0.1M the final concentration in the anodic chamber. The mineral medium was prepared according to Kennes *et al.*, containing (per litre): 4.5 g KH₂PO₄, 0.5 g K₂HPO₄, 2 g NH₄Cl, 0.1 g MgSO₄·7H₂O, 1 mL of a trace mineral solution, and 1 mL of a vitamin solution. The experiment lasted 90 days, during which the anodic chamber was fed with the acetate solution (1 mL of anolyte was replaced by 1 mL pulse of acetate solution 2.95 g/L in mineral medium) each time the voltage decreased to the baseline value. The cathodic chamber was filled up with 10 mL of a chemical solution containing (per litre): 16.5 g K₃Fe(CN)₆ as final electron acceptor and 4.5 g KH₂PO₄ + 0.5 g K₂HPO₄ as phosphate buffer.

5.2.2. Inoculum

The MFC anodic chamber was inoculated with 1 mL of digestate (49 g COD/L and 2.5 g NH₄⁺-N/L) from a bench-scale mesophilic methanogenic continuously stirred reactor fed with slaughterhouse waste under hydraulic retention times of 20-30 days, organic loading rates of 2-3 g COD/L/d, and nitrogen loading rates of 0.08-0.14 g N/L/d, as previously described by Rodríguez-Abalde *et al.*

5.2.3. Electrochemical characterization

The voltage in the external circuit of the MFC was recorded every 10 minutes using a data acquisition unit (Mod. 34970A, Agilent Technologies, Loveland, CO,

USA). The current density (I) was then calculated according to the Ohm's law (equation 5.1), and the power density (P) was calculated with (equation 5.2):

$$\text{(Equation 5.1)} \quad I=V/R$$

$$\text{(Equation 5.2)} \quad P=I^2 \cdot R$$

where, I stands for current density (mA), V stands for the voltage (mV), R is the external resistance (Ω), P is the power density (mW m^{-2}) and A stand as the electrode surface area (m^2) and P stands for power density (mW m^{-2}).

Polarization curves (P versus I) were performed at different moments of the experiment to estimate the enrichment of the exoelectrogenic community and calculate the maximum value of P , which is obtained with the internal resistance (Ω) of the system. The procedure to obtain a polarization curve was as follows: after leaving the system 1 hour in open circuit, the circuit was closed and the external resistance was varied in the range from 30000 to 1.2 Ω . Upon the connexion of each resistance, the system was left for stabilization during 30 min before recording the voltage data.

The Coulombic efficiency (CE), defined as the fraction of electrons recovered as current versus the maximum theoretical recovery from the substrate oxidation (Logan et al., 2006) was calculated using data collected after acetate pulses and using (equation 5.3),

$$\text{(Equation 5.3)} \quad CE=C_p/C_{\pi} * 100$$

where CE is the Coulombic efficiency (%), C_p is the total number of Coulombs estimated by integrating the electric current over time and C_{π} is the theoretical amount of Coulombs that can be produced from acetate, calculated assuming total removal of the acetate added, similarly as previously described by Liu and Logan.

5.2.4. Scanning Electron Microscopy

At the end of the experiments, the occurrence of different kind of material accumulations on the IEM surface was also assessed. The used IEMs were observed with a Scanning Electron Microscope (SEM) (mod. Quanta 200, FEI Co., Hillsboro, OR, USA) operated at 15 kV and high vacuum. The samples were

placed on stubs using double-stick tape and coated with carbon. The surface of the samples on the slides was observed through secondary electrons (SE) and back-scattered electrons (BSE) imaging, and X-ray energy dispersive spectroscopy (EDS). Surface IEMs measurements were performed at Nanometric unit in Scientific and Technological Centers of the University of Barcelona (CCiTUB).

5.2.5. Denaturing gradient gel electrophoresis molecular profiling

Culture-independent molecular techniques were applied in order to analyse the eubacterial and archaeal microbial communities in the digestate used as inoculum, supernatant in the anodic chamber, and anodic biofilm formed in the carbon fibre tissue working as electrode. Samples from the MFC anodic chamber supernatant were taken at 7, 20, and 60 days of operation, when an electricity production peak was observed (peaks number 1, 2, and 3, respectively), while anode biofilms were sampled at the end of the experimental phase from carbon fibre tissue material in the anode compartment after 90 days.

Total DNA was extracted in triplicate from known volumes/weights of each sample with the PowerSoil® DNA Isolation Kit (MoBio Laboratories Inc., Carlsbad, CA, USA), according to manufacturer's instructions. Universal eubacterial forward F341 and reverse R907 primers were used to amplify the hypervariable V3-V5 region from the 16S rRNA gene by the polymerase chain reaction (PCR), as previously reported (Yu et al., 2004). For archaeal population a NESTED-PCR approach was performed by using the primer pairs Arch0025/R1517 and F344-R915-GC for the PCR and the nested reaction, respectively (Palatsi et al., 2010). All PCR reactions were carried out in a Mastercycler (Eppendorf, Hamburg, Germany) and each reaction mix (25 µL mix/reaction) contained 1.25 U of Ex TaqDNA polymerase (Takara Bio Inc., Otsu, Shiga, Japan), 12.5 mM dNTPs, 0.25 µM of each primer, and 100 ng of DNA.

The PCR amplicons (20 µL) were loaded in an 8% (w/v) polyacrylamide gel (0.75 mm thick) with a chemical denaturing gradient ranging from 30% to 70% (100% denaturant stock solution contained 7 M urea and 40% (w/v) of formamide). The electrophoresis was carried out in a DGGE-4001 system (CBS Scientific Company Inc., Del Mar, CA, USA) at 100 V and 60°C for 16 h in a 1x TAE buffer solution (40 mM Tris, 20 mM sodium acetate, 1 mM EDTA, pH 7.4) (Muyzer et al., 1993). The DGGE gels were stained in darkness for 45 min with 15 mL of 1x TAE buffer solution containing 3 µL of SYBR® Gold 10,000x (Molecular Probes, Eugene, OR, USA). The gels were scanned under blue light by means of a blue converter plate (UV Products Ltd., Cambridge, UK) and a transilluminator (GeneFlash, Synoptics Ltd.,

Cambridge, UK). Predominant DGGE bands were excised with a sterile filter tip, suspended in 50 µL of molecular biology grade water, and stored at 4°C. The resuspended bands were subsequently reamplified by PCR as described above. Sequencing was accomplished by using the ABI Prism Big Dye Terminator Cycle-Sequencing Reaction Kit v.3.1 and an ABI 3700 DNA sequence (both Perkin–Elmer Applied Biosystems, Waltham, MA, USA), according to manufacturer’s instruction.

Sequences were processed by BioEdit software package v.7.0.9 (Ibis Biosciences, Carlsbad, CA, USA) and aligned by BLAST basic local alignment search tool (NCBI, Bethesda, MD, USA) and the Naïve Bayesian Classifier tool of RDP (Ribosomal Database Project) v.10 (East Lansing, MI, USA) for the taxonomic assignment. After the alignment, Bellerophon v.3 (GreenGenes, Berkeley, CA, USA) was used to eliminate chimeric sequences. The eubacterial and archaeal 16S rRNA gene nucleotide sequences determined in this study were deposited in the Genbank (NCBI) under accession numbers JQ307401-JQ307412 and JQ394939-41, JQ394943- JQ394944, JQ394946-JQ394948, JQ394950-JQ394952, JQ394954, JQ394959- JQ394961, JQ394964- JQ394966 for eubacterial and JQ394967-JQ394968, JQ394970- JQ394971, JQ394977-JQ394979.

Changes on the microbial community structure were analysed by covariance-based Principal Component Analysis (PCA) based on the position and relative intensity of the bands present on the DGGE profiles previously digitalized. The MS Excel application StatistiXL v.1.4 (Broadway, Nedlands, Australia) was used for this purpose.

5.2.6. Quantitative PCR assay

Gene copy numbers of eubacterial 16S rRNA gene and *mcrA* gene (methanogenic archaeal methyl coenzyme-M reductase) were quantified by means quantitative real-time PCR (qPCR). Each sample was analyzed in triplicate by means of three independent DNA extracts as elsewhere described (Prenafeta-Boldú et al., 2012). The analysis was carried out by using Brilliant II SYBR Green qPCR Master Mix (Stratagene, La Jolla, CA, USA) in a Real-Time PCR System Mx3000P (Stratagene) operated with the following protocol: 10 min at 95°C, followed by 40 cycles of denaturation at 95°C for 30 s, annealing for 30 s at 50°C and 54°C (for 16S rRNA and *mcrA* gene, respectively), extension at 72°C for 45 s, and fluorescence capture at 80°C. The specificity of PCR amplification was determined by observations on a melting curve and gel electrophoresis

profile. Melting curve analysis to detect the presence of primer dimers was performed after the final extension by increasing the temperature from 55 to 95°C 95°C at heating rates of 0.5°C each 10 s. Image capture was performed at 82°C to 82°C to exclude fluorescence from the amplification of primer dimers. Each reaction was performed in a 25 µL volume containing 2 µL of DNA template, 200 nM of each *16S rRNA* primer, 600nM of each *mcrA* primer, 12.5 µL of the ready reaction mix, and 30 nM of ROX reference dye. The primer set for eubacterial population was 519FqPCR (5'-GCCAGCAGCCGCGGTAAT-3') and 907RqPCR (5'-CCGTC AATTCCTTGAGT-3'). The primer set for archaeal *mcrA* gene was ME1F (5'-GCMATGCARATHGGWATGTC-3') and ME3R (5'-TGTGTGAASCKACDCCACC-3'); (Hales et al., 1996), both primer pairs were purified by HPLC. The standard curves were performed with the following reference genes: *16S rRNA* gene from *Desulfovibrio vulgaris* ssp. *vulgaris* ATCC 29579, and *mcrA* gene fragment obtained from *Methanosarcina barkeri* DSM 800, both inserted in a TOPO TA vector (Invitrogen Ltd., Paisley, UK). All reference genes were quantified by NanoDrop 1000 (Thermo Scientific). Ten-fold serial dilutions of known copy numbers of the plasmid DNA in the range 10 to 10⁸ copies were subjected to a qPCR assay in duplicate to generate the standard curves. The qPCR efficiencies of amplification were greater than 98%. All results were processed by MxPro QPCR Software (Stratagene).

5.3. Results and discussion

5.3.1. Electrochemical activity

The electricity production capacity of the MFCs was compared in terms of voltage generation and polarisation curves. A sharp increase in the voltage was observed in all the reactors after an acetate feeding pulse, but the voltage decrease patterns were different depending on the type of membrane (**Figure 5.1**).

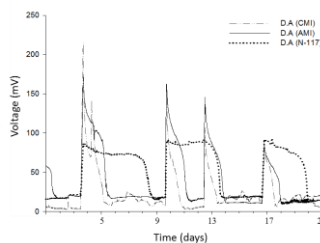


Figure 5.1. Voltage produced in MFCs working with an external resistance of 1000 Ω after three consecutive substrate loads and depending on the ion exchange membrane used: CMI (- -), AMI (-), and N-117 (· ·).

The MFCs equipped with Nafion N-117 exhibited a greater electricity production than those built with Ultrex CMI-7000 and Ultrex AMI-7000 membranes, with a CE for one acetate feeding cycle of 13%. The CE in the MFCs using CMI-7000 and AMI-7000 membranes was 5.7% and 6.7%, respectively.

Similarly, the highest voltage and power density when performing the polarization curves were achieved again with the N-117 membrane, with 433 mV and 71 mW/m², respectively (**Figure 5.2 and Table 5.1**). These results are in the same range than the values reported elsewhere for small-sized MFCs, accounting for a similar potential but higher internal resistance (2200 Ω) and lower CE values (Sun et al., 2008; Ieropoulos et al., 2010). However, it is well known that Nafion N-117 contains sulfonic acid groups that bind with the ammonia present in the anolyte. Hence, this membrane could display a low stability and trap free nitrogen (Rabaey et al., 2005). Results of the MFC equipped with the N-117 membrane were followed by those of the MFC equipped with the CMI-7000 membrane. Finally, a significantly lower electricity production was observed with the AMI-7000 membrane compared to the other two membranes tested in this study (**Figure 5.1 and Figure 5.2**). Although little is known on the performance of anion exchange membranes such as AMI-7000, there are some studies reported in literature that show even better results with AEMs than with CEMs (Rozendal et al., 2008; Jung et al., 2007).

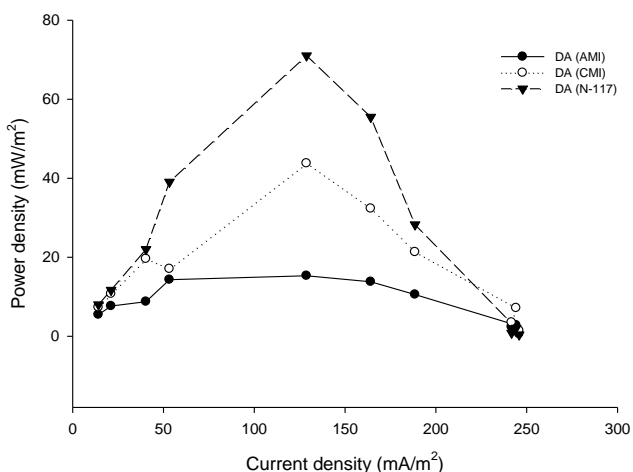


Figure 5.2. Effect of current density on the power density depending on the type of membrane used: CMI (●), AMI (○), and N-117 (▼).

Table 5.1. Maximum voltage (V_{max}), maximum power density (P_{max}), and internal resistance (Ω_{int}) obtained for the three reactors through a polarization curve test (**Figure 5.2**).

	Polarization curve		
	V_{max} (mV)	P_{max} (mW/m ²)	Ω_{int}
DA (CMI)	340	44	2200
DA (AMI)	201	15	2200
DA (N-117)	433	71	2200

Depletion of the current density production was observed in all the MFCs after 10 acetate feeding cycles (two months). Membrane fouling and clogging could be responsible for this progressive decay in the current density production. In order to have more insight of this phenomenon, the IEMs were analysed by means of SEM and EDS. The results showed the predominance of Fe and K crystallites in both membrane sides and for the three materials tested (**Figures 5.3, 5.4, 5.5**). It is well known that CEMs such as N-117 or CMI-7000 may be permeable to certain chemicals such as oxygen, ferricyanide and other ions (Logan et al., 2006). In the present study, the N-117 membrane apparently had less precipitates attached (**Figure 5.5**) and maintained the activity of the MFC for longer time, which contrasts with results reported in some previous works (Rabaey et al., 2003).

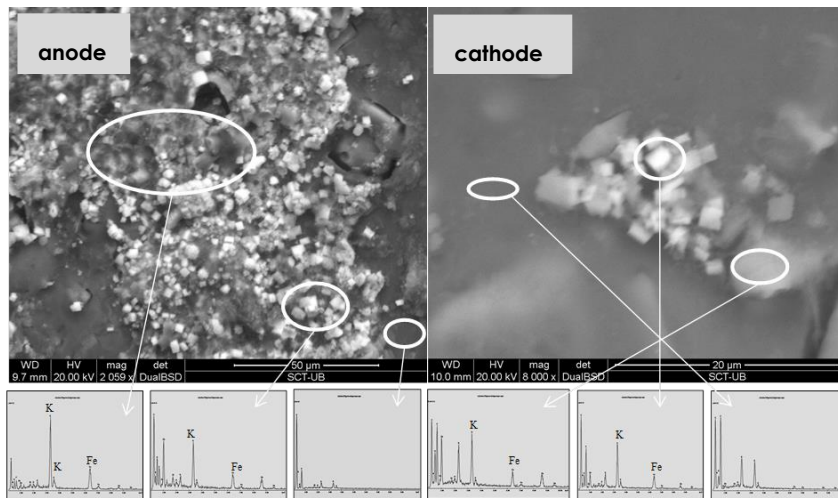


Figure 5.3. Results obtained through SEM and EDS concerning the CMI-7000 anode and cathode side respectively.

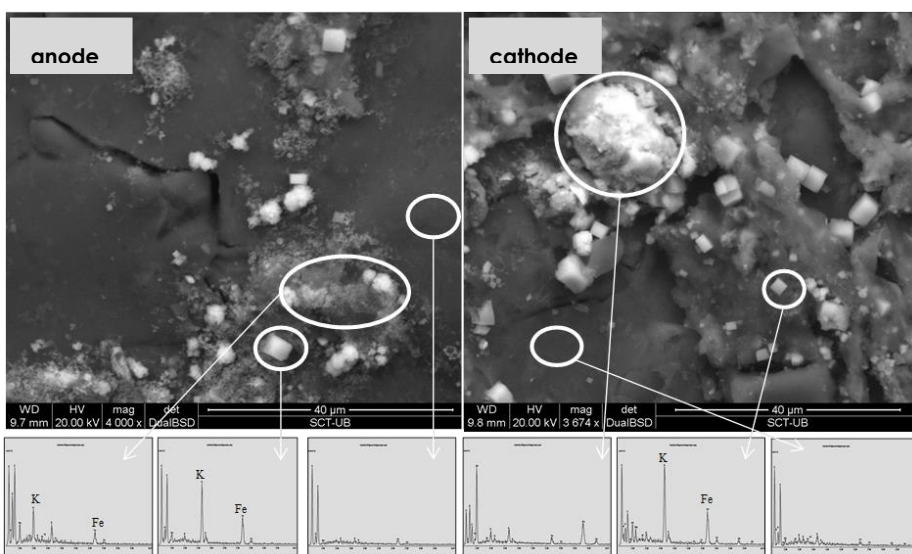


Figure 5.4. Results obtained through SEM and EDS concerning the AMI-7000 anode and cathode side respectively.

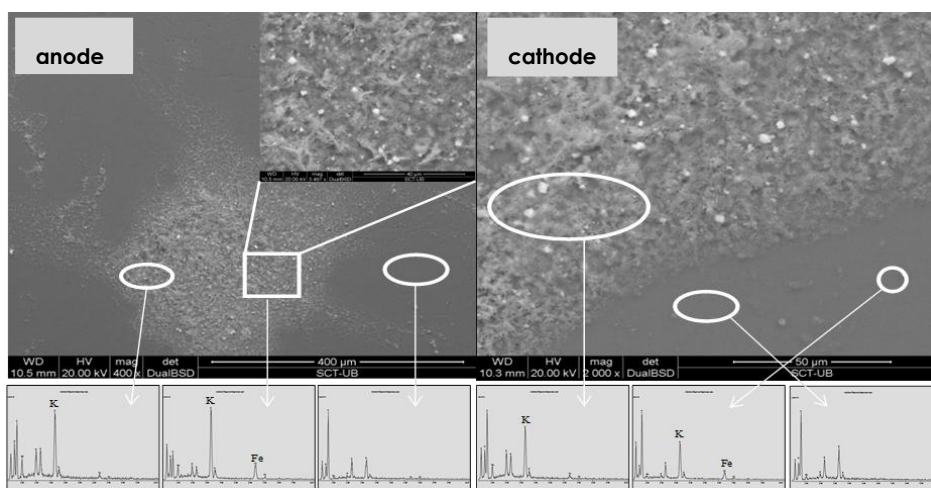


Figure 5.5. Results obtained through SEM and EDS concerning the N-117 anode and cathode side respectively.

5.3.2. Microbial community analysis

Microbial community characterization (*Eubacteria* and *Archaea* domains) was performed by means of DGGE profiling (*16S rRNA* genes) and qPCR technique (*16S rRNA* and *mcrA* genes) on samples encompassing three acetate feeding cycles. The obtained DGGE results (**Figure 5.6a** and **Figure 5.7**) showed a significant microbial population shift of both eubacteria and archaea overtime, concomitantly with an increment in electricity production. Such microbial community changes, as observed in the DGGE patterns, might be related to the adaptation of the initial inoculum, obtained from an anaerobic digester, to the presence of an external electric circuit. Population dynamics in eubacteria were rather independent on the type of membrane used in MFC experiments. Principal Component Analysis (PCA) on parameterized eubacterial *16S rRNA* DGGE profiles (**Figure 5.6b**), showed that the most significant changes in the microbial community structure coincided with the second and third peak of voltage production. Yet, it is noteworthy that the most differentiated microbial community has been observed in the MFC equipped with the N-117 membrane (third peak) (**Figure 5.6b**), which it also displayed the best performance. Band 36 (**Figure 5.6a**) belong to *Mollicutes* (*Acholeplasmataceae*) has been identified only for the sample corresponding to the third peak of N-177 sample.

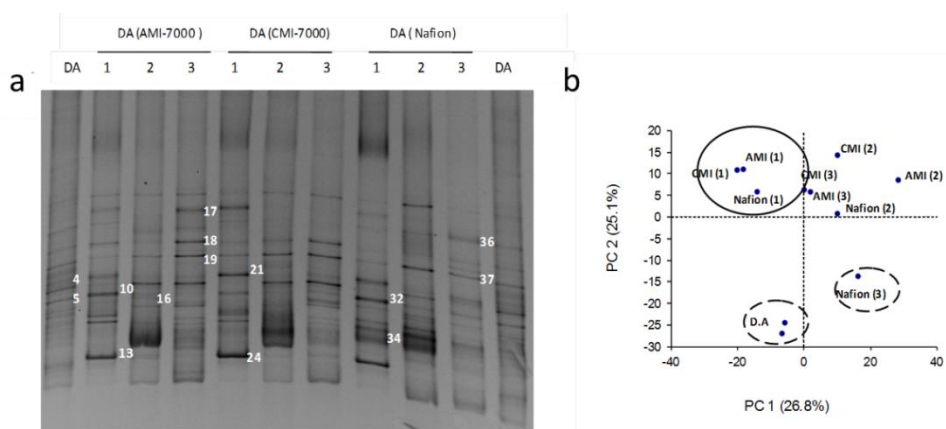


Figure 5.6. (a) DGGE profiles on eubacterial *16S rDNA* amplified from samples obtained in MFCs. (b) Principal component analysis (PCA) 2D-plot from digitalized DGGE profiles. DA: initial inoculum. 1, 2, and 3: electricity production peak number.

Conversely, changes on the archaeal microbial community over time were strongly dependent on the membrane material (**Figure 5.7** and **Figure 5.8**). The membrane materials are different, such as N-117 membrane contains sulfonic acid groups which could directly affect the archaea metabolisms. It is noteworthy that ribotypes closely related to the methanogenic genus *Methanosarcina* (DGGE band 1 (**Figure 5.7**) and DGGE bands 27, 35, 36, and 39 (**Figure 5.8**) were only found in MFC equipped with cationic membranes (N-117 and CMI-7000), whereas ribotypes belonging to Methanosateaceae were detected both in anionic and cationic membranes (bands 10, 13, 15, 38). Such important occurrence of *Methanosarcina* detected in cationic membranes-MFC was also coincident with a higher electricity production in Nafion N-117-MFC.

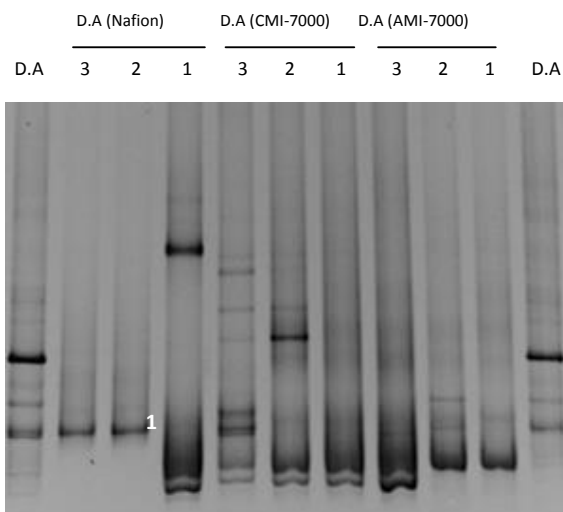


Figure 5.7. DGGE profiles on archaeal 16S rDNA amplified from samples obtained in MFCs. DA: initial inoculum. 1, 2, and 3: electricity production peak number.

In addition, the *mcrA* gene copy numbers quantified by qPCR revealed a high abundance of methanogenic archaea in the three MFC systems, representing the 6-20% in relation to the total eubacterial 16S rRNA gene copy numbers (**Figure 5.9**).

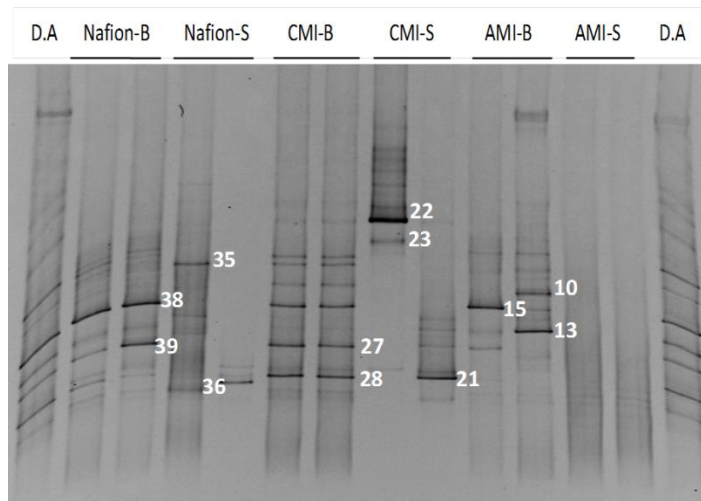


Figure 5.8. DGGE profile 16S rDNA for the total archaea community. D.A: initial inoculums; Nafion-B: biofilm of the MFC equipped with Nafion; Nafion-S: supernatant of the MFC (Nafion); CMI-B:biofilm of the MFC (CMI-Ultrex™); CMI-S: supernatant of the MFC (CMI-Ultrex™). AMI-B: biofilm of the MFC (AMI-Ultrex™); AMI-S: supernatant of the MFC (AMI-Ultrex™).

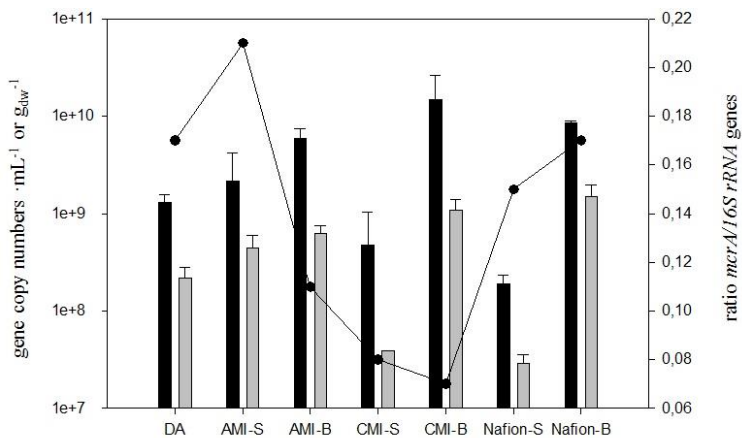


Figure 5.9. qPCR results for 16S rRNA (in black) and *mcrA* (in gray) genes, for the initial inoculum and for the three different MFCs equipped with the three tested membranes and ratio *mcrA*/16S rRNA genes. D.A: initial inoculum; AMI-B: biofilm of the MFC (AMI-Ultrex™); AMI-S: supernatant of the MFC (AMI-Ultrex™); CMI-B:biofilm of the MFC (CMI-Ultrex™); CMI-S: supernatant of the MFC (CMI-Ultrex™); N117-B: biofilm of the MFC equipped with Nafion; N117-S: supernatant of the MFC (Nafion).

In addition, it is noteworthy, that Nafion-MFC harboured the highest methanogenic population on the anode biofilm (10^9 *mcrA* gene/ g_{dw} anode) accounting for 17% of total population, compared with CMI-MFC (7%) and AMI-MFC (11%). Previous studies reported also a high prevalence of methanogenic archaea close to the anode on MFC and MEC bioelectrochemical systems (Kiely et al., 2011; Croese et al., 2013). Although methanogenic archaea could compete for the electrons and have been pointed as responsible for the low CE, they could play a role in the establishment and function of an anodophilic biofilm by improving the bioavailability of cofactors, and other molecules such as electron shuttles enhancing electron transfer among microorganisms (Eggleston et al., 2008; Pham et al., 2008).

It is noteworthy that no significant differences were found in relation to the microbial community structure of supernatant (planktonic cells) and biofilm-forming eubacteria (**Figure 5.9**), in agreement with a recent work from Bonmati et al. 2013 where the predominant bands in both supernatant and biofilm belonged to the same phylum. Contrary, the archaeal communities from the biofilm and the supernatant were significantly different and dependent on the membrane material (**Figure 5.8**). Such spatial differentiation in the archaeal community composition could be explained by the enrichment of archaea in contact with the anode, which could encompass specialized representatives both in cooperation and in competence with exoelectrogenic eubacteria. However, further research is needed in this field to confirm such potential interaction between eubacteria and targeted methanogens belonging to Methanosarcinaeae and Methanosaetaceae in our MFC reactors.

Sequences of most predominant eubacterial ribotypes from DGGE bands (**Figure 5.6a** and **5.9**) are presented on **Tables 5.2** and **5.3**. The most predominant eubacterial ribotypes found in the supernatant and the biofilm are associated to *Bacteroidetes* (*Prophyromonadaceae*) and β -*Proteobacteria* (*Alcaligenaceae* and *Comamonadaceae*). Representatives of these microbial groups have previously been described as being able to exchange electrons with an electrode (Logan et al., 2006). Within the β -*Proteobacteria* class, we observed several bands on the DGGE profiles with sequences belonging to the *Alcaligenaceae* and *Comamonadaceae* families. Representatives of these families have been previously described as electrochemically active in studies also performed with methanogenic sludge as inoculum (Higgins et al., 2013; Rabaey et al., 2004).

Table 5.2. Characteristics of the sequenced bands from Eubacterial 16S rRNA gene based-DGGE from samples obtained in the MFCs. DA: initial inoculum. 1, 2, and 3: electricity production peak number (**Figure 5.6**).

Band	Length (bp)	Accession number	Phylogenetic group (RDP)	Reference species, strain or uncultivated microorganism (environmental source)	Accession number	H (%)
4	480	JQ307401	<i>Bacteroidetes</i>	Uncultured (ASBR reactor treating swine waste)	GQ135359	99
				<i>Sphingobacterium thermophilum</i> strain CKTN2 ^T	NR_108120	87
5	357	JQ307402	<i>Bacteroidetes</i>	Uncultured (mesophilic anaerobic digester)	KF147566	98
				<i>Cellulophaga tyrosinoydans</i> strain VSW306	KC534369	86
10=32	425	JQ307403	γ - <i>proteobacteria</i> <i>Moraxellaceae</i>	<i>Acinetobacter</i> sp. WX-19	JF730216	100
				<i>Acinetobacter seohaensis</i> ^T	AY633608	99
13	415	JQ307404	<i>B-proteobacteria</i> <i>Comamonadaceae</i>	<i>Comamonas testosteroni</i> strain BK1R	KC864773	99
16	270	JQ307406	<i>B-proteobacteria</i> <i>Alcaligenaceae</i>	<i>Advenella kashmirensis</i> strain 20rA (bioanode in MEC)	KF528154	98
				<i>Advenella kashmirensis</i> WT001 ^T	NR_074872	97
17	440	JQ307407	<i>Bacteroidetes</i>	Uncultured (mesophilic anaerobic digester)	EU104338	98
				<i>Paludibacter propionigenes</i> WB4 ^T	NR_074577	90
18	499	JQ307408	<i>Bacteroidetes</i>	Uncultured (ASBR reactor treating swine waste)	GQ134808	99
				Uncultured (microbial fuel cell)	JX174653	97
19=37	471	JQ307409	<i>Bacteroidetes</i> <i>Porphyromonadaceae</i>	Uncultured (MFC with phosphate buffer and acetate)	GQ152958	99
				<i>Proteiniphilum acetatigenes</i> strain TB107 ^T	NR_043154	97
21	432	JQ307410	<i>Bacteroidetes</i> <i>Bacteroidaceae</i>	<i>Bacteroides coprosuis</i> strain JCM 13475 ^T	AB510699	99
24	361	JQ307405	<i>B-proteobacteria</i> <i>Comamonadaceae</i>	Uncultured (MFC fed with sucrose)	HM043267	100
				<i>Comamonas jiangduensis</i> strain YW1 ^T	NR_109655	99
34	438	JQ307411	<i>B-proteobacteria</i> <i>Alcaligenaceae</i>	<i>C. kerstersii</i> strain CIP 107987 ^T	EU024144	99
				<i>Alcaligenes faecalis</i> strain MUN1	KF843701	100
36	475	JQ307412	<i>Mollicutes</i> <i>Acholeplasmataceae</i>	<i>Acholeplasma parvum</i> strain H23M	NR_042961	92
				<i>A. palmae</i> strain J233	NR_029152	92

The most homologous sequence and the closest phylogenetically relevant match are shown (preferably type strains^T).

Regarding the archaeal DGGE profiles (**Figure 5.7** and **Figure 5.8**) the phylogenetic assignment on basis of the DNA sequence homology searches has been summarized in **Table 5.3**. The observed diversity of archaea was significantly lower than that of eubacteria. It is remarkable that all methanogenic sequences belonged to the *Methanosaetaceae*, *Methanomicrobiaceae* and *Methanosarcinaceae* families. There is one particular ribotype sequence belonging to the *Methanosarcinaceae* which is apparently enriched over time in the reactors equipped with cationic membrane (band 27) (**Figure 5.8**), and specially with N-117 membrane (band 1) (**Figure 5.7**). Yet, those bands belonging to *Methanosaetaceae* and *Methanosarcinaceae* were found to be predominant in the biofilm for the three studied MFC configurations. It is noteworthy that methanosarcinaceae are specially enriched in MFC equipped with cationic

membranes. So far, relatively few studies have focussed on the archaea that are present in anode compartment of a MFC reactor. Also, we quantified the population by means of qPCR and we can conclude that there is a high number of methanogenic archaea, both in the biofilm ($6.3 \cdot 10^8$ - $1.5 \cdot 10^9$ *mcrA* gene copies g_{dw}^{-1} anode) and in the planktonic community ($2.8 \cdot 10^7$ - $4.5 \cdot 10^8$ *mcrA* gene copies mL^{-1} anolyte) (Figure 5.10).

Table 5.3. Characteristics of the bands from the 16S rRNA DGGE eubacteria gel from the following samples: D.A: initial inocula; Nafion-B: biofilm of the MFC equipped with Nafion N-117; Nafion-S: supernatant of the MFC (Nafion N-117); CMI-B: biofilm of the MFC (Ultrex CMI-7000); CMI-S: supernatant of the MFC (Ultrex CMI-7000). AMI-B: biofilm of the MFC (Ultrex AMI-7000); AMI-S: supernatant of the MFC (Ultrex AMI-7000) (Figure 5.10).

Band	Length (bp)	Accession number	Phylogenetic group (RDP)	Reference species, strain or uncultivated microorganism (environmental source)	Accession number	H (%)
1=4	495	JQ394939	<i>Bacteroidetes</i>	Uncultured (ASBR reactor treating swine waste)	GQ134808	100
2	498	JQ394940	<i>Bacteroidetes</i> <i>Porphyromonadaceae</i>	Uncultured (MFC with phosphate buffer and Acetate)	GQ152958	99
3	517	JQ394941	<i>Bacteroidetes</i>	<i>Proteiniphilum acetatigenes</i> strain TB107 ^T Uncultured (biogas reactor) <i>Sphingobacterium thermophilum</i> strain CKTN2 ^T	NR_043154 HG007883 NR_108120	98 99 87
5	325	JQ394943	<i>Bacteroidetes</i> <i>Porphyromonadaceae</i>	Uncultured (anodic biofilm of double-chamber MFC) <i>Proteiniphilum acetatigenes</i> strain TB107 ^T	JX944537 NR_043154	98 95
7	476	JQ394944	<i>α-proteobacteria</i>	<i>Brevundimonas olei</i> strain MJ15 ^T	GQ250440	91
9	484	JQ394946	<i>Bacteroidetes</i>	Uncultured (ASBR treating swine waste)	GQ134808	100
16=44	516	JQ394947	<i>Bacteroidetes</i> <i>Porphyromonadaceae</i>	Uncultured (biofilm from electrode material in a MFC) <i>Proteiniphilum acetatigenes</i> strain TB107 ^T	JQ724340 NR_043154	98 96
17	522	JQ394948	<i>Bacteroidetes</i>	Uncultured (biogas reactor)	AB826041	99
21=28	516	JQ394950	<i>B-proteobacteria</i> <i>Alcaligenaceae</i>	<i>Kerstersia gyiorum</i> strain LMG 5906 ^T	NR_025669	99
22=43	484	JQ394951	<i>Bacteroidetes</i>	Uncultured (ASBR treating swine waste)	GQ134808	97
24	331	JQ394952	<i>Bacteroidetes</i>	Uncultured (biogas reactor) <i>Cytophaga fermentas</i> strain NBRC15936 ^T	HG007883 AB517712	91 86
26	522	JQ394954	<i>γ-proteobacteria</i>	<i>Pseudomonas xiamenensis</i> strain JD6	JQ246783	91
36	504	JQ394959	<i>Acholeplasmataceae</i> <i>Tenericutes</i>	<i>Tenericutes bacterium</i> P19x10x-fac	JQ411296	93
41	344	JQ394960	<i>Deferribacteres</i>	Uncultured (anaerobic microbial consortium growing in MFC anode fed with microalgal biomass) <i>Geovibrio thiophilus</i> strain AAFu3	JN676221 NR_028005	86 87
42	453	JQ394961	<i>B-proteobacteria</i> <i>Alcaligenaceae</i>	<i>Alcaligenes faecalis</i> strain G	KJ000880	99
45	501	JQ394964	<i>B-proteobacteria</i> <i>Alcaligenaceae</i>	<i>Alcaligenes faecalis</i> strain CPO 4.0058	KF921605	99
46	357	JQ394965	<i>α-proteobacteria</i>	<i>Brevundimonas</i> sp. P10	JX908719	93
52	428	JQ394966	<i>α-proteobacteria</i> <i>Phyllobacteriaceae</i>	<i>Defluviobacter lusatiensis</i> strain ST39	FJ982919	96

The most homologous sequence and the closest phylogenetically relevant match are shown (preferably type strains¹).

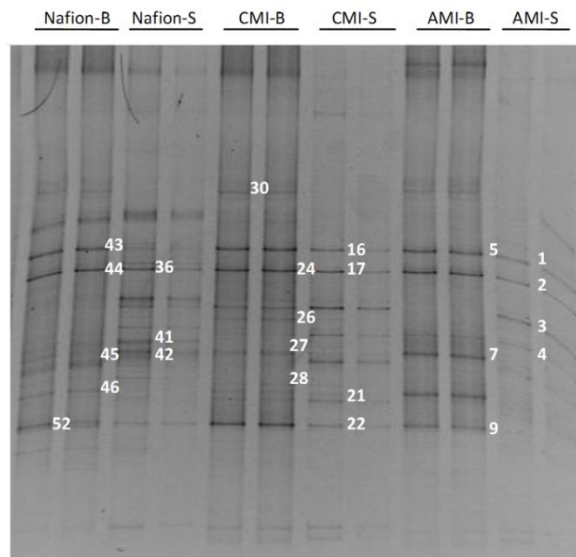


Figure 5.10. DGGE profile 16S rRNA for the total eubacteria community. Nafion-B: biofilm of the MFC equipped with Nafion N-117; Nafion-S: supernatant of the MFC (Nafion N-117); CMI-B: biofilm of the MFC (Ultrex CMI-7000); CMI-S: supernatant of the MFC (Ultrex CMI-7000). AMI-B: biofilm of the MFC (Ultrex AMI-7000); AMI-S: supernatant of the MFC (Ultrex AMI-7000).

Table 5.4. Characteristics of the bands from the 16S rRNA DGGE archaea gel from the following samples: D.A: initial inoculums; Nafion-B: biofilm of the MFC equipped with Nafion N-117; Nafion-S: supernatant of the MFC (Nafion N-117); CMI-B: biofilm of the MFC (Ultrex CMI-7000); CMI-S: supernatant of the MFC (Ultrex CMI-7000). AMI-B: biofilm of the MFC (Ultrex AMI-7000); AMI-S: supernatant of the MFC (Ultrex AMI-7000) (**Figure 5.8**).

Band	Length (bp)	Accession number	Phylogenetic group (RDP)	Reference species, strain or uncultivated microorganism (environmental source)	Accession number	H (%)
10	488	JQ394967	<i>Methanomicrobia</i> <i>Methanosetaeaceae</i>	<i>Methanosaeta concilii</i> strain Opfikon ^T	NR_028242	99
13=15=38	488	JQ394968	<i>Methanomicrobia</i> <i>Methanosetaeaceae</i>	Anaerobic <i>methanogenic archaeon</i> E15-4	AJ244290	99
21=28	488	JQ394970	<i>Methanomicrobia</i> <i>Methanomicrobiaceae</i>	<i>Methanoculleus bourgensis</i> strain Mcu(1)	JN413087	99
22=23	491	JQ394971	<i>Thermolasmata</i>	<i>Thermoplasmata archaeon</i> Kjm51s	AB749767	100
35=36	486	JQ394977	<i>Methanomicrobia</i> <i>Methanosarcinaceae</i>	<i>Methanosarcina barkeri</i> strain DSM 800 ^T	NR_025303	99
39=27	486	JQ394979	<i>Methanomicrobia</i> <i>Methanosarcinaceae</i>	<i>Methanosarcina soligelidi</i> strain SMA-21 ^T <i>M. barkeri</i> strain MS ^T	NR_109423 JQ346756	98 98

The most homologous sequence and the closest phylogenetically relevant match are shown (preferably type strains¹).

The unravelled low diversity high abundance of methanogenic archaea would suggest that specific methanogenic archaea could play an important role in the MFC performance. In this regard, Chung and Okabe 2009 reported FISH and SEM images where methanogenic archaea were colonizing the anode surface in concomitance with several eubacteria. Moreover, Croese *et al.* 2013 reported the presence of methanogenic archaea in the bulk between electrode fibres, but in this case, they are not physically attached to the anode. Besides, it has been reported that some methanogens can directly reduce solid iron Fe (III) oxide,⁵ pointing out the possibility that methanogenic archaea could contribute to electricity generation by means of exoelectrogenic strategies, which is being reinforced in recent experiments by Rotaru *et al.*, 2014 and Malvankar *et al.*, 2014, where it has been reported that methanogenic archaeae, like *Methanosaeta* and *Methanosarcina* species, are capable of exchange electrons via direct interspecies electron transfer and this would have outstanding implications in the field of anaerobic digesters and MFCs.

5.4. Conclusions

Microbial community population profiles show a clear enrichment in specific microbial ribotypes regardless of the type of membrane tested. Concerning the electrochemical activity, different patterns depending on the type of membrane were observed. The highest power density values were obtained with the MFC equipped with the N-117 membrane. These differences indicate that the eubacterial community was not affected by membrane materials, while the archaeal counterpart appears to be highly dependent on the type of membrane used, as evidencing by the selective enrichment of *Methanosarcina* spp. in the MFC equipped with cationic membranes, especially with Nafion (N-117). The specific microbial diversity contained in the anode biofilm and the minor extent of crystallite deposition in the N-117 membrane could explain the highest potential and power density achieved with this set-up.

Based on our results it has been proposed that further studies are needed in order to better understanding synergic eubacteria and methanogenic archaea interactions in BES reactors such as MFC community.

5.5. References

Abrevaya, X.C., Sacco, N., Mauas, P.J., Cort'on, E., 2011. Archaea-based microbial fuel cell operating at high ionic strength conditions. *Extremophiles*. 15, 633-642.

- Beecroft, N.J., Zhao, F., Varcoe, JR., Slade, R.C.T., Thumser, A.E., Avignone-Rossa, 2012. Dynamics changes in the microbial community composition in microbial fuel cells fed with sucrose. *Appl. Microbiol. Biotechnol.* 93, 423-437.
- Bond, D.R., Lovley, D.R., 2002. Reduction of Fe(III) oxide in the presence and absence of extracellular quinones. *Environ. Microbiol.* 4, 115-124.
- Bonmatí, A., Sotres, A., Mu, Y., Rozendal, R., Rabaey, K., 2013. Oxalate degradation in a bioelectrochemical system: reactor performance and microbial community characterization. *Bioresour. Technol.* 143, 147-153.
- Chung, K., Okabe, S., 2009. Continuous power generation and microbial community structure of the anode biofilms in a three-stage microbial fuel cell system. *Appl. Microbiol. Biotechnol.* 83 965-977.
- Croese, E., Keesman, K.J., Widjaja-Greefkes, H.C.A., Geelhoed, J.S., Plugge, C.M., Sleutels, T.H.J.A., Stams, A.J.M., Euverink, G-J.W., 2013. Relating MEC population dynamics to anode performance from DGGE and electrical data. *Syst. Appl. Microbiol.* 36, 408-416.
- Dhar, Br., Lee, H.S., 2013. Membranes for bioelectrochemical systems: challenges and research advances. *Environ. Technol.* 34,1751-64.
- Eggleston, C.M., Vörös, J., Shi, L., Lower, B.H., Droubay, T.C., Colberg, P.J.S., 2008. Binding and direct electrochemistry of OmcA, an outer-membrane cytochrome from an iron reducing bacterium, with oxide electrodes: A candidate biofuel cell system. *Inorg. Chim. Acta.* 361, 769-777.
- Franks, A., 2012. What's current with electric microbes?. *J. Bacteriol. Parasitol.* 3(9), e116.
- Hales, B.A., Edwards, C., Ritchie, D.A., Hall, G., Pickup, R.W., Saunders, J.R., 1996. Isolation and identification of methanogen-specific DNA from blanket bog peat by PCR amplification and sequence analysis. *Appl. Environ. Microbiol.* 62, 668-675.
- Hamelers, H., Ter, Heijne, A., Sleutels, T.H., Jeremiasse, A.W., Strik, D.P., Buisman, C.J., 2010. New applications and performance of bioelectrochemical systems. *Appl. Microbiol. Biotechnol.* 85, 1673-85.
- Higgins, S.R., López, R.J., Pagaling, E., Yan, T., Cooney, M.J., 2013. Towards a hybrid anaerobic digester-microbial fuel cell integrated energy recovery system: An overview of the development of an electrogenic biofilm. *Enzyme Microb. Technol.* 52, 344-351.
- Ieropoulos, I.A., Winfield, J., Greenman, J., Melhuish, C., 2010. Small scale microbial fuel cells and different ways of reporting output. *ECS Trans.* 28, 1-9.
- Jung, S.H., Regan, J.M., 2007. Comparison of anode bacterial communities and performance in microbial fuel cells with different electron donors. *Appl. Microbiol. Biotechnol.* 77, 393-402.
- Kennes, C., Cox, H.H.J., Harder, W., 1996. Design and performance of biofilters for the removal of alkylbenzene vapors. *Chem. Technol. Biotechnol.* 66, 300-304.
- Kiely, P.D., Cusick, R., Call, D.F., Selembo, P.A., Regan, J.M., Logan, B.E., 2011. Anode microbial communities produced by changing from microbial fuel cell to microbial

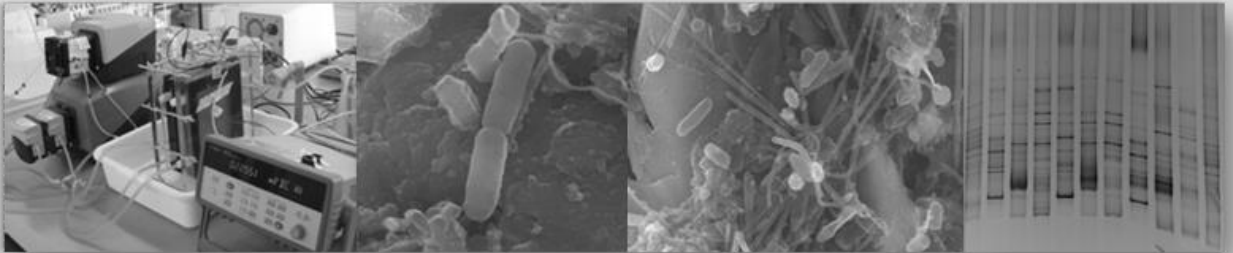
- electrolysis cell operation using two different wastewaters. *Bioresour. Technol.* 102, 388-394.
- Kim, J.R., Cheng, S., Oh, S.E., Logan, B.E., 2007. Power generation using different cation, anion, and ultrafiltration membranes in microbial fuel cells. *Environ. Sci. Technol.* 41, 1004-1009 (2007).
- Liu, H., Logan, B.E., 2004. Electricity generation using an air-cathode single chamber microbial fuel cell in the presence and absence of a proton exchange membrane. *Environ. Sci. Technol.* 38, 4040-4046.
- Logan, B.E., Regan, J.M., 2006. Electricity-producing bacterial communities in microbial fuel cells. *Trends Biotechnol.* 14, 512-518.
- Logan, B.E., Hamelers, B., Rozendal, R., Schröder, U., Keller, J., Freguia, S., Aelterman, P., Verstraete, W., Rabaey, K., 2006. Microbial fuel cells: Methodology and technology. *Environ. Sci. Technol.* 40, 5181-5192 (2006).
- Malvankar, N.S., Lovley, D.R., 2014. Microbial nanowires for bioenergy applications. *Curr. Opin. Biotechnol.* 27, 88-95 (2014).
- Muyzer, G., DeWaal, E.C., Uitterlinden, A.G., 1993. Profiling of complex microbial populations by denaturing gradient gel electrophoresis analysis of polymerase chain reaction-amplified genes coding for 16S rRNA. *Appl. Environ. Microbiol.* 59, 695-700.
- Nevin, K.P., Richter, H., Covalla, S.F., Johnson, J.P., Woodard, T.L., Orloff, A.L., Jia, H., Zhang, M., Lovley, D.R., 2008. Power output and columbic efficiencies from biofilms of *Geobacter sulfurreducens* comparable to mixed community microbial fuel cells. *Environ. Microbiol.* 10, 2505-2514.
- Oh, S.T., Kim, J.R., Premier, G.C., Lee, T.H., Kim, C., Sloan, W.T., 2010. Sustainable wastewater treatment: How might microbial fuel cells contribute. *Biotechnol. Adv.* 28, 871-881.
- Palatsi, J., Illa, J., Prenafeta-Boldú, F.X., Laureni, M., Fernandez, B., Angelidaki, I., Flotats, X., 2010. Long-chain fatty acids inhibition and adaptation process in anaerobic thermophilic digestion: Batch tests, microbial community structure and mathematical modelling. *Bioresour. Technol.* 101, 2243-2251 (2010).
- Pant, D., Van, Bogaert, G., Diels, L., Vanbroekhoven, K., 2010. A review of the substrates used in microbial fuel cells (MFCs) for sustainable energy production. *Bioresour. Technol.* 101, 1533-1543.
- Park, D.H., Zeikus, J.G., 2000. Electricity generation in microbial fuel cells using neutral red as an electronophore. *Appl. Environ. Microbiol.* 66, 1292-1297.
- Pham, T.H., Boon, N., Aelterman, P., Clauwaert, P., De Schampelaire, L., Vanhaecke, L., De Maeyer, K., Höfte, M., Verstraete, W., Rabaey, K., 2008. Metabolites produced by *Pseudomonas* sp. enable a Gram-positive bacterium to achieve extracellular electron transfer. *Appl. Microbiol. Biotechnol.* 77, 1119-1129.
- Pham, T.H., Rabaey, K., Aelterman, P., Clauwaert, P., De Schampelaire, L., Boon, N., Verstraete, W., 2006. Microbial fuel cells in relation to conventional anaerobic digestion technology. *Eng. Life Sci.* 6, 285-292.

- Prenafeta-Boldú, F.X., Guivernau, M., Gallastegui, G., Viñas, M., de Hoog, G.S., Elías, A., 2012. Fungal/bacterial interactions during the biodegradation of TEX hydrocarbons (toluene, ethylbenzene and *p*-xylene) in gas biofilters operated under xerophilic conditions. *FEMS Microbiol. Ecol.* 80, 722-734.
- Rabaey, K., Boon, N., Siciliano, S.D., Verhaege, M., Verstraete, W., 2004. Biofuel cells select for microbial consortia that self-mediate electron transfer. *Appl. Environ. Microbiol.* 70, 5373-5382.
- Rabaey, K., Lissens, G., Siciliano, S.D., Verstraete, W., 2003. A microbial fuel cell capable of converting glucose to electricity at high rate and efficiency. *Biotechnol. Lett.* 25, 1531-1535.
- Rabaey, K., Lissens, G., Verstraete W. Microbial fuel cells: performances and perspectives. In: Lens P, Westermann P, Haberbauer M, Moreno A, editors. *Biofuels for fuel cells: renewable energy from biomass fermentation*. London, UK: IWA Publishing; 2005. p. 377–99.
- Richter, H., Mc Carthy, K., Nevin, K.P., Johnson, J.P., Rotello, V.M., Lovley, D.R., 2008. Electricity generation by *Geobacter sulfurreducens* attached to gold electrodes. *Langmuir.* 24, 4376-4379.
- Ringeisen, B.R., Henderson, E., Wu, P.K., Pietron, J., Ray, R., Little, B., Biffinger, J.C., Jones-Meehan, J.M., 2006. High power density from a miniature microbial fuel cell using *Shewanella oneidensis* DSP10. *Environ. Sci. Technol.* 40, 2629-2634.
- Rodríguez-Abalde, A., Juznic-Zonta, Z., Fernández, B., 2010. Anaerobic co-digestion of treated slaughterhouse wastes, in: *Libro de Actas del II Congreso Español de Gestión Integral de Deyecciones Ganaderas, International Workshop on Anaerobic Digestion of Slaughterhouse Waste*, ed by Bonmatí A, Palatsi J, Prenafeta-Boldú FX, Fernández B and Flotats X. Service Point, Barcelona, pp. 347-356.
- Rotaru, A., Shrestha, P., Liu, F., Shrestha, M., Shrestha, D., Embree, M., Zengler, K., Wardman, C., Nevin, K.P., Lovley, D.R., 2014. A new model for electron flow during anaerobic digestion: direct interspecies electron transfer to *Methanosaeta* for the reduction of carbon dioxide to methane. *Energy Environ. Sci.* 7, 408-415.
- Rozendal, R.A., Hamelers, H.V.M., Buisman, C.J.N., 2006. Effects of membrane cation transport on pH and microbial fuel cell performance. *Environ. Sci. Technol.* 40, 5206-5211.
- Rozendal, R.A., Hamelers, H.V.M., Rabaey, K., Keller, J., Buisman, C.J.N., 2008. Towards practical implementation of bioelectrochemical wastewater treatment. *Trends Biotechnol.* 26, 450-459.
- Schröder, U., 2007. Anodic electron transfer mechanisms in microbial fuel cells and their energy efficiency. *Phys. Chem. Chem. Phys.* 9, 2619-2629.
- Sun, Y.J., Zuo, J.E., Cui, L.T., Dang, Y., 2008. Analysis of microbial diversity in microbial fuel cells under different wastewater. *China Environ. Sci.* 28, 1068-1073.
- Wrighton, K.C., Agbo, P., Warnecke, F., Weber, K.A., Brodie, E.L., DeSantis, T.Z., Hugenholtz, P., Andersen, G.L., Coates, J.D., 2008. A novel ecological role of the Firmicutes identified in thermophilic microbial fuel cells. *ISME J.* 2, 1146-1156.

Yu, Z., Morrison, M., 2004. Comparisons of different hypervariable regions of *rrs* genes for use in fingerprinting of microbial communities by PCR-denaturing gradient gel electrophoresis. *Appl. Environ. Microbiol.* 70, 4800-4806.

Chapter 6

Microbial community dynamics in a continuous microbial fuel cell fed with synthetic wastewater and pig slurry



Sotres, A., Tey, L., Bonmati, A. Viñas, M. (2015)
Submitted to peer reviewed journal

Abstract

Two-chambered microbial fuel cells (MFCs) were operated with synthetic media and pig slurry under a continuous fed mode. Additionally, the use of 2-bromoethanesulfonate (BES-Inh.) to prevent methanogenesis was studied. Synthetic-fed MFC (MFC_{SW}) showed a maximum power density (PD_{max}) of 2138.2 mW m⁻³, and the addition of BES-Inh. (10 mM) did not show any improvement on the performance (PD_{max} = 2077.5 mW m⁻³). When pig slurry was used as fed (MFC_{PS}), PD_{max} increased till (5622.7 mW m⁻³). Microbial community composition was affected by the type of substrate used. While, *Brachymonas* sp., *Alcaligenes* sp., *Delftia* sp., *Massilia* sp., *Acidovorax* sp., and *Pseudomonas* sp. belonging to *Proteobacteria* were the most representative phlotypes with synthetic medium, *Clostridium* sp., *Acholeplasma* sp., and *Syntrophomonas* sp., belonging to *Firmicutes*, and *Paludibacter* sp. and *Meniscus* sp., belonging to *Bacteroidetes* were predominant when pig slurry was used as feed. Despite all the difference in the microbial community, 6 OTUs belonging to *Comamonadaceae*, *Intrasporangiaceae*, *Flavobacteriaceae* and *Porphyromonadaceae*, were common in both biofilms, and therefore they could be consider the core microbiome of the system. Otherwise, the eubacterial microbial community composition was strongly modified by the addition of BES-Inh., promoting enrichment in *Bacteroidetes* and *Firmicutes* phyla, while *Spirochaetes* and *Actinobacteria* were newly identified under this condition. Contrary, archaeal community was less affected by the addition of BES-Inh. and *Methanosarcina* sp., appeared roughly in the same relative abundance in both situations.

6.1. Introduction

In a microbial fuel cell (MFC), microorganisms can convert chemical energy present in organic compounds directly into electricity by transferring electrons to an anode (Logan and Regan, 2006). The formation of a biofilm on the anode surface is essential for the efficient transfer of electrons in a MFC (Franks et al., 2010). These microorganisms can use a wide range of substrates from pure and mineral compounds to complex organic compounds present in wastewater (Pant et al., 2010). Hence, depending on the substrates feed, the microbial community as well as the MFC performance might be different.

Up to date, many studies have investigated the effect of synthetic substrates on MFC performance and microbial diversity; nevertheless, fewer studies have focused on the effect of using complex substrates (e.g. pig slurry). Otherwise, the study of microbial communities on anodes is being increasingly investigated in

order to understand the electron transfer mechanisms and current generation by anode biofilm microorganisms (Lovley, 2006; Rabaey et al., 2007). For application purposes, mixed cultures are more appropriate, as generally pure cultures are not able to produce such a high power, and the range of organic compounds metabolizable is limited.

It is well known that methanogens compete with anodophiles for substrate and thus the efficiency, in terms of power generation and coulombic efficiency (CE) of the MFCs (Rajesh et al., 2014). Both exoelectrogens and methanogens present similar growth conditions, therefore there is an active competition for the substrate in the anodic chamber (Chae et al., 2009; Freguia et al., 2007b). Especially, methane production is common in MFCs which have been inoculated with inocula from anaerobic digesters. Therefore, there has been an increasing interest in searching strategies to inhibit the methanogenesis, and thus avoiding a decrease on the MFC performance.

So far, many types of methanogenesis inhibitors have been previously described (Liu et al., 2011), standing out the 2-bromoethanesulfonate ($\text{BrCH}_2\text{CH}_2\text{SO}_3^-$) (BES-Inh.), due to its specificity as inhibitor of methanogenesis from acetate (acetoclastic pathway) (Nollet et al., 1997; Zinder et al., 1984). BES-Inh. is a structural analogue of coenzyme M (2-mercaptoethanesulfonic acid, HS-CoM) only present in methanogenic archaea and is directly involved in the final enzymatic reaction in methane biosynthesis (Chiu and Lee, 2001) (**Figure 6.1**). BES-Inh. binds to methylreductase, a membrane bound enzymatic system, thus avoiding methane formation. Several analogues have been found to be methylreductase inhibitors, being the most efficient 2-bromoethanesulfonate (DiMarco et al., 1990).

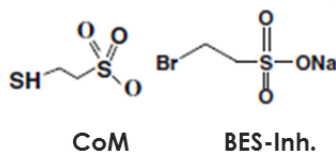


Figure 6.1. The structure of the CoM of methanogens and the BES-Inh. analog.

Although, effective concentrations vary depending on the application system (Liu et al., 2011), most of these studies are related with reactor performance; but, so far, knowledge about their effects over the microbial community composition is limited.

As aforementioned above exoelectrogens and methanogens are in an active competition for the substrate in the anodic chamber, but the possibility that methanogenic archaea could establish syntrophic relationship with exoelectrogenic microorganisms is being intensively study in last years (Rotaru et al., 2014; Liu et al., 2012). These works reported that methanogenic archaea (*Methanosaeta* and *Methanosarcina* sp.) can form syntrophic associations with a *Geobacter* species via direct electron transfer. A better understanding of these syntrophic relationships could have implications in the anodophilic microbial community and in the overall MFC performance. As far as we know, up to date, the eubacteria and archaea community shifts in the anode biofilm after the addition of BES has not been studied with 454-pyrosequencing.

The objectives of the present study, were i) to evaluate the performance of two MFCs operating with different inocula (anaerobic inoculum and MFC inoculum), and different substrates types, synthetic wastewater and liquid fraction of pig slurry; ii) to study the evolution over time of the microbial community developed on the anodic chamber under these different operational conditions; and iii) to evaluate the effect of 2-bromoethanesulfonate on the microbial community established in the anodic biofilm aiming to find out putative exoelectrogenic microorganisms hampered by active methanogenic microbial communities.

6.2. Materials and methods

6.2.1. MFC configuration

Two identical two-chamber MFC were used in this study. The two MFCs were constructed with methacrylate plates, each chamber had a size of 0.14 x 0.12 x 0.02 m³, separated by a cation exchange membrane (CEM) (14x12 cm) (Ultrex CMI-7000, Membranes International Inc., Ringwood, NJ, USA). The anodes were made of granular graphite (2 to 6 mm diameter) (El Carb 100, Graphite Sales Inc., U.S.A.) and Carbon felt, 3.18 mm thick, 99.0% (Cymit Química, S.L.), resulting in a net anode volume (NAV) of 165 mL and 269 mL for the MFC fed with synthetic wastewater (MFC_{sw}) and the MFC fed with pig slurry (MFC_{ps}) respectively, and a net cathode volume of 250 mL (NCV) for both MFCs. The cathodes were made with stainless steel mesh in both cases. The anode and cathode were connected to 1000, 500 and 100 Ω external resistors. Prior to its use, both electrodes, granular graphite and carbon felt, were sequentially soaked in 1M of HCL, and 1M of NaOH, in each case for 24 hours, and finally rinsed in deionised water, in order to remove organic and inorganic impurities.

6.2.2. MFC operation

The MFC_{SW} was feed with synthetic wastewater containing (per litre) CaCl₂ 0.0147 g; KH₂PO₄, 3 g; Na₂HPO₄, 6 g; MgSO₄, 0.246 g; and 1 mL trace elements solution per litre was prepared as described elsewhere (Lu et al. 2006), and CH₃COONa and NH₄Cl, as carbon and nitrogen source respectively. Their concentrations were increased along the experiment ranged between 0.46-2.91 g · L⁻¹ for CH₃COONa and 0.26-3.82 g · L⁻¹ for NH₄Cl. The catholyte used in both MFC consisted of buffer phosphate (KH₂PO₄, 3 g L⁻¹ and Na₂HPO₄ 6 g L⁻¹). 2-bromoethanesulfonate (BES-Inh.) was added to the synthetic medium in a ranged between 0.16-10Mm in the experiments to study the effect of BES over the microbial community and over the MFC performance. The cell was inoculated with biomass taken from a bench-scale mesophilic methanogenic digester continuously stirred reactor fed with slaughterhouse waste (In.AD).

The MFC_{PS} was feed with liquid fraction of pig slurry (PS) collected from the farm Sat Caseta d'en Grau (Calldetenes, Catalonia). The characterization of PS used for the experiments, previously sieved, was: pH, 7.72; total and soluble chemical oxygen demand, COD_t (mg O₂ kg⁻¹), 6908; COD_s (mg O₂ kg⁻¹), 3462; N-NH₄⁺ (mg N-NH₄⁺ · N L⁻¹), 858.15; Kjeldahl-N (mg N L⁻¹), 1068.47; TS (%), 0.78; VS (%), 0.42 and EC (mS cm⁻¹), 7.73. In order to procure the expected concentrations for the different assays, specific dilutions were carried out. The inoculum used in the MFC_{PS} was the anode biofilm from the MFC_{SW} after one year of operation named B₂ MFC_{SW}. A schematic diagram of the inoculum and feeding used for both MFCs and the samples collected are illustrated in **Figure 6.2.**, and an overview of the operational conditions during experiments is described in **Table 6.1.**

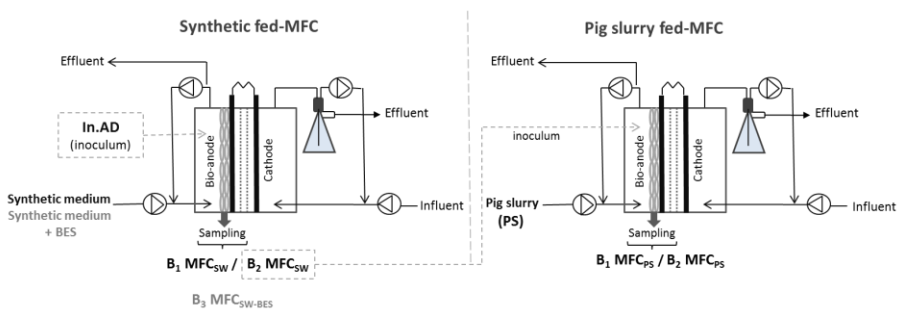


Figure 6.2. Schematic diagram of both two chambered MFCs, and the biofilm samples collected from the anode compartments.

Table 6.1. Overview of the operational conditions during experiments with synthetic and pig slurry feeding.

	Synthetic-fed MFC (MFC _{SW})				Pig slurry-fed MFC (MFC _{PS})			
	PI	PII	PIII	PIV	PI ^a	PII	PIII	PIV
OLR (g COD L ⁻¹ d ⁻¹)	0.7	1.7	9.1	8.6	0.7	3.0	5.4	10.7
NLR (g N-NH ₄ L ⁻¹ d ⁻¹)	0.3	0.5	4.2	4.2	2.0	2.7	4.7	7.4
HRT (h) (anode)	7.0	6.2	7.6	9.5	6.9	7.2	8.1	7.6
[BES]mM	n.a.	n.a.	n.a.	0.16-10	n.a.	n.a.	n.a.	n.a.
Biofilm sample	B ₁ MFC _{SW}	-	B ₂ MFC _{SW}	B ₃ MFC _{SW-BES}	-	B ₁ MFC _{PS}	-	B ₂ MFC _{PS}

n.a. = not applicable

PI^a = during this period the MFC_{PS} was feeding with synthetic medium (0-26 days)

6.2.3. Chemical and electrochemical measurements

The voltage (V) was measured using a multimeter data acquisition unit (Mod. 34970A, Agilent Technologies, Loveland, CO, USA). The current density (*I*) was then calculated using Ohm's Law, and the maximum power density (PD_{max}), open circuit voltage (OCV) and internal resistance (*R*_{int}) were obtained through polarization curves following the procedure described by Sotres et al., 2014.

The chemical oxygen demand (COD) was measured following an optimized APHA–AWWA–WPCF Standard Method 5220 (Noguerol et al., 2012) and filtering the samples through a 0.45 μm pore diameter Nylon syringe filter (Scharlau, S.L.). Coulombic efficiency (*CE*), defined as the ratio of electrons used as current to the theoretical maximum electron production, was calculated as described elsewhere (Logan et al., 2006).

Methane was determined by a CP-3800 gas chromatograph (Varian, USA) fitted with Haysep-Q 80-100 Mesh (2mx1/8" × 2.0mm) column (Varian, USA) and thermal conductivity detector (TCD). Helium was used as carrier gas (45 ml min⁻¹) and the temperature of the injection port, oven and detector were 50, 150 and 180°C, respectively.

6.2.4. Anode community characterization

6.2.4.1 Biofilm morphology

In order to determinate the biofilm morphology, samples from biofilm were examined with SEM microscopy (mod. Hitachi S-4100FE). A small portion of granular graphite and carbon felt (both biofilm-harboring) were carefully removed from the anodic compartment of both MFCs. Biofilm were fixed immersing samples in 2%

glutaraldehyde buffer at pH 7.4. Then, samples were dried and sputter-coated with a graphite layer. As a control, both electrodes without biofilm were also examined.

6.2.4.2. DNA extraction and PCR amplification

Genomic DNA was extracted in triplicate from the granular graphite and carbon felt with the PowerSoil® DNA Isolation Kit (MoBio Laboratories Inc., Carlsbad, CA, USA), following the manufacturer's instructions. Two primer sets were used to amplify eubacterial and archaeal partial 16S rRNA genes. Universal eubacterial forward F341-GC and reverse R907 primers were used to amplify the hypervariable V3-V5 region by a polymerase chain reaction (PCR) (Yu and Morrison, 2004). For archaeal population a Nested PCR approach was performed by using the primer pairs ArchF0025/R1517, and F344/R915-GC for the nested and PCR reaction respectively (Palatsi et al., 2010). All PCR reactions were carried out in a Mastercycler (Eppendorf, Hamburg, Germany) and the PCR samples were checked on a 1% agarose gel for size of the product.

6.2.4.3. DGGE molecular profiling

The eubacterial and archaeal community populating the electrodes of both MFC setups were analysed by means of Denaturing gradient gel electrophoresis (DGGE). Amplicons (20 µL) were run on an 8% (w/v) polyacrylamide gel (0.75 mm thick) containing a formamide (40% (w/v)) and urea (7M) denaturant gradient of 30-70%. Gels were run in a DGGE-4001 system (CBS Scientific Company Inc., Del Mar, CA, USA) at 100 V and 60°C for 16h in a 1x TAE buffer solution (40 mM Tris, 20 mM sodium acetate, 1 mM EDTA, pH 7.4) (Muyzer et al., 1993).

The bands were excised from the gel for subsequent identification. These bands were previously suspended in 50 µL of molecular biology grade water and stored at 4 °C overnight and subsequently reamplified by PCR. Then, amplicons of the expected size were sequenced following Sanger's method at Macrogen (Macrogen, the Netherlands).

Sequences were processed using the BioEdit software package v.7.0.9 (Ibis Biosciences, Carlsbad, CA, USA) and aligned with the BLAST basic local alignment search tool (NCBI, Bethesda, MD, USA) and the Naïve Bayesian Classifier tool of RDP (Ribosomal Database Project) v.10 (East Lansing, MI, USA) for the taxonomic assignment.

6.2.4.4. 454-pyrotag sequencing of massive 16S rRNA gene libraries pyrosequencing

Total DNA extract was used for pyrosequencing purposes. Each sample was amplified with 16S rRNA eubacteria and archaea genes. The primer set used was 27Fmod (5'-AGRGTTTGATCMTGGCTCAG-3') / 519R modBio (5'-GTNTACNGCGGCKGCTG-3') (Kuske et al., 2006; Callaway et al., 2009) and Arch 349F (5'-GYGCASCAGKCGMGAAW-3') / Arch 806R (5'-GGACTACVSGGTATCTAAT-3') (Takaii and Horikoshi 2000) for the eubacterial and archaeal analysis population. For the amplification 2µl of each DNA was used and reaction was carried out in 50 µl which contained 0.4 mM of fusion primers, 0.1 mM of dNTPs, 2.5 U of Taq ADN polymerase (Qiagen) and 5 µl of reaction buffer (Qiagen). The PCR amplification operated with the following protocol: 30 s at 95 °C, followed by 30 cycles at 94 °C for 30 s, annealing at 55 °C for 30 s, extension at 72 °C for 10 min and the PCR was carried out in a termocicler GeneAmp_PCRsystem 9700 (Applied Biosystems). The obtained DNA reads were compiled in FASTq files for further bioinformatic processing. Trimming of the 16S rRNA barcoded sequences into libraries was carried out using QIIME software version 1.8.0 (Caporaso et al., 2010). Quality filtering of the reads was performed at Q25 quality, prior to the grouping into Operational Taxonomic Units (OTUs) at a 97% sequence homology cutoff. The following steps were performed using QIIME: Denoising using Denoiser (Reeder and Knight, 2010). Reference sequences for each OTU (OTU picking up) were obtained via the first method of UCLUST algorithm (Edgar, 2010). For sequence alignment was used PyNASt (Caporaso et al., 2010b) and Chimera detection was used ChimeraSlayer (Haas et al., 2011). OTUs were then taxonomically classified using GreenGenes database and compiled into each taxonomic level (DeSantis and Hugenholtz, 2006; Wang et al., 2007).

6.2.4.5. Analysis of pyrosequencing data

Rarefaction curves, the microbial richness estimators (S_{obs} and $Chao1$) and diversity indices estimators ($Shannon$, $inv Simpson$ and $sampling coverage$) were calculated with the defined OTUs table (shared.file) using MOTHUR software version 1.33.3 for each sample (Schloss et al., 2009). Venn diagram analysis was performed using MOTHUR and VENNY software (Oliveros, 2007). The XLSTAT 2014 software package for multivariate analysis (Addinsoft, Paris, France) was used for performing a Correspondence Analysis (CA) on the OTUs abundance matrix of both Eubacteria and Archaeobacteria. The obtained samples and OTUs scores were

depicted in a 2D biplot, which represented the phylogenetic assignment of the predominant OTUs (relative abundance >0.5%).

6.3. Results and discussion

6.3.1. MFC performance

6.3.1.1. Synthetic-fed MFC performance

The evolution of voltage for the MFC_{SW} is shown in **Figure 6.3**. The polarization curves performed through time revealed that MFC_{SW} increased their PD_{max} and I_{max}, indicating the continued development of the biofilm. PD_{max} values were 34.4, 197.0 and 200.5 mW m⁻³ at 14, 23 and 25 weeks respectively and continued increasing in subsequent stages (**Figure 6.4a and 6.4b**). When the first biofilm sample was taken (B₁ MFC_{SW}) after 28 weeks of operation, PD_{max} was 287.1 mW m⁻³, suggesting that the exoelectrogenic biofilm was already developed. In successive periods nitrogen loading rate was increased from 0.32 to 4.2 g N-NH₄⁺ L⁻¹d⁻¹ and PD_{max} enhanced from 366.8 to 652.4 mW m⁻³. A second biofilm sample (B₂ MFC_{SW}) was sampled when the highest nitrogen loading rate (4.2 g N-NH₄⁺ L⁻¹d⁻¹) was tested and when PD_{max} was almost two-fold higher compared to the moment when B₁ MFC_{SW} was taken.

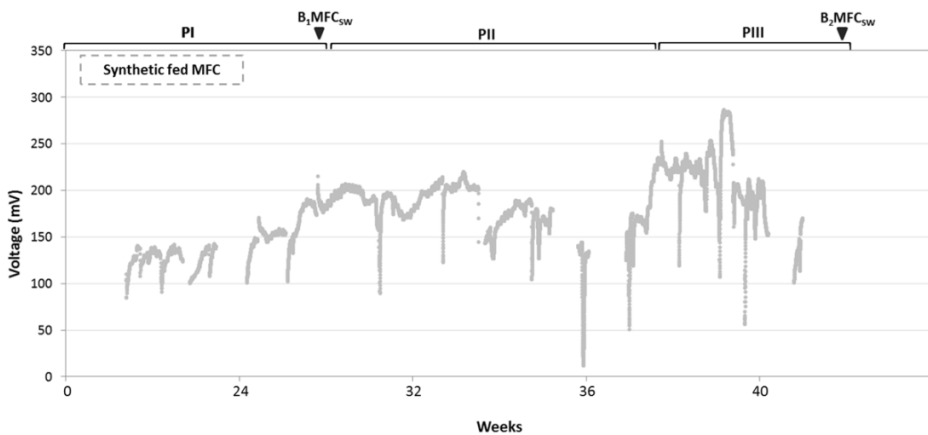


Figure 6.3. Evolution of voltage during the synthetic-fed MFC performance (R_{ext} 500 Ω).

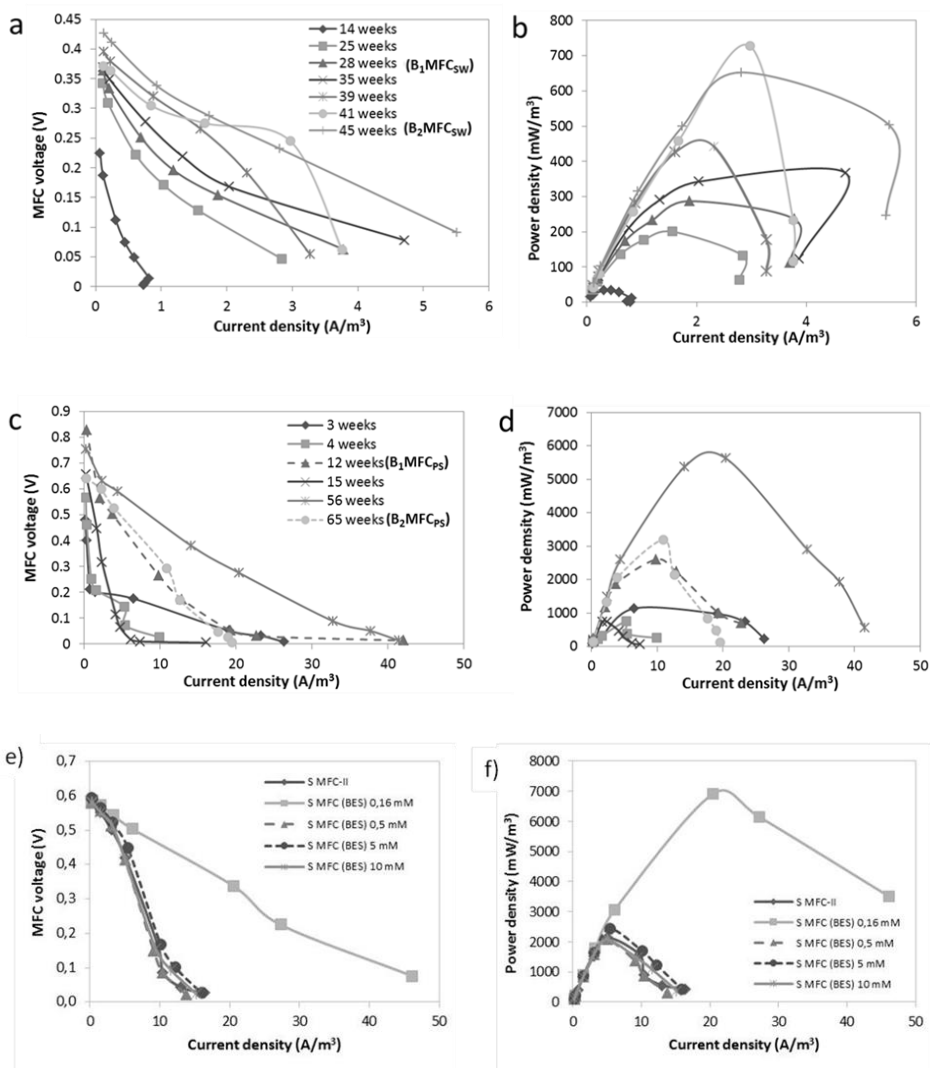


Figure 6.4. Polarization curves and power density curves (a) and (b) of synthetic fed-MFC; (c) and (d) of pig slurry-fed MFC; (e) and (f) of synthetic fed-MFC operated with different BES-Inh. concentrations.

6.3.1.2. Pig slurry-fed MFC performance

MFC_{PS} was inoculated with B₂ MFC_{SW} and feed during the first 26 days with the same synthetic wastewater as MFC_{SW}. As **Figure 6.5** shows, the voltage during the start-up of the MFC_{PS} was higher than in the MFC_{SW}. Likely the use of a biomass previously adapted to a MFC anode (B₂ MFC_{SW}) expedited the adaptation process.

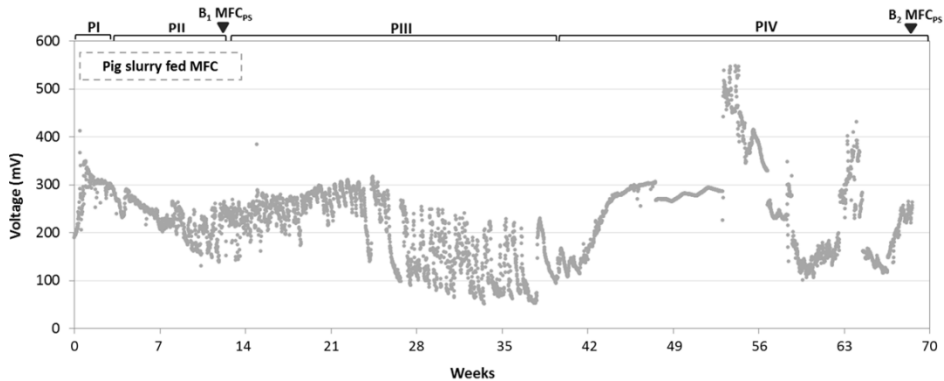


Figure 6.5. Evolution of voltage during the pig slurry-fed MFC performance (R_{ext} 500-100 Ω). This MFC was inoculated with a biomass taken from the synthetic-fed MFC (B₂ MFC_{SW}) after 45 weeks of operation.

PD_{max} increase rapidly attaining 1144.9 mW m⁻³ after 3 weeks (**Figure 6.4c and d**), slightly higher values than those obtained after 45 weeks with the synthetic-fed MFC (MFC_{SW}). This showed that the inoculum used (B₂ MFC_{SW}) was well adapted, shortening greatly the required time for the start-up of the MFC

After 26 days of acclimatization, the feed was changed to liquid fraction of pig slurry, and after 5 weeks PD_{max} reached 2608.1 mW m⁻³ and a biofilm sampled was taken (B₁ MFC_{PS}). From week 12 to week 65 organic and nitrogen loading rates were increased until 10.7 g COD L⁻¹ d⁻¹ and 7.4 g N L⁻¹ d⁻¹ respectively, with a PD_{max} of 3191.4 mW m⁻³ and at final period a sample of the anode biomass was taken (B₂ MFC_{PS}). **Figure 6.5c** and **d**, shows that higher polarization performance was achieved at weeks 12, 56 and 65, as PD_{max} results revealed.

The pig slurry-fed MFC generated higher values of PD_{max} and I_{max} compared to synthetic-fed MFC in early stages, presumably because of the initial inoculum used to start this MFC was a sample from an already running MFC after 11 months of operation (B₂ MFC_{SW}), so the start-up can be expedited. Accordingly, **Figure 6.4c and d**, showed that during the first months of operation (still fed with synthetic medium), PD_{max} attained 1144.9 and 763.5 mW m⁻³ at 3 and 4 weeks, slightly higher

values than those obtained after 45 weeks with the synthetic-fed MFC (B_2 MFC_{SW}) (Figure 6.4d).

6.3.1.3. Synthetic-fed MFC performance after the addition of BES inhibitor

Increasing BES-Inh. concentrations, from 0.16 to 10 mM, were applied in order to investigate its effect over MFC performance as well as the microbial community structure (see section 6.3.3).

Electricity generation showed that there were no significant changes during the operational period applying different BES-Inh. concentrations. The generated voltage remained between 300 – 400 mV (0.72 – 0.79 mA) (Figure 6.6). After each BES-Inh. addition a polarization curve was done (Figure 6.4e and f). The addition of BES-Inh. to the MFC_{SW}, resulted on a PD_{max} increase from 2138 $mW\ m^{-3}$ till 6924 $mW\ m^{-3}$ before and after the first BES-Inh. concentration (0.16 mM) respectively. However, in the followings additions of BES-Inh. (0.5, 5 and 10 mM) the PD_{max} remained in similar values than those obtained just before the addition BES-Inh. (2078, 2432 and 2078 $mW\ m^{-3}$). Since the BES-Inh. did not affect the MFC performance in terms of PD_{max} obtained under this range of concentration, it would be interesting to substantiate if it has caused any effect over microbial communities.

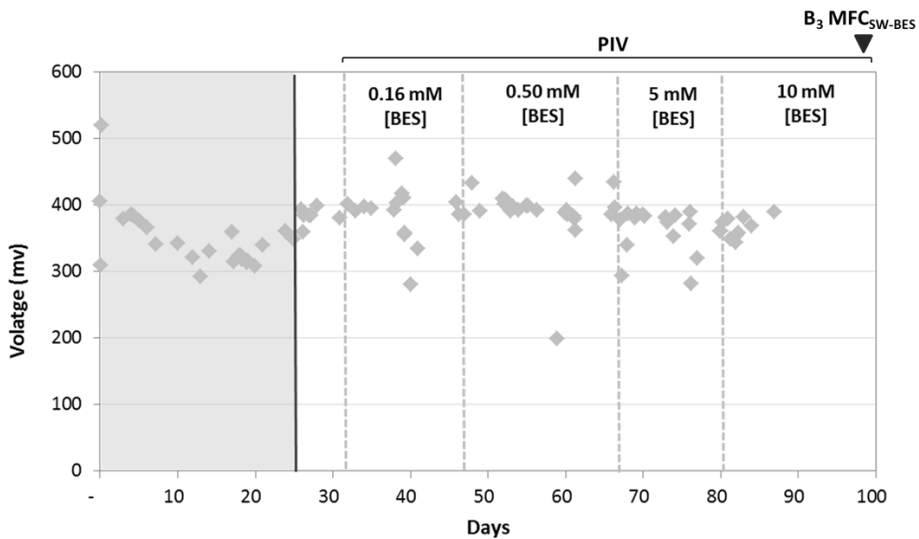


Figure 6.6. Evolution of voltage during the synthetic-fed MFC performance ($R_{ext} 500\Omega$), when BES-Inh. was added to the medium.

An overview of the outstanding parameters obtained from the polarization curves are summarized in **Table 6.2**.

Table 6.2. Electrochemical parameters obtained from the polarization curves for the synthetic wastewater and pig slurry feed MFC, and for the synthetic feed MFC before and after the addition of BES inhibitor.

		$R_{\text{internal}} (\Omega)$	$PD_{\text{max}} (\text{mW m}^{-3})$	OCV (mV)
MFC_{SW}	14 weeks	1874	34	284
	25 weeks	698	200	386
	28 weeks (B ₁ MFC _{SW})	566	287	396
	35 weeks	474	367	386
	39 weeks	570	442	402
	41 weeks	234	728	502
	45 weeks (B ₂ MFC _{SW})	416	652	428
	69 weeks	256	2138	574
MFC_{PS}	3 weeks	67	1145	533
	4 weeks	94	763	763
	5 weeks (B ₁ MFC _{PS})	57	2608	832
	8 weeks	137	746	657
	49 weeks	61	5623	717
	50 weeks (B ₂ MFC _{PS})	115	3191	613
MFC_{SW-BES}	0.16 mM [BES]	66	6924	512
	0.5 mM [BES]	250	2078	575
	5 mM [BES]	218	2432	591
	10 mM [BES]	225	2078	572

According to **Table 6.2**, the highest internal resistance (1874 Ω) is achieved in the first weeks of MFC_{SW}, which was decreasing progressively till reach the lowest values around 416-234 Ω , attributable to the growth and adaptation of a biofilm at the anode chamber. Lower internal resistance values are obtained in MFC_{PS} in all cases (ranged between 137-57 Ω) compared to those obtained in the MFC_{SW}. This could be explained for the faster adaptation of the biofilm resulting in a better MFC performance.

In the case of MFC_{SW-BES}, the internal resistance has not shown significant changes during the addition of BES-Inh. remained 200 Ω , except for the first concentration which is lower.

Although the voltage and thus the current density remained stable over time, COD degradation was roughly half lower during this period, showing similar values with the different BES-Inh. concentrations (40.5% [0.16mM], 29.1% [0.5mM], 30.5% [5mM], and 38.1% [10 mM]). With the addition of BES-Inh., it would be expected a decrease in CH₄ production. However dissolved CH₄ in the anode chamber remained stable between 36 – 45 mg CH₄ mg/L. CH₄ formed without BES-Inh. represented 6% of the COD removed, while with the addition BES-Inh. this CH₄ represented between 12-19%. Even so, CE increased slightly during this operational period, increasing from 0.27 to a range between 0.53 – 0.75%. Despite no noteworthy difference were observed before and after the addition of BES-Inh. at these concentrations, it is recommended to study the microbial community composition onto the biofilm in both cases.

6.3.2. Biofilm morphology

In order to determine the morphology of the biofilms attaching onto the anode electrodes, a small amount of biofilm harbouring granular graphite and carbon felt were taken from both MFCs feeding with synthetic and pig slurry, and analysed by means of SEM. In order to compare and confirm the presence of biofilm on the electrodes, clean electrodes were also analysed as control.

As can be seen in **Figure 6.7**, developed biofilm adhered to the granular graphite and the carbon felt is shown in panels **a** to **d**, and panels **e** to **h**, respectively. Both anode surfaces were covered by different microorganisms with different morphology and size, and this may be due to the type of feeding and electrodes material used. High amount of straight pili-like filaments, rods and cocci shape bacteria were observed in both biofilms and in some cases cells were intertwined with each other (**Figure 6.7a and h**). However, the biofilm seems to be spread over the electrode in the MFC_{SW} (**Figure 6.7a and b**) and more scattered in clumps upon the carbon felt electrode in the MFC_{PS} (**Figure 6.7h**). It can be also observed a bacteria pili-based or nanowire-like morphology in some of these images (**Figure 6.7b and d**). Moreover, in MFC_{PS} it is observed morphology that it could be a group of *Spirochaetes* represented by a group of elongated microbial cells which are helically wound (**Figure 6.7g**).

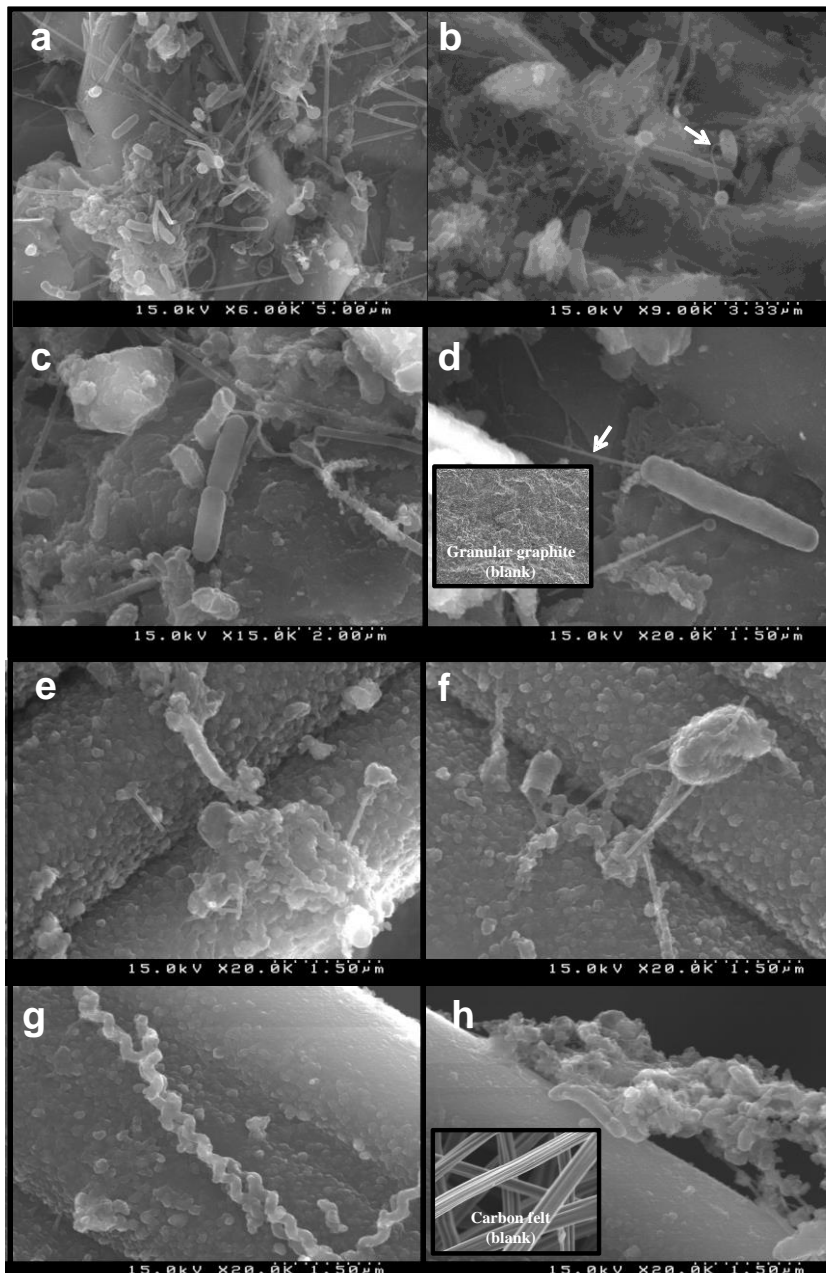


Figure 6.7. SEM images for anode biofilms; a-d) anode biofilm adhering onto granular graphite in the MFC_{sw}, and e-h) anode biofilm onto carbon felt in the MFC_{ps}. The squares in the figures on the right indicate the SEM images for both controls (granular graphite and carbon felt). The arrow indicates a typical rod cell with a long appendage-like filament.

6.3.3. Microbial community dynamics

In order to analyze the microbial community dynamics and structure and compare the microbial community adaptation over the time and under different operational conditions, such as the effect of different substrates and the effect of BES-Inh., samples were analyzed by means of 16SrRNA DGGE and 454-pyrosequencing such for bacteria and archaea.

A brief diagram of the samples that has been compared in the present work and their aim is represented in **Figure 6.8**.

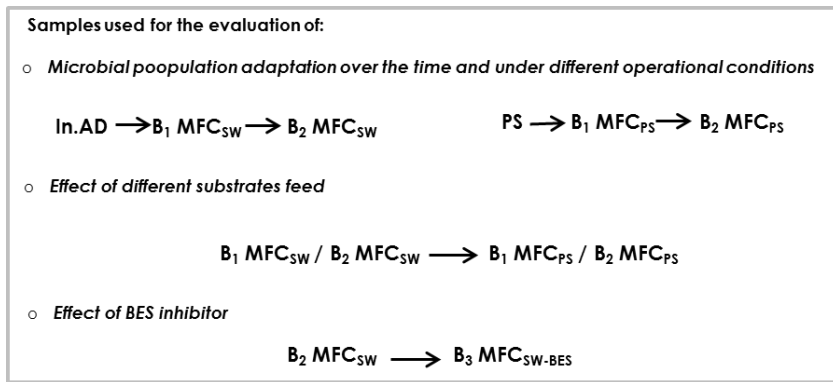


Figure 6.8. Diagram of the samples taken and compared in the present work.

The composition, dynamics and taxonomic of the bacterial communities in the anodic biofilm were also analysed foremost by means of DGGE, in order to have an overview of the band patterns and the predominant phylogenetic groups of each samples.

6.3.3.1. Microbial population adaptation over time and under different operational conditions

The MFC_{SW} analysis of the DGGE pattern (**Figure 6.9a**) revealed that the microbial diversity growing on the anode biofilm was significantly different from that of the In.AD, which indicates that some microorganisms were enriched at the electrode of the anodic compartment. However, the diversity of the microbial population did not change apparently, according to the pattern profile, during the nitrogen increasing concentration, comparing B₁ and B₂ MFC_{SW} samples. The sequenced bands from In.AD belong to *Bacteroidetes* and *Firmicutes* phyla, while greater phyla diversity is found in anode biofilms, with bands belonging to

Bacteroidetes, *Firmicutes*, and *Proteobacteria* (β and γ -*proteobacteria*). As the banding profile is fairly constant in B₁ and B₂ MFC_{SW}, all the obtained DGGE bands from anode biofilms appear to be present in both samples (B₁ and B₂ MFC_{SW}), and are described in **Table 6.3**. Three of those bands (bands 8, 24 and 16) belonging to *Chitinophagaceae*, *Pseudomonadaceae* and *Alcaligenaceae*, stand out for being the most intensive.

The MFC_{PS} analysis of the DGGE pattern (**Figure 6.9b**) revealed that in this case the pattern profile between PS and B₁ MFC_{PS}, is not such as different as the one observed for the MFC_{SW}, probably due to the high effect of the background of the feed (PS) over the microbial community. The sequenced bands from PS and B₁ and B₂ MFC_{PS} belong mainly to *Bacteroidetes* phyla (**Table 6.4**). Nevertheless, a shift in the microbial community was observed after increasing organic and nitrogen loading rates (B₂ MFC_{PS}). The most intensive bands in B₂ MFC_{PS} belong to *Proteiniphulum* sp., and to *Porphyromonadaceae* (band 23), and band 30, belonging to α -*proteobacteria*, was only found in B₂ MFC_{PS}.

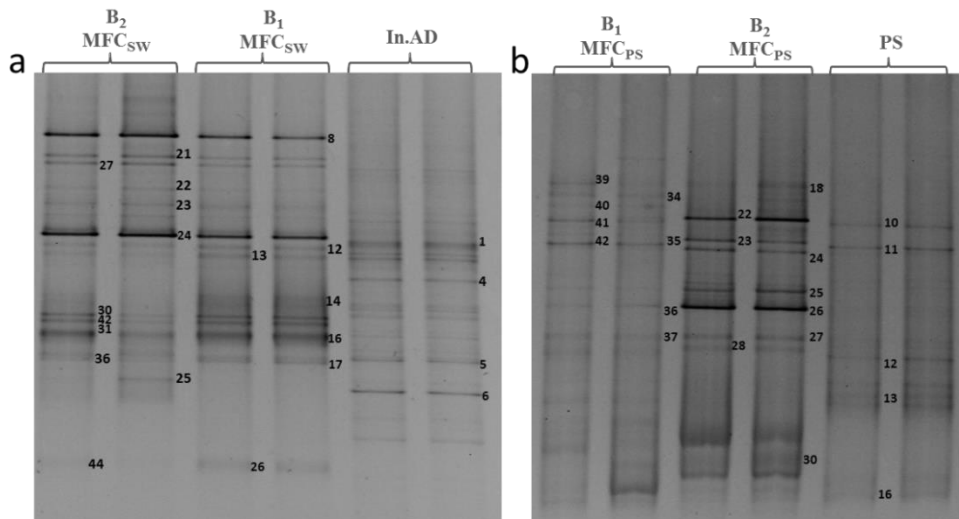


Figure 6.9. DGGE of PCR-amplified 16S rRNA gene fragments (*V*₃-*V*₅ regions) of Eubacterial communities **(a)** from In.AD: initial inoculum, and B₁ MFC_{SW} / B₂ MFC_{SW}: biofilm samples from the synthetic wastewater-fed MFC, and **(b)** from PS: pig slurry, and B₁ MFC_{PS} / B₂ MFC_{PS}: biofilm samples from the pig slurry-fed MFC.

Table 6.3. Closest match for bands excised from the 16S rRNA DGGE Eubacterial gel from the MFC_{sw} (Figure 6.9a).

DGGE band	Band detection			Length (bp)	Similar sequence (genbank)	% Sim.	Phylogenetic group
	In.AD	B ₁ MFC _{sw}	B ₂ MFC _{sw}				
1	×	-	-	446	Uncultured bacterium (GQ136285)	79	<i>Bacteroidetes</i>
4	×	-	-	301	Uncultured bacterium (JQ307402)	99	<i>Bacteroidetes</i>
5	×	-	-	354	Uncultured <i>Clostridiales</i> (JN173135)	98	<i>Firmicutes</i>
6	×	-	-	450	Uncultured bacterium (GQ468300)	100	<i>Firmicutes</i>
8	-	× ^a	×	522	Uncultured <i>Sphingobacterium</i> (FJ756565)	95	<i>Chitinophagaceae</i> (<i>Bacteroidetes</i>)
12	-	× ^a	×	470	Uncultured bacterium (GQ133291)	98	<i>Firmicutes</i>
13	-	× ^a	×	511	Uncultured <i>Cytophagaceae</i> (HM205113)	99	<i>Cytophagaceae</i>
17	-	×	-	335	<i>Delftia</i> sp. (FR682925)	97	<i>Comamonadaceae</i> (<i>β-proteobacteria</i>)
23=26=21=22	-	×	×	495	<i>Bacteroides</i> sp. (AY554420)	100	<i>Porphyromonadaceae</i> (<i>Bacteroidetes</i>)
24	-	× ^a	×	257	<i>Pseudomonas</i> sp. (AM110955)	88	<i>Pseudomonadaceae</i> (<i>γ-proteobacteria</i>)
30	-	× ^a	×	511	Uncultured bacterium (HE583040)	90	<i>Comamonadaceae</i> (<i>β-proteobacteria</i>)
42=16=31=36=27	-	×	×	528	<i>Alcaligenes</i> sp. (AB695233)	98	<i>β-proteobacteria</i>
44=25	-	-	×	511	<i>Defluviobacter</i> sp. (HQ890470)	100	<i>Alcaligenaceae</i> (<i>β-proteobacteria</i>)

^aBand detected by means of gel migration. Band not sequenced.

Table 6.4. Closest match for bands excised from the 16S rRNA DGGE Eubacterial gel from the MFC_{PS} (Figure 6.9b).

DGGE band	PS	Band detection		Length (bp)	Similar sequence (genbank)	% Sim.	Phylogenetic group
		B ₁ MFC _{PS}	B ₂ MFC _{PS}				
10=41	×	×	-	492	Uncultured bacterium (CU927836)	96	<i>Porphyromonadaceae</i> (<i>Bacteroidetes</i>)
11=35=42	×	×	-	389	Uncultured bacterium (EU358742)	94	<i>Bacteroidetes</i>
18=22=39	-	× ^a	×	484	Uncultured bacterium (JX126832)	97	<i>Bacteroidetes</i>
23	-	-	×	400	Uncultured bacterium (JN196916)	96	<i>Porphyromonadaceae</i> (<i>Bacteroidetes</i>)
24=26=36	-	×	×	488	Bacterium NLAE-zl-C76 (JQ607775)	99	<i>Proteiniphilum</i> (<i>Bacteroidetes</i>)
25	-	-	×	350	Uncultured bacterium (JN196883)	91	<i>Bacteroidetes</i>
30	-	-	×	200	Uncultured <i>Sphingomonadeodaceae</i> (EU630871)	89	<i>α-proteobacteria</i>
40	-	×	-	350	Uncultured bacterium (JQ409177)	91	<i>Bacteroidetes</i>

^aBand detected by means of gel migration. Band not sequenced.

Table 6.5. Closest match for bands excised from the 16S rRNA DGGE Eubacterial gel from the MFC_{SW} before and after BES addition (Figure 6.10).

DGGE band	Band detection		Length (bp)	Similar sequence (genbank)	% Sim.	Phylogenetic group
	B ₂ MFC _{SW}	B ₃ MFC _{SW-BES}				
3=4	×	-	490	Uncultured bacterium (JX126832)	99	<i>Bacteroidetes</i>
5=14=15	×	× ^a	485	Uncultured bacterium (HM008283)	99	<i>Porphyromonadaceae</i> (<i>Bacteroidetes</i>)
6	×	× ^a	490	Uncultured bacterium (GU90348)	99	<i>Porphyromonadaceae</i> (<i>Bacteroidetes</i>)
25	-	×	360	Uncultured <i>Bacteroidetes</i> (JQ724358)	100	<i>Bacteroidetes</i>
27	-	×	437	Uncultured Bacterium (JX174653)	99	<i>Bacteroidetes</i>
28	-	×	435	Uncultured Bacterium (GQ139189)	100	<i>Bacteroidetes</i>
31	× ^a	×	385	Iron-reducing bacterium (FJ269105)	98	<i>Firmicutes</i>

^aBand detected by means of gel migration. Band not sequenced.

6.3.3.2. Effect of different substrates feed

DGGE profiles results revealed the band pattern of the anodic microbial community in B₁ and B₂ MFC_{SW} was very different to that observed in B₁ and B₂ MFC_{PS} (**Figure 6.9a and b**). Also the affiliation of sequenced bands showed some differences, founding Bacteroidetes, Firmicutes and Proteobacteria (β and γ -proteobacteria) in MFC_{SW} and mostly Bacteroidetes and also Proteobacteria (α -proteobacteria) in MFC_{PS} (**Tables 6.3 and 6.4**).

6.3.3.3. Effect of BES inhibitor

Figure 6.10 show the DGGE profile for eubacterial and archaeal community just before and after the addition on BES-Inh. DGGE profiles obtained from the B₂ MFC_{SW} for archaeal community did not changed with BES-Inh. addition (B₃ MFC_{SW-BES}) (**Figure 6.10**). Bands absence in these profiles could be due to the low microbial diversity, fact that causes massive migration of a few bands. However, eubacterial community DGGE profiles did show significant changes between microbial community structure before (B₂ MFC_{SW}) and after the addition of BES-Inh. (B₃ MFC_{SW-BES}) (**Figure 6.10**). Before the addition of BES-Inh., predominant sequences belonging to Bacteroidetes phyla were found, and after the addition of BES-Inh. besides Bacteroidetes, sequences belonging to Firmicutes phyla were detected (**Table 6.5**).

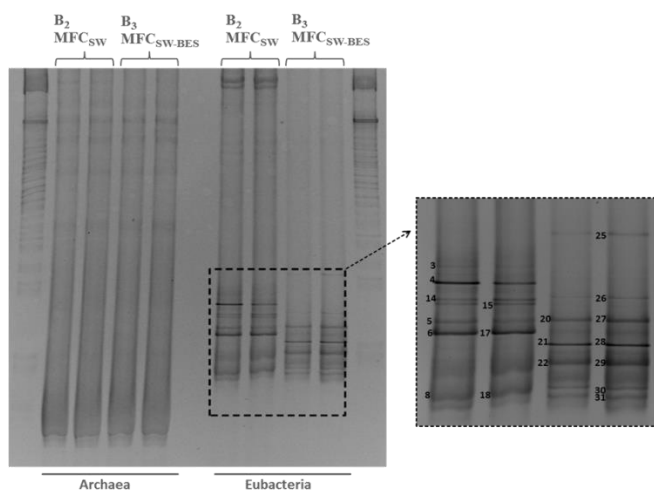


Figure 6.10. DGGE of PCR-amplified 16S rRNA gene fragments (V_3 - V_5 regions) of Archaeal and Eubacterial communities before (B₂ MFC_{SW}) and after (B₃ MFC_{SW-BES}) the addition of BES-Inh.

6.3.4. Richness and diversity of bacteria phylotypes

Statistical analyses were performed in order to obtain the richness and diversity indices and sample coverage γ means of 454-pyrosequencing. The number of quality reads per sample ranged from 2631 to 18493 (**Table 6.6**) with an average number of 7382 reads per sample for Eubacterial communities, while for Archaeal communities the number of quality reads per sample ranged from 1654 to 6417 (**Table 6.7**) with an average number of 3756 reads per sample.. As can be seen in **Table 6.6**, there is a strong proportionality between the richness estimators (Sobs and Chao 1) and the diversity indices (Shannon and 1/Simpson) for the Eubacterial community. The more the richness the sample has the more the diversity has. Contrary, for Archaeal community, the proportionality between richness and diversity is not so clear (**Table 6.7**).

6.3.4.1. Microbial population adaptation overtime and under different operational conditions

Diversity indices for eubacterial community indicate that In.AD inoculum had higher diversity (Shannon = 5.5) than the anode biofilms in the MFC_{sw} (Shannon = 4.7 and 3.8 for B₁ MFC_{sw} and B₂ MFC_{sw}, respectively). Therefore, based on diversity index, a microbial community specialization can be assumed (**Table 6.6**). In the case of the richness estimators, results indicated that richness in In.AD (Chao = 719.7) is quite high and more than two-fold higher compared to that of the anode biofilm samples B₁ MFC_{sw} (Chao = 583.3) and B₂ MFC_{sw} (Chao = 352.2).

However, for the pig slurry-fed MFC the diversity indices showed an increase of diversity comparing PS (Shannon = 4.5), with the biofilms B₁ MFC_{ps} (Shannon = 6.0), and B₂ MFC_{ps} (Shannon = 5.6). Similarly, Chao richness estimator are higher for the biofilm samples, B₁ MFC_{ps} (Chao = 979.8) and B₂ MFC_{ps} (Chao = 655.0), than PS (Chao = 551.7).

Richness estimator results for the archaeal community indicated that richness in In.AD sample (Chao 1= 166.0) is more than two-fold higher compared to that of the anode biofilms MFC_{sw} (Chao 1 = 67.6 (B₁ MFC_{sw}) and Chao 1 = 62.9 (B₂ MFC_{sw}). Thus, it can be concluded that the number of species in archaeal community is higher in the initial inoculum (In.AD) than later in the biofilms for the synthetic-fed MFC. For the pig slurry-fed MFC the Archaeal community diversity also decreased through time from PS (Shannon = 4.1), to B₁ MFC_{ps} (Shannon = 3.9) and B₂ MFC_{ps} (Shannon = 2.7) (**Table 6.7**). Regarding the Chao richness estimator, it increased from PS (Chao = 155.0) to the B₁ MFC_{ps} (Chao = 208.1), and in the last sample decreased fairly B₂ MFC_{ps} (Chao = 67.0).

Table 6.6. N° of sequences, and OTUs, estimated richness (S_{obs} and Chao1), diversity indices (Shannon and 1/Simpson) and sample coverage values for Eubacterial operational taxonomic units (OTUs), calculated with MOTHUR at the 3% distance level.

Sample	nseqs	sobs OTUs	Chao1		Shannon		1/Simpson		Coverage* (%)
			mean	c.i.**	mean	c.i.**	mean	c.i.**	
In.AD	5110	620	719.7	681.3-782.4	5.5	5.5-5.6	100.0	93.1-107.9	97.8
B ₁ MFC _{SW}	18493	514	585.3	552.3-646.8	4.7	4.6-4.7	39.9	38.6-41.2	99.3
B ₂ MFC _{SW}	5630	300	352.2	328.9-394.3	3.8	3.8-3.9	12.0	11.2-12.8	98.7
B ₃ MFC _{SW-BES}	8259	514	595	560.2-656.0	5.1	5.0-5.1	70.2	67.2-73.4	99.0
PS	5403	491	551.7	526.7-594.3	4.5	4.4-4.5	16.0	15.7-18.0	98.3
B ₁ MFC _{PS}	6151	840	979.8	933.4-1049.2	6.0	5.0-6.1	197.1	183.6-212.7	97.4
B ₂ MFC _{PS}	2631	514	655.0	605.9-730.5	5.6	5.6-5.7	150.4	136.0-168.2	94.6

*Estimated sample coverage: $C_x = 1 - (N_x/n)$, where N_x is the number of unique sequences and n is the total number of sequences. ** c.i. 95% confidence intervals

Table 6.7. N° of sequences, and OTUs, estimated richness (S_{obs} and Chao1), diversity indices (Shannon and 1/Simpson) and sample coverage values for Archaeal operational taxonomic units (OTUs), calculated with MOTHUR at the 3% distance level.

Sample	nseqs	sobs OTUs	Chao1		Shannon		1/Simpson		Coverage* (%)
			mean	c.i.**	mean	c.i.**	mean	c.i.**	
In.AD	3784	146	166.0	153.6-198.9	3.5	3.5-3.6	13.2	12.3-14.2	99.3
B ₁ MFC _{SW}	6411	65	67.6	65.5-79.7	2.1	2.0-2.1	3.1	3.0-3.2	99.9
B ₂ MFC _{SW}	2518	55	62.9	57.0-86.5	2.1	2.1-2.2	3.5	3.3-3.7	99.6
B ₃ MFC _{SW-BES}	6417	113	128.5	118.2-159.6	2.7	2.6-2.7	5.4	5.2-5.7	99.7
PS	1654	142	155.0	147.0-176.2	4.1	4.0-4.2	37.4	34.7-40.5	98.4
B ₁ MFC _{PS}	3663	186	208.1	195.2-239.4	3.9	3.9-4.0	20.1	18.6-21.8	99.2
B ₂ MFC _{PS}	1843	67	67.0	67.0-67.0	2.7	2.6-2.7	4.6	4.3-5.1	100

*Estimated sample coverage: $C_x = 1 - (N_x/n)$, where N_x is the number of unique sequences and n is the total number of sequences. ** c.i. 95% confidence intervals

6.3.4.2. Effect of different substrates feed

The MFC_{SW}, fed with synthetic waste water, clearly showed a decrease in the diversity indices, as well as the richness estimators, showing a major specialization on the anodic microbial community. However, in the MFC_{PS}, it is difficult to see a clear trend probably due to the masking effect of the continuous feeding with pig slurry.

6.3.4.3. Effect of BES inhibitor

The addition of BES to the synthetic-fed MFC produced an increase in the Eubacterial Shannon diversity index (Shannon = 5.1) with respect to the precedent sample of the anode biofilm B₂ MFC_{SW} (Shannon = 3.8) (**Table 6.6**). In the case of archaeal community, Shannon index increased slightly from 2.1 to 2.7 (**Table 6.7**). Chao richness estimator increase two-fold after BES addition, from Chao = 352.2 to Chao = 595; and the same trend occurs for the archaeal community, increasing from Chao = 62.9 to Chao = 128.5.

These results were also supported by the rarefaction curves performed on each sample for Eubacteria and Archaea community (**Figure 6.11**), with 5110 (In.AD), 18493 (B₁ MFC_{SW}), 5630 (B₂ MFC_{SW}), 8259 (B₃ MFC_{SW-BES}) 5403 (PS), 6151 (B₁ MFC_{PS}) and 2631 (B₂ MFC_{PS}) high-quality reads for eubacteria community and 3784 (In.AD), 6411 (B₁ MFC_{SW}), 2518 (B₂ MFC_{SW}), 6417 (B₃ MFC_{SW-BES}), 1654 (PS), 3663 (B₁ MFC_{PS}) and 1843 (B₂ MFC_{PS}) high-quality reads for archaea community. These results also indicates that both Eubacterial and Archaeal microbial diversity decreased from In.AD sample to B₁ and B₂ MFC_{SW} samples. Contrary, for the pig slurry-fed MFC a diversification of the microbial community is observed from the PS to B₁ MFC_{PS}, probably due to the background of the pig slurry, although the diversity decreased overtime (B₁ MFC_{PS}). Besides, there is an increase in the microbial diversity promoted by the addition of BES (B₂ MFC_{SW} versus B₃ MFC_{SW-BES}). Finally, the eubacterial microbial diversity as well as the archaeal microbial diversity tended to increase from PS to B₁ MFC_{PS}, but then a noticeable decrease from B₁ MFC_{PS} to B₂ MFC_{PS} is observed.

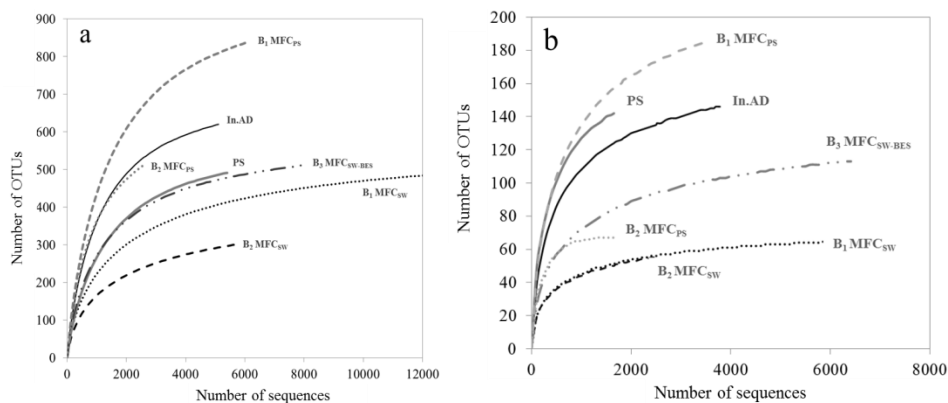


Figure 6.11. Rarefaction curves of a) eubacterial and b) archaeal number of operational taxonomic units (OTUs) obtained from the 454-pyrosequencing results, for the different samples (B_1 MFC_{sw}, B_2 MFC_{sw}, B_1 MFC_{ps} and B_2 MFC_{ps}) in relation to the initially inoculated biomass (In.AD) and the liquid fraction of pig slurry (PS) using as feed. The OTUs were defined by 3% distances using MOTHUR software.

6.3.5 Comparative analysis of microbial communities

To have an overview of the dynamics and similar or different composition of all samples together, a correspondence analysis (CA) based on the pyrosequencing results were carried out with all samples. The CA based on the relative abundance of all OTUs (obtained by pyrosequencing analysis) was for the Eubacterial communities can be seen in **Figure 6.12a**, and the CA based on the relative abundance of all families for Eubacterial and Archaeal communities can be seen in **Figure 6.12b** and **Figure 6.13**, respectively. The two components (F1 and F2) explain 41.9% and 56.3% of the total variation among the samples for **Figure 6.12a** and **b**, respectively. The CA based on the OTUs analysis (**Figure 6.12a**) indicated that the microbial community on the anode compartment for MFC_{sw} (B_1 and B_2 MFC_{sw}) was modified from the initial inoculum (In.AD). These exoelectrogenic communities (B_1 and B_2 MFC_{sw}) clustered together, and were also separated from communities on anode compartments of the MFC_{ps} (B_1 and B_2 MFC_{ps}). Therefore, these results indicated that anode communities were enriched in specific exoelectrogenic populations based on type of substrates used, as it has been previously described elsewhere (Lu et al., 2012; Ishii et al., 2013).

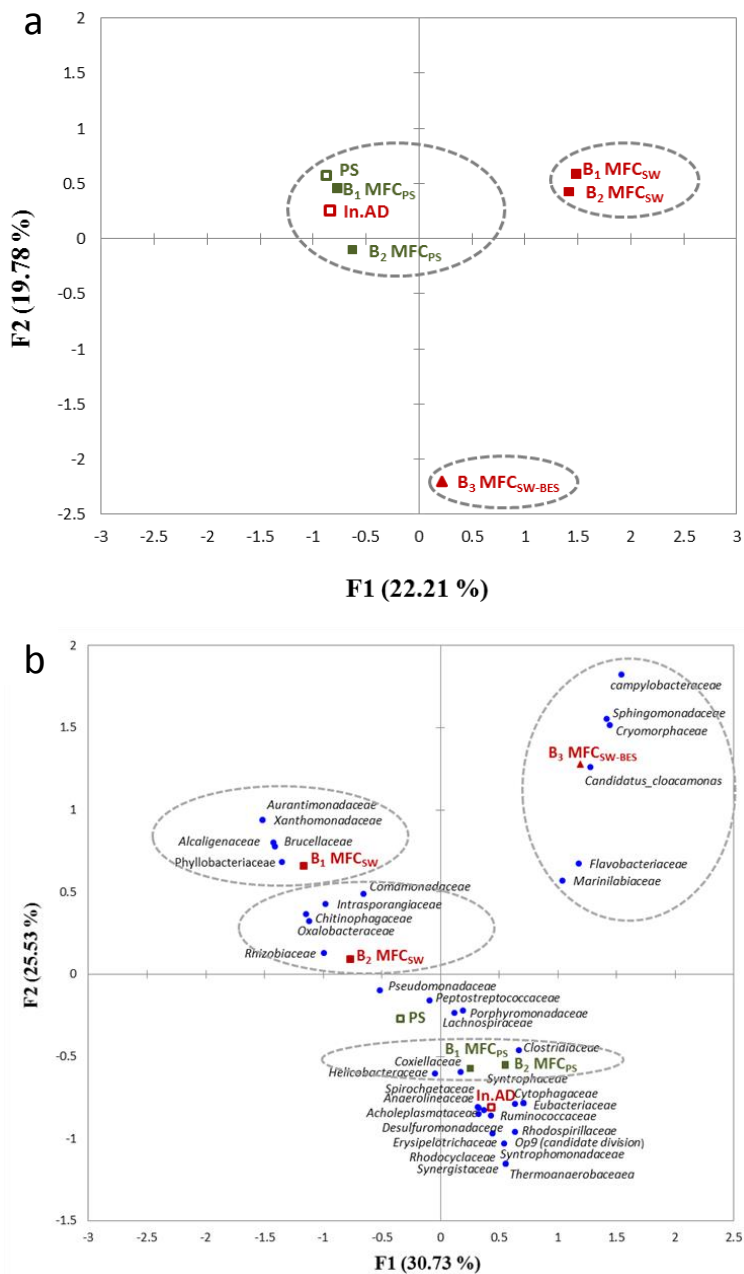


Figure 6.12. Correspondence analysis (CA) of bacterial communities from In.AD, B₁ MFC_{SW}, B₂ MFC_{SW}, B₃ MFC_{SW-BES}, PS, B₁ MFC_{PS} and B₂ MFC_{PS} samples, based on pyrosequencing of archaea 16S rRNA gene based on, **a)** OTUs matrix, **b)** family level taxonomy.

Results of the CA based on the family level (**Figure 6.12b**) indicated that *Aurantimonadaceae*, *Xanthomonadaceae*, *Brucellaceae*, *Alcaligenaceae* and *Phyllobacteraceae* were most associated with B₁ MFC_{SW}, *Comamonadaceae*, *Intrasporangiaceae*, *Chitinophagaceae*, *Oxalobacteraceae* and *Rhizobiaceae* were assigned to B₂ MFC_{SW}, and *Clostridiaceae*, *Coxiellaceae* and *Helicobacteraceae* were related to both B₁ and B₂ MFC_{PS}.

The liquid fraction of pig slurry (PS), as can be expected, is also clustered together with both anode biofilms (B₁ and B₂ MFC_{PS}), which means they share a lot of OTUs, since PS is the substrate used as feeding for this MFC.

The microbial community after BES addition, B₃ MFC_{SW-BES}, was considerably different from that of the B₂ MFC_{SW} (**Figure 6.12a**). This community was the most distant to the rest, but still in the same quadrant than B₁ and B₂ MFC_{SW}. **Figure 6.12b** showed that several families were associated with the changes caused by the addition of BES, as *Campylobacteraceae*, *Sphingomonadaceae*, *Cryomorphaceae*, *Flavobacteriaceae* and *Marinilabiaceae*.

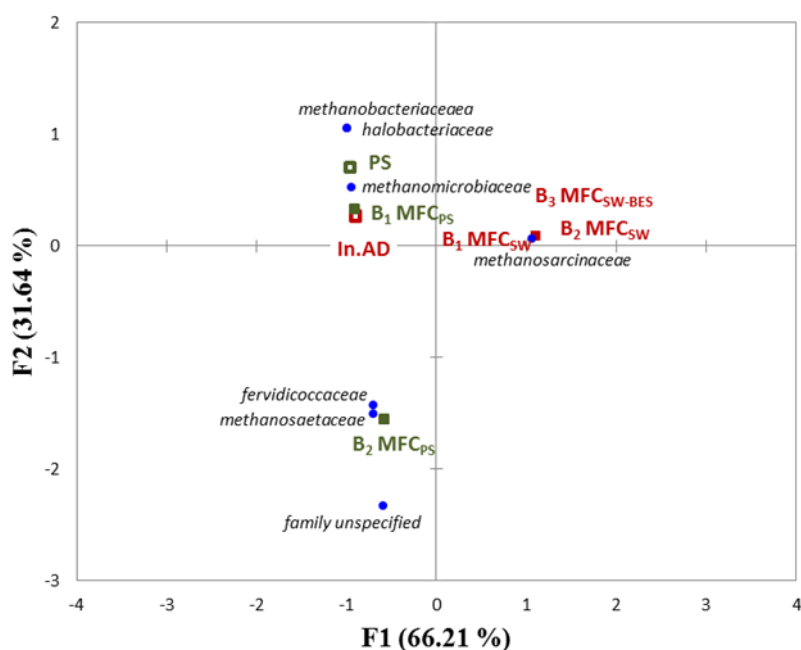


Figure 6.13. Correspondence analysis (CA) of Archaeal communities from AD, S MFC-I, S MFC-II, S MFC(BES), PS, PS MFC-I and PS MFC-II samples, based on 454-pyrosequencing of archaea 16S rRNA gene, based on family level taxonomy.

The CA diagram for archaeal community explains 97.85% of the total variation among all sample for the two components F1 and F2 (**Figure 6.13**). The CA based on the presence and absence of the archaeal families is strongly different from that of the eubacterial communities. While **Figure 6.12a** and **b** showed that the addition of BES-Inh. caused noticeable shifts in eubacterial population, it did not promote an archaeal population shift though (**Figure 6.13**). The most distant community is B₂ MFC_{PS} and *Fervidicoccaceae* and *Methanosaetaceae* were associated to the difference between this archaeal community and the rest.

In order to find out which OTUs show greater trend to establish in anodophilic biofilms, the OTUs present in the samples has been compared.

6.3.5.1. Microbial population adaptation overtime and under different operational conditions

In order to analyze the evolution of the microbial community of the MFC_{sw}, the inoculum (In.AD), was compared with the tow biofilm samples, B₁ and B₂ (**Figure 6.14a**). The total observed OTUs in the three samples was 1151, but only 6 OTUs, equivalent to 0.52% of the total OTUs, were shared by them. The major part of these 6 OTUs in common (66.7%) were *Bacteroidetes* phylum, represented by three families, *Flavobacteriaceae* (33.3%), *Porphyromonadaceae* (16.7%), and *Marinilabiaceae* (16.7%). The rest was distributed into two phyla, β -proteobacteria, represented by *Comamonadaceae* (16.7%), and *Synergistetes*, represented by *Synergistaceae* (16.7%). Otherwise, as it might be expected, the number of shared OTUs increase significantly, 261 (22.7% of the total OTUs), when comparing the two samples of anode biofilm (B₁ and B₂ MFC_{sw}).

Similarly, the anode communities in the biofilm of pig slurry-fed MFC were analyzed (**Figure 6.14b**). In this case, the total observed OTUs was 1332, and 99 (7.43% of the total OTUs) were shared by the three samples. The majority of the shared OTUs (36.4%) were *Bacteroidetes*, following by γ -proteobacteria (20.2%), *Firmicutes* (12.1%), *Tenericutes* (11.1%), β -proteobacteria (6.1%) and the rest of the phyla were below 3% of relative abundance (*Chloroflexi*, *Synergistetes*, *Actinobacteria*, *Spirochaetes*, *Lentisphaerae*, *Fibrobacteres* and α -proteobacteria). These phyla were represented by 29 families (**Figure 6.15**), but just four of them accounted for 60.6%, *Porphyromonadaceae* (27.3%), *Pseudomonadaceae* (17.2%), *Acholeplasmataceae* (11.1%) and *Comamonadaceae* (5.1%). When comparing B₁ and B₂ MFC_{PS} the number of common OTUs increases till 130 OTUs, representing 9.8% of the total OTUs.

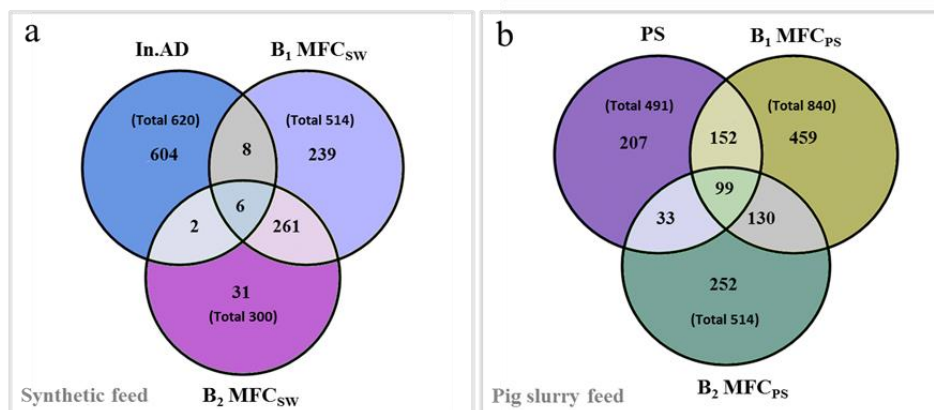


Figure 6.14. Overlap of the three bacterial communities: **a)** from the initial inoculum (In.AD) and the synthetic-fed MFC (B_1 MFC_{sw} and B_2 MFC_{sw}), **b)** from the liquid fraction of pig slurry (PS) and pig slurry-fed MFC (B_1 MFC_{ps} and B_2 MFC_{ps}), based on OTU (3% distance), and the taxonomic identities of the shared OTUs at family level. The total number of OTUs in each sample is shown between parentheses.

Finally, the three samples of the MFC_{ps} (PS, B_1 MFC_{ps} and B_2 MFC_{ps}) were compared with the sample B_2 MFC_{sw}, as it was the inoculum used in the start up of this MFC (**Figure 6.15**). The total OTUs in the four samples was 1585. The four communities did not share any OTU, but the three anode biofilm samples (B_2 MFC_{sw}, B_1 MFC_{ps}, and B_2 MFC_{ps}) shared 6 OTUs (0.38% of the total OTUs). This analysis showed that the majority (66.7%) of the shared OTUs were *Bacteroidetes*, represented by two families, *Flavobacteriaceae* (33.3%) and *Porphyromonadaceae* (33.3%), following by two groups in the same relative abundance (16.7% each one), β -proteobacteria represented by *Comamonadaceae*, and *Actinobacteria* represented by *Intrasporangiaceae*. These 6 OTUs have remained among all three communities from the initial inoculum to the last conditions, and they could be considered the core microbiome and vital to the function of the community, as it has been previously described (Shade and Handelsman, 2012), for the OTUs shared by all samples overtime. It is noteworthy that three families, *Comamonadaceae*, *Flavobacteriaceae* and *Porphyromonadaceae* were found in all samples (In.AD, B_1 and B_2 MFC_{sw}, B_3 MFC_{sw-BES}, PS, B_1 and B_2 MFC_{ps}) regardless of the inoculum, the substrates and the type of electrode used.

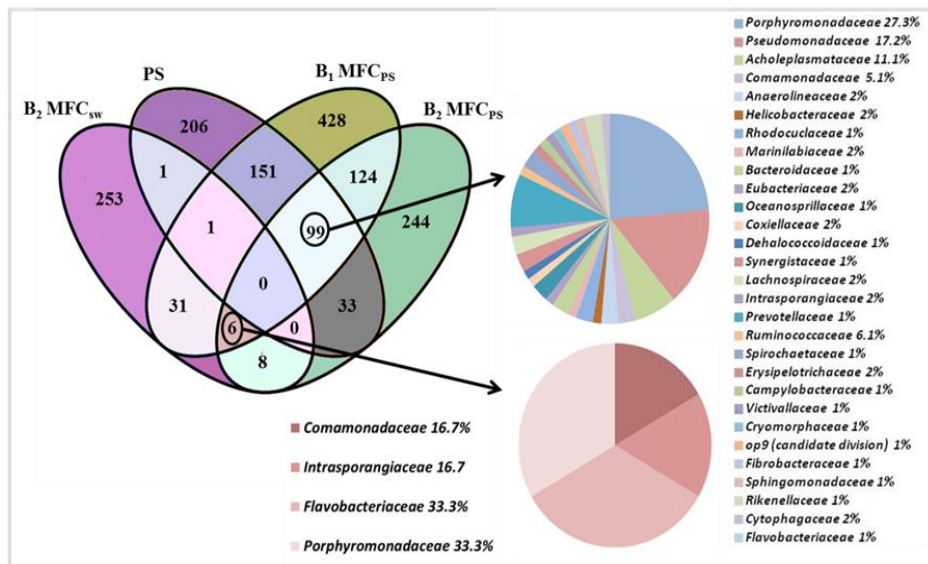


Figure 6.15. Overlap of the four bacterial communities for B₂ MFC_{sw}, PS, B₁ MFC_{ps} and B₂ MFC_{ps}, based on OTU (3% distance), and the taxonomic identities of the shared OTUs at family level. The total number of OTUs in each sample is shown between parentheses.

6.3.5.2. Effect of BES inhibitor

A comparative population analyses was also performed between B₂ MFC_{sw} and B₃ MFC_{sw-BES}. As can be seen in **Figure 6.16** only 83 OTUs (11.4%) of the 731 identified are in common in the anodic biofilm before and after the injection of BES. This 83 of OTUs shared, are distributed in *Bacteroidetes*, α -proteobacteria (22% each one), *Firmicutes*, β -proteobacteria, *Actinobacteria* (11.1% each one), and γ -proteobacteria, δ -proteobacteria, *Synergistetes* and *Chloroflexi* (5.6% each one). Eighteen families are represented within this 83 OTUs shared, but 6 of them, *Porphyromonadaceae* (24.1%), *Pseudomonadaceae* (18.1%), *Lachnospiraceae* (14.5%), *Alcaligenaceae* (9.6%), *Desulfovibrionaceae* (6.0%) and *Comamonadaceae* (4.8%), should be highlighted due to their high percentage and their importance in exoelectrogenic communities (**Figure 6.16**).

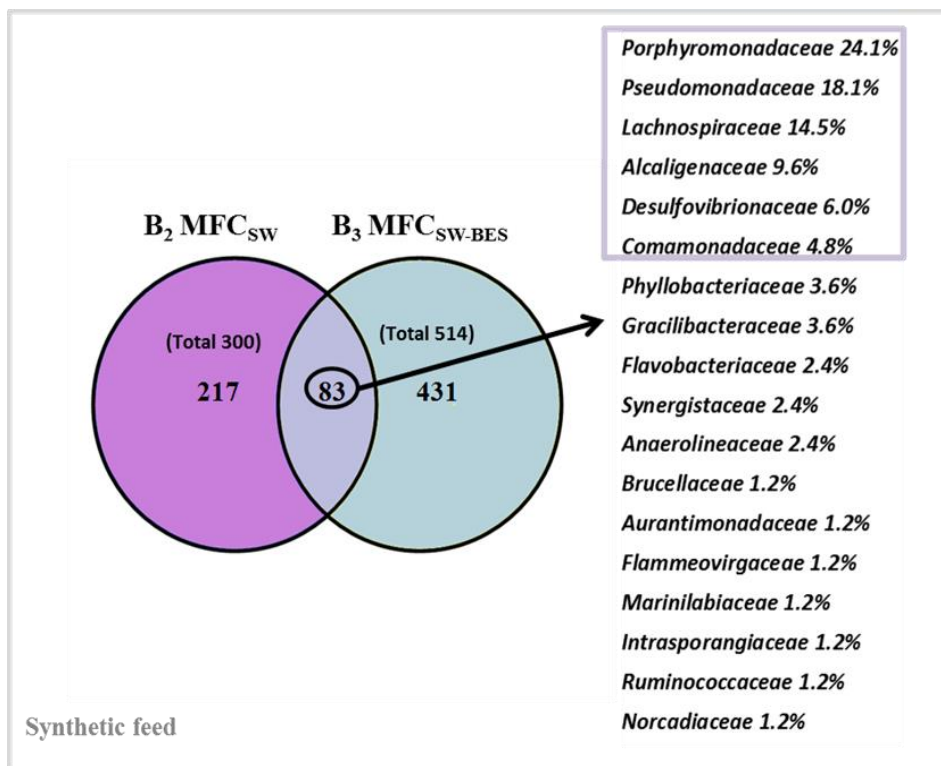


Figure 6.16. Overlap bacterial communities from the synthetic-fed MFC before (B_2 MFC_{SW}) and after (B_3 MFC_{SW-BES}) BES addition, based on OTU (3% distance), and the taxonomic identities of the shared OTUs at family level. The total number of OTUs in each sample is shown between parentheses.

6.3.6. Eubacteria community composition

6.3.6.1. Microbial population adaptation overtime and under different operational conditions

Clear variation in community composition was already observed at phylum level from the inoculum (In.AD) to the anode biofilm and even between the anodes samples over the biofilm development over time and under different operating conditions for the MFC_{SW}. Seven different phyla were identified in In.AD sample, *Bacteroidetes*, *Firmicutes*, *Proteobacteria*, *Tenericutes*, *Actinobacteria*, *Synergistetes*, *Spirochaetes* and *Chloroflexi*) and only four (*Bacteroidetes*, *Firmicutes*, *Proteobacteria* and *Actinobacteria*) and three (*Bacteroidetes*, *Firmicutes* and *Proteobacteria*) phyla in B_1 and B_2 MFC_{SW} respectively. Besides, a clear enrichment in some phyla from the initial inoculum to the anode biofilms was observed (**Figure 6.17a**). The clearest difference between the three communities was the different relative abundance of the three dominant phyla *Bacteroidetes*, *Firmicutes* and

Proteobacteria, but the three phyla accounted by 79.5% (In.AD), 96% (B₁ MFC_{SW}), and 98.9% (B₂ MFC_{SW}). However, *Proteobacteria* was clearly lower in In.AD (6.8%) in contrast to B₁ MFC_{SW} (76.3%) and B₂ MFC_{SW} (73.3%), where this phylum was the most abundant, decreasing the relative abundance of *Bacteroidetes* and *Firmicutes*, that are the dominant phyla in In.AD (**Figure 6.17a**).

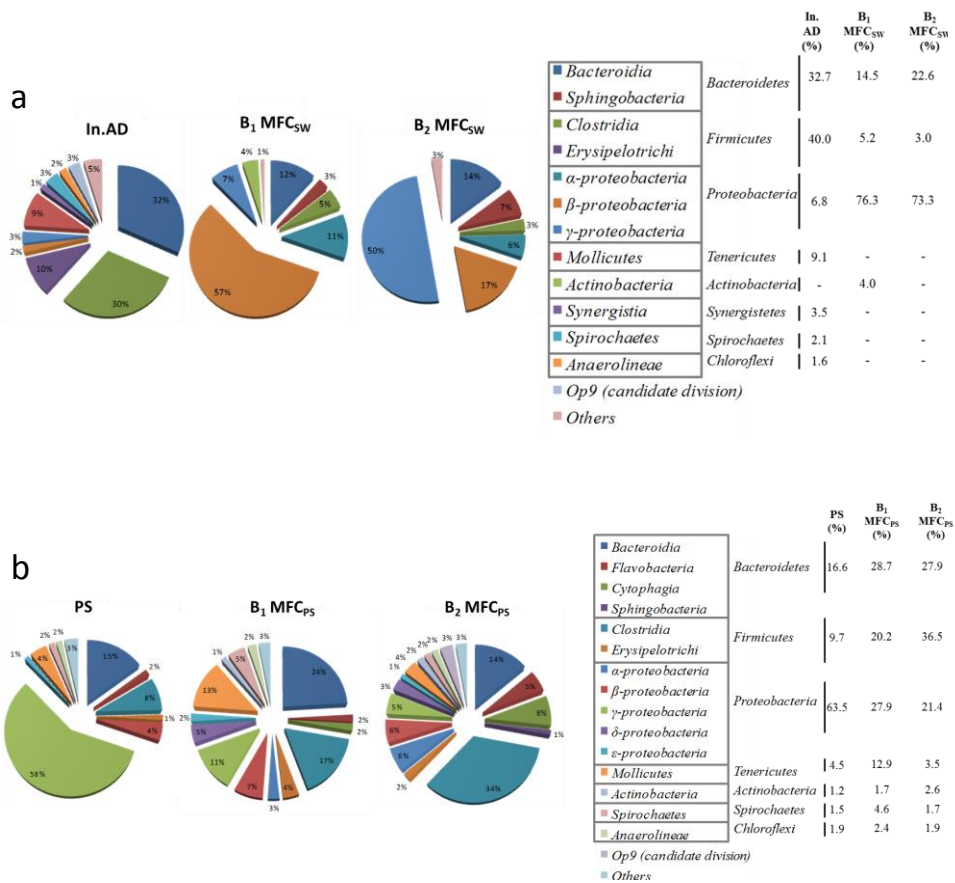


Figure 6.17. Taxonomic classification of 454-pyrosequencing of 16S rRNA gene from Eubacterial communities of **a)** In.AD, B₁ MFC_{SW}, B₂ MFC_{SW}, and **b)** PS, B₁ MFC_{PS}, B₂ MFC_{PS} at phylum, class and order levels. Groups making up less than 1% of the total number of sequences per sample were classified as "others".

Focusing the MFC_{PS} (**Figure 6.17b**), seven phyla were identified in three communities (*Bacteroidetes*, *Firmicutes*, *Proteobacteria*, *Tenericutes*, *Actinobacteria*, *Spirochaetes* and *Chloroflexi*), being the three main phyla, as the previous samples, *Bacteroidetes*, *Firmicutes* and *Proteobacteria*. Nonetheless, a selective enrichment of *Firmicutes* was observed. PS had 9.7% of *Firmicutes* while B₁ MFC_{PS} and B₂ MFC_{PS} presented 20.2% and 36.5% respectively.

6.3.6.2. Effect of different substrates feed

Phylum and class level indicated an enrichment in specific groups on the anode biofilms respect to the initial inoculum in the case of MFC_{SW} (**Figure 6.17a**) but an increasing in the diversity at class level is observed in MFC_{PS} though (**Figure 6.17b**). This fact is attributable to different feeding of the two MFC; as they were continuously fed with sterilized synthetic wastewater and liquid fraction of pig slurry, respectively. Comparing the class composition in both anodes biofilms (MFC_{SW} and MFC_{PS}), the difference between them is the appearance of *Flavobacteria*, *Cytophaga*, *δ-proteobacteria* and *ε-proteobacteria* in MFC_{PS}.

Standing on the order and family levels allowed better understanding of the function of certain microbial community members within the anodophilic structure community.

Nine families were maintained in the MFC_{SW} biofilms under different operational conditions (**Figure 6.18**), highlighting that *Alcaligenaceae* and *Comamonadaceae* are clearly dominant in B₁ MFC_{SW}, 33.0% and 22.9% respectively, reducing thrice their relative abundance to 7.0% and 5.6% respectively in B₂ MFC_{SW} when increasing nitrogen concentrations to the anode influent. In these conditions, with the highest nitrogen concentration used, three families were enriched, *Chitinophagaceae* from 2.6% to 6.5%, *Oxalobacteraceae* from 1.4% to 4.4% in B₁ and B₂ MFC_{SW} respectively, and the most dominant with high nitrogen concentration was *Pseudomonadaceae*, which enriched from 6.2% in B₁ MFC_{SW} to 50% B₂ MFC_{SW}. *Rhizobiaceae* appeared in B₂ MFC_{SW} at a 1.4% relative abundance.

Pyrosequencing results detected 10 bacterial families in B₂ MFC_{SW} and 21 in B₂ MFC_{PS}, but some of those members could be considered "background" due to continuous feeding with the liquid fraction of pig slurry to the MFC_{PS}. Despite this "background", in general terms the community composition was enriched in certain families from PS to B₁ MFC_{PS}, as *Porphyromonadaceae* (from 12% to 20%), *Ruminococcaceae* (from 4.5% to 7.9%), *Erysipelotrichaceae* (from 1.4% to 4.0%), *Acholeplasmataceae* (from 4.4% to 12.5%), *Anaerolineaceae* (from 1.5% to 2.3%).

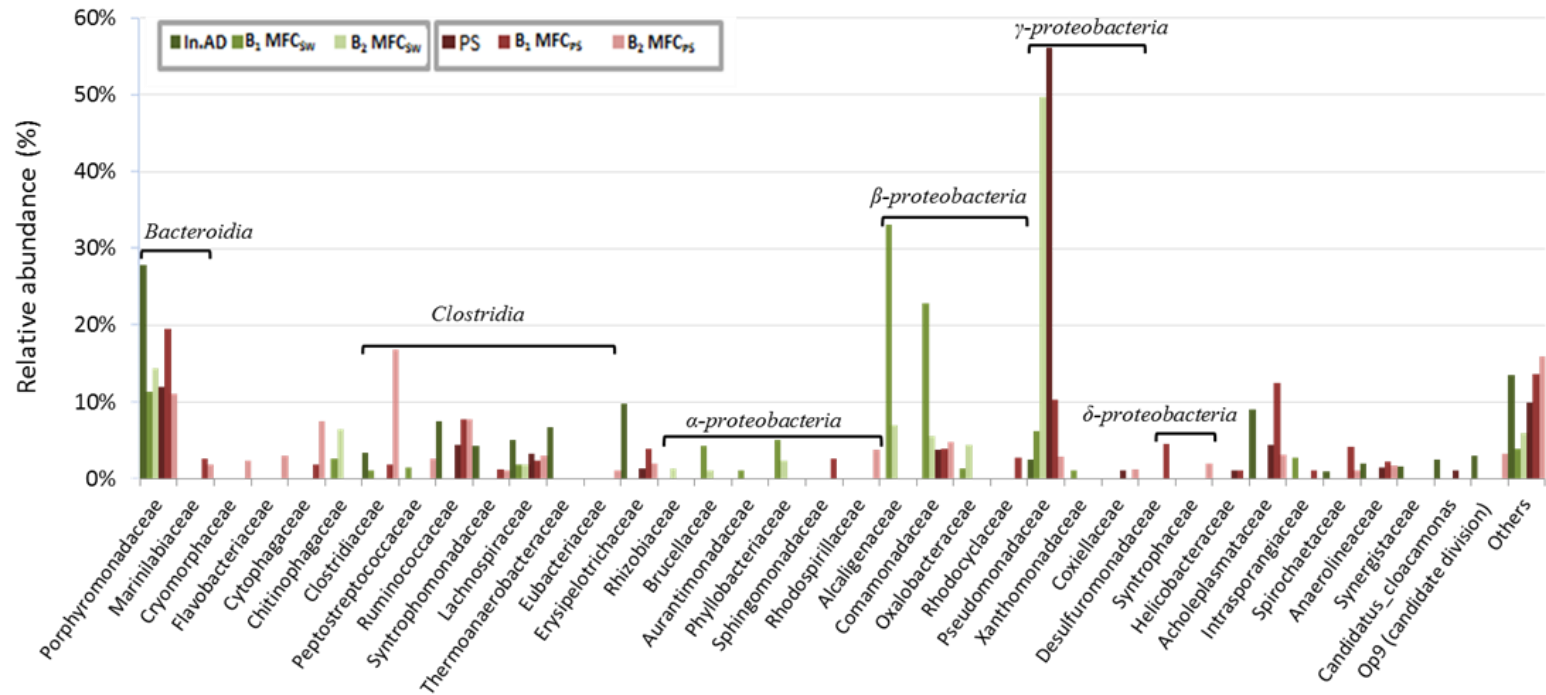


Figure 6.18. Taxonomic classification of 454-pyrosequencing of 16S rRNA gene from eubacterial communities of In.AD, B₁ MFC_{sw}, B₂ MFC_{sw}, PS, B₁ MFC_{ps} and B₂ MFC_{ps} at a family level. Groups making up less than 1% of the total number of sequences per sample were classified as “others”.

A large percentage of bacteria are within the group of “other” bacteria. The In.AD inoculum contained 13.6%, two-fold higher than B₁ MFC_{SW} (4%) and B₂ MFC_{SW} (6%). In the case of MFC_{PS}, values are similar to those found in In.AD, 10%, 14% and 16% for PS, B₁ and B₂ MFC_{SW} respectively, those similar percentages of the three samples, as mention before, can be attributable to the continuous feeding with the liquid fraction of pig slurry. This large quantity of bacteria encompassed in “others” has been described elsewhere (Lesnik et al., 2014).

6.3.6.3. Effect of BES inhibitor

The phyla, order and family level identification in the anodic biofilm before and after the addition of BES-Inh. are illustrated in **Figure 6.19**. This figure clearly shows that the inhibitor caused a dramatic shift in the relative abundance of the dominant Eubacterial phyla within the anodic biofilm.

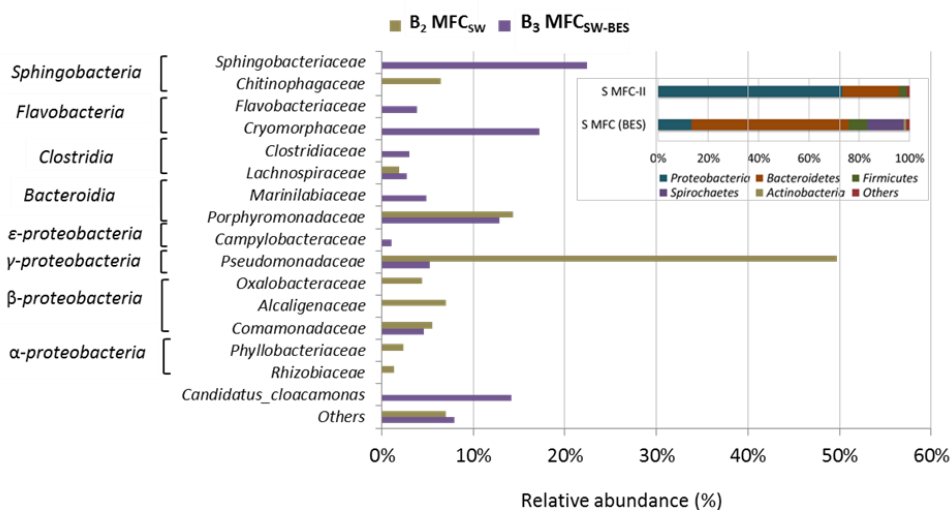


Figure 6.19: Taxonomic classification of 454-pyrosequencing of 16srRNA from eubacterial communities of B₂ MFC_{SW} and B₃ MFC_{SW-BES} at a class and family level. In the box above the phyla classification level. Groups making up less than 1% of the total number of sequences per sample were classified as “others”.

Proteobacteria decreased their relative abundance from 73.3% (B₂ MFC_{SW}) to 13.1% (B₃ MFC_{SW-BES}), and contrary *Bacteroidetes* increased from 22.6% (B₂ MFC_{SW}) to 62.5% (B₃ MFC_{SW-BES}). Besides, two more phyla were detected after the addition of BES-Inh., *Spirochaetes* (14.4%) and *Actinobacteria* (1.0%). Regarding the family level, only three families maintained their abundances after the addition of BES-Inh., *Porphyromonadaceae* (14.3% to 13.0%), *Comamonadaceae* (5.5% to 4.6%) and *Lachnospiraceae* (1.9% to 2.7%).

The abundances in genus level can be very helpful to understand the role of specified populations to MFC performance. Consequently, a list of sequence abundance in the established genera is presented in **Table 6.8**. The genera of *Proteiniphilum* sp. (26.4%), *Bacteroides* sp. (2.8%), *Acholeplasma* sp. (9.1%), *Thermacetogenium* sp. (5.4%), *Fastidiosipila* sp. (3.4%), *Clostridium* sp. (2.7%), *Pseudomonas* sp. (2.5%), and *Anaerobaculum* sp. (1.1%), were the predominant in the initial inoculum from the anaerobic digester (In.AD). After long term acclimation, the population composition and abundance in the anodic biofilm of B₁ MFC_{SW} were, *Alcaligenes* sp. (32.4%), *Brachymonas* sp. (18.6%) and *Proteiniphilum* sp. (10.30%) in a very high abundance, and below but also in a significant abundance were *Pseudomonas* (6.1%), *Delftia* sp. (2.8%), *Tetrasphaera* sp. (2.8%), *Pseudochrobactrum* sp. (2.2%) and *Ochobactrum* sp. (2.1%). When organic and nitrogen concentrations were increased in the synthetic medium, *Proteiniphilum* sp. (13.5%) and *Alcaligenes* sp. (6.4%) remained in a high abundance in the anodic biofilm of B₂ MFC_{SW}, but abundance of *Pseudomonas* sp. greatly increased accounted 49.7% of total sequences. In much lower percentage, *Massilia* sp. (4.4%) and *Acidovorax* sp. (2.2%) were identified in this condition.

Microbial community composition in the anodic biofilm after the addition of BES-Inh. (B₃ MFC_{SW-BES}) was strongly altered. After the last BES concentration (10 mM), *Shingobacterium* sp. (22.1%), *Owenweeksia* sp. (10.4%) and *Brumimicrobium* sp. (6.8%) were extremely high abundant and identified for the first time since the addition of BES. Two populations were found before (B₂ MFC_{SW}) and after (B₃ MFC_{SW-BES}) the addition of BES-Inh. but in different abundance, as *Proteiniphilum* sp. 13.5% vs 5.35%, *Pseudomonas* sp. 49.7% vs 5.3%. However, the main difference between B₂ MFC_{SW} and B₃ MFC_{SW-BES} is a number of genera identified after the addition of BES, *Paludibacter* sp. (5.8%), *Actibacter* sp. (2.6%), *Arcobacter* sp. (1.1%), *Marinifilum* sp. (1.2%), *Meniscus* sp. (0.7%), *Parabacteroides* sp. (0.5%), *Flexithrix* sp. (0.5%), *Odoribacter* sp. (0.4%), *Maritimimonas* sp. (0.4%), *Croceibacter* sp. (0.4%), *Lutispora* sp. (0.4%), *Azospira* sp. (0.3%), *Thiothrix* sp. (0.3%), *Syntrophus* sp. (0.2%) and *Mucilaginitibacter* sp. (0.1%).

Table 6.8. Changes in relative abundances of the bacteria genera.

Taxonomy		Abundance (%)							
Phyla or Classes	Genera	In.AD	B ₂			PS	B ₁		
			MFC _{SW}	MFC _{SW}	MFC _{SW-BES}		MFC _{PS}	MFC _{PS}	
<i>Bacteroidetes</i>	<i>Proteiniphilum</i>	26.44	10.30	13.46	5.30	9.07	12.57	6.20	
	<i>Bacteroides</i>	2.78	0.12	0.00	0.00	1.15	0.44	0.30	
	<i>Paludibacter</i>	0.84	0.00	0.00	5.86	1.11	4.88	2.93	
	<i>Owenweeksia</i>	0.65	0.00	0.00	10.36	0.13	0.00	1.75	
	<i>Alkaliflexus</i>	0.37	0.00	0.20	1.02	0.46	1.07	0.99	
	<i>Petrimonas</i>	0.20	0.92	0.85	0.63	1.00	1.72	1.71	
	<i>Paraprevotella</i>	0.16	0.00	0.00	0.00	0.00	0.00	0.27	
	<i>Meniscus</i>	0.16	0.00	0.00	0.68	0.26	1.82	7.41	
	<i>Actibacter</i>	0.00	0.14	0.44	2.58	0.00	0.00	1.63	
	<i>Pedobacter</i>	0.00	0.00	0.64	0.18	0.00	0.00	0.00	
	<i>Flavobacterium</i>	0.00	0.00	0.41	0.16	0.17	0.37	0.68	
	<i>Sphingobacterium</i>	0.00	0.00	0.00	22.12	0.00	0.80	0.87	
	<i>Brunimicrobium</i>	0.00	0.00	0.00	6.84	0.00	0.00	0.00	
	<i>Marinifilum</i>	0.00	0.00	0.00	1.17	0.00	0.00	0.23	
	<i>Parabacteroides</i>	0.00	0.00	0.00	0.50	0.00	0.00	0.00	
	<i>Flexithrix</i>	0.00	0.00	0.00	0.47	0.00	0.00	0.00	
	<i>Odoribacter</i>	0.00	0.00	0.00	0.41	0.00	0.00	0.19	
	<i>Maritimimonas</i>	0.00	0.00	0.00	0.38	0.00	0.00	0.00	
	<i>Croceibacter</i>	0.00	0.00	0.00	0.38	0.00	0.00	0.00	
	<i>Mucilaginitibacter</i>	0.00	0.00	0.00	0.11	0.00	0.00	0.00	
	<i>Myroides</i>	0.00	0.00	0.00	0.00	0.59	0.00	0.00	
	<i>Alispires</i>	0.00	0.00	0.00	0.00	0.30	0.23	0.00	
	<i>Fluviicola</i>	0.00	0.00	0.00	0.00	0.28	0.00	0.42	
	<i>Cryomorpha</i>	0.00	0.00	0.00	0.00	0.26	0.00	0.15	
	<i>Barnesiella</i>	0.00	0.00	0.00	0.00	0.17	0.00	0.00	
	<i>Rikenella</i>	0.00	0.00	0.00	0.00	0.00	0.28	0.00	
	<i>Aequorivita</i>	0.00	0.00	0.00	0.00	0.00	0.00	0.11	
	<i>Flexibacter</i>	0.00	0.00	0.00	0.00	0.00	0.00	0.11	
	<i>Firmicutes</i>	<i>Acholeplasma</i>	9.08	0.00	0.00	0.00	4.40	12.36	3.19
		<i>Thermacetogenium</i>	5.44	0.00	0.00	0.00	0.00	0.00	0.00
		<i>Fastidiosipila</i>	3.39	0.00	0.00	0.36	0.28	1.30	1.22
		<i>Clostridium</i>	2.72	0.19	0.11	2.81	0.00	0.46	16.08
		<i>Caldicoproductor</i>	2.43	0.00	0.00	0.00	0.00	0.00	0.00
		<i>Gelria</i>	0.98	0.00	0.00	0.00	0.00	0.20	0.00
		<i>Coprothermobacter</i>	0.88	0.00	0.00	0.00	0.00	0.00	0.00
		<i>Alkaliphilus</i>	0.61	0.00	0.00	0.12	0.00	1.28	0.19
		<i>Turcibacter</i>	0.55	0.00	0.00	0.00	0.00	0.00	0.99
		<i>Syntrophomonas</i>	0.45	0.00	0.00	0.00	0.00	1.14	1.10
		<i>Lutispora</i>	0.43	0.00	0.00	0.39	0.00	0.00	0.00
		<i>Anaerotruncus</i>	0.37	0.00	0.00	0.00	0.11	0.15	0.00
<i>Moorella</i>		0.37	0.00	0.00	0.00	0.00	0.00	0.00	
<i>Catenibacterium</i>		0.35	0.00	0.00	0.00	0.00	0.00	0.00	
<i>Saccharofermentas</i>		0.20	0.00	0.00	0.00	0.11	0.00	0.15	
<i>Tissierella</i>		0.16	0.00	0.00	0.00	0.00	0.91	0.00	
<i>Ethanoligenens</i>		0.16	0.00	0.00	0.00	0.00	0.00	0.00	
<i>Erysipelothrix</i>		0.12	0.00	0.00	0.00	0.15	0.72	0.00	
<i>Clostridiisalibacter</i>		0.00	0.71	0.36	0.00	0.00	0.00	0.00	
<i>Gracilibacter</i>		0.00	0.00	0.00	0.11	0.00	0.00	0.00	
<i>Faecalibacterium</i>		0.00	0.00	0.00	0.00	0.74	0.00	0.30	
<i>Coprococcus</i>		0.00	0.00	0.00	0.00	0.39	0.00	0.00	
<i>Blautia</i>		0.00	0.00	0.00	0.00	0.19	0.00	0.00	
<i>Proteiniclasticum</i>		0.00	0.00	0.00	0.00	0.00	0.00	0.42	
<i>Streptococcus</i>		0.00	0.00	0.00	0.00	0.00	0.00	0.38	
<i>Pelotomaculum</i>		0.00	0.00	0.00	0.00	0.00	0.00	0.27	
<i>Anaerostipes</i>		0.00	0.00	0.00	0.00	0.00	0.00	0.19	
<i>Sarcina</i>		0.00	0.00	0.00	0.00	0.00	0.00	0.15	
<i>Vulcanibacillus</i>		0.00	0.00	0.00	0.00	0.00	0.00	0.11	
<i>Peptoniphilus</i>		0.00	0.00	0.00	0.00	0.00	0.00	0.11	

Table 6.8. Changes in relative abundances of the bacteria genera (continuation).

Taxonomy		Abundance (%)						
Phyla or Classes	Genera	In.AD	B ₁ MFC _{SW}	B ₂ MFC _{SW}	B ₃ MFC _{SW-BES}	PS	B ₁ MFC _{PS}	B ₂ MFC _{PS}
<i>α</i> -proteobacteria	<i>Methylosinus</i>	0.16	0.00	0.00	0.00	0.00	0.00	0.00
	<i>Sphingomonas</i>	0.14	0.00	0.00	0.00	0.00	0.00	0.00
	<i>Blastomonas</i>	0.14	0.00	0.53	0.00	0.00	0.00	0.34
	<i>Pseudochrobactrum</i>	0.00	2.17	0.52	0.00	0.00	0.00	0.00
	<i>Ochrobactrum</i>	0.00	2.09	0.55	0.00	0.00	0.00	0.00
	<i>Aquamicrobium</i>	0.00	1.88	1.58	0.00	0.00	0.00	0.00
	<i>Brevundimonas</i>	0.00	0.29	0.00	0.00	0.00	0.00	0.00
	<i>Rhizobium</i>	0.00	0.17	0.67	0.00	0.00	0.00	0.91
	<i>Agrobacterium</i>	0.00	0.00	0.71	0.00	0.00	0.00	0.00
	<i>Sphingopyxis</i>	0.00	0.00	0.20	0.00	0.00	0.00	0.00
	<i>Hypomicrobium</i>	0.00	0.00	0.00	0.00	0.00	0.15	0.61
	<i>Thalassospira</i>	0.00	0.00	0.00	0.00	0.00	0.00	3.23
	<i>Dongia</i>	0.00	0.00	0.00	0.00	0.00	0.00	0.38
	<i>Rhodobacter</i>	0.00	0.00	0.00	0.00	0.00	0.00	0.23
	<i>β</i> -proteobacteria	<i>Brachymonas</i>	0.61	18.56	1.07	0.00	3.52	1.25
<i>Azospira</i>		0.35	0.00	0.00	0.30	0.48	1.56	0.15
<i>Azoarcus</i>		0.14	0.00	0.00	0.00	0.00	0.00	0.00
<i>Simplicispira</i>		0.14	0.14	0.00	0.17	0.00	0.18	0.61
<i>Conchiformibius</i>		0.14	0.00	0.00	0.00	0.00	0.00	0.00
<i>Pusillimonas</i>		0.12	0.00	0.00	0.00	0.00	0.00	0.00
<i>Alcaligenes</i>		0.00	32.35	6.39	0.30	0.00	0.00	0.00
<i>Delftia</i>		0.00	2.83	0.91	0.00	0.00	0.20	0.00
<i>Massilia</i>		0.00	1.38	4.37	0.00	0.00	0.00	0.00
<i>Acidovorax</i>		0.00	0.71	2.18	0.00	0.00	0.88	0.11
<i>Achromobacter</i>		0.00	0.56	0.00	0.00	0.00	0.00	0.00
<i>Paucibacter</i>		0.00	0.23	0.00	0.00	0.00	0.00	0.00
<i>Alicyclophilus</i>		0.00	0.00	0.00	0.00	0.00	0.54	0.00
<i>Comamonas</i>		0.00	0.00	0.00	0.00	0.00	0.46	0.00
<i>Hydrogenophaga</i>		0.00	0.00	0.00	0.00	0.00	0.29	0.00
<i>Thiobacillus</i>	0.00	0.00	0.00	0.00	0.00	0.00	0.57	
<i>Limnibacter</i>	0.00	0.00	0.00	0.00	0.00	0.00	0.23	
<i>Lamproedia</i>	0.00	0.00	0.00	0.00	0.00	0.00	0.19	
<i>γ</i> -proteobacteria	<i>Pseudomonas</i>	2.47	6.13	49.68	5.29	56.10	10.28	2.43
	<i>Thiomicrospira</i>	0.12	0.00	0.00	0.00	0.00	0.00	0.00
	<i>Methylomonas</i>	0.12	0.00	0.00	0.00	0.00	0.00	0.00
	<i>Stenotrophomonas</i>	0.00	1.01	0.39	0.00	0.00	0.15	0.00
	<i>Thiothrix</i>	0.00	0.00	0.00	0.25	0.00	0.00	0.00
	<i>Coxiella</i>	0.00	0.00	0.00	0.00	1.07	0.34	1.22
	<i>Marinospirillum</i>	0.00	0.00	0.00	0.00	0.31	0.00	0.00
	<i>Thermomonas</i>	0.00	0.00	0.00	0.00	0.00	0.28	0.11
	<i>Rhodanobacter</i>	0.00	0.00	0.00	0.00	0.00	0.00	0.61
	<i>Pseudofulvimonas</i>	0.00	0.00	0.00	0.00	0.00	0.00	0.19
<i>δ</i> -proteobacteria	<i>Syntrophus</i>	0.41	0.00	0.00	0.15	0.00	0.00	1.63
	<i>Arcobacter</i>	0.22	0.00	0.00	1.08	0.94	0.00	0.53
	<i>Phaselicystis</i>	0.20	0.00	0.00	0.00	0.00	0.00	0.00
	<i>Desulfovibrio</i>	0.18	0.28	0.57	0.38	0.00	0.00	0.00
	<i>Smithella</i>	0.00	0.14	0.00	0.00	0.00	0.00	0.19
	<i>Desulfuromonas</i>	0.00	0.00	0.00	0.00	0.00	4.46	0.00
	<i>Cystobacterineae</i>	0.00	0.00	0.00	0.00	0.00	0.00	0.27
	<i>Nannocystineae</i>	0.00	0.00	0.00	0.00	0.00	0.00	0.15
	<i>Desulfobulbus</i>	0.00	0.00	0.00	0.00	0.00	0.00	0.15
	<i>Nitratifactor</i>	0.37	0.00	0.00	0.13	0.00	0.00	0.00
<i>ε</i> -proteobacteria	<i>Sulfurovum</i>	0.00	0.00	0.00	0.00	0.89	1.07	0.11
	<i>Sulfurinomas</i>	0.00	0.00	0.00	0.00	0.15	0.00	0.00
	<i>Sulfurospirillum</i>	0.00	0.00	0.00	0.00	0.00	0.00	0.11

Table 6.8. Changes in relative abundances of the bacteria genera (continuation).

Taxonomy		Abundance (%)						
Phyla or Classes	Genera	In.AD	B ₁	B ₂	B ₃	PS	B ₁	B ₂
			MFC _{SW}	MFC _{SW}	MFC _{SW-BES}		MFC _{PS}	MFC _{PS}
Actinobacteria	<i>Dermatophilus</i>	0.23	0.00	0.00	0.00	0.00	0.00	0.00
	<i>Virgisporangium</i>	0.14	0.00	0.00	0.00	0.00	0.00	0.00
	<i>Tetrasphaera</i>	0.00	2.80	0.55	0.00	0.41	1.15	0.49
	<i>Gordonia</i>	0.00	0.41	0.00	0.00	0.00	0.00	0.00
	<i>Rhodococcus</i>	0.00	0.36	0.00	0.00	0.00	0.00	0.00
	<i>Mycobacterium</i>	0.00	0.32	0.14	0.00	0.00	0.00	0.00
	<i>Iamia</i>	0.00	0.00	0.00	0.16	0.00	0.00	0.00
	<i>Eggerthella</i>	0.00	0.00	0.00	0.00	0.39	0.20	0.00
	<i>Streptomyces</i>	0.00	0.00	0.00	0.00	0.00	0.11	0.11
	<i>Corynebacterium</i>	0.00	0.00	0.00	0.00	0.00	0.00	0.11
	<i>Arthrobacter</i>	0.00	0.00	0.00	0.00	0.00	0.00	0.11
Synergistetes	<i>Anaerobaculum</i>	1.14	0.00	0.00	0.00	0.00	0.00	0.00
Spirochaetes	<i>Spirochaeta</i>	0.74	0.00	0.00	0.11	0.22	0.29	0.91
	<i>Treponema</i>	0.00	0.00	0.00	0.00	0.15	0.00	0.46
Thermotogae	<i>Kosmotoga</i>	0.31	0.00	0.00	0.00	0.00	0.00	0.00
Chloroflexi	<i>Dehalococcoides</i>	0.00	0.00	0.00	0.00	0.30	0.11	0.00
Tenericutes	<i>Haloplasma</i>	0.00	0.00	0.00	0.00	0.00	0.00	0.34
Gemmatimonadetes	<i>Gemmatimonas</i>	0.00	0.00	0.00	0.00	0.00	0.00	0.15
Lentisphaeria	<i>Victivallis</i>	0.00	0.00	0.00	0.00	0.00	0.00	0.15
Deinococcus-Thermus	<i>Truepera</i>	0.00	0.00	0.00	0.00	0.00	0.00	0.11

Relative abundance (%)



As for the MFC_{PS}, some difference of dominant genera (above 1.0% in abundance) were newly detected in comparison to the MFC_{SW}, *Paludibacter* sp., *Owenweeksia* sp., *Alkaliflexus* sp., *Meniscus* sp., *Acholeplasma* sp., *Fastidiosipila* sp., *Alkaliphilus* sp., *Syntrophomonas* sp., *Thalassospira* sp., *Azospira* sp., *Coxiella* sp., *Synthrophus* sp., *Desulfuromonas* sp. and *Sulfurovum* sp.

6.3.7. Archaea community composition

6.3.7.1. Microbial population adaptation overtime and under different operational conditions

Two orders of Archaea are dominant in In.AD sample, *Methanomicrobiales* (81.3%) and *Methanosarcinales* (16.7%). However, there is a clear enrichment in *Methanosarcinales* in the MFC_{SW} anodic compartment, reaching almost 100% in B₁ and B₂ MFC_{SW} (Figure 6.20).

Regarding pig slurry (PS), four orders were detected: *Methanomicrobiales* (90.3%), *Methanosarcinales* (3.9%), *Methanobacteriales* (2.6%) and *Halobacteriales* (2.2%), and a selective enrichment throughout incubation promoted *Methanosarcinales* in the MFC_{PS}, founding *Methanomicrobiales* (81.6%) and *Methanosarcinales* (15.6%) for the B₁ MFC_{PS} and inversely *Methanomicrobiales* (13.9%) and *Methanosarcinales* (81.8%) for the B₂ MFC_{PS}.

6.3.7.2. Effect of different substrates feed

The genus and family level classification illustrated in **Figure 6.20** revealed that the dominant genus in the MFC_{SW} accounted for over 99% in the three samples (In.AD, B₁ and B₂ MFC_{SW}) was *Methanosarcina* sp. Nevertheless, *Methanosarcina* sp., was not identified in B₁ MFC_{PS} and just with 9.7% in B₂ MFC_{PS}. Contrary, the archaeal community structure showed a shift among the time in the MFC_{PS}. In B₁ MFC_{PS}, *Methanomicrobium* sp. accounted for 68.9% of the total Archaea population, following by *Methanosaeta* sp. (14.7%), *Methanoculleus* sp. (5.8%) and *Methanogenium* sp. (6.7%). The community composition in B₂ MFC_{PS} is quite similar to B₁ MFC_{PS} but with different relative abundances. So in this case, the majority (71.9%) of the total Archaea community is *Methanosaeta* sp., and three minority genus as *Methanoculleus* sp. (8.2%), *Methanomicrobium* sp. (4.2%) and *Fervicoccaceae* (3.4%). Thus, an acetoclastic methanogens, *Methanosaeta* sp., and *Methanosarcina* sp., which have the acetoclastic and hydrogenotrophic pathway, were dominant in B₁ and B₂ MFC_{SW}, B₃ MFC_{SW-BES} and B₂ MFC_{PS}. Contrary, an hydrogenotrophic methanogen, *Methanomicrobium* sp., was dominant in B₁ MFC_{PS}. Both *Methanosarcina* sp. and *Methanosaeta* sp. are an acetate oxidizers (Garcia et al., 2006), thus in these MFCs, mainly in the MFC_{SW}, methanogenic archaea was competing with the exoelectrogenic bacteria for the substrate. Hydrogenotrophic methanogens as *Methanomicrobium* sp., which is dominant in PS and in B₁ MFC_{PS}, was also members in the anodic community of a MFC feed with glucose or cellulose (Borole et al., 2009).

6.3.7.3. Effect of BES inhibitor

The order of *Methanosarcinales* is almost reaching 100% in B₃ MFC_{SW-BES}, thus these results indicated that the addition of BES-Inh. ranging from 0.16 to 10 mM did not inhibited the methanogenic pathway, contrary to others studies report (Chae et al., 2019; Zhuang et al., 2012). **Figure 6.20** shows that the addition of BES-Inh. did not change any effect over the archaeal community, being also *Methanosarcina* sp. the dominant genus after the addition of BES-Inh.

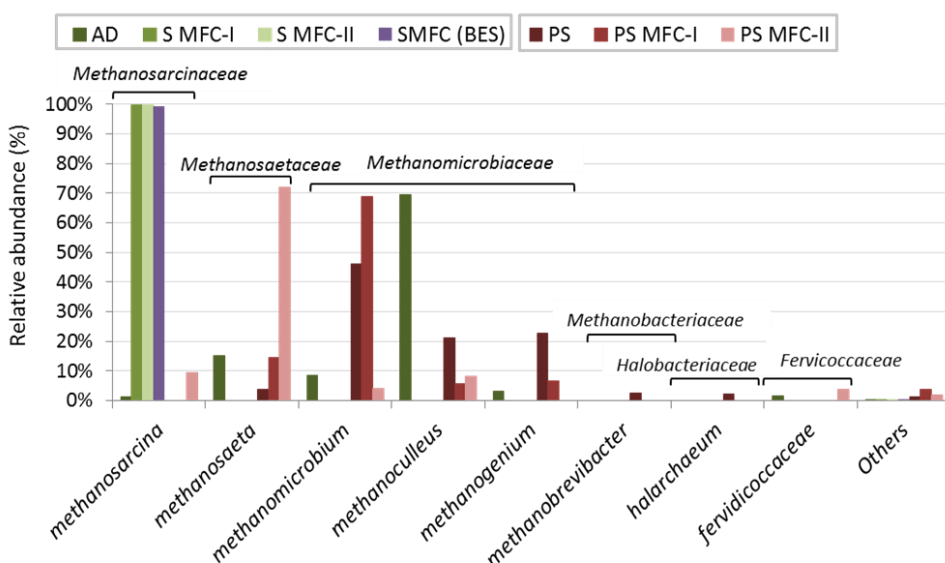


Figure 6.20. 1 **Figure 6.20.** Taxonomic classification of 454-pyrosequencing data from archaeal communities of In.AD, B₁ MFC_{SW}, B₂ MFC_{SW}, B₃ MFC_{SW-BES}, PS, B₁ MFC_{PS} and B₂ MFC_{PS} at a family and genus level. Groups making up less than 1% of the total number of sequences per sample were classified as "others".

6.4. Conclusions

Molecular biology techniques as DGGE and 454-pyrosequencing, were used to analyse and compare the anodophilic biofilms in a two-chamber MFC operating with synthetic wastewater and liquid fraction of pig slurry. Both anodophilic biofilms presented different species, belonging some of them to well-known exoelectrogenic microorganisms, so it was clearly demonstrated that the type of substrate and the operational conditions determined the biofilm developed. Although the literature and the present results suggested that there is no typical MFC microbial community in all anode biofilms, since it is extremely dependent on other factors, we could identify three common families found in all conditions in this study, *Comamonadaceae*, *Flavobacteriaceae* and *Porohyromonadaceae*, which could be considered majority exoelectrogens without dependence of others intermediaries.

Archaeal communities showed much less diversity than eubacterial communities. Acetoclastic methanogens were predominant in B₁ and B₂ MFC_{SW} (*Methanosarcina* sp.), and B₂ MFC_{PS} (*Methanosaeta* sp.), while hydrogenotrophic methanogens was the the most abundant in B₁ MFC_{PS} (*Methanomicrobium* sp.).

BES addition did not inhibit completely methanogenesis at concentrations between 0.16 and 10 mM. These concentrations could produce the inhibition of acetoclastic pathway associated to *Methanosarcina* sp., enhancing hydrogenotrophic pathway. Nevertheless, a shift in eubacterial community diversity is observed, as well as a shift in relative abundance of phyla such as Bacteroidetes, which could play an important role in the increasing of the coulombic efficiency.

6.5. References

- Borole, A.P., Hamilton, C.Y., Vishnivetskaya, T.A., Leak, D., Andras, C., Morrel-Falvey, J., Keller, M., Davison, B., 2009. Integrating engineering design improvements with exoelectrogen enrichment process to increase power output from microbial fuel cells. *J Power Sour.* 191, 520-527.
- Caporaso, J.G., K. Bittinger, F.D. Bushman, T.Z. DeSantis, G.L. Andersen, R. Knight., 2010. PyNASt: A flexible tool for aligning sequences to a template alignment, *Bioinformatics.* 26, 266-267.
- Chae, K.J., Choi, M.J., Lee, J.W., Kim, K.Y., Kim, I.S., 2009. Effect of different substrates on the performance, bacterial diversity, and bacterial viability in microbial fuel cells. *Bioresour. Technol.* 100, 3518-3525.
- Chae, K.J., Choi, M.J., Kim, K.Y., Ajayi, F.F., Park, W., Kim, C.W., Kim, I.S., 2010. Methanogenesis control by employing various environmental stress conditions in two-chambered microbial fuel cells. *Bioresour. Technol.* 101, 5350-5357.
- Chiu, P.C., Lee, M., 2001. 2-Bromoethanesulfonate affects bacteria in a trichloroethenedechlorinating culture. *Appl. Environ. Microbiol.* 67(5), 2371-2374.
- DeSantis, T. Z., P. Hugenholtz., 2006. Greengenes, a chimera-checked 16S rRNA gene database and workbench compatible with ARB. *Appl Environ Microbiol* 72(7), 5069-5072.
- DiMarco, A.A., Bobik, T.A., Wolfe, R.S., 1990. Unusual coenzymes of methanogenesis. *Annu. Rev. Biochem.* 59, 355-394.
- Edgar, R.C., 2011. Search and clustering orders of magnitude faster than BLAST. *Bioinformatics.* 26, 2460-2461.
- Franks, A.E., Malvankar, N., Nevin, K.P., 2010. Bacterial biofilms: the powerhouse of a microbial fuel cell. *Biofuels.* 1, 589-604.
- Freguia, S., Rabaey, K., Yuan, Z., Keller, J., 2007a. Non-catalyzed cathodic oxygen reduction at graphite granules in microbial fuel cells. *Electrochimica Acta.* 53, 598-603.
- Freguia, S., Rabaey, K., Yuan, S., Keller, J., 2007b. Electron and carbon balances in microbial fuel cells reveal temporary bacterial storage behaviour during electricity generation. *Environ. Sci. Technol.* 41, 2915-2921.
- Garcia, J.L., Ollivier, B., Whitman, W.B., 2006. The order Methanomicrobiales. *The Prokaryotes.* Springer Science, New York, USA, pp 208-230.

- Ishii, S., Suzuki, S., Norden-Krichmar, T.M., Wu, A., Yamanaka, Y., Nealson, K.H., Bretschger, O., 2013. Identifying the microbial communities and operational conditions for optimized wastewater treatment in microbial fuel cells. *Water Res.* 47, 7120-7130.
- Jung, S., Regan, J.M., 2007. Comparison of anode bacterial communities and performance in microbial fuel cells with different electron donors. *Appl. Microbiol. Biotechnol.* 77(2), 393-402.
- Lesnik, K.L., Liu, H., 2014. Establishing a core microbiome in acetate-fed microbial fuel cells. *Appl. Microbiol. Biotechnol.* 98 (9), 4187-4196.
- Liu, H., Wang, A., Chen, J., 2011. Chemical inhibitors of methanogenesis and putative applications. *Appl. Microbiol. Biotechnol.* 89, 1333-1340.
- Liu, F., Rotaru, A.E., Shrestha, P.M., Malvankar, N.S., Nevin, K.P., Lovley, D.R., 2012. Promoting direct interspecies electron transfer with activated carbon. *Energy Environ. Sci.* DOI: 10.1039/c2ee22459c
- Logan, B.E., Regan, J.M., 2006. Electricity-producing bacterial communities in microbial fuel cells. *Trends Microbiol.* 15, 512-518.
- Lovley, D.R., 2006. Bug juice: harvesting electricity with microorganisms. *Nature Reviews Microbiol.* 4, 497-508.
- Lu, H., Oehmen, A., Virdis, B., Keller, J., Yuan, Z., 2006. Obtaining highly enriched cultures of *Candidatus Accumulibacter* phosphates through altering a carbon sources. *Water Res.* 40, 3838-3848.
- Lu, L., Xing, D., Ren, N., 2012. Pyrosequencing reveals highly diverse microbial communities in microbial electrolysis cells involved in enhanced H₂ production from waste activated sludge. *Water Res.* 46, 2425-2434.
- Muyzer G, DeWaal, E.C., Uitterlinden, A.G., 1993. Profiling of complex microbial populations by denaturing gradient gel electrophoresis analysis of polymerase chain reaction-amplified genes coding for 16S rRNA. *Appl. Environ. Microbiol.* 59, 695-700.
- Noguerol-Arias, J., Rodríguez-Abalde, A., Romero-Merino, E., Flotats, X., 2012. Determination of Chemical Oxygen Demand in Heterogeneous Solid or Semisolid Samples Using a Novel Method Combining Solid Dilutions as a Preparation Step Followed by Optimized Closed Reflux and Colorimetric Measurement. *Anal. Chem.* 84, 5548-5555.
- Nollet, L., Demeyer, D., Verstraete, W., 1997. Effect of 2-bromoethanesulfonic acid and Peptostreptococcus products ATCC 35244 addition on simulation of reductive acetogenesis in the ruminal ecosystem by selective inhibition of methanogenesis. *Appl. Environ. Microbiol.* 63(1), 194-200.
- Oliveros, J.C., 2007. VENNY. An interactive tool for comparing lists with Venn Diagrams. <http://bioinfogp.cnb.csic.es/tools/venny/index.html>.
- Palatsi J, Illa J, Prenafeta-Boldú FX, Laurení M, Fernández B, Angelidaki I, Flotats, X., 2010. Long-chain fatty acids inhibition and adaptation process in anaerobic thermophilic digestion: Batch tests, microbial community structure and mathematical modelling. *Bioresour. Technol.* 101, 2243-2251.
- Pant, D., Van Bogaert, G., Diels, L., and Vanbroekhoven, K. (2010). A review of the substrates

- used in microbial fuel cells (MFCs) for sustainable energy production. *Bioresor. Technol.* 101, 1533-1543.
- Rajesh, P.P., Noori, M.D.T., Ghangrekar, M.M., 2014. Controlling methanogenesis and improving power production of microbial fuel cell by lauric acid dosing. *Water Sci. Technol.* 70(8), 1363-1369. doi: 10.2166/wst.2014.386.
- Rabaey, K., Rodríguez, J., Blackall, L.L., 2007. Microbial ecology meets electrochemistry: electricity-driven and driving communities. *The ISME Journal.* 1, 9-18.
- Reeder, J., R. Knight., 2010. Rapidly denoising pyrosequencing amplicon reads by exploiting rank-abundance distributions. *Nature Methods.* 7, 668-669.
- Rotaru A.E., Shrestha P, Liu F, Shrestha M, Shrestha D, Embree M, Zengler K, Wardman C, Nevin K.P., Lovley, D.R., 2014. A new model for electron flow during anaerobic digestion: direct interspecies electron transfer to *Methanosaeta* for the reduction of carbon dioxide to methane. *Energy Environ Sci* 7: 408-415.
- Sotres, A., Diaz-Marcos, J., Guivernau, M., Ila, J., Magrñi, A., Prenafeta-Boldú, F.X., Bonmati, A., Viñas, M., 2014. Microbial community dynamics in two-chambered microbial fuel cells: Effect of different ion exchange membranes. *J. Chem. Technol. Biotechnol.* DOI:10.1002/jctb.4465.
- Schloss, P.D., Westcott, S.L., Ryabin, T., Hall, J.R., Hartmann, M., Hollister, E.B., Lesniewski, R.A., Oakley, B.B., Parks, D.H., Robinson, C.J., Sahl, J.W., Stres, B., Thallinger, G.G., Van Horn, D.J., Weber, C.F., 2009. Introducing mother: open-source, platform-independent, community-supported software for describing and comparing microbial communities. *Appl. Environ. Microbiol.* 75, 7537-7541.
- Shade, A., Handelsman, J., 2012. Beyond the Venn diagram: the hunt for a core microbiome. *Environ. Microbiol.* 14, 4-12. doi:10.1111/j.1462-2920.2011.02585.x
- Takai, K., Horikoshi, K., 2000. Rapid Detection and Quantification of Members of the Archaeal Community by Quantitative PCR Using Fluorogenic Probes. *Appl. Environ. Microbiol.* 66(11), 5066-5072.
- Yu, Z., Morrison, M., 2004. Comparisons of different hypervariable regions of *rrs* genes for use in fingerprinting of microbial communities by PCR-denaturing gradient gel electrophoresis. *Appl. Environ. Microbiol.* 70, 4800-4806.
- Zhuang, L., Chen, Q., Zhou, S., Yuan, Y., Yuan, H., 2012. Methanogenesis control using 2-bromoethanesulfonate for enhanced power recovery from sewage sludge in air-cathode microbial fuel cells. *Int. J. Electrochem. Sci.* 7, 6512-6523.
- Zinder, S.H., Anguish, T., Cardwell, S.C., 1984. Selective Inhibition by 2-Bromoethanesulfonate of Methanogenesis from Acetate in a Thermophilic Anaerobic Digester. *Appl. Environ. Microbiol.* 47(6), 1343-1345.

Chapter 7

Nitrogen recovery from pig slurry in a two-chambered bioelectrochemical system



Sotres, A., Cerrillo, M., Viñas M., Bonmati, A.

2nd EU-ISMET.3-5, September, Alcalá de Henares (Spain)(2014): [oral presentation](#)

Sotres, A., Cerrillo, M., Viñas M., Bonmati, A. (2015)

Submitted to peer reviewed journal

Abstract

Abiotic batch experiments showed that ammonia migration from anode to cathode was favoured by an increase in voltage, from 24.9% to 44.6%, using synthetic wastewater. A slight increase in ammonia migration was observed when using pig slurry, reaching a maximum ammonia migration of 49.9%. In a continuously MFC fed with pig slurry with a stripping/absorption unit coupled to the cathode chamber, the highest nitrogen flux ($7.23 \text{ g N d}^{-1} \text{ m}^{-2}$) was achieved using a buffer as catholyte. Nitrogen flux increased to $10.26 \text{ g N d}^{-1} \text{ m}^{-2}$ when shifting to MEC mode. A clear improvement in nitrogen flux ($25.51 \text{ g N d}^{-1} \text{ m}^{-2}$) was observed when using NaCl as catholyte. Besides, ammonia stripping was favoured, reaching a nitrogen recovery of 94.3% in the absorption column, due to the high pH reached in the cathode. The microbial community analysis revealed an enrichment of certain taxonomic Eubacterial and Archaeal groups when the system shifted from MFC to MEC mode.

7.2. Introduction

A conventional electrochemical system consists of a chemical anode and a chemical cathode separated by an ion exchange membrane, where the oxidation and reduction reactions take place in each compartment respectively. Bio-electrochemical systems (BESs) came upon the discovery of electrochemically active microorganisms which can catalyze the oxidation/reduction reactions being able to transfer the electrons to a solid surface such as the electrode (Pant et al., 2011; Clauwaert et al., 2008; Rabaey et al., 2010). A BES is considered a microbial fuel cell (MFC) if it gathers electrical power, and is considered microbial electrolysis cell (MEC) if electrical energy is supplied to drive an otherwise non-spontaneous reaction (Hamelers et al., 2010).

One advantage of a BES with a two chamber configuration is that the oxidation and reduction products are produced in separated compartments, making possible to recover “clean” products out of wastes (Hamelers et al., 2010). For this reason, BES are increasingly becoming a novel technological solution for environmental issues related to wastewater treatment, nutrient recovery, and the production of valuable compounds, with the advantage that they can help to reduce energy costs.

Nitrogen is one of the key contaminants and its discharge regulation is becoming stricter hence, to develop or further improve a technology for nitrogen removal/recovery is becoming a challenge in BES research. It is well known that nitrogen can affect the BES performance since the concentration of total

ammonia nitrogen (TAN) can inhibit the activity of the microbial community, and accordingly can affect the anodophilic population reducing electricity generation (Nam et al., 2010). Nevertheless, and as it is reported that microorganisms can acclimatise to increasing TAN concentrations, the inhibition concentration threshold is not clear. In this sense, Kim et al. (2011) reported a higher TAN inhibition threshold in MFCs operating in continuous mode, than in batch mode. Besides ammonia inhibition depends on the anolyte pH (Kuntke et al., 2011). With a low anolyte pH, an increase in ammonia concentration does not affect the performance of a MFC in the same way, owing to the low anolyte pH which results in less free ammonia. Therefore, understanding how nitrogen can affect a BES performance is a key factor to improve strategies for nitrogen removal/recovery from organic wastes.

So far, different processes have been studied for nitrogen removal/recovery using BES technologies. It has been reported that nitrogen can be removed by using biological processes such as external nitrification and subsequent denitrification, accomplished by microorganisms in the cathode chamber (Clauwaert et al., 2007; Virdis et al., 2008), or even with simultaneous nitrification-denitrification in the cathode (Virdis et al., 2010). Another strategy for nitrogen recovery is to combine biological and physicochemical processes. The fundament of this strategy in a BES system is the fact that ammonium ions can diffuse from the anode onto the cathode compartment throughout the cation exchange membrane (Rozendal et al., 2008), either via diffusion or current-driven migration (Kuntke et al., 2011). Then, the ammonia can be recovered by means of stripping, promoted by active aeration and a high catholyte pH, and its subsequent adsorption in an acid solution. This strategy has been previously described by Kuntke et al. (2012), who developed a MFC reactor to simultaneously produce energy and recover ammonium from real urine, reaching an ammonium recovery rate of $3.29 \text{ gN d}^{-1} \text{ m}^{-2}$, at a current density of 0.50 A m^{-2} . Later on, Desloover et al. (2012) developed a non biological electrochemical cell in which a stripping unit was coupled to the cathode chamber, reaching a nitrogen flux of $120 \text{ gN d}^{-1} \text{ m}^{-2}$, with synthetic wastewater. Although this technology has already been reported as a sustainable process to recover ammonia from wastewater, further research is needed when applied to high strength and nitrogen rich wastewater, such as pig slurries, and equally to investigate more in depth its performance in MFC and MEC modes.

Setting up a biofilm on the electrode surface is essential for efficient performance in a BES (Franks et al., 2010). Although both MFCs and MECs favour the growth of exoelectrogenic bacteria, microbial communities in MECs may be

different from those in MFCs, because distinct conditions favour the growth of different microorganisms, as previously described (Logan et al., 2008). So far, there is a lack of knowledge about the best method for enriching an exoelectrogenic microbial community, but a common practice described by Ditzig et al. (2007) is to switch from MFC mode to MEC mode for the inoculum to be initially acclimated and for an exoelectrogenic community to be preselected in the anode of the MFC.

In this work, the use of both synthetic wastewater and the liquid fraction of pig slurry and the effect of the applied voltage on ammonia recovering, were studied. Furthermore, the feasibility of nitrogen recovery using a stripping unit coupled to the cathode of a continuously fed BES was investigated. Whereas the stripping system was operated under MFC and MEC modes, a third goal was to analyze the effect of shifting from MFC mode to MEC mode on the microbial community (Eubacteria and Archaea) of the bio-anode, by means of 454-pyrosequencing.

7.2. Material and methods

7.2.1. Experimental set-up

The experimental set up consisted of a two-chambered bioelectrochemical system (BES). The BES was built using methacrylate plates, with the anode and cathode compartment ($0.14 \times 0.12 \times 0.02 \text{ m}^3$) separated by a cation exchange membrane CEM (14 x 12 cm) (Ultrex CMI-7000, Membrane International Inc., Ringwood, NJ, USA). The anode frame had a window which allowed taking samples from the biomass attached to the electrode. A carbon felt mesh, 3.18 mm thick, 99.0% Carbon (Cymit Química, S.L.) and stainless steel mesh, were used as anode and cathode electrodes respectively. Before use, organic and inorganic impurities were eliminated from the carbon felt sequentially soaking it in HCl 1M and NaOH 1M, each time for 24 hours, and then rinsing it with deionised water. The projected anode surface area was of 0.0209 m^2 . Copper wires were used to connect the electrodes to an external 100Ω resistance (MFC mode) or to a power supply unit (MEC mode).

When the BES was fed with the liquid fraction of pig slurry a stripping/absorption unit was coupled to the cathode compartment, following to the set up previously described by Desloover et al. (2012) (**see Chapter 3, section 3.1.3**). The system consisted of two tubular columns (height: 70 cm, external diameter: 7 cm, internal diameter: 5.5 cm) both filled with Raschig rings (length: 5-7 mm, internal diameter: 3 mm, external diameter: 5 mm) (**Figure 7.1**). The stripping column was filled with 80 mL of medium from the cathode chamber and the absorption column with 500 mL

of H_2SO_4 1 M. The spraying of the catholyte over the stripping column was completed installing a Mini diaphragm vacuum pump (VP 86, VWR International) at the bottom of the column; a water trap was also connected to protect the pump.

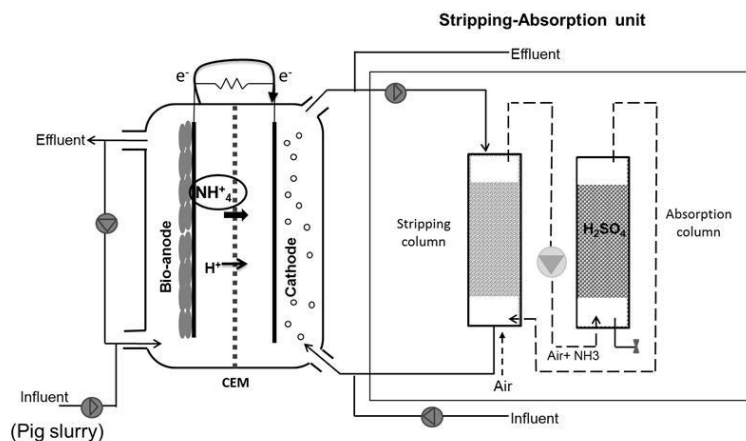


Figure 7.1. Scheme of the BES coupled with the stripping/absorption unit.

7.2.2. Batch experiments

Batch experiments were performed at room temperature (23 ± 1 °C) in abiotic conditions. The anode feed consisted of either synthetic wastewater or the liquid fraction of pig slurry with an ammonium concentration of $523 \text{ mg N-NH}_4^+ \text{ L}^{-1}$; and a buffer solution or sodium chloride for the cathode compartment, depending on the experimental design. All abiotic experiments were performed under different voltages: passive diffusion (P.D.), 0.3 V and 0.6 V, using a power supply unit (PS23032, Diotronic, S.A.). Each experiment lasted 56 hours and every condition was tested in triplicate.

7.2.3. Continuous experiments

For the continuous experiments, the anode and cathode were continuously fed with a hydraulic retention time (HRT) of 6.9 ± 0.7 and 4.3 ± 0.3 hours for the anode and cathode chamber, respectively. The organic loading rate (OLR) and the nitrogen loading rate (NLR) were increased stepwise from 3.0 to $10.7 \text{ g COD L}^{-1} \text{ d}^{-1}$ and 1.1 to $7.4 \text{ g N L}^{-1} \text{ d}^{-1}$, respectively. MEC mode experiments were performed applying a voltage (E_{op}) of 0.1- 0.8 V using a (PS23032 Diotronic, S.A.) power

source, as elsewhere described by Call and Logan (2008). A 10 Ω resistor was connected to one of the leads with the power supply, allowing for voltage measurement across the resistor.

The duration of the stripping experiments was of 72 hours for each assay performed. Three samples from the anode and cathode compartments and the absorption column were taken per day.

7.2.4. Medium composition

The synthetic wastewater used in the batch experiments contained (per litre of tap water): CaCl_2 , 0.0147 g ; KH_2PO_4 , 3 g ; Na_2HPO_4 , 6 g and MgSO_4 , 0.34 g. Additionally, 2 g L^{-1} NH_4Cl were added to the anode solution once the synthetic wastewater was prepared. The cathode feed consisted of either a buffer phosphate (KH_2PO_4 , 3 g L^{-1} and Na_2HPO_4 6 g L^{-1}) or sodium chloride (NaCl , 0.1 g L^{-1}).

The pig slurry used was collected from a pig farm located in Calldetenes (Catalonia) and was centrifuged (4991 g during 10 minutes) before feeding it to the cell. The main physicochemical characteristics of the liquid fraction of the pig slurry were: pH, 7.72; COD_t ($\text{mgO}_2 \text{ kg}^{-1}$), 6908; COD_s ($\text{mg O}_2 \text{ kg}^{-1}$), 3462; N-NH_4^+ ($\text{mg N-NH}_4^+ \text{ L}^{-1}$), 858.15; Kjeldahl-N (mg N L^{-1}), 1068.47; TSS (%), 0.78; VSS (%), 0.42; alkalinity (g $\text{CaCO}_3 \text{ L}^{-1}$), 3.2; conductivity (mS cm^{-1}), 7.73. In order to procure the desired concentrations for the different assays, specific dilutions were carried out.

7.2.5. Electrochemical characterization

Voltage (V) across a given external resistance (Ω) was recorded at 20 min intervals using a multimeter data acquisition unit (Mod. 34970A, Agilent Technologies, Loveland, CO, USA). Current density (I) was then calculated using Ohm's Law, and power density (P) was obtained using $P = IV/A$, where I stands for the current density (A), V stands for the voltage (V), A stands for the electrode surface area (m^2) and P stands for the power density (mW m^{-2}).

Including a resistor in the external circuit results in additional voltage loss, thus the applied voltage (E_{ap}), over the anode and cathode, was smaller than the power source applied voltage, (E_{ps}). The applied voltage can be calculated with the following equation (Logan et al., 2008):

(Equation 7.1)

$$E_{ap} = E_{ps} - IR_{ext}$$

where, E_{ap} stands for the voltage applied to the cell (V), E_{ps} for the applied voltage of the power source (V), I is the current density (A) calculated from the voltage across the resistor, and R_{ext} is the load (10 Ω).

Polarization curves (P versus I) were carried out in order to obtain maximum power densities and internal resistance within the system, thus evaluating the performance of the cell. The procedure to obtain a polarization curve was as follows: after leaving the system in an open circuit for 1 hour, the circuit was closed and the external resistance changed from 10000 to 1.2 Ω (10000, 1000, 500, 100, 50, 10, 5 and 1.2). Upon the connexion of each resistance, the system was left to stabilize for 30 min, before recording the voltage data.

Coulombic efficiency (CE), defined as the ratio of electrons used as current to the theoretical maximum electron production, was calculated as described in Logan et al. (2006).

7.2.6. Chemical analysis and calculations

Ammonium $\text{NH}_4^+\text{-N}$, total solids (TS), volatile solids (VS), Total Kjeldahl nitrogen (TKN), soluble COD (CODs), total COD (CODt), and pH were analysed according to Standard Method 5220 (APHA, 2005). Sodium (Na^+), potassium (K^+), calcium (Ca^{2+}) and magnesium (Mg^{2+}) concentrations were quantified by ion chromatography (Metrohm 861 Advanced Compact IC), using a Metrohm Metrosep A Supp 4 column and a Metrosep A Supp 4/5 Guard pre-column with a 4 mmol $\text{C}_4\text{H}_6\text{O}_6/\text{L}$ (tartaric acid) and 0.75 mmol pyridine-2,6-dicarboxylic acid/L effluent, once filtered through a 0.2 μm pore diameter PTFE syringe filter (VWR International). Ammonium ($\text{NH}_4^+\text{-N}$) was analysed with a Büchi B-324 distiller, and a Metrohm 702 SM autotitrator. Bulk solution pH was measured with a pH electrode CRISON 2000. CODs and CODt were measured according to an optimized method: the APHA–AWWA–WPCF Standard Method 5220 (Noguerol et al., 2012). The CODs sample was previously filtered through a 0.45 μm pore diameter Nylon syringe filter (Scharlau, S.L.).

Nitrogen flux (J_N , $\text{g N m}^{-2} \text{d}^{-1}$) from anode to cathode was calculated as:

$$\text{(Equation 7.2)} \quad J_N = \frac{(C_{An,in} - C_{An,out}) \times Q}{A}$$

where $C_{An,in}$ (g N L^{-1}) and $C_{An,out}$ (g N L^{-1}) are the measured NH_4^+ -N concentrations coming in and out of the anode compartment, respectively. Q (L d^{-1}) is the anode flow rate, and A (m^2) is the ion exchange membrane projected surface area.

The statistical analysis was performed using R software (R project for statistical computing) and ANOVA and Tukey tests were carried out to analyze the results.

7.2.7. Microbial community analysis

In order to study the microbial community attached to the electrodes when shifting from MFC mode to MEC mode, three different spots of the anode carbon felt were sampled. Samples were taken at the end of the MFC period (55 days of operation) and at the end of the MEC mode (41 days of operation). Total genomic DNA was extracted considering the known weight of each sample with a PowerSoil® DNA Isolation Kit (MoBio Laboratories Inc., Carlsbad, CA, USA), following the manufacturer's instructions. The quantity and quality of the extracted DNA was checked measuring them in a NanoDrop 1000 (Thermo Scientific).

This DNA extract was used for 454-pyrosequencing purposes. *16SrRNA* genes were amplified from each sample. The primer set used was 27Fmod (5' – AGRGTITGATCMTGGCTCAG-3') / 519R modBio (5' – GTNTACNGCGGCKGCTG-3') (Kuske et al., 2006; Callaway et al., 2009) and Arch 349F (5' – GYGASCAGKCGMGAAW-3') / Arch 806R (5' – GGACTACVSGGGTATCTAAT-3') (Takaii and Horikoshi, 2000) for the eubacterial and archaeal analysis population. For amplification, 2 μl of each DNA was used and a reaction was carried out in 50 μl containing 0.4 mM of fusion primers, 0.1 mM of dNTPs, 2.5 U of Taq ADN polymerase (Qiagen), and 5 μl of the reaction buffer (Qiagen). The PCR amplification was carried out in a thermocycler GeneAmp_PCRsystem 9700 (Applied Biosystems) and operated with the following protocol: 30 s at 95 °C, followed by 30 cycles at 94 °C for 30 s, annealing at 55 °C for 30 s, extension at 72 °C for 10 min. The obtained DNA reads were compiled in FASTq files for further bioinformatic processing. The trimming of the *16SrRNA* bar-coded sequences into libraries, was carried out using QIIME software, version 1.8.0 (Caporaso et al., 2010). Quality filtering of the reads was performed at Q25, prior to the grouping into Operational Taxonomic Units (OTUs) at a 97% sequence homology cutoff. The following steps were performed using QIIME: Denoising using a Denoiser (Reeder and Knight, 2010). Reference sequences for each OTU (OTU picking up) were obtained via the first method of UCLUST algorithm (Edgar, R.C., 2010). A PyNASt (Caporaso et al., 2010b) was used for sequence alignment and a ChimeraSlayer (Haas et al., 2011) for chimera detection. OTUs were then taxonomically classified using BLASTn against GreenGenes and RDP Bayesian Classifier databases, and compiled into each taxonomic level (DeSantis et al., 2006). These pyrosequencing data were also taxonomically classified using the Ribosomal

Database Project Group (RDP), in order to compare the results obtained in both databases.

The data from pyrosequencing datasets was submitted to the Sequence Read Archive of the National Center for Biotechnology Information (NCBI) under the study accession number SRP054973 for eubacterial and archaeal populations.

7.3. Results and discussion

7.3.1. Ammonia recovery in batch experiments

Batch abiotic experiments were carried out to assess the effect of voltage on ammonia diffusion through the cation exchange membrane. These experiments were performed using synthetic wastewater and the liquid fraction of pig slurry and in both cases different applied voltages (passive diffusion, 0.3 and 0.6 V) and different catholytes (phosphate buffer and sodium chloride) were studied.

When using synthetic wastewater and phosphate buffer as catholyte, ammonium migration through the membrane increased from 39.9 to 44.6 after 56 hours when the working voltage was set at 0.3 V and 0.6 V respectively. When using NaCl as catholyte, ammonium migration was significantly lower, 24.9 at 0.6 V. These results clearly show that nitrogen recovery percentage (%) increases when applying voltage and performs better using the phosphate buffer (**Figure 7.2a and b**).

Results obtained when the liquid fraction of pig slurry was used were slightly better. Pig slurry presented a higher nitrogen migration N-NH_4^+ , again even higher when the phosphate buffer was used as catholyte, reaching 49.9 at 0.6 V, compared to 29.1 when using a NaCl catholyte (**Figure 7.2c and d**).

Regarding pH in the cathode compartment, it remained in a range between 7 and 8 when using a phosphate buffer; while the use of NaCl lead to a pH increase up to values of 9 - 10. This difference in pH affected ammonia losses, 3% (buffer) and 22% (NaCl). Nevertheless, if a NH_3 stripping unit is coupled to the cathode compartment, an increase in pH will presumably favour ammonia recovery.

Results of the cation concentrations at the cathode chamber at the beginning and at the end of each experiment are shown in **Figure 7.3**. As previously mentioned a higher ammonia transport is shown when using pig slurry and a phosphate buffer at the cathode. These differences could be related with a higher cation concentration –mainly Na^+ and K^+ – in the cathode chamber than in the anode chamber, at the beginning of the experiments; so this causes transport by diffusion of these cations to the anode compartment and therefore transport of NH_4^+ to the cathode, so as to maintain the balance in cation concentrations. A similar behaviour has been previously described by Kuntke et al. (2011).

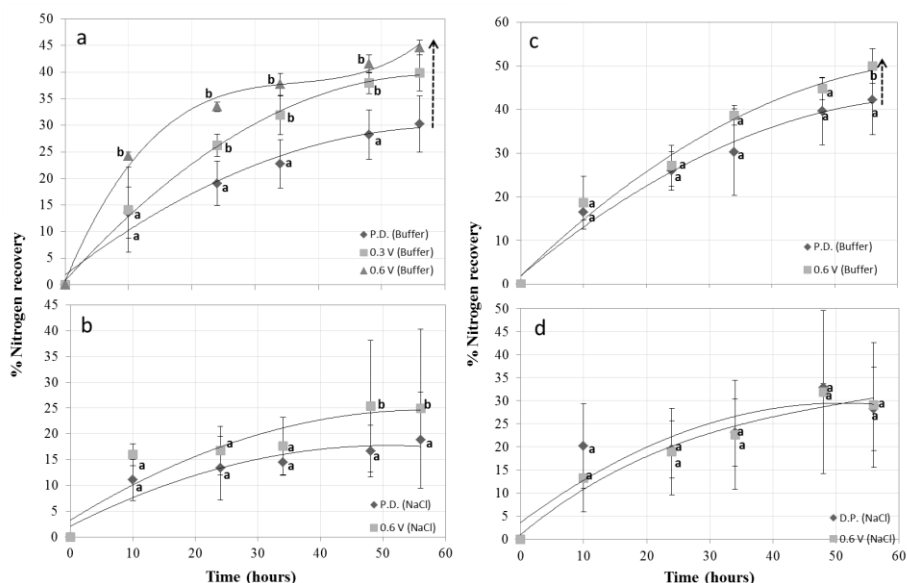


Figure 7.2. Ammonia transported through the CEM at the abiotic two-chambered cell at different working voltages and passive diffusion in batch mode. (a and b) cell fed with synthetic wastewater and buffer phosphate and NaCl as catholyte, (c and d) cell fed with liquid fraction of pig slurry and buffer phosphate and NaCl as catholyte. The significance of the differences between values is represented in lowercase.

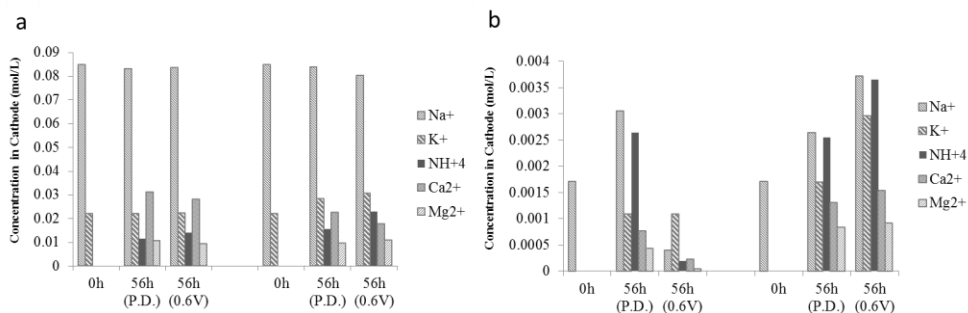


Figure 7.3. Cations concentration at the cathode, at the beginning (0 h) and at the end (56 h) of the abiotic batch experiment, in passive diffusion (P.D.) and 0.6V. (a) cathode fed with phosphate buffer, and b) cathode fed with sodium chloride.

7.3.2. Ammonia recovery in a continuously fed BES

The effect of organic and nitrogen loading rates, anolyte and catholyte pH, and the operating mode (MFC and MEC modes), over nitrogen flux and recovery in a subsequent stripping/absorption system, as well as over the BES overall performance, was assessed in a continuous BES fed with the liquid fraction of pig slurry.

7.3.2.1. Influence of organic and nitrogen loading rate

As a first step, and before coupling the stripping/absorption unit, the effect of the organic loading rate (OLR) and the nitrogen loading rate (NLR) over the MFC performance was assessed. Three different OLR (ranged from 2.2 to 7.1 g COD L⁻¹d⁻¹) and NLR (ranged from 0.3 to 2.1 g NH₄-N L⁻¹d⁻¹) were tested diluting the liquid fraction of pig slurry. Polarization curves were carried out to check the performance of the MFC. As seen in **Figure 7.4**, an increase in OLR and NLR did not affect microbial activity in the anode, but rather a slight increase in electricity production was observed. Thereby, the maximum power density showed in the polarization curves changed from 363 mW m⁻³ (at 2.2 g COD L⁻¹ d⁻¹; 0.6 g NH₄-N L⁻¹ d⁻¹), to 668 mW m⁻³ (at 6.4 g COD L⁻¹ d⁻¹; 1.55 g NH₄-N L⁻¹ d⁻¹), and finally to 1.569 mW m⁻³ (at 7.1 g COD L⁻¹ d⁻¹; 2.1 g NH₄-N L⁻¹ d⁻¹). These results are found to be in agreement with those described by Kuntke et al. (2011), where no adverse effect was observed when using urine with an ammonium concentration range between 0.07 g NH₄-N L⁻¹ to 4.0 g NH₄-N L⁻¹.

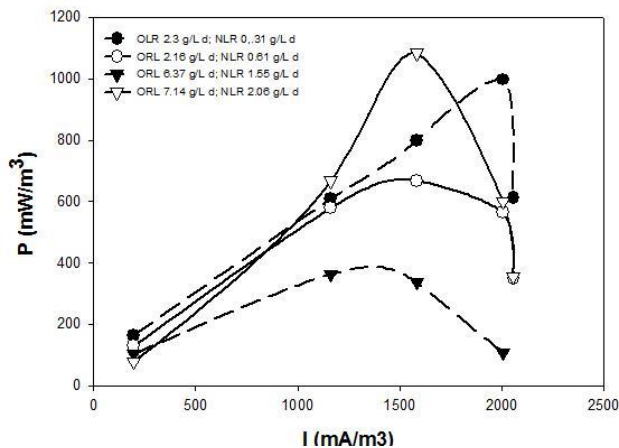


Figure 7.4. Polarization curves of continuously-fed MFC with liquid fraction of pig slurry at different OLR and NLR.

7.3.2.2. Stripping experiments in MFC mode

A total of five assays with different organic and nitrogen loading rates were assessed operating under MFC mode. **Table 7.1** shows the main characteristics and the results obtained under these conditions.

As can be seen, the increase of organic loading rate using phosphate buffer as catholyte, resulted in an increase on voltage and current density, from an average of 138.8 mV and 66.4 mA m⁻² at 3.0 g COD L⁻¹ d⁻¹ to 306.9 mV and 146.8 mA m⁻² at 11.5 g COD L⁻¹ d⁻¹ (**Figure 7.5**).

Table 7.1. Operational conditions and results obtained in the continuous experiment working with pig slurry and the stripping/absorption unit coupled with the BES (MFC mode).

Continuous experiments in MFC mode					
Assay n°	1	2	3	4	5
Catholyte	Buffer phosphate				NaCl
ORL (g COD/L d)	3.0	5.4	9.2	11.5	10.7
NLR (g N-NH₄⁺/L d)	2.7	4.5	1.1	7.4	7.4
N-NH₄⁺ influent (ppm)	940	1600	800	2500	2500
Voltage (mV)	138.8±0.2	157.8±0.1	211.5±0.2	306.9±0.2	139.3±0.1
I (mA m⁻²)	66.4±0.2	75.5±0.08	101.2±0.2	146.8±0.1	66.6±0.1
P (mW m⁻²)	9.5±0.3	12.0±0.2	21.9±0.3	46.1±0.3	9.4±0.2
pH anode	7.7	7.8	7.9	7.7	7.8
pH cathode	7.2	7.3	7.1	7.3	8.1
HRT (h) anode	5.4	5.6	6.9	5.8	5.7
HRT (h) cathode	6.4	7.0	3.9	9.0	6.1
COD removal (%)	50	19	13	31	18
CE (%)	0.7	1.5	6.9	3.3	6.5
N flux (g N m⁻²d⁻¹)	4.34 ± 0.1	4.69 ± 0.2	2.28 ± 0.6	7.23 ± 0.2	3.70 ± 0.2

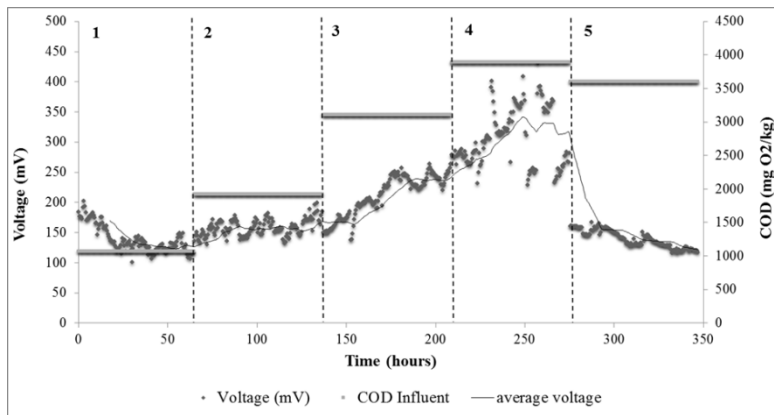


Figure 7.5. Voltage evolution and COD influent through the different periods of the continuous fed MFC experiment.

Accordingly, and as shown in **Figure 7.6a**, the higher the current density the higher the nitrogen flux to the cathodic compartment. The highest nitrogen flux ($7.23 \text{ g N m}^{-2} \text{ d}^{-1}$) was shown in assay number 4 (146.8 mA m^{-2}) which was three-fold higher than the flux achieved with the lower organic and nitrogen loading rates in assay number 1 ($2.28 \text{ g N m}^{-2} \text{ d}^{-1}$) (**Table 7.1**). On the other hand, a slight decrease in COD removal was observed when increasing the OLR, and low Coulombic efficiencies (CE) were obtained in all cases (**Table 7.1**).

When using NaCl as catholyte, and keeping the same OLR and NLR, both the voltage profile (Fig. 4) and the overall performance of the MFC were significantly cut down –as shown by the low power density obtained, 9.4 mW m^{-2} (**Table 7.1**)–, which slowed down the nitrogen flux to $3.70 \text{ g N m}^{-2} \text{ d}^{-1}$ (**Figure 7.6a**), as a result.

As expected, in all assays carried out with phosphate buffer as catholyte, the bulk pH in the cathode compartment remained stable at 7.3, whereas pH values slightly increased up to 8.1 when NaCl was used as catholyte.

7.3.2.3. Stripping experiments in MEC mode

In order to investigate the effects of an increase in current density applying different voltages, MEC mode assays were performed under fixed organic and nitrogen loading rates; $10.7 \text{ g COD L}^{-1} \text{ d}^{-1}$ and $7.4 \text{ g NH}_4\text{-N L}^{-1} \text{ d}^{-1}$, respectively.

As shown in **Table 7.2**, the MEC mode operation showed a higher COD removal efficiency and CE than in the MFC mode. As for nitrogen transport to the cathode compartment, the first four assays ($E_{\text{ap}} = 0.1 \text{ V} - E_{\text{ap}} = 0.6 \text{ V}$) showed a nitrogen flux between 5.69 and $6.94 \text{ g N m}^{-2} \text{ d}^{-1}$, similar to the highest flux obtained in MFC experiments. When a higher voltage was applied (0.8 V), nitrogen flux increased

up to $10.26 \text{ g N m}^{-2} \text{ d}^{-1}$ (**Figure 6b**). These results are in agreement with Kuntke et al. (2012) and Desloover et al. (2012), where nitrogen flux increased together with an increase in the voltage applied. The highest nitrogen flux was reached when using NaCl as catholyte, with a nitrogen flux up to $25.51 \text{ g N m}^{-2} \text{ d}^{-1}$ (**Figure 6b**).

Table 7.2. Operational conditions and results obtained in the continuous experiment working with pig slurry and the stripping/absorption unit coupled with the BES (MEC mode).

Continuous experiments in MEC mode						
Assay n°	1	2	3	4	5	6
V applied	0.1	0.2	0.4	0.6	0.8	0.4
Catholyte	Buffer phosphate					NaCl
ORL (g COD/L d)	10.7 ± 1.0					
NLR (g NH ₄ ⁺ /L d)	7.4 ± 1.1					
HRT (h) anode	6.9 ± 0.7					
HRT (h) cathode	4.3 ± 0.3					
pH anode	7.7	7.6	7.5	7.4	7.3	7.2
pH cathode	6.9	7.5	7.5	7.6	8.0	11.2
COD removal (%)	46.80	13.52	53.79	38.74	19.67	31.59
CE (%)	3.2	10.0	26.6	56.9	15.3	30.4
N flux (g N m ⁻² d ⁻¹)	6.39 ± 0.2	7.0 ± 0.1	5.69 ± 0.05	6.94 ± 0.2	10.26 ± 0.2	25.51 ± 0.01

With respect to the bulk pH in the cathode compartment, when working with the phosphate buffer it remained between 7.5 and 8.0. Contrary to the MFC mode, pH dramatically increased up to a value of 11.2 when using NaCl as catholyte. This pH increase was concomitant to the highest ammonia recovery rates achieved in the stripping-absorption unit, reaching up to 94.3% as opposed to the 38.4% reported in MFC mode (**Table 7.3**). These results confirm a high pH at the cathode compartment as the key factor to ensure a proper ammonia recovery in BES systems coupled to stripping-absorption units.

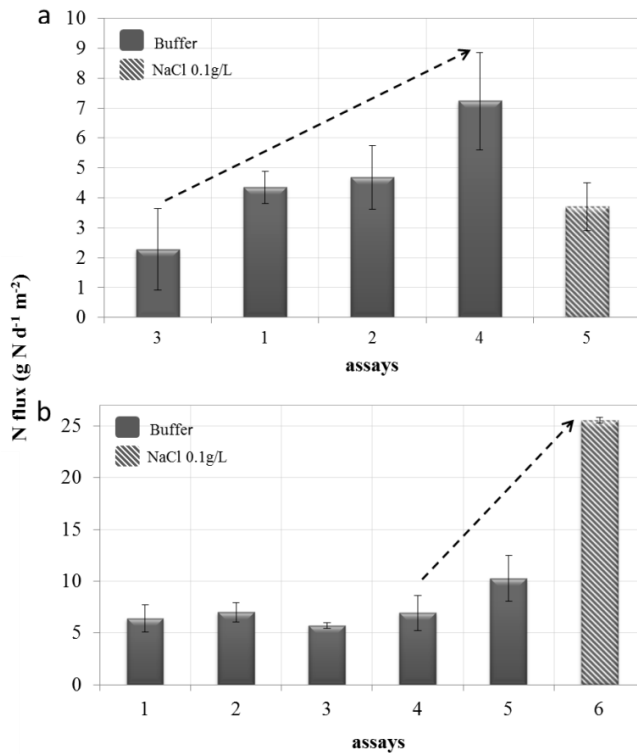


Figure 7.6. Nitrogen flux ($\text{g N d}^{-1} \text{m}^{-2}$), a) for the five assays carried out on the MFC under different organic ($\text{g COD L}^{-1} \text{d}^{-1}$) and nitrogen ($\text{g N-NH}_4^+ \text{L}^{-1} \text{d}^{-1}$) loading rates.

Table 7.3. pH of the cathode and nitrogen recovered (%) in the absorption column during the continuous experiment working with pig slurry and the stripping/absorption unit coupled with the BES (MFC and MEC mode).

	V applied	Catholyte	pH cathode	N absorbed (%)
MFC mode	n.a.	Buffer	7.3	6.4
	n.a.	NaCl	8.1	38.4
MEC mode (assay n°)	0.2 (2)	Buffer	7.5	6.3
	0.4 (3)	Buffer	7.5	15.6
	0.6 (4)	Buffer	7.6	11.3
	0.8 (5)	Buffer	8.0	24.8
	0.4 (6)	NaCl	11.2	94.3

n.a.: not applicable

7.3.2. Microbial community analysis

The study of microbial communities attached to the electrodes in a BES system has been so far of growing interest. In the present study, as aforementioned, a BES coupled with the stripping/absorption unit was operated under MFC and MEC modes, providing the opportunity to investigate the effects of voltage application on the microbial community attached to the anode electrode.

A 16S rRNA based 454-pyrosequencing analysis of all Eubacteria and Archaea was carried out to characterize the microbial community structure from the microbial biomass attached to the carbon felt (bio-anode), at the end of MFC and MEC experiments.

Seven identified phyla were detected in both MFC and MEC mode samples. Breakdown of the bacterial phyla on the bio-anode for the MFC and MEC is detailed in **Figure 7.7** and **Table 7.4**. The three predominant phyla in both samples were *Firmicutes*, *Bacteroidetes* and *Proteobacteria*. The sum of those phyla accounted for 85% and 81% of the total reads in each MFC and MEC sample respectively. Comparing the two MFC and MEC samples, *Firmicutes* was the only one which increased its relative abundance from 36.49% to 50.05%, while *Bacteroidetes* remained relatively constant, 28% and 23%, and *Proteobacteria* decreased its relative abundance to 21% and 8% in the MFC and MEC samples respectively. The other phyla (*Chloroflexi*, *Actinobacteria*, *Tenericutes* and *Spirochaetes*) presented relative abundances below 8%.

The relative abundance of all taxonomic levels in the MFC and MEC samples is represented in **Table 7.4**. Results revealed a selective enrichment at a family and genus level. Seven families were enriched under MEC mode, *Clostridiaceae* (from 14.5% to 25.9%), *Ruminococcaceae* (from 6.7% to 11.3%), *Anaerolineaceae* (from 1.4% to 6.2%), *Erysipelotrichaceae* (from 1.7% to 5.2%), *Peptostreptococcaceae* (from 2.2% to 3.4%), *Acholeplasmataceae* (from 2.8% to 3.0%) and *Porphyromonadaceae* (from 9.6% to 18.7%) (**Figure 7.7**). The most abundant sequences in MEC mode were affiliated with the family *Porphyromonadaceae*, affiliated to OTUs belonging to *Proteiniphilum* sp. with relative abundances of 1.9% and 4.4% in the MFC and MEC communities respectively. As can be seen, a high diverse microbial community consortium was present in both the MFC and MEC anode. This high diversity has been previously described in many studies (Aelterman, 2009; Kiely et al., 2011), since such factors as inoculums, BES configuration, substrate, and operational conditions directly affect the structure of the microbial community. However, a wide trend may be expected as in several

BES systems, regardless of configuration, inoculum or substrate, the predominant phyla on the anode is usually found to be *Proteobacteria* and *Firmicutes* (Bonmati et al., 2013; Goud and Mohan, 2013; Sotres et al., 2014).

Regarding the archaeal community, an important change was revealed when shifting from MFC to MEC mode. Under MEC mode a two-fold increase on the relative predominance of hydrogenotrophic methanogens such as *Methanomicrobiaceae* –as previously described in the MFC anode by Sotres et al. (2014)–, and non-methanogenic *Fervidicoccaceae* was observed; whereas both *Methanosaetaceae* and *Methanosarcinaceae* significantly decreased in relative abundance under MEC mode **Figure 7.8.** and **Table 7.5.** Taking into account that both the MEC and MFC were fed with the same influent, such an important change in Archaeal community could be related with changes in metabolism and therefore, on the diversity of fermentative eubacteria as well.

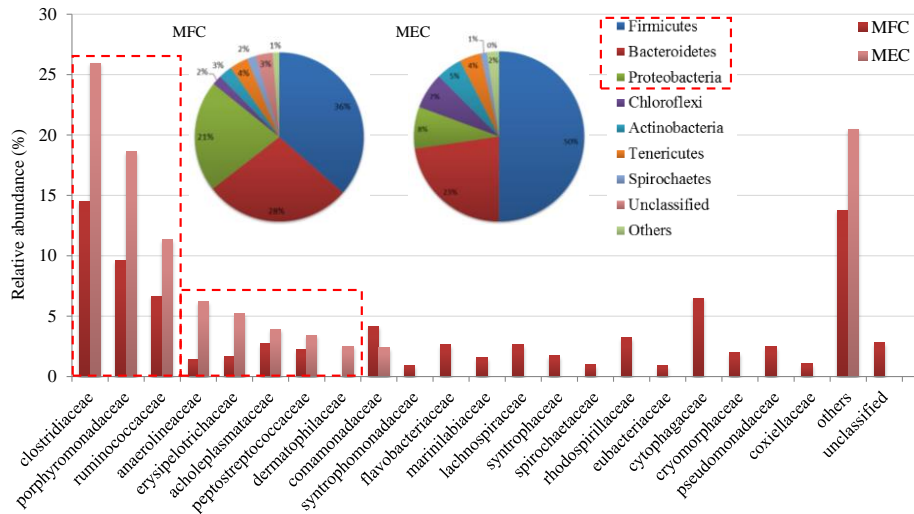


Figure 7.7. Taxonomic classification of pyrosequencing from Eubacterial community of MFC and MEC mode. At the family (bar chart), and phylum (pie chart) levels. (Note: relative abundance was defined as the number of sequences affiliated with that taxon divided by the total number of sequences per sample. Phylogenetic groups with relative abundance lower than 1% were categorized as “others”).

Table 7.5. . Archaeal microbial community enriched in MFC and MEC mode (percentage of total 16S rRNA reads).

Phylum	MFC	MEC	Class	MFC	MEC	Order	MFC	MEC	Family	MFC	MEC	Genus	MFC	MEC
Euryarchaeota	96.0	88.2	Methanomicrobia	95.7	88.0	<i>Methanosarcinales</i>	81.8	49.6	<i>Methanosaetaceae</i>	72.7	48.5	<i>Methanosaeta</i>	72.7	48.5
									<i>Methanosarcinaceae</i>	10.0	1.2	<i>Methanosarcina</i>	9.8	1.2
												<i>Methanimicrococcus</i>	0.2	0
						<i>Methanomicrobiales</i>	13.9	38.4	<i>Methanomicrobiaceae</i>	12.8	37.5	<i>Methanomicrobium</i>	4.3	31.2
												<i>Methanogenium</i>	0.2	0.8
												<i>Methanoculleus</i>	8.3	5.5
Crenarchaeota	3.9	11.9	Methanobacteria	0.3	0.1	<i>Methanobacteriales</i>	0.3	0.1						
			Thermoprotei	3.9	11.9	<i>Fervidicoccales</i>	3.9	11.9	<i>Fervidicoccaceae</i>	4.0	11.9			

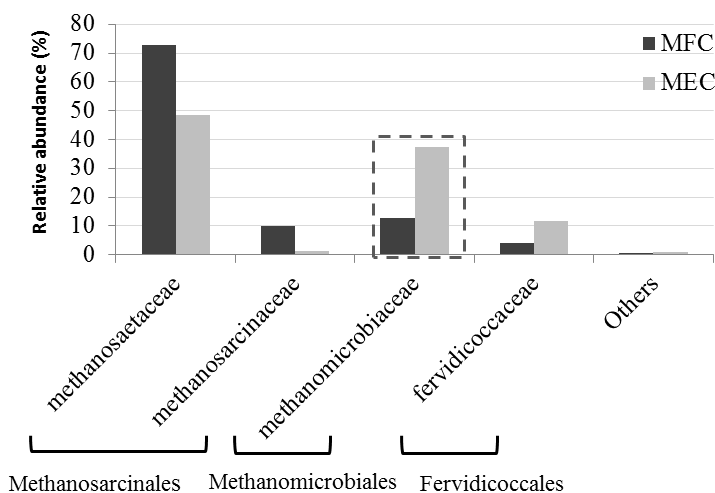


Figure 7.8. Taxonomic classification of pyrosequencing from Archaeal community of MFC and MEC mode. At the family and order levels. (Note: relative abundance was defined as the number of sequences affiliated with that taxon divided by the total number of sequences per sample. Phylogenetic groups with relative abundance lower than 1% were categorized as "others").

Pyrosequencing results were further compared in two databases –GreenGenes and RDP Bayesian Classifier– in order to reinforce confidence in the taxonomic affiliation. Taxonomy assignment of individual datasets using the RDP Bayesian Classifier was performed with an 80% and 50% bootstrap cutoff. Eubacterial and Archaeal population comparison in the MEC sample is shown in **(Figure 7.9)**. As can be seen, there is an overlap between the dominant taxons in the Eubacteria community, but some differences in minority groups are also shown. The lineages represented at the highest level of the taxonomic classification presented some differences in relative abundance but not in new group appearance. However, at the lower level of the taxonomic classification some new taxons are displayed in the RDP database but not in the GreenGenes one, this agrees with a higher relative abundance of 'others' obtained when using GreenGenes. These results are not exactly comparable for Archaea community, for in this case significant differences were found both in highest and lowest levels of the taxonomic classification, because in this particular case most of the taxonomic groups were not described in the RDP database.

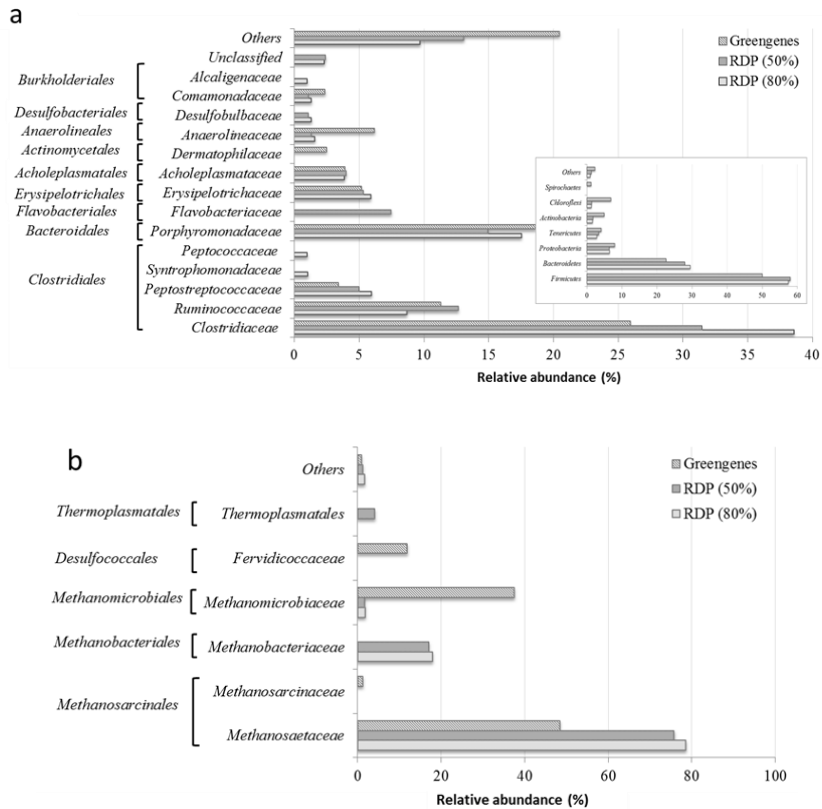


Figure 7.9. Comparison of the phyla and family candidate division between Greengenes and RDP (50% and 80% threshold) databases: a) comparison for the Eubacterial community, and b) for the Archaeal community under MEC operational mode.

The results obtained suggest that, despite some differences both in specific taxonomic groups and in relative abundance, the general pattern for the majority and minority groups does not vary subject to the database used, although contrasting results in both databases is highly recommend.

7.4. Conclusions

Batch experiments showed that ammonia migration through the CEM is enhanced by voltage, and that maximum ammonia migration was achieved when using pig slurry as feed (49.9%). Besides, ammonia recovery from pig slurry was made feasible using a stripping/absorption-BES system. A clear improvement in ammonia migration was shown when using NaCl under MEC mode. The advantage of using sodium chloride as a catholyte is related to a sharp pH increase in the cathode and, accordingly, ammonia stripping/absorption are favoured. 454-pyrosequencing

results revealed that microbial communities are affected when shifting from MFC to MEC mode, promoting a relative enrichment of *Firmicutes* and hydrogenotrophic archaea.

7.5. References

- Aelterman, P., 2009. Microbial fuel cells for the treatment of waste streams with energy recovery. PhD Thesis, Gent University, Belgium.
- APHA, AWA, WEF, 2005. Standard methods for the examination of water and waste water, 21th ed. American Public Health Association/American Water Works Association/Water Environment Federation, Washington, DC, USA.
- Bonmati, A., Sotres, A., Mu, Y., Rozendal, R. and Rabaey, K., 2013. Oxalate degradation in a bioelectrochemical system: reactor performance and microbial community characterization. *Bioresour. Technol.* 143, 147-153.
- Bruce, L., Call, D., Cheng, Sh., Hamelers, H.M., Sleutels, T.H.J.A., Jeremiasse, A., Rozendal, R., 2008. Microbial electrolysis cells for high yield hydrogen gas production from organic matter. *Environ. Sci. Technol.* 42(23), 8630-8640.
- Call, D., Bruce, L., 2008. Hydrogen production in a single chamber microbial electrolysis cell lacking a membrane. *Environ. Sci. Technol.* 42, 3401-3406.
- Callaway, T. R., Dowd, S. E., Wolcott, R. D., Sun, Y., McReynolds, J. L., 2009. Evaluation of the bacterial diversity in fecal contents of laying hens fed various molting diets by using bacterial tag-encoded FLX amplicon pyrosequencing. *PoultSci.* 88, 298-302.
- Caporaso, J.G., K. Bittinger, F.D. Bushman, T.Z. DeSantis, G.L. Andersen, R. Knight., 2010a. PyNAST: A flexible tool for aligning sequences to a template alignment, *Bioinformatics.* 26(2), 266-267.
- Caporaso, J. G., J. Kuczynski, J. Stombaugh, K. Bittinger, F.D. Bushman, E.K. Costello, N. Fierer, A. Gonzalez-Pena, J.K. Goodrich, J.I. Gordon, G.A. Huttley, S.T. Kelley, D. Knights, J.E. Koenig, R.E. Ley, C.A. Lozupone, D. McDonald, B.D. Muegge, M. Pirrung, J. Reeder, J.R. Sevinsky, P.J. Turnbaugh, W.A. Walters, J. Widmann, T. Yatsunenko, J. Zaneveld, R. Knight.. 2010b. QIIME allows analysis of high-throughput community sequencing data, *Nature Methods.* 7(5), 335-336.
- Clauwaert, P., Rabaey, K., Aelterman, P., DeSchampelaire, L., Pham, T.H., Boeckx, P., Boon, N., Verstraete, W., 2007a. Biological denitrification in microbial fuel cells. *Environ. Sci. Technol.* 41(9), 3354-3360.
- Clauwaert, P., Aelterman, P., Pham, T., De Schampelaire L., Carballa, M., Rabaey, K., Verstraete, W., 2008. Minimizing losses in bio-electrochemical systems: the road to applications. *Appl. Microbiol. Biotechnol.* 79, 901-913.
- DeSantis, T.Z., Hugenholtz, P., Larsen, N., Rojas, M., Brodie, E.L., Keller, K., Huber, T., Dalevi, D., Hu, P., Andersen, G.L., 2006. Greengenes, a chimera-checked 16S rRNA gene database and workbench compatible with ARB. *Appl Environ. Microbiol.* 72(7), 5069-5072.

- Desloover, J., Woldeyohannis, A.A., Vestraete, W., Boon, N., Rabaey, K., 2012. Electrochemical resource recovery from digestate to prevent ammonia toxicity during anaerobic digestion. *Environ. Sci. Technol.* 46(21), 12209-12216.
- Ditzig, J., Liu, H., Logan, B.E., 2007. Production of hydrogen from domestic wastewater using a bioelectrochemically assisted microbial reactor (BEAMR). *Int. J. Hydrogen Energy.* 32, 2296-2304.
- Edgar, R.C., 2011. Search and clustering orders of magnitude faster than BLAST, *Bioinformatics.* 26, 2460-2461.
- Franks, A.E., Malvankar, N., Nevin, N.P., 2010. Bacterial biofilms: the powerhouse of a microbial fuel cell. *Biofuels.* 1, 589-604.
- Goud, R.K., Mohan, S.V., 2013. Prolonged applied potential to anode facilitate selective enrichment of bio-electrochemically active Proteobacteria for mediating electron transfer: microbial dynamics and bio-catalytic analysis. *Bioresour. Technol.* 137, 160-170.
- Haas, B.J., Gevers, D., Earl, A.M., Feldgarden, M., Ward, D.V., Giannoukos, G., 2011. Chimeric 16S rRNA sequence formation and detection in Sanger and 454-pyrosequenced PCR amplicons, *Gen. Res.* 21, 494-504.
- Hamelers, H.V., Ter Heijne, A., Sleutels, T.H., Jeremiasse, A.W., Strik, D.P., Buisman, C.J., 2010. New applications and performance of bioelectrochemical systems. *Appl. Microbiol. Biotechnol.* 85(6), 1673-1685.
- Kiely, P.D., Cusick, R., Call, D.F., Selembo, P.A., Regan, J.M., Logan, B.E., 2011. Anode microbial communities produced by changing from microbial fuel cell to microbial electrolysis cell operation using two different wastewaters. *Bioresour. Technol.* 102, 388-394.
- Kim, H.W., Nam, J.Y., Shin, H.S., 2011. Ammonia inhibition and microbial adaptation in continuous single-chamber microbial fuel cells. *J. Power Sources.* 196, 6210-6213.
- Kuntke, P., Geleji, M., Bruning, H., Zeeman, G., Hamelers, H.V.M. and Buisman, C.J.N., 2011. Effects of ammonium concentration and charge exchange on ammonium recovery from high strength wastewater using a microbial fuel cell. *Bioresour. Technol.* 102, 4376-4382.
- Kuntke, P., Smiech, K.M., Bruning, H., Zeeman, G., Saakes, M., Sleutels, T.H., Hamelers, H.V., Buisman C.J., 2012. Ammonium recovery and energy production from urine by a microbial fuel cell. *Water Res.* 46(8), 2627-2635.
- Kuske, C. R., Barns, S. M., Grow, C. C., Merrill, L., Dunbar, J., 2006. Environmental survey for four pathogenic bacteria and closely related species using phylogenetic and functional genes. *Journal of Forensic Science.* 51(3), 548-558.
- Logan, B., Hamelers, B., Rozendal, R., Schröder, U., Keller, J., Freguia, S., Aelterman, P., Verstraete, W, Rabaey, K., 2006. Microbial fuel cells: methodology and technology. *Environ. Sci. Technol.* 40, 5181-5192.
- Logan, B., Shaoan Cheng, D., Hamelers, H.M., Sleutels, Tom, H.J.A., Jeremiasse, A., Rozendal, R., 2008. Microbial electrolysis cells for high yield hydrogen gas production from organic matter. *Environ. Sci. and Technol.* 42, 8630-8640.
- Noguerol, J., Rodríguez-Abalde, A., Romero, E., Flotats, X., 2012. Determination of Chemical Oxygen Demand in Heterogeneous Solid or Semisolid Samples Using a Novel Method

- Combining Solid Dilutions as a Preparation Step Followed by Optimized Closed Reflux and Colorimetric Measurement. *Analytical Chemistry*. 84, 5548–5555.
- Pant, D., Singh, A., Van Bogaert, G., Olsen, S., Nigam, P., Diels, L., Vanbroekhoven, K., 2011. Bioelectrochemical systems (BES) for sustainable energy production and product recovery from organic wastes and industrial wastewaters. *RSC Advances* 2, 1248-1263.
- Rabaey, K., Buetzer, S., Brown, S., Keller, J., Rozendal, R., 2010. High current generation coupled to caustic production using a lamellar Bioelectrochemical system. *Environ. Sci. Technol.*, 44(11), 4315-4321.
- Reeder, J., Knight, R., 2010. Rapidly denoising pyrosequencing amplicon reads by exploiting rank-abundance distributions, *Nature Methods*. 7, 668-669.
- Rozendal, R.A., Sleutels, T., Hamelers, H.V.M., Buisman, C.J.N., 2008. Effect of the type of ion exchange membrane on performance, ion transport, and pH in biocatalyzed electrolysis of wastewater. *Water Sci. Technol.* 57, 1757-1762.
- Sotres, A., Díaz-Marcos, J., Guivernau, M., Illa, J., Magrí, A., Prenafeta-Boldú, F.X., Bonmatí, A., Viñas, M., 2014. Microbial community dynamics in two-chambered microbial fuel cells: effect of different ion exchange membranes. DOI 10.1002/jctb.4465.
- Takai, K. and Horikoshi, K., 2000. Rapid Detection and Quantification of Members of the Archaeal Community by Quantitative PCR Using Fluorogenic Probes. *Applied and Environmental Microbiology*. 66(11), 5066-5072.
- Viridis, B., Rabaey, K., Yuan, Z., Keller, J., 2008. Microbial fuel cells for simultaneous carbon and nitrogen removal. *Water Res.* 42(12), 3013-3024.
- Viridis, B., Read, S.T., Rabaey, K., Rozendal, R.A., Yuan, Z., Keller J., 2010. Biofilm stratification during simultaneous nitrification and denitrification (SND) at a biocathode. *Bioresour. Technol.* 102(1), 334-341.

Chapter 8

Nitrogen removal in a two-chambered microbial fuel cell- Establishment of a nitrifying- denitrifying microbial community on an intermittent aerated cathode.



Sotres, A., Cerrillo, M., Viñas M., Bonmati, A.

4th International MFC conference. 1 - 4 September, Cairns (Australia)(2013): [oral presentation](#)

Sotres, A., Cerrillo, M., Viñas M., Bonmati, A. (2015)

Submitted to peer reviewed journal

Abstract

A Microbial fuel Cell (MFC) was used to study nitrogen dynamics and its feasibility for high strength wastewater treatment. The system, harbouring active microbial biomass both at the anode and cathode chambers, was operated in a continuous mode, fed with acetate as the sole electron donor (OLR: 1.7 g COD L⁻¹d⁻¹), and had a nitrogen loading rate of 4.2 g N-NH₄⁺ L⁻¹d⁻¹. To achieve a simultaneous nitrification and denitrification process, intermittent aeration was applied on the cathode chamber accomplishing the establishment of a nitrifying-denitrifying microbial community. The reactor achieved a power density of 459.7 mW m⁻³ while removing 53.8-69.1% of COD. A total of 30.4% of the N-NH₄⁺ migrated through the ion exchange membrane being primarily nitrified at the cathode chamber. When intermittent aeration was applied in the cathode, denitrification also occurred achieving 17.8% of nitrate removal without acetate addition, and 41.2% with acetate addition.

The microbial community analysis was performed by means of 16S rRNA gene-based DGGE, qPCR, and 454-pyrosequencing analysis. Results revealed that the nitrification process at the cathode chamber could be explained due to a high predominance of *Nitrosomonas* sp. as ammonia-oxidizing bacteria and other *Comamonadaceae* phylotypes as potential denitrifiers. Parallel batch denitrification assays, carried out outside the MFC using the cathode effluent, confirm the existence of heterotrophic denitrification processes with other well known denitrifying dominant phylotypes enrichment (*Burkholderiaceae*, *Comamonadaceae*, *Alcaligenaceae*), some of them also shown to be enriched in the cathode chamber during the intermittent aeration periods.

8.1. Introduction

Nitrogen removal from wastewaters is increasingly becoming more relevant as a cause for serious environmental problems such as eutrophication of rivers, the deterioration of water sources, and as a serious hazard for human and animal health (Mousavi et al., 2011). Ammonia (NH₃), ammonium (NH₄⁺), nitrite (NO₂⁻) and nitrate (NO₃⁻) are the most important forms of reactive nitrogen found in the environment, and nitrate in particular (NO₃⁻), is one of the most problematic compounds found in water and wastewaters. Therefore, efforts to improve the removal of nitrogen have been increased in the last decades. Nitrification/Denitrification is a well known process applied to remove nitrogen from wastewaters. Nevertheless, as different microbial populations are involved with different requirements of oxygen, temperature, etc., it is often fairly complicated and expensive to implement. Finding new treatment methods to achieve an

effective and less expensive nitrogen removal is still an issue to be adequately solved.

Bioelectrochemical systems (BESs) offer a promising technology for nutrient removal while at the same time recovering bioenergy (Zhang et al, 2013). These systems are capable of converting the chemical energy of organic wastes into electricity. Among all BESs, microbial fuel cells (MFCs) are the most widely researched. Microbial fuel cells (MFC) use bacteria as a catalysts to oxidize organic and inorganic matter and generate electrical currents since the electrons derived from these metabolic reactions are transferred from the anode (negative terminal) to the cathode (positive terminal) producing a current flow running through an external circuit (Logan et al., 2006). A two-chamber MFC, consisting of an anode and a cathode separated by an ion exchange membrane, is the most common configuration found, where, at least one of the anodic or cathodic reactions, is microbologically catalysed (Rabaey et al., 2007).

So far, nitrogen removal by MFCs has been focused on two different strategies – MFC ammonium removal under anaerobic conditions (Min et al., 2005) or, being that ammonia can be diffused from anode to cathode through the cation exchange membrane (Rozendal et al., 2008), hence ammonia can be stripped and subsequently absorbed (Desloover et al., 2012). Instead of recovering ammonia at the cathode chamber, another strategy is to remove it by external nitrification and a subsequent denitrification accomplished by microorganisms on the cathode chamber (Clauwaert et al., 2007a; Viridis et al., 2008), or by simultaneous cathodic nitrification-denitrification (Viridis et al., 2010). So far very few studies referring to nitrogen removal via simultaneous nitrification and denitrification (SND) processes as an alternative of using an external nitrifying bioreactor, which is known to be more difficult and expensive to scale up, have been reported. Afterwards, to simplify the reactor structure and reduce the costs associated others designs were investigated in order to carry out SDN in MFC systems. However, to date majority of studies are performed using groundwater or synthetic wastewater, and contrary the use of high strength animal wastewater, particularly pig slurries, has received little attention so far. Thus, there is a lack of knowledge about the feasibility of using a MFC-SND, and its potential application for treatment high strength animal wastewater to accomplish the requirements for agricultural uses.

Nitrification is the biological oxidation of ammonia (NH_4^+) to nitrite (NO_2^-) and then to nitrate (NO_3^-) (equation 1). It is an aerobic process performed by autotrophic ammonia-oxidizing bacteria (AOB), ammonia-oxidizing archaea (AOA) and nitrite-oxidizing bacteria (NOB). The first step of nitrification is the oxidation of ammonia to nitrite catalysed by bacteria containing the ammonia monooxygenase gene

This study aims to evaluate nitrogen dynamics and microbial community structure in a two-chamber microbial fuel cell operating with an intermittently aerated cathode, and its feasibility as a treatment for high strength (organic and nitrogen) wastewater simulating a liquid fraction of pig slurry. This work focuses on three main goals: i) to study nitrogen dynamics in a MFC harbouring active microbial biomass both in the anode and cathode chambers; ii) to enhance the nitrification-denitrification process at the cathode chamber, and iii) to assess the microbial community enriched both in the cathode compartment and in the anode.

8.2. Materials and Methods

8.2.1. Experimental set-up

A methacrylate two-chamber MFC reactor was built with the anode and cathode compartments (0.14 x 0.12 x 0.02 m³) separated by a cation exchange membrane (CEM) (14x12 cm) (Ultrex CMI-7000, Membranes International Inc., Ringwood, NJ, USA). Granular graphite rods with a diameter ranging from 2 to 6 mm (El Carb 100, Graphite Sales Inc., U.S.A.), and stainless steel mesh were used as anode and cathode respectively, resting in 165 mL of net anodic volume (NAV) and 250 mL of net cathodic volume (NCV). Prior to its use, the granular graphite was sequentially soaked in 1M of HCL, and 1M of NaOH, in each case for 24 hours, and finally rinsed in deionised water. Copper wires were used to connect the electrodes to a 500 Ω external resistance.

8.2.2. MFC operation

The anodic chamber was inoculated with 1 mL of digestate from a bench-scale mesophilic methanogenic continuously stirred tank reactor fed with slaughterhouse waste harbouring a high content of N-NH₄⁺ (Rodríguez-Abalde et al., 2010).

The feed solutions were prepared containing (distilled water): CaCl₂, 0.0147 g; KH₂PO₄, 3 g; Na₂HPO₄, 6 g; MgSO₄, 0.246 g; and 1 mL L⁻¹ trace elements solution as described in Lu et al. (2006). Additionally the anode feed solution contained 2.9 g L⁻¹ CH₃COONa, as carbon source, and 3.82 g L⁻¹ NH₄Cl; accordingly, the COD:N ratio of the medium was 2.23. The feed solution for the cathode chamber contained KH₂PO₄, 3 g L⁻¹; Na₂HPO₄, 6 g L⁻¹. The MFC was operated at a room temperature of ~ 23 °C and in a continuous mode with a flow rate of 0.628 L d⁻¹, resulting in organic and nitrogen loading rates of 1.7 g COD L⁻¹ d⁻¹ and 4.2 g N-NH₄⁺ L⁻¹ d⁻¹ respectively. The operated hydraulic retention time (HRT) was of 6.3 and 9.4 h at the anode and cathode respectively (**Table 8.1**). To keep the cathode under aerobic conditions, air was supplied at a flow rate of 2 L min⁻¹. Then, a side batch

assay, as described in point 2.3, was performed to assess the occurrence of denitrification biomass in the cathode. Finally, and in order to accomplish our second objective, three different cathode aeration patterns were carried out: (i) short intermittent aerated periods (P. 2.1), followed by (ii) long intermittent aerated periods (P. 2.2), and (iii) long intermittent aerated periods plus acetate addition (P. 2.3). Samples were taken from the anode and the cathode compartment three times a day during the continuous cathode aeration period (P. 1), and during the intermittent aeration, before and after each different aerated period (P. 2.1, 2.2 and 2.3).

Table 8.1. Set up and operational characteristics of the anode and cathode chambers.

Methacrylate chamber (internal dimensions)	0.14 x 0.12 x 0.002 m ³
Net anodic volume (NAV)	165 mL
Net cathodic volume (NCV)	250 mL
HRT (A)	6.3 h
HRT (C)	9.4 h
Initial inoculum	Anaerobic biomass
Organic loading rate (OLR)	9.5 g COD L ⁻¹ d ⁻¹
Nitrogen loading rate (NLR)	4.2 g N-NH ₄ ⁺ L ⁻¹ d ⁻¹
Electrode (anode)	Granular graphite
Electrode (cathode)	Stainless steel mesh
External resistor	500 Ω
Cation exchange membrane	Ultrex CMI-7000

8.2.3. Denitrification batch assays

Denitrification batch assays were carried out to confirm the presence of denitrifiers on the MFC cathode. Glass vials of 120 mL volume were filled with 60 mL of cathode effluent and different biomass sources. Four experimental conditions were studied: (i) the cathode effluent, (ii) the cathode effluent plus acetate, (iii) the cathode effluent plus the anode effluent, and iv) a negative control (autoclaved cathode effluent).

To create anaerobic conditions, oxygen was removed bubbling up each bottle with N₂ during 10 minutes. All conditions were carried out per triplicate and, to

avoid substrate limitations, COD in condition (ii) was added in excess. Batch assays lasted 160 h, and samples were taken every 24 hours.

8.2.4. Electrochemical analysis

Voltage (V) across the external resistance (Ω) was recorded at 20 min intervals using a multimeter data acquisition unit (Mod. 34970A, Agilent Technologies, Loveland, CO, USA) The current density (I) was then calculated using Ohm's Law, and the power density (P) was obtained using $P = IV/A$, where I stands for current density (mA), V stands for the voltage (mV), A stands for the cell volume (m^3) and P stands for the power density ($mW m^{-3}$).

Polarization curves (P versus I) were carried out in order to obtain the maximum power densities and the internal resistance of the system. The procedure to obtain a polarization curve was set up as follows: after leaving the system in open circuit for 1 hour, the circuit was closed and the external resistance was changed from 20000 to 10 Ω (20000, 10000, 2200, 1000, 500, 100, 50 and 10). Upon the connection of each resistance, the system was left to stabilize for 30 min before recording the voltage data.

8.2.5. Chemical analysis and calculations

Ammonium NH_4^+ -N, nitrate NO_3^- -N, nitrite NO_2^- -N, pH, and soluble COD were analysed according to Standard Method 5220 (APHA, 1999). Nitrate (NO_3^- -N) and nitrite (NO_2^- -N) concentrations were analysed by ion chromatography (Metrohm 861 Advanced Compact IC), using a Metrohm Metrosep A Supp 4 column and pre-column, a Metrosep A Supp 4/5 Guard with 1.8 mmol $NaCO_3/L$, and 1.7 mmol $NaHCO_3/L$ effluent once filtered through a 0.2 μm pore diameter PTFE syringe filter (VWR International, LLC.). Ammonium (NH_4^+ -N) was analysed using a Büchi B-324 distiller, and a Metrohm 702 SM autotitrator. The bulk solution pH in each experiment was tested using a CRISON 2000 pH electrode. Soluble COD was measured following an optimized APHA-AWWA-WPCF Standard Method 5220 (Noguerol et al., 2012) and filtering the samples through a 0.45 μm pore diameter Nylon syringe filter (Scharlau, S.L.).

Total nitrogen (TN) was defined as the sum of ammonium (NH_4^+ -N), nitrite (NO_2^- -N), and nitrate (NO_3^- -N) concentrations. And the total nitrogen and nitrate removal efficiency, η_{TN} and $\eta_{NO_3^-}$ respectively, was calculated based on the difference between initial and final concentrations in the bulk solution at the beginning and at the end of every sampling period divided by its initial concentration.

Coulombic efficiency (CE), defined as the ratio of electrons used as current to the theoretical maximum electron production, was calculated as described elsewhere (Logan et al., 2006).

8.2.6. Microbial community analysis

Samples from each of the experiments were taken and analysed using different culture-independent techniques such as the *16S rRNA* gene-based PCR-DGGE, and 454-Pyrosequencing, as well as real time PCR (qPCR) for the *16S rRNA* gene and two other functional genes (*amoA* and *nosZ*) in order to gain insight on the microbial community structure.

8.2.6.1. Denaturing gradient gel electrophoresis

The bacterial communities enriched on the anode and cathode chamber of the MFC were analysed by means DGGE. Total DNA was extracted in triplicate from known volumes/weights of each sample with the PowerSoil® DNA Isolation Kit (MoBio Laboratories Inc., Carlsbad, CA, USA), following the manufacturer's instructions. Universal eubacterial forward (F341) and reverse (R907) primers were used to amplify the hypervariable (V3-V5) region of the *16S rRNA* gene by a polymerase chain reaction (PCR), as previously reported (Yu and Morrison, 2004). All PCR reactions were carried out in a Mastercycler (Eppendorf, Hamburg, Germany) and each reaction mix (25 µL mix/reaction) contained 1.25 U of Ex TaqDNA polymerase (Takara Bio Inc., Otsu, Shiga, Japan), 12.5 mM dNTPs, 0.25 µM of each primer, and 100 ng of DNA.

The PCR amplicons (20 µL) were loaded in an 8% (w/v) polyacrylamide gel (0.75 mm thick) with a chemical denaturing gradient ranging from 30% to 70% (100% denaturant stock solution contained 7 M urea and 40% (w/v) of formamide).

The electrophoresis was carried out in a DGGE-4001 system (CBS Scientific Company Inc., Del Mar, CA, USA) at 100 V and 60 °C for 16 h in a 1x TAE buffer solution (40 mM Tris, 20 mM sodium acetate, 1 mM EDTA, pH 7.4) (Muyzer et al., 1993). The DGGE gels were stained in darkness for 45 min with 15 mL of a 1x TAE buffer solution containing 3 µL of SYBR® Gold 10,000x (Molecular Probes, Eugene, OR, USA). The gels were scanned under blue light by means of a blue converter plate (UV Products Ltd., Cambridge, UK) and a transilluminator (GeneFlash, Synoptics Ltd., Cambridge, UK). Predominant DGGE bands were excised with a sterile filter tip, suspended in 50 µL of molecular biology grade water, and stored at 4 °C overnight. The resuspended bands were subsequently reamplified by PCR as described above. Amplicons of the expected size were externally sequenced following Sanger's method at Macrogen (Macrogen, the Netherlands).

Sequences were processed using the BioEdit software package v.7.0.9 (Ibis Biosciences, Carlsbad, CA, USA) and aligned with the BLAST basic local alignment search tool (NCBI, Bethesda, MD, USA) and the Naïve Bayesian Classifier tool of RDP (Ribosomal Database Project) v.10 (East Lansing, MI, USA) for the taxonomic assignment.

Changes on the microbial community structure were analysed by covariance-based Principal Component Analysis (PCA) based on the position and relative intensity of the bands present on the DGGE profiles previously digitalized. The MS Excel application StatistiXL v.1.4 (Broadway, Nedlands, Australia) was used for this purpose.

8.2.6.2. Quantitative PCR assay

The gene abundance of nitrifying, denitrifying and total eubacteria community was determined using quantitative PCR (qPCR). The qPCR amplification was performed for the functional genes: ammonium monooxygenase (pair of primers *amoAF/amoAR*), which catalyzes the oxidation from ammonium to nitrite, and secondly the nitrous oxide reductase gene (pair of primers *nosZF/nosZR* (Kandeler et al 2006)), which catalyzes the last step of the denitrification pathway from nitrous oxide to nitrogen gas. For the entire eubacteria community the *16S rRNA* gene was tested. Each sample was analyzed in triplicate by means of three independent DNA extracts as elsewhere described (Prenafeta-Boldú et al., 2012). All reactions were performed using Brilliant II SYBR Green qPCR Master Mix (Stratagene, La Jolla, CA, USA) in a Real-Time PCR System Mx3000P (Stratagene) operated with the following protocol: 10 min at 95 °C, followed by 40 cycles of denaturation at 95 °C for 30 s, annealing for 30 s at 50 °C, 54 °C and 56 °C (for *16S rRNA*, *amoA* and *nosZ* gene, respectively), extension at 72 °C for 45 s, and fluorescence capture at 80 °C. The specificity of PCR amplification was determined by observations on a melting curve and gel electrophoresis profile. A melting curve analysis to detect the presence of primer dimers was performed after the final extension increasing the temperature from 55 to 95 °C at heating rates of 0.5 °C every 10 s. Image capture was performed at 82 °C to exclude fluorescence from the amplification of primer dimers. In all cases, the PCR reactions were performed in a total volume of 25 µL containing: 2 µL of DNA template, 200 nM of each *16S rRNA* primer, 600 nM of each primer, 12.5 µL of the ready reaction mix, and 30 nM of ROX reference dye. The primer set for *16S rRNA* and functional genes (*amoA* and *nosZ*) is described in Table 2. The standard curves were performed with the following reference genes: *16S rRNA* gene from *Desulfovibrio vulgaris* ssp. *vulgaris* ATCC 29579 and *nosZ* gene from

Pseudomonas fluorescens DSM 50415 as previously described (Calderer et al., 2014) and a custom-made *amoA* synthetic gBlock™ gene fragment (IDT, IA, Coralville, USA) from *Nitrosomonas europaea* ATCC 19718, and a set of *amoA*/*amoAR* primers (Shimomura et al 2012).

All reference genes were quantified by NanoDrop 1000 (Thermo Scientific). Serial dilutions from 10^2 to 10^9 copies/reactions of plasmids/GBlocks™ containing known sequences of the targeted genes in duplicate were used to generate the standard curves. The qPCR efficiencies of amplification for the *16S rRNA*, *nosZ*, and *amoA* genes were 108%, 83.1%, and 110.7% respectively. All results were processed with the MxPro qPCR Software (Stratagene).

8.2.6.3. Pyrosequencing and data analysis

The same DNA extracted from anode and cathode compartments and used for DGGE and qPCR analysis was used for pyrosequencing purposes. Each DNA sample was amplified separately using fusion primers containing adapters-barcode-forward primers (5'-3' direction) and a bead adapter-reverse primer (5'-3' direction). Reverse primers were bound to the beads by means of a specific bead adapter. Each sample was amplified with the *16S rRNA* eubacteria gene. The primer set for the eubacterial analysis population is described in Table 2. For the amplification 2 µl of each DNA were used and the reaction was carried out in 50 µl containing 0.4 mM of fusion primers, 0.1 mM of dNTPs, 2.5 U of Taq ADN polymerase (Qiagen), and 5 µl of a reaction buffer (Qiagen). The PCR amplification operated with the following protocol: 30 s at 95 °C, followed by 30 cycles at 94 °C for 30 s, annealing at 55 °C for 30 s, and extension at 72 °C for 10 min. The PCR was carried out in a GeneAmp_PCRsystem 9700 thermocycler (Applied Biosystems). Massive eubacterial *16S rRNA* gene libraries targeting the V3-V5 region were sequenced using the 454 FLX Titanium equipment developed by Roche Diagnostics (Branford, CT, USA). All PCR products obtained from the different samples using fusion primers were mixed in equal concentrations with the Quant-iT PicoGreen dsDNA Kit (Invitrogen, Carlsbad, CA, USA). Purification was achieved with Agencourt Ampure beads (Agencourt Bioscience Corporation, MA, USA). All sequencing protocols and reagents were executed as detailed by the manufacturer's guidelines.

The DNA readings obtained were compiled in FASTq files for further bioinformatics processing. Trimming of *16S rRNA* bar-coded sequences into libraries was carried out using QIIME software version 1.8.0 (Caporaso et al., 2010). Quality filtering of the readings was performed at Q25, prior to the grouping into Operational Taxonomic Units (OTUs) at a 97% sequence homology cut-off. The following steps were performed using QIIME: Denoising, using a Denoiser (Reeder

and Knight, 2010); reference sequences for each OTU (OTU picking) were obtained via the first method of UCLUST algorithm (Edgar, R.C., 2010); sequence alignment using PyNAST (Caporaso et al., 2010b), and Chimera detection using ChimeraSlayer (Haas et al., 2011). OTUs were then taxonomically classified using BLASTn against GreenGenes databases and compiled into each taxonomic level (DeSantis, Hugenholtz et al. 2006).

8.2.6.4. Nucleotide Sequence Accession Numbers

All sequences derived from DGGE results have been submitted to the GenBank database under accession numbers, and data from pyrosequencing datasets were submitted to the Sequence Read Archive (SRA) of the National Centre for Biotechnology Information (NCBI) under the study accession number SRP051329.

8.3. Results and discussion

8.3.1. Nitrogen dynamics in the continuous aerated cathode period

8.3.1.1. MFC operation and nitrogen dynamics

The MFC operating under the conditions described in **Table 8.1** (P.1) achieved an average voltage (V) of 193.9 mV, with a current density (I) of 2.3 A m⁻³ and a power density of 459.7 mW m⁻³ while removing 53.8-69.1% of COD. The maximum power density obtained in polarization curves was 767.2±0.07 mW m⁻³.

Figure 8.2 shows the nitrogen dynamics in a MFC harbouring active biomass both in the anode and cathode chambers. The results show that a range between 25.8±2.6% and 33.8±0.6% of total N-NH₄⁺ migrated through the cation exchange membrane and, in the cathode, the diffused nitrogen found was: N-NH₄⁺ (9.0±1.1% - 14.4±0.8%), N-NO₃⁻ (10.8±0.1% - 20.9±0.6%) and N-NO₂⁻ (<0.11%), with respect to the nitrogen transferred, resulting in nitrogen losses (notwithstanding the nitrites) ranging between (3.7±1.5% and 8±0.2%). This indicates that the ammonium diffused though the membrane is being mostly nitrified at the cathode compartment. Although the optimum pH for nitrifying processes ranges from 8 to 9 (Anthonisen et al., 1976), such process occurs as the main event in the cathode chamber with an average pH of 6.8±0.01 over time. Our results concur with those reported by Zhang and He (2011), where the pH of the aerobic cathode was 6.7±0.2. These results were not as high as those for the MFCs reported by others (Zhao et al., 2006) probably due to nitrification, which reduces alkalinity.

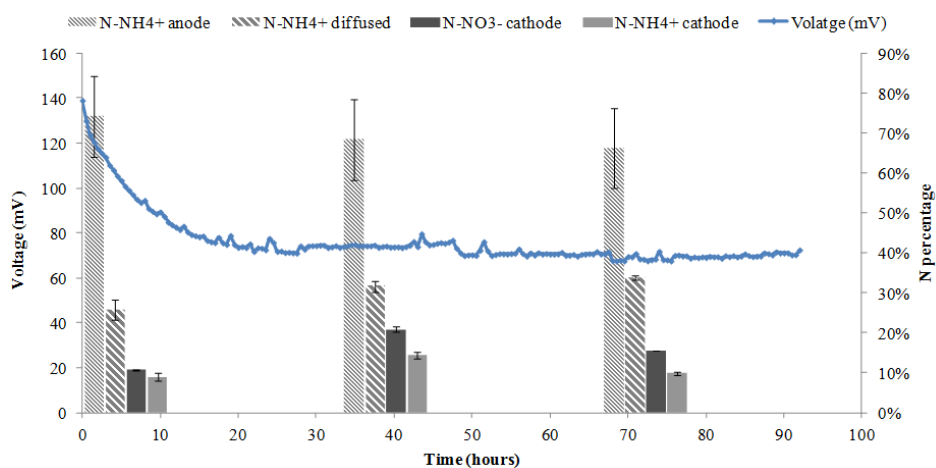


Figure 8.2. Voltage and nitrogen evolution over time during continuous aeration cathode (P. 1) (data shows 3 samples periods).

8.3.1.2. Microbial community assessment

In order to gain insight on the microbial community structure and its potential function related with the MFC operation, molecular biology methods such as DGGE and qPCR were applied to biomass from both the anode and the cathode chambers. As expected, DGGE results show a higher microbial diversity on the anode than in cathode chamber (**Figure 8.3a**). The predominant bands in the biofilm attached to the graphite granules of the anode chamber belonged to *Firmicutes*, *Bacteroidetes* and *Proteobacteria*. The most abundant classes within the *Proteobacteria* phylum, have been β -*Proteobacteria*, as already reported in previous studies (Bonmatí et al., 2013; Sotres et al., 2014). Park et al. (2006) reported that β -*Proteobacteria* appears as the main population, rather than α -*Proteobacteria*, γ -*Proteobacteria* and *Flavobacteria*. The FISH analysis also shows that β -*Proteobacteria* was dominant on the biofilm-electrode, being α -*Proteobacteria* and γ -*Proteobacteria* rarely detected. They concluded that β -*Proteobacteria* was likely to play a key role in biofilm reactors.

The DGGE results from cathode chamber reveal *Nitrosomonas* sp. as the most predominant band which could highly contribute to nitrification process as an ammonium oxidizer (band 1 in **Figure 8.3a**). Although *Nitrosomonas* sp. was identified as the main nitrifying bacteria linked to the nitrification process, an important phylotype belonging to *Comamonadaceae* (band 2 in **Figure 8.3a**) –a well-known potential denitrifier family–, was also present in the aerated cathode.

Regarding qPCR analyses, the *16S rRNA* gene copy number revealed a high abundance of total eubacterial populations both in the anode and cathode chamber (1.1×10^9 gene copy number g^{-1} and 6.2×10^8 gene copy number mL^{-1} ,

respectively). We also observed in the aerated cathode a high abundance of the *amoA* gene (8.9×10^9 gene copy number mL^{-1}), and even the presence of *nosZ* although at much lower concentrations (3.3×10^7 gene copy number mL^{-1}) (**Figure 8.3b**).

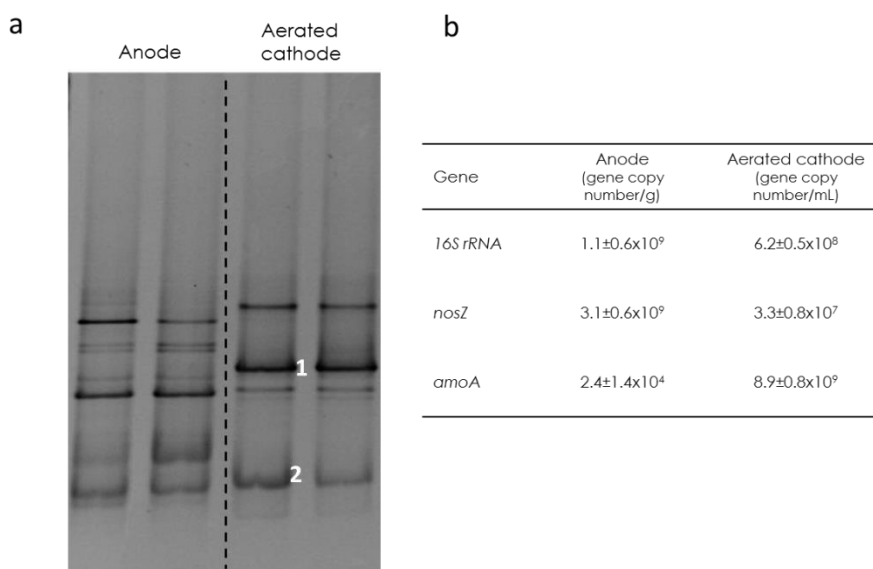


Figure 8.3. (a) Total eubacterial community DGGE profile in the anode biofilm-electrode and in the biomass located in the supernatant aerated cathode chamber. **(b)** *16S rRNA*, *nosZ* and *amoA* genes for both compartments.

To bear out the DGGE results from cathode chamber and analyse the cathodic microbial community in more detail, a 454-pyrosequencing was carried out on the cathode compartment. The results obtained revealed that the microbial community was mainly accounted for with three phyla, *Proteobacteria* (71.9%), *Bacteroidetes* (26.4%) and *Actinobacteria* (1.5%) in a minor degree. Looking at the family level, *Nitrosomonadaceae* (44.5%) appears to be the most predominant family whereas an important community belonging to *Comamonadaceae* (21.4%) and *Chitinophagaceae* (11.9%) is also concomitant to the nitrifying community of the cathode chamber (**Figure 8.4a**), as also observed in the DGGE results (**Figure 8.3a**).

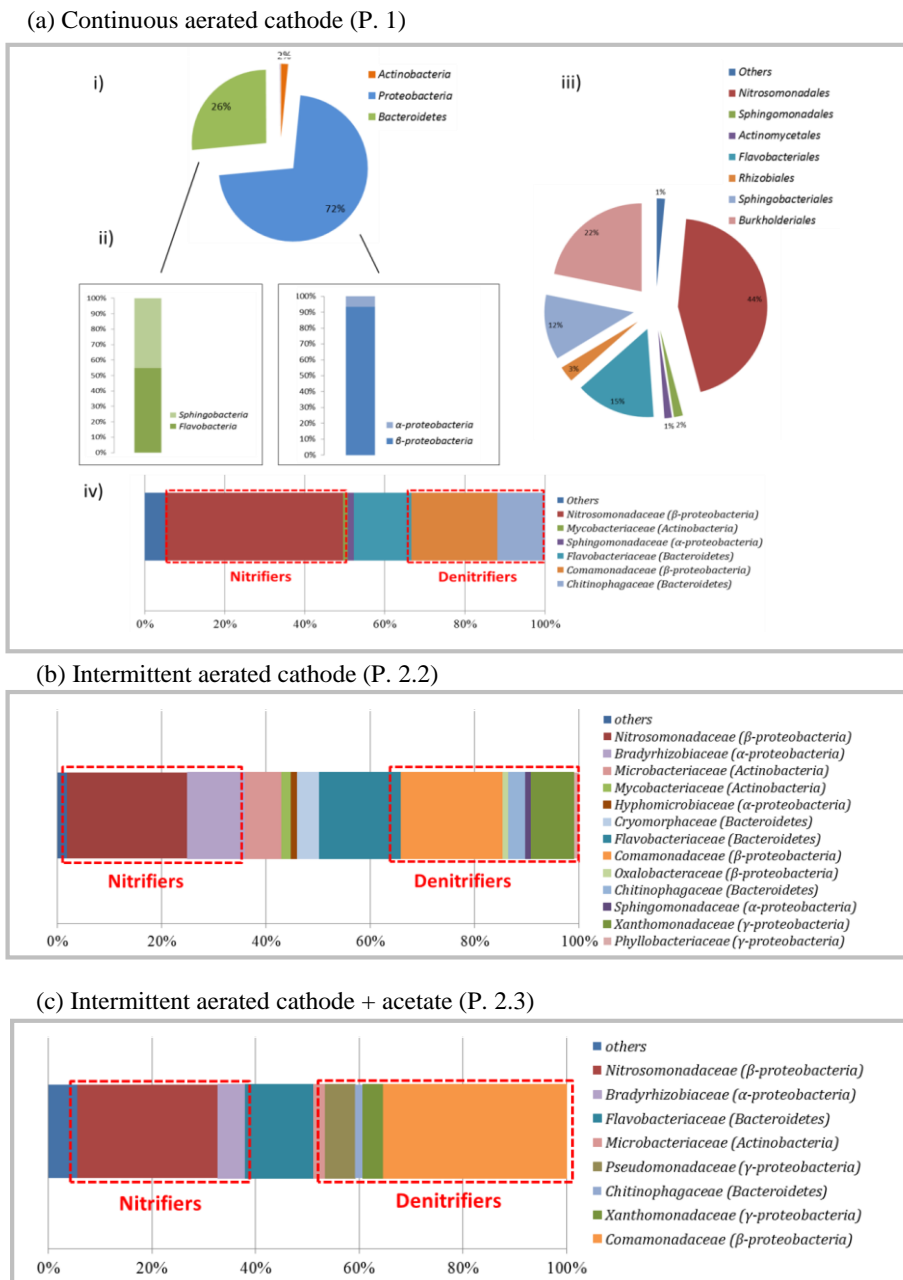


Figure 8.4. Taxonomic assignment of 16SrRNA based-pyrosequencing assessment of bacterial community at the aerated cathode chamber during the different periods: **(a)** continuous aerated cathode - P. 1 - (phylum (i), class (ii), order (iii) and family (iv) level); **(b)** intermittent aerated period - P. 2.2 - (family level); and **(c)** during the intermittent aerated period + acetate - P. 2.3- (family level). Note: Phylogenetic groups with relative abundance lower than 1% were categorized as "others".

Pyrosequencing data also revealed class β -Proteobacteria as the dominant group of bacteria accounting for 66.4%, followed by Flavobacteria with 14.5%, and Sphingobacteria with 11.9% of the relative abundance on reads obtained from the cathode chamber, as previously described by Park et al., 2006. The group of α -Proteobacteria scarcely appeared with only 4.7% of the sequences and γ -Proteobacteria were not identified at all. These results are in excellent agreement with Cong et al. (2013) who found a pronounced enrichment in β -Proteobacteria and Sphingobacteria attached to the biofilm-electrode and demonstrated that bacteria consortiums with current acclimation had higher levels of β - than α -Proteobacteria. Moreover, Sphingobacteria were identified to be dominant in denitrifying cathode biofilms. In our study, the β -proteobacteria class was mainly comprised by Nitrosomonas sp. (44.5%), and Comamonas sp. (19.9%), whereas the Flavobacteria class included Kaistella sp. (10.8%).

These results point out to the possibility of enhancing denitrification by promoting sequential aerobic-anoxic conditions in the cathode. Nevertheless, as a first step, and in order to confirm the presence of a denitrifying microbial community, the cathodic biomass was grown in a set of different denitrification batch assays.

8.3.2. Denitrification batch assays

Batch experiments were carried out in anoxic conditions to confirm the occurrence of denitrification processes on biomass harvested from cathode chamber. Denitrification occurred when acetate was added to the cathode effluent, reaching up to 99.7% (from 128.9 to 0.4 mg N-NO₃⁻ L⁻¹) of the nitrate removal in 7 days. However, nitrate removal was quite low, reaching just 16.5% (from 64.5 to 53.8 mg N-NO₃⁻ L⁻¹) when an anode effluent was combined with the cathode effluent (without acetate amendment but containing the non-degraded acetate), and only 5.1% (from 128.9 to 122.4 mg N-NO₃⁻ L⁻¹) of nitrate removal was accomplished using just the cathode effluent without additional acetate in these batch experiments (**Figure 8.5**). These results suggest that there is no autotrophic denitrification under these conditions; however, the existence of a heterotrophic denitrification is confirmed by the microbial community analysis (**Figure 8.5** and **8.6a**).

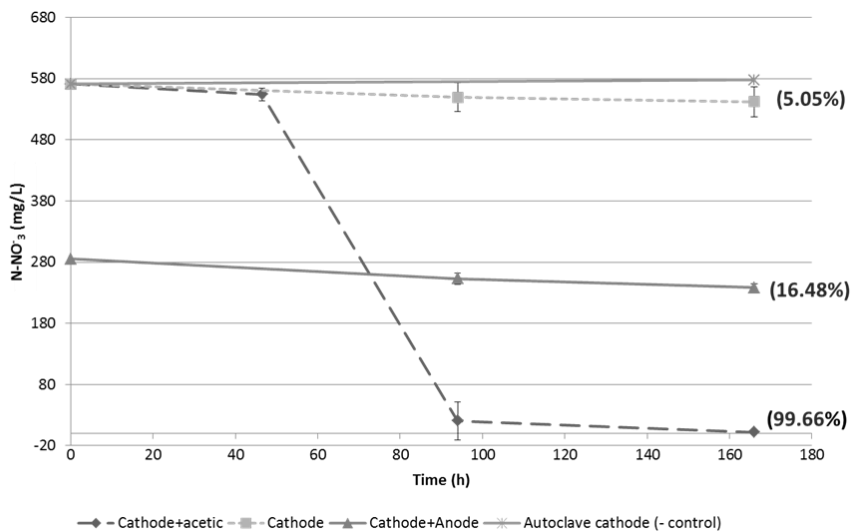


Figure 8.5. $N\text{-NO}_3^-$ removal in the denitrification batch assays using cathode effluent from MFC cathode chamber and different biomass sources after 7 days. In brackets, nitrate removal percentage.

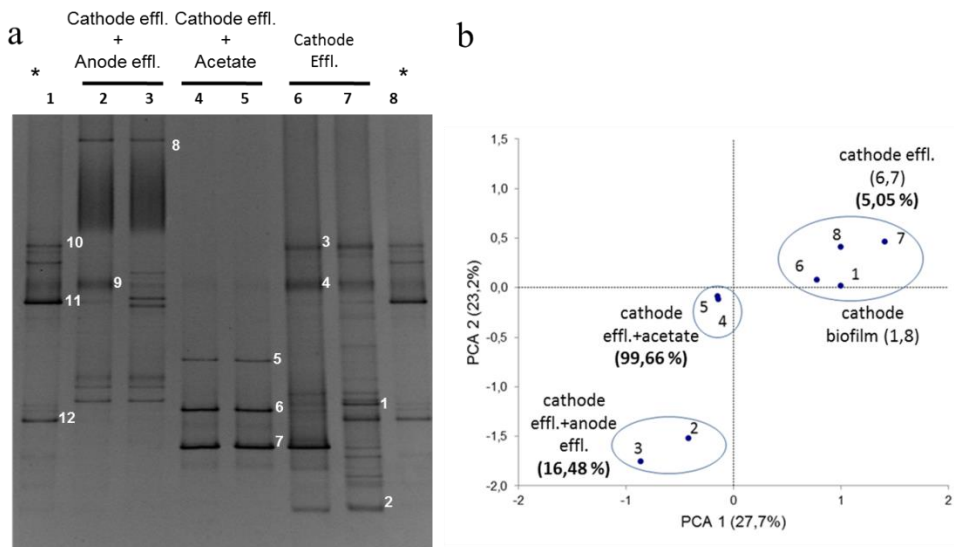


Figure 8.6. (a) DGGE 16S rDNA ($V_3\text{-}V_5$ region) of the total eubacteria microbial community from the different batch assays and (*) sample from MFC cathode chamber. (b) Principal Component Analysis (PCA) 2D-Plot from DGGE profiles. In brackets, the percentage of nitrate removal after 7d of incubation in the denitrification batch assays.

8.3.2.1. Microbial community assessment

Comparison between the physicochemical analysis and the DGGE results revealed the presence of well known denitrifying phylotypes, when acetate was added to cathode effluent. The three predominant bands (bands 5, 6 and 7) (**Figure 8.6a**) belonged to *Burkholderiaceae*, *Alcaligenaceae* and *Comamonadaceae*, (**Table 8.2**), which have been previously reported as key players in cathodic nitrate reduction in a closed circuit (Wrighton et al., 2010).

In the other batch conditions, without acetate amendment, minority bands (bands 4 and 11) like *Comamonadaceae* and *Alcaligenaceae*, (**Table 8.2**) were identified as potential denitrifiers.

The rest of the bands identified on the DGGE belong mostly to *Bacteroidetes* (*Porphyromonadaceae*) and *Proteobacteria* (β and γ -*Proteobacteria*), which have been also described as dominant phyla in other MFCs systems (Huang et al., 2014; Sotres et al., 2014).

The Multivariate Principal Component Analysis (PCA) of the DGGE profiles (**Figure 8.6b**) showed three distinct main groups. One group corresponds to the samples from the cathode chamber and the batch experiments with cathode effluent without acetate addition. Although nitrate was not consumed during the denitrification batch experiment performed with only the cathode effluent, some bands showing phylotypes potentially related with denitrification processes were described. It is worth noting that acetate addition into the cathode effluent caused a significant shift on the DGGE profile, with the occurrence of potential denitrifying phylotypes as well as the enhancement of the denitrification process. DGGE profile differentiation of the cathode effluent + the acetate and cathode effluent + the anode effluent batch experiments, displayed as separate groups on the PCA, might be explained by the different microbial communities encompassed in both compartments, as well as by the difference in acetate availability, being residual in the anode effluent and clearly higher when acetate was added directly to the batch experiment (COD of 1.120 mg O₂ L⁻¹).

Therefore, denitrification batch assays confirm the existence of a potential denitrifying population in the cathode chamber which could be enhanced if the cathode is adequately handled.

Table 8.2. Characteristics of the bands excised and sequenced from Eubacterial 16S rRNA gene based-DGGE (**Figure 8.6**) from samples obtained in denitrification batch experiments.

Band	Length (bp)	Accession number	Closest organism in GenBank database (accession number)	Similarity (%)	Phylogenetic group (RDP)
1	480	JQ307401	Uncultured Bacteroidetes bacterium (GU112204)	99%	Bacteroidetes
2	357	JQ307402	Uncultured bacterium (EF559196)	98%	Bacteroidetes
3	425	JQ307403	<i>Acinetobacter seohaensis</i> (FJ392126)	100%	Moraxellaceae Gammaproteobacteria Comamonadaceae
4	415	JQ307404	<i>Comamonas</i> sp (HM365952)	99%	Betaproteobacteria Comamonadaceae
5	361	JQ307405	<i>Comamonas</i> sp (FJ426595)		Betaproteobacteria Alcaligenaceae
6	270	JQ307406	<i>Tetrathibacter mimigardefordensis</i> (HM031463)	99%	Betaproteobacteria
7	440	JQ307407	Uncultured Bacteroidetes bacterium (CU923099)	94%	Porphyromonadaceae Bacteroidetes
8	499	JQ307408	Uncultured bacterium (AM982611)	95%	Bacteroidetes
9	471	JQ307409	<i>Proteiniphilum acetatigenes</i> (AY742226)	97%	Porphyromonadaceae Bacteroidetes
10	432	JQ307410	<i>Bacteroides coprosuis</i> (AF319778)	99%	Bacteroidaceae Bacteroidetes
11	438	JQ307411	<i>Alcaligenes faecalis</i> (HM597239)	99%	Alcaligenaceae Betaproteobacteria
12	475	JQ307412	<i>Acholeplasma</i> sp (FN813713)	95%	Acholeplasmataceae Mallicutes

8.3.3. Nitrogen dynamics during the intermittent aerated cathode periods

8.3.3.1. MFC operation and nitrogen dynamics

Since the previous experiments pointed out that a potential denitrifying community was concomitant with the nitrifying population, the cathode compartment was submitted to different working conditions in order to achieve simultaneous nitrification-denitrification processes. The oxidation of ammonium to nitrate, conducted as shown mainly by *Nitrosomonas* sp., in the continuous aerated cathode (P.1) was one of the main processes taking place and, as a result, a high accumulation of nitrate was detected in the cathode chamber (169.4 ± 0.21 mg N-NO₃⁻ L⁻¹). These results, and the finding of a potential denitrifying community, suggested that establishing nitrification-denitrification processes may

be feasible if the cathode is submitted to aerobic-anoxic cycles, similar to a SBR reactor as already described elsewhere (Magrí et al., 2009).

In order to evaluate whether the intermittent aerated periods had an influence on the cathode denitrifying community and its ability to reduce nitrate, the evolution of nitrogen (N-NH_4^+ , N-NO_3^- and N-NO_2^-) both in the anode and in the cathode compartments was studied. The initial nitrate concentration in the cathode was $169.4 \pm 0.21 \text{ mg N-NO}_3^- \text{ L}^{-1}$, which was higher than other concentrations from previous studies on autotrophic nitrate reduction such as 26 and $50 \text{ mg N-NO}_3^- \text{ L}^{-1}$ (Vilar-Sanz et al., 2013; Lee and Rittmann, 2002), though two-fold lower than the experimental conditions described by Park et al. (2006). **Figure 8.7a)** shows the evolution of the different forms of nitrogen during three short intermittent aerated cycles (P. 2.1). As it can be seen, ammonia concentrations decreased during the aerated periods whereas nitrates decreased during the non-aerated periods. In **Table 8.3** we can see that the reported average N-NO_3^- removal efficiency was 17.8% (P. 2.1). The same behaviour, though with a lower N-NO_3^- 8.3% removal efficiency, was also observed during the long intermittent aerated period (P. 2.2). Nevertheless, when acetate was added (P. 2.3) the removal efficiency increased up to 41.2% (**Figure 8.7b**).

As nitrate reduction to di-nitrogen gas occurs through four consecutive reactions where two of them tend to accumulate (NO_2^- and N_2O) (Virdis et al., 2009), nitrite concentrations were as well monitored. During the two first non-aerated cycles of the intermittent aerated period (P. 2.1) the accumulation of nitrite was 4.3 and $10.9 \text{ mg N-NO}_2^- \text{ L}^{-1}$, respectively (**Figure 8.7b**), although this concentration reached 0 during the second non-aerated period (P. 2.2). The decrease in nitrite accumulation after some non-aerated cycles could be due to an acclimation of the denitrification processes. Pous et al. (2012) reported concentrations close to 0 after 84 days. Nevertheless it is surprising that in the last non-aerated period, when the acetate was added, nitrite concentrations rose to higher values than in previous periods, reaching up to $15.8 \text{ mg N-NO}_2^- \text{ L}^{-1}$.

Although residual nitrogen was still present, the use of MFC to partially remove nitrogen could be a good strategy to adjust the composition of either high strength wastewater or livestock wastewater, to be used as fertilizer.

The initial pH of the catholyte was 7.2 ± 0.02 and it began to decrease during the intermittent aerated periods down to about 6.5 ± 0.04 and 6.8 ± 0.23 . Although the optimum pH for denitrification processes is between 7 and 8 (Ahn, 2006), these values, lower than 7, do not seem to affect the presence of potential nitrous oxide reductase gene to catalyse the last step of the denitrification pathway taking place with a pH value below 6 (Einsle and Kroneck, 2004).

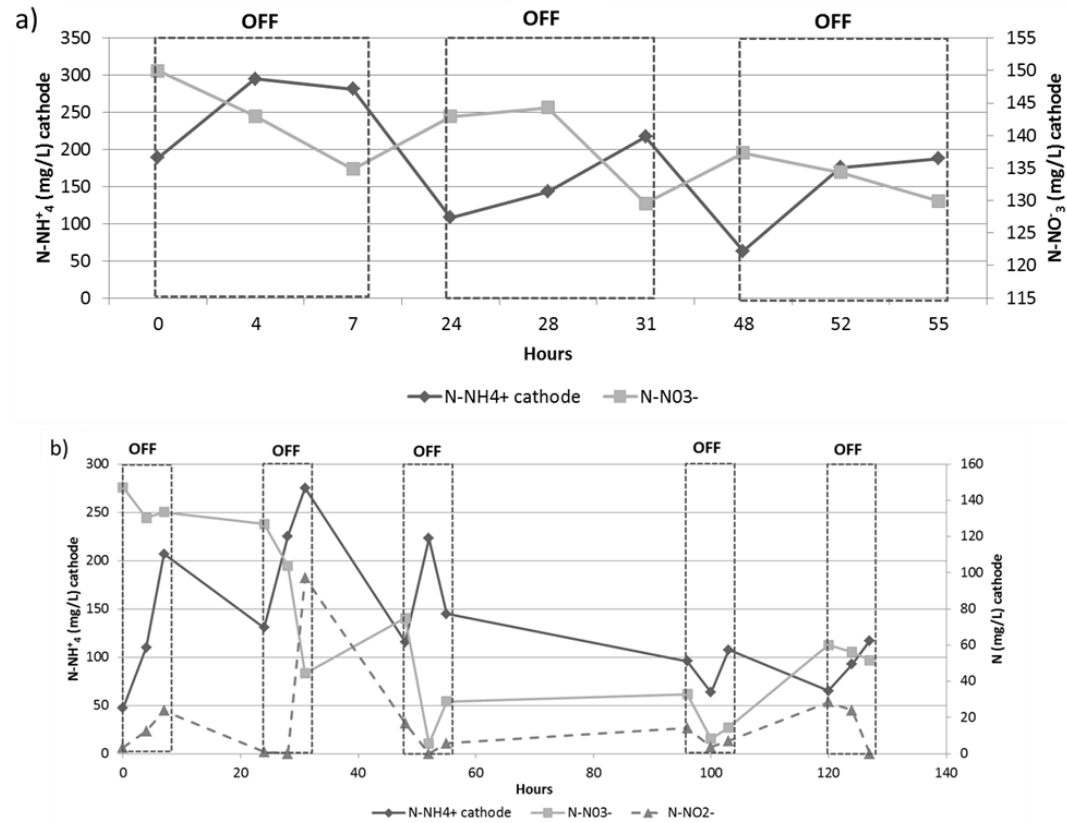


Figure 8.7. Nitrogen dynamics ($N\text{-NO}_3^-$, $N\text{-NO}_2^-$ and $N\text{-NH}_4^+$) in the cathode during the intermittent aerated periods. **(a)** Short intermittent aerated cycles (P. 2.1), and **(b)** Long intermittent aerated cycles with addition of acetate (P. 2.3).

Table 8.3. Effect of the intermittent aerated periods on the nitrate removal efficiency at cathode chamber.

Period	N-NH ₄ ⁺ transferred	η _{N-NO₃⁻}
P. 2.1 (Short intermittent aerated cathode)	29.9±0.1 %	17.8±2.5 %
P. 2.2 (Long intermittent aerated cathode)	21.8±0.1 %	8.3±2.5 %
P. 2.3 (Long intermittent aerated cathode + acetate)	32.6±0.1 %	41.2±4.4 %

8.3.3.2. Microbial community assessment

The microbial community was quantified by means of qPCR and pyrosequencing, both in the aerated cathode and in the last stage of each intermittent aerated period. The results showed that the abundance of the *16S rRNA* gene varied between 5.9×10^9 gene copy number mL⁻¹ on the aerated cathode (P. 1) and a range between 3.1×10^{10} - 4.7×10^{10} gene copy number mL⁻¹ on the intermittent aerated cathode periods (P. 2.1, 2.2 and 2.3) (**Figure 8.8**). The amount of *16S rRNA* genes increased slightly during the intermittent aerated periods. Likewise, the *amoA* gene increased during the intermittent aerated cathode periods (P. 2.1, 2.2 and 2.3), compared with the continuous aerated cathode period (P. 1) ranging from 8.9×10^9 to 3.1×10^{10} gene copy number mL⁻¹. Regarding the *nosZ* gene, linked to denitrification, its gene copy number experienced a 3-7 fold increase, from 3.3×10^7 gene copy number mL⁻¹ on the continuous aerated cathode period (P. 1) to 9.6×10^7 - 1.6×10^8 on the intermittent aerated cathode periods (P. 2.1 and 2.2); and to 2.4×10^8 on the intermittent aerated cathode period with the addition of acetate (P. 2.3). Besides, the gene ratio *nosZ/16S rRNA* shifted from 0.08 to 0.15 after the intermittent aerated periods, which speaks of an enrichment of denitrifying populations when aeration is stopped and the cathode chamber is fed with acetate as a carbon source and an alternative electron donor.

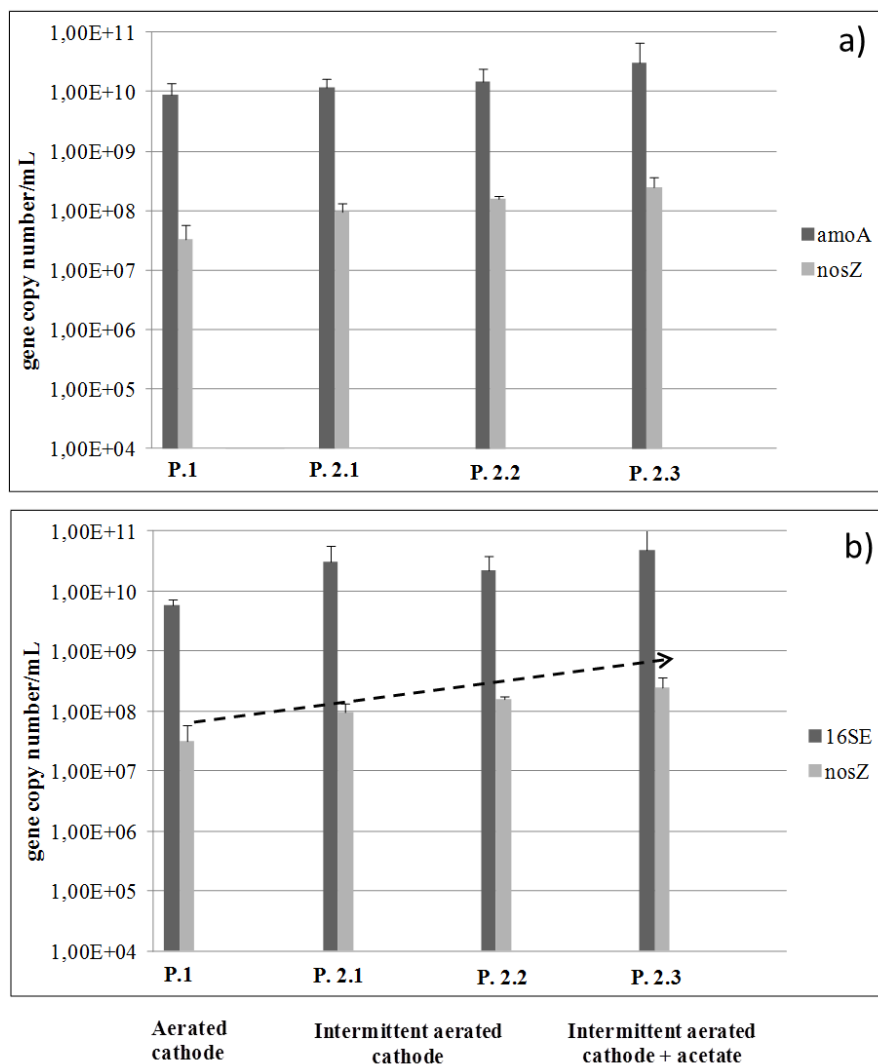


Figure 8.8. Abundances of the 16S rRNA and two functional genes (*amoA* and *nosZ*) according to the last point of four periods studied. The number of copies for these genes (a) functional genes (*amoA* and *nosZ*) and (b) 16S rRNA and *nosZ* at aerated cathode, after two non-aerated cathode periods and non-aerated period with acetate pulses. Standard errors of the mean (n=3) are indicated.

As for the pyrosequencing analysis, although the Phyla *Proteobacteria*, *Bacteroidetes* and *Actinobacteria* are still dominant, a clear shift at lower taxonomic levels is noticed during different operational conditions. Under intermittent aerated periods new denitrifying families such as *Phyllobacteriaceae* (1.0%), *Xanthomonadaceae* (8.2%), *Sphingomonadaceae* (1.1%), and

Oxalobacteriaceae (1.1%) were also enriched (**Figure 8.4b**). When acetate was added to the intermittent aerated period this denitrifying community was clearly enriched in *Comamonadaceae* phylotypes, increasing from 19.5% to 35.4% (**Figure 8.4c**). Regarding the nitrifying community, its diversity and structure was quite stable and represented by a high relative abundance of *Nitrosomonas* sp. (as AOB) (44.5%, 23.0% and 27.2% in P. 1, 2.2 and 2.3 respectively) and *Nitrobacter* sp. (as nitrite oxidizer, NOB) (1.0%, 10.9% and 5.1% in P. 1, 2.2 and 2.3 respectively); also in samples from the intermittent aerated cathode periods. The diversity indexes – the inverted Simpson index and Shannon-Wievers index–, confirm that the overall diversity of the samples remained stable over the different periods, with values of 21.5 (P. 1), 32.2 (P. 2.2) and 24.9 (P. 2.3) for the inverted Simpson index, and 3.9 (P. 1), 3.9 (P. 2.2) and 3.8 (P. 2.3) for the Shannon-Wievers index.

Summing up, while the nitrifying community abundance remains stable in quantity and diversity throughout time, regardless of the working conditions, the denitrifying community increases under the application of intermittent aeration periods. Further research is needed to ascertain the real denitrification mechanisms (either heterotrophic or mixotrophic) that have been occurring in the cathode in the presence of low concentration of organic compounds and electron donors, which compete with the electrons coming from the circuit.

8.4. Conclusions

An average of 30.4% of the ammonia contained in the anode is diffused through the membrane to the cathode during the stable operation of a MFC loaded with high strength wastewater (organic matter and nitrogen). The nitrification of the ammonia diffused was the main process happening at the aerated cathode and denitrification processes could be enhanced to reach a nitrate removal efficiency of 41.2%, when intermittent aeration cycles plus acetate were applied.

Regarding the microbial community involved in these processes, its analysis showed that the predominance of *Nitrosomonas* sp. at the aerated cathode chamber explains the active nitrification process and, besides, phylotypes belonging to known denitrifying bacteria (*Alcaligenaceae*, *Burkholderiaceae* and *Comamonadaceae*) are concomitant with *Nitrosomonas* sp.; a fact which could explain the loss of nitrogen on a global nitrogen balance basis. The presence of potential heterotrophic denitrification processes in the cathode chamber was also confirmed under batch denitrification assays. Moreover, when intermittent aerated

periods were applied, mixotrophic-driven denitrification could be the main mechanism for denitrification at the cathode compartment under these conditions.

These results show that the microbial community structure was dominated by concomitant nitrifying and denitrifying members, confirming the feasibility of nitrification-denitrification processes in the cathode provided that intermittent aeration is applied.

8.5. References

- Ahn, YH., 2006. Sustainable nitrogen elimination biotechnologies: A review. *Process Biochem.* 41(8), 1709-1721.
- Anthonisen, R.C., Loehr, R.C., Prakam, T.B.S., Srinath, E.G., 1976. Inhibition of nitrification by ammonia and nitrous acid. *Water Environm. Federation.* 48, 835-852.
- Bonmatí, A., Sotres, A., Mu, Y., Rozendal, R. Rabaey, K., 2013. Oxalate degradation in a bioelectrochemical system: reactor performance and microbial community characterization. *Bioresour. Technol.* 143, 147-153.
- Calderer, M., Martí, V., De Pablo, J., Guivernau, M., Prenafeta-Boldú, F.X., Viñas, M., 2014. Effects of enhanced denitrification on hydrodynamics and microbial community structure in a soil column system. *Chemosphere.* 111, 112-119.
- Callaway, T. R., Dowd, S. E., Wolcott, R. D., Sun, Y., McReynolds, J. L., 2009. Evaluation of the bacterial diversity in fecal contents of laying hens fed various molting diets by using bacterial tag-encoded FLX amplicon pyrosequencing. *Poult. Sci.* 88, 298-302.
- Caporaso, J. G., J. Kuczynski, J. Stombaugh, K. Bittinger, F.D. Bushman, E.K. Costello, N. Fierer, A. Gonzalez-Pena, J.K. Goodrich, J.I. Gordon, G.A. Huttley, S.T. Kelley, D. Knights, J.E. Koenig, R.E. Ley, C.A. Lozupone, D. McDonald, B.D. Muegge, M. Pirrung, J. Reeder, J.R. Sevinsky, P.J. Turnbaugh, W.A. Walters, J. Widmann, T. Yatsunencko, J. Zaneveld, R. Knight., 2010. QIIME allows analysis of high-throughput community sequencing data. *Nat. Methods.* 7, 335-336.
- Caporaso, J.G., K. Bittinger, F.D. Bushman, T.Z. DeSantis, G.L. Andersen, R. Knight., 2019. PyNAST: A flexible tool for aligning sequences to a template alignment. *Bioinformatics.* 26, 266-267.
- Clauwaert, P., Rabaey, K., Aelterman, P., DeSchampelaire, L., Pham, T.H., Boeckx, P., Boon, N., Verstraete, W., 2007a. Biological denitrification in microbial fuel cells. *Environ. Sci. Technol.* 41(9), 3354-3360.
- Cong, Y., Xu, Q., Feng, H., Shen, D., 2013. Efficient electrochemically active biofilm denitrification and bacteria consortium analysis. *Bioresour. Technol.* 132, 24-27.
- DeSantis, T.Z., Hugenholtz, P., Larsen N., Rojas, M., Brodie, E.L., Keller, K., Huber, T., Dalevi, D., Hu, P., Andersen, G.L., 2006. Greengenes, a chimera-checked 16S rRNA gen database and workbench compatible with ARB. *Appl. Environ. Microbiol.* 72(7), 5069-5072.

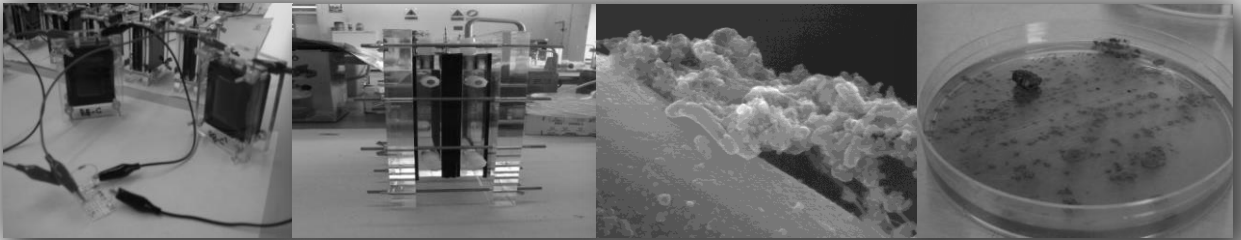
- Desloover, J., Woldeyohannis, A.A., Verstraete, W., Boon, N., Rabaey, K., 2012. Electrochemical resource recovery from digestate to prevent ammonia toxicity during anaerobic digestion. *Environ. Sci. Technol.* 46(21), 12209-12216.
- Edgar, R.C., 2010. Search and clustering orders of magnitude faster than BLAST. *Bioinformatics.* 26, 2460-2461.
- Einsle, O., Kroneck, P.M.H., 2004. Structural basis of denitrification. *Biol. Chem.* 385(10), 875-883.
- Haas, B.J., D. Gevers, A.M., Earl, M., Feldgarden, D.V. Ward, G. Giannoukos., 2011. Chimeric 16S rRNA sequence formation and detection in Sanger and 454-pyrosequenced PCR amplicons. *Gen. Res.* 21, 494-504.
- He, Z., Kan, J., Mansfeld, F., Angenent, L.T., Nealson, K.H., 2009. Self-sustained phototrophic microbial fuel cells based on the synergistic cooperation between photosynthetic microorganisms and heterotrophic bacteria. *Environ. Sci. Technol.* 43, 1648-1654.
- Huang, J., Wang, Z., Zhu, Ch., Ma, J., Zhang, X., Wu, Z., 2014. Identification of microbial communities in open and closed circuit bioelectrochemical MBRs by High-throughput 454 pyrosequencing. *PLoS One* 9(4), e93842.
- Kandeler, E., Deiglmayr, K., Tschirko, D., Bru, D., Philippot, L., 2006. Abundance of narG, nirS, nirK, and nosZ genes of denitrifying bacteria during primary successions of a glacier foreland. *Appl. Environ. Microbiol.* 72, 5957-5962.
- Karanasios, K.A., Vasiliadou, I.A., Pavlou, S., Vayenas, D.V., 2010. Hydrogenotrophic denitrification of potable water: a review. *J. Hazard. Mater.* 180, 121-125.
- Kuske, C. R., Barns, S. M., Grow, C. C., Merrill, L., Dunbar, J., 2006. Environmental survey for four pathogenic bacteria and closely related species using phylogenetic and functional genes. *J. Forensic. Sci.* 51(3), 548-558.
- Lee, K.C., Rittman, B.E., 2002. Applying a novel autohydrogenotrophic hollowfiber membrane biofilm reactor for denitrification of drinking water. *Water Res.* 36, 2040-2052.
- Logan, B., Hamelers, B., Rozendal, R., Schröder, U., Keller, J., Freguia, S., Aelterman, P., Verstraete, W., Rabaey, K., 2006. Microbial fuel cells: methodology and technology. *Environ. Sci. Technol.* 40, 5181-5192.
- Lu, H., Oehmen, A., Virdis, B., Keller, J., Yuan, Z., 2006. Obtaining highly enriched cultures of *Candidatus Accumulibacter phosphatus* through alternating carbon sources. *Water Res.* 40, 3838-3848.
- Magrí, A., Guivernau, M., Baquerizo, G., Viñas, M., Prenafeta-Boldú, F. X., Flotats, X., 2009. Batch treatment of liquid fraction of pig slurry by intermittent aeration: process simulation and microbial community analysis. *J. Chem. Technol. Biotechnol.* 84, 1202-1210.
- Martens-Habbena, W., Berube, P. M., Urakawa, H., de la Torre, J. R., Stahl, D. A., 2009. Ammonia oxidation kinetics determine niche separation of nitrifying Archaea and Bacteria. *Nature.* 461, 976-981.
- Mousavi, S.A.R., Ibrahim, S., Aroua, M.K., Ghafari, S., 2011. Bio-electrochemical denitrification- A review. *Intern. J. Chem. Environ. Engin.* 2 (2).
- Min, B., Kim, J., Oh, S., Regan, J.M., Logan, B.E., 2005. Electricity generation from swine wastewater using microbial fuel cells. *Water Res.* 39(20), 4961-4968.

- Muyzer, G., DeWaal, E.C., Uitterlinden, A.G., 1993. Profiling of complex microbial populations by denaturing gradient gel electrophoresis analysis of polymerase chain reaction-amplified genes coding for 16S rRNA. *Appl. Environ. Microbiol.* 59, 695-700.
- Noguerol-Arias, J., Rodríguez-Abalde, A., Romero-Merino, E., Flotats, X., 2012. Determination of Chemical Oxygen Demand in Heterogeneous Solid or Semisolid Samples Using a Novel Method Combining Solid Dilutions as a Preparation Step Followed by Optimized Closed Reflux and Colorimetric Measurement. *Anal. Chem.* 84, 5548-5555.
- Park, Ho Il, Kim, J.S., Kim, D.K., Choi, Y.-J., Pak, D., 2006. Nitrate-reducing bacterial community in a biofilm-electrode reactor. *Enzyme Microb. Technol.* 39, 453-458.
- Prenafeta-Boldú, F.X., Guivernau, M., Gallastegui, G., Viñas, M., de Hoog, G.S., Elías, A., 2012. Fungal/bacterial interactions during the biodegradation of TEX hydrocarbons (toluene, ethylbenzene and *p*-xylene) in gas biofilters operated under xerophilic conditions. *FEMS Microbiol. Ecol.* 80, 722-734.
- Rabaey, K., Rodríguez, J., Blackall, L.L., Keller, J., Gross, P., Batstone, D., 2007. Microbial ecology meets electrochemistry: electricity-driven and driving communities. *ISME J.* 1, 9-18.
- Reeder, J., R. Knight., 2010. Rapidly denoising pyrosequencing amplicon reads by exploiting rank-abundance distributions. *Nat. Methods.* 7, 668-669.
- Rodríguez-Abalde, A., Juznic-Zonta, Z., Fernández, B., 2010. Anaerobic co-digestion of treated slaughterhouse wastes, in: *Libro de Actas del II Congreso Español de Gestión Integral de Deyecciones Ganaderas, International Workshop on Anaerobic Digestion of Slaughterhouse Waste*, ed by Bonmatí, A., Palatsi, J., Prenafeta-Boldú, F.X., Fernández, B., Flotats, X. Service Point, Barcelona, pp. 347-356.
- Rozendal, R.A., Sleutels, T., Hamelers, H.V.M., Buisman, C.J.N., 2008. Effect of the type of ion exchange membrane on performance, ion transport, and pH in biocatalyzed electrolysis of wastewater. *Water Sci. Technol.* 57, 1757-1762.
- Shao, M.F., Zhang, T., Fang H.H., 2010. Sulfur-driven autotrophic denitrification: diversity, biochemistry, and engineering applications. *Appl. Microbiol. Biotechnol.* 88(5), 1027-1042.
- Shimomura, Y., Morimoto, S., Takada Hoshino, Y., Uchida, Y., Akiyama, H., Hayatsu, M., 2012. Comparison among amoA primers suited for quantification and diversity analyses of ammonia-oxidizing bacteria in soil. *Microbes Environ.* 27:94-8.
- Sotres, A., Diaz-Marcos, J., Guivernau, M., Illa, J., Magrñi, A., Prenafeta-Boldú, F.X., Bonmati, A., Viñas, M., 2014. Microbial community dynamics in two-chambered microbial fuel cells: Effect of different ion exchange membranes. *J. Chem. Technol. Biotechnol.* DOI:10.1002/jctb.4465.
- Takai, K., Horikoshi, K., 2000. Rapid Detection and Quantification of Members of the Archaeal Community by Quantitative PCR Using Fluorogenic Probes. *Appl. Environ. Microbiol.* 66(11), 5066-5072.
- Vilar-Sanz, A., Puig, S., García-Lledó, A., Trías, R., Balaguer, M.D., Colprim, J., Bañeras Ll., 2013. Denitrifying bacterial community affect current production and nitrous oxide accumulation in a microbial fuel cell. *PLoS One* 8(5), e63460.

- Viridis, B., Rabaey, K., Yuan, Z., Keller, J., 2008. Microbial fuel cells for simultaneous carbon and nitrogen removal. *Water Res.* 42(12), 3013-3024.
- Viridis, B., Rabaey, K., Yuan, Z., Rozendal, R.A., Keller, J., 2009. Electron fluxes in a microbial fuel cell performing carbon and nitrogen removal. *Environ. Sci. Technol.* 43(5), 5144-5149.
- Viridis, B., Read, S.T., Rabaey, K., Rozendal, R.A., Yuan, Z., Keller, J., 2010. Biofilm stratification during simultaneous nitrification and denitrification (SND) at a biocathode. *Bioresour. Technol.* 102(1), 334-341.
- Wrighton, K.C., Viridis, B., Clauwaert, P., Read, S.T., Daly, R.A., Boon, N., Piceno, Y., Arington, K.C., Viridis, B., Clauwaert, P., Read, S.T., Daly, R.A., Boon, N., Piceno, Y., Andersen, G.L., Coates, J.D., Rabaey, K., 2010. Bacterial community structure corresponds to performance during cathodic nitrate reduction. *ISME J.* 4, 1443-1455.
- Yu, Z., Morrison, M., 2004. Comparisons of different hypervariable regions of *rrs* genes for use in fingerprinting of microbial communities by PCR-denaturing gradient gel electrophoresis. *Appl. Environ. Microbiol.* 70, 4800-4806.
- Zhang, F., and He, Z., 2011. Simultaneous nitrification and denitrification with electricity generation in dual-cathode microbial fuel cells. *J. Chem. Technol. Biotechnol.* 87, 153-159.
- Zhang, F., He, Z., 2013. A cooperative microbial fuel cell system for waste treatment and energy recovery. *Environ. Technol.* 34, 1905-1913.
- Zhao, F., Hamisch, F., Schroder, U., Scholz, F., Bogdanoff, P., Hermann, I., 2006. Challenges and constraints of using oxygen cathodes in microbial fuel cells. *Environ. Sci. Technol.* 40, 5193-5199.
- Zumft, W.G., 1997. Cell biology and molecular basis of denitrification. *Microbiol. Mol. Biol. Rev.* 61, 533-616.

Chapter 9

General conclusions



Based on the proposed objectives, the present chapter gives an overview of the main conclusions of this dissertation. Suggestions for further research and perspectives of BESs technology are also presented.

9.1. General conclusions

This last chapter gives an overview of the main conclusions drawn from the research done. The studies reported in this dissertation were carried out using different sized MFC under different operational conditions so as to gain insight on those microbial communities enriched on electrode materials and nitrogen removal/recovery strategies using BES. Thus, from the overall results, the following major conclusions have been reached:

1. *With regards to study the effect of different membrane materials and inocula over the general performance of a two-chambered MFC, the major conclusions are:*

- Electricity production is linked to a microbial population shift encompassed the anode material in comparison with the initial inoculum.
- The Eubacterial community showed a clear enrichment in specific microbial ribotypes, predominantly *Bacteroidetes* and β -*proteobacteria*, regardless of the type of membrane tested.
- The Archaeal community was highly dependent on the type of membrane used, as evidenced by the selective enrichment of *Methanosarcina* sp. in the MFC equipped with Nafion N-117 membrane - the MFC showing the highest current production.

2. *Regarding the study of diversity and dynamics of the microbial community on the biofilm attached onto the anode electrode, under different substrates and continuous-fed operational conditions, it can be stated that:*

- A highly diverse microbial community consortium was present in both synthetic wastewater and pig slurry-fed MFCs, and the microbial community is specialized under increasing organic and nitrogen loading rates over time.
- The type of substrate used (synthetic wastewater or pig slurry) led to distinct a difference between the final anodophilic microbial communities of each substrate. However, 6 OTUs belonging to *Flavobacteriaceae*, *Porphyromonadaceae*, *Comamonadaceae* and *Intrasporangiaceae* remained present in both anodophilic communities under different operational conditions.

General conclusions

Thus, they could be considered as the core microbiome and good candidates to be the main exoelectrogenic players in the MFC.

- The archaeal community composition was highly affected by the type of substrate used, being *Methanosarcina* sp. predominant in the synthetic fed-MFC, whereas *Methanosaeta* sp., was the most abundant in the pig slurry-fed MFC, along with other minor groups such as *Methanomicrobium* sp., *Methanosarcina* sp., and *Methanoculleus* sp.
- The effect of 2-bromoethanesulfonate (BES-Inh.) was also tested as methanogenesis inhibitor in the synthetic-fed MFC, and although the overall MFC performance was not affected, the addition of BES-Inh. caused a dramatic change in eubacterial community, but it did not significantly affect the Archaea community.
- The microbial community phylotypes highly enriched following the addition of BES-Inh., were *Sphingobacteriaceae*, *Flavobacteriaceae*, *Cryomorphaceae* and *Marinilabiaceae*.

The results obtained from these two objectives clearly demonstrated that there is no unique microbial community found in all anodes, and factors like MFC configuration and materials used, inoculum, and substrate, determine the composition of the final microbial community on the anodes. On the other hand, based on these results, Archaea population seemed not to necessarily have an antagonist role in these consortiums, and further research will be needed in order to better understand synergic/interactions between eubacteria and archaea in MFC anodophilic communities.

3. Regarding the study of nitrogen dynamics in a two chambered MFC operated in a batch mode, the major conclusions are:

- When synthetic wastewater was used, 44.6% of the ammonium migrated through the membrane at 0.6V, using phosphate buffer as catholyte. Nevertheless, ammonium migration decreased to 24.9% at 0.6V when using NaCl as catholyte.

- Higher ammonium migration percentages through the membrane were obtained when using the liquid fraction of pig slurry, reaching 29.1% and 49.9% when NaCl and phosphate buffer were used as catholyte, respectively.
- pH at the cathode chamber remained between a range of 7 and 8, using phosphate buffer, and rose up till 9-10 using NaCl, which supports the subsequent stripping processes.

It can be concluded that higher ammonium migration percentages were obtained using the liquid fraction of pig slurry and a phosphate buffer as catholyte. But the advantage of using NaCl lies on an increase in pH up to 10. This increase in pH at the cathode chamber will presumably favour ammonia stripping and its subsequent recovery.

4. With regards to the development of a physicochemical strategy to recover nitrogen in a continuous system fed with the liquid fraction of pig slurry, it can be stated that:

- In a pig slurry-fed MFC system, the voltage increases when increasing the organic loading rate, and as a consequence the nitrogen flux also increases, from 2.3 g N m⁻²d⁻¹ at 9.2 g COD L⁻¹ d⁻¹ to 7.23 g N m⁻²d⁻¹ at 11.5 g COD L⁻¹ d⁻¹.
- Shifting to MEC mode clearly improved nitrogen flux to 10.3 g N m⁻²d⁻¹ at 10.7 g COD L⁻¹ d⁻¹.
- As observed in batch experiments, pH values in the cathode rise when using NaCl as catholyte, reaching 8 in MFC mode and increasing dramatically rising to 11.2 in MEC mode.
- High pH values at the cathode compartment is the key factor to ensure the proper ammonia recovery in BES systems coupled to a stripping-absorption unit, reaching up to 94.3% of stripped/absorbed nitrogen in MEC mode.
- Pyrosequencing analysis revealed that a shift from MFC to MEC mode led to a 10% enrichment in relative abundance for certain taxonomic Eubacterial groups: Clostridiaceae, Porphyromonadaceae and Ruminococcaceae.

- Shifting from MFC to MEC mode also promoted an increase in the relative predominance of hydrogenotrophic methanogens such as *Methanomicrobiaceae*, and the depletion of *Methanosarcinaceae* and *Methanosaetaceae*.

Accordingly, using stripping-BES systems is a good strategy for the recovery of ammonia from pig slurries; nevertheless further optimization is needed.

5. As for the biological strategy to remove nitrogen in the cathode chamber, it can be concluded that:

- Nitrification of migrated ammonia was the main process occurring at the aerated cathode.
- The migration of ammonia, from the anode to the aerated bio-cathode, resulted in the selective enrichment of a microbial community composed mainly by nitrifying (*Nitrosomonas* sp.) and potential denitrifying phylotypes (*Alcaligenaceae*, *Burkholderiaceae* and *Comamonadaceae*).
- When intermittent aeration was applied to the bio-cathode, acetate – dependent, and independent denitrification occurred, achieving values of 17.8% and 41.2% respectively.

Thus, nitrification-denitrification processes in the cathode compartment were feasible and stimulated under intermittent aeration cycles applied in a two-chambered MFC, fed continuously with high strength synthetic animal wastewater, simulating the liquid fraction of pig slurries.

As a general conclusion it can be said that the feasibility to remove/recover nitrogen from high strength animal wastewaters, such as pig slurries, in bioelectrochemical systems and establishing different strategies has been demonstrated. Hence, this technology can be considered as an alternative for high strength (organic and nitrogen) wastewater treatment, to accomplish the requirements needed for agricultural uses. Microbial community assessment revealed that a highly diverse microbial community was harboured in the anode biofilms, strongly dependent on the type of electrodes used, on operational conditions, and on the substrate used as feed. Potential microbial exoelectrogenic candidates, commonly shared in all

anode biofilms, were described. The microbiology study of the anodophilic communities is a key factor to better understand the performance of these systems.

9.2. Further research

Based in our results, it has been demonstrated that animal wastewaters can be processed with bioelectrochemical systems using different implementable processes for nitrogen removal and/or recovery. Nevertheless, there are still several challenges to overcome before this technology can be implemented at large scale. Many factors contribute to the overall BES and ammonia nitrogen removal/recovery efficiency, such as system configuration, type of membrane, wastewater ammonium, current density, and catholyte pH. As several of these factors are interrelated, further studies are required in order to optimize and scale up the technology.

Interest regarding its microbiological aspects has grown tremendously in the last five years, as new angles are being discovered. However, there are different aspects in need of further research, to better understand the behaviour of exoelectrogenic communities, aiming to optimize BES performance. Aspects related to the syntrophic relationship established between anodophilic populations and synergic/interactions between Eubacteria and methanogenic Archaea, both in the anode and cathode compartment are relevant topics that also need further research.

Chapter 10

Annexed Information

10.1. Annex: Research stays

Internship during two months in the Laboratory of Microbial Ecology and Technology (LabMET) (Ghent, Belgium 08/2012 – 09/2012).

Supervisor: Prof. Korneel Rabaey.

During this period I was helping Dr. Joachim Desloover in the last months of his PhD, in a project related with nitrogen recovery in electrochemical systems. The aim of this project was to optimize current efficiency of a two compartment reactor working under different conditions: OCV, 10, 20 and 30 mA m⁻², introducing changes in architecture of the system (electrode distance from the membrane, different membranes, using or not spacer in the anode compartment).

Experimental set-up

The experimental set-up consisted of a two-chambered electrochemical cell of which the cathode compartment is coupled to a strip and absorption unit. The experimental set-up is presented in **Figure 10.1**.

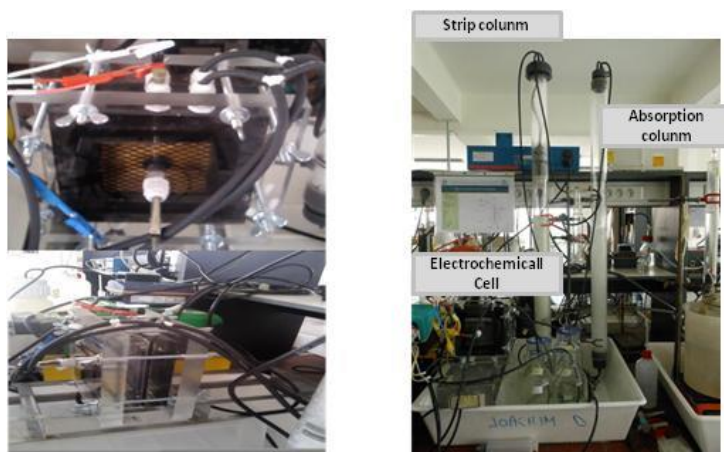


Figure 10.1. Pictures of the electrochemical cell used during the experiments.

The two-chambered electrochemical system was assembled by placing two square Perspex frames (internal dimensions: 8 x 8 x 1.9 cm) side by side, separated by a different cation exchange membrane depending on the experiment. The total volume of each compartment was 122 mL. The anode used was a Ti electrode (dimensions: 7.8 x 7.8 cm; 1 mm thickness). The cathode used was a stainless steel

mesh (dimensions: 7.8 x 7.8; wire thickness: 140 μm). Both the anode and cathode had a projected electrode surface area of 61 cm^2 , and were placed in close contact or away to the membrane.

General results:

- No differences in current density were observed between membranes (CMI ultrex and lanxess) or the use or not of spacer. Only there was a clear difference in the pH of the anode. At 10A m^{-2} the pH in the anode was not as low as in the case of 20 and 30 A m^{-2} .
- Current efficiency of 25% was obtained using digestate as feed at 30A m^{-2} , whilst working with pig manure a current efficiency of 40% was obtained. The small drop in pH thanks to high manure alkalinity, can explain this difference.
- In the cell working with liquid fraction of pig manure at 30 A/ m^2 the efficiency improves from 43% (electrode against membrane) to 60% (distance between electrode and membrane).
- Similar results were obtained, with distance between electrode and membrane and working with the thicker spacer (in the anode) and the electrode against the membrane.
- The best results were reached working at 30A m^{-2} . A clearly improvement on N flux was obtained with a distance between electrode and membrane. This results are similar to those obtained working with a thicker spacer in the anode and in both compartments.

Research stay during six months at the University of Queensland's Advanced Water Management Centre (AWMC) (Brisbane, Australia, 09/2013 – 02/2014). Supervisor: Dr. Stefano Freguia.

The main objective of this internship was to help on the start-up of BES reactors for nitrogen removal, to try to answer the following questions:

- It is possible to have a fully autotrophic cathodic nitrogen removal?
- Is there a difference in community structure in treated/untreated Plasma electrodes surfaces?
- Is there a difference in community structure when applying different potentials (-0.4 and -0.6 V vs Ag/AgCl)?

The experimental plan is detailed in **Table 10.1**. Six reactors (A to F) were used to carry out the experiments. All reactors were inoculated with the same inoculum, which was a mix from different denitrifying reactors. Reactors A from D were used to study the heterotrophic and autotrophic nitrogen removal applying the same potential (-0.4V). Reactor E was used to test the effected plasma treatment under the electrodes in a heterotrophic conditions, and reactor F was compared to reactor A/B to study the effect of applying different potentials.

Table 10.1. Experimental plan made to carry out experiments.

	Pot. Ag/AgCl	Medium	Plasma treatm.	Stirr	CE	Electrodes		*Inoc.	
						Type	Surf. Area (cm ²)		Electrodes per reactor
A/B	-0.4V	Heterot. Acetate	Yes					3	
C/D	-0.4V	Aut. - No acetate	Yes	Batch	Separate anodic chamber	Cloth	15.4 (ea)	3	Mixed (10 ml)
E	-0.6V	Heterot. Acetate	Yes (2x) No (2x)	350 rpm	Pt wire			4	
F	-0.6V	Heterot. Acetate	Yes					3	

*Mix from denitrifying reactors

Experimental set-up:

The main set-up was the same for all reactors (**Figure 10.2**). The abiotic anode consisted in a glass tube with a cation exchange membrane and the electrode used was platinum. The anolyte and catholyte is described in **Figure 10.2**. And the electrodes were made with two pieces of carbon cloth (5.5 cm x 0.7 cm) connectec with titanium mesh and titanium wire to make a good connection. **Figure 10.3** shows how the reactors look like.

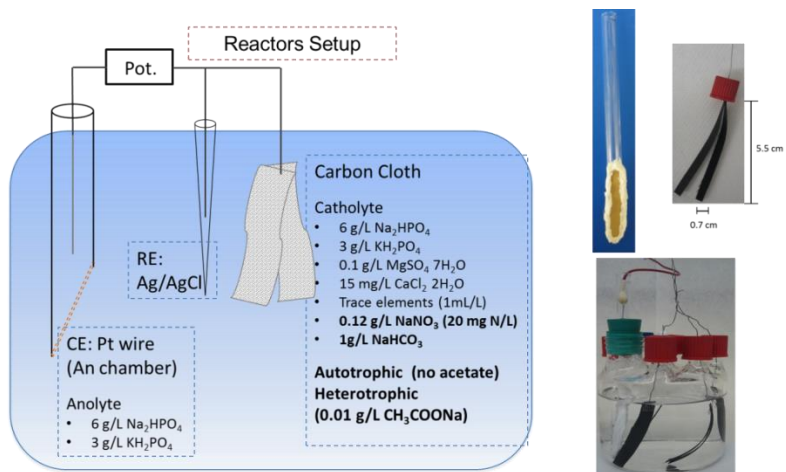


Figure 10.2. Diagram of the reactors setup and pictures of the materials used.

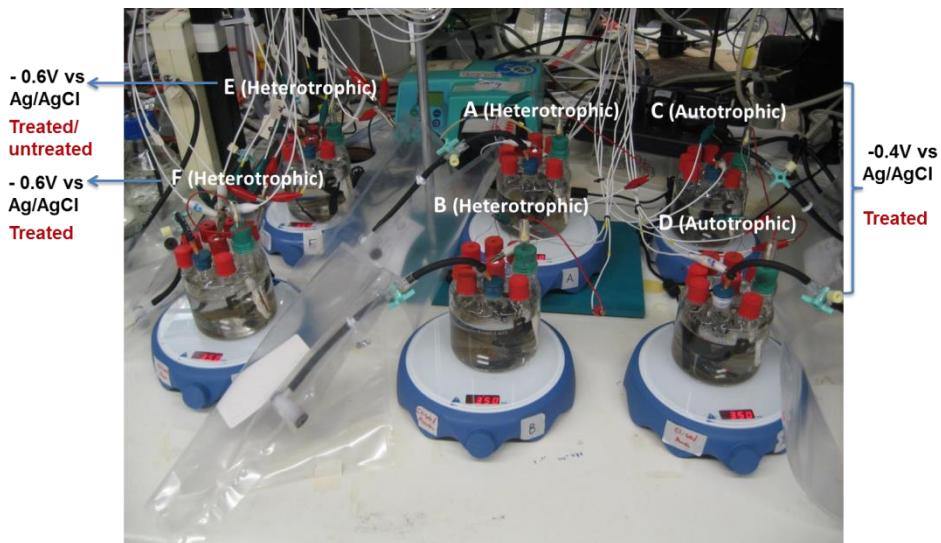


Figure 10.3. Picture of the reactors used during the experiments.

General results:

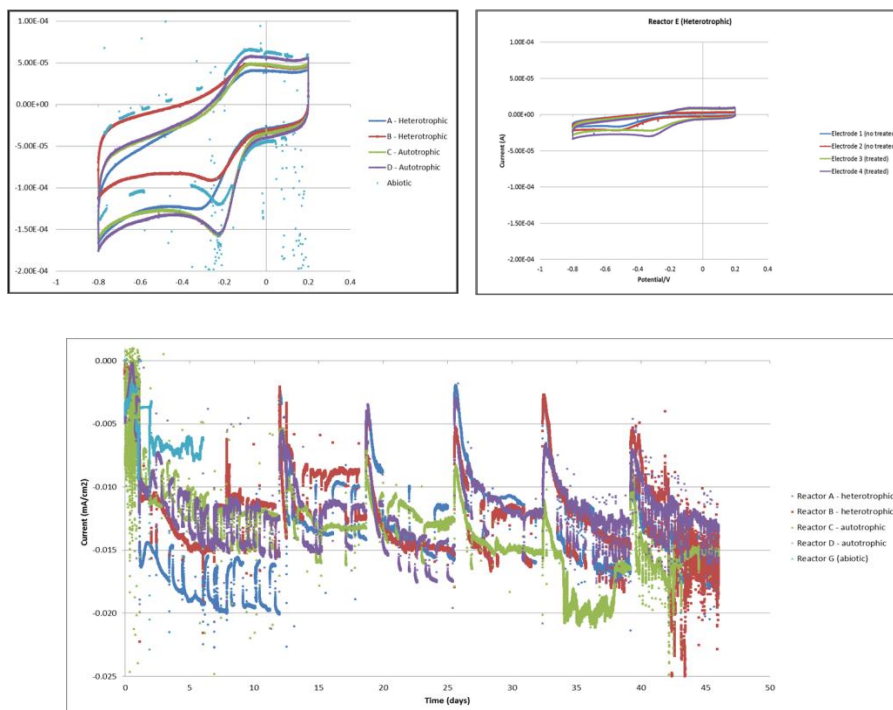


Figure 10.4. Current progress profile.

The preliminary results showed very low current generation and very noisy current profiles (**Figure 10.4**). Therefore, it was decided to increase the speed and media replacement done in longer periods.

Besides nitrate is not being consumed and acetate is consumed in two days, therefore pulses of acetate weekly and daily were applied.

Curriculum Vitae

Personal information



Surname (s): Sotres Fernández
Name: Ana
Date of birth: 19/05/1982
Telephone: 677 37 43 27
Email address: sotresana@gmail.com

Training received

Current thesis in Environmental Engineering program for the Polytechnic University of Catalonia (UPC) (2010-2015).

Title dissertation: “Microbial fuel cell running on high strength animal wastewater – Nitrogen removal strategies and microbial community characterization”

Supervisors: Marc Viñas Canals and August Bonmatí Blasi

Thesis Proposal: “Nitrogen dynamics and microbial processes associated to a Microbial Fuel Cells (MFCs) fed with pig slurry” in Environmental Engineering program for the Polytechnic University of Catalonia (UPC) (2011).

PhD courses and Advanced Studies Diploma (D.E.A) at the University of Oviedo (2007-2009).

BSc- Biology, in the field of Environmental Sciences at the University of Oviedo (2000-2005).

Training experience

Researcher in the project “Integration of bioelectrochemical reactors and anaerobic digesters for Viable Energy yield and Nitrogen Trapping” (INVENT). IRTA,GIRO.- Joint research unit IRTA-UPC (Barcelona, 2013-2014).

Research stay grant at the University of Queensland – Brisbane (Australia) (6 months), funded by the AGAUR (Government of Catalonia) (2013-2014).

Research stay grant at the University of Ghent (two months), funded by the Spanish Ministry of Science and Innovation (MICINN). University of Ghent, Belgium (2012).

Researcher in the project “Nitrogen dynamics in a Microbial Fuel Cell running on pig slurries: electrochemical and microbial characterization”, funded by the Spanish Ministry of Science and Innovation (MICINN project CTM2009-12632). IRTA,GIRO.- Joint research unit IRTA-UPC (Barcelona, 2010-2013).

Preparation of teaching materials, teaching classes and collaboration practices on the subject of Environmental Microbiology on Biology degree, (100 h. period 2008-2009). University of Oviedo (2008-2009).

Research grant under a Project CLEAM-CENIT,AIE called "CLEAM (Construcción Limpia, Eficiente y Amigable con el Medio Ambiente)". University of Oviedo (2008-2009).

Grant in a project "Functional, genetic and biochemical analysis and biotechnological applications of *Steptomyces* programmed cellular death". University of Oviedo (2007).

Leonardo Da Vince fellowship grant (six months) at the Molecular Ecology and Microbiology department at Plymouth Marine Laboratory (PML), England (2007).

Assistance to conference

2nd EU-ISMET (European International Society for Microbial Electrochemical Technologies Meeting). Oral presentation: **A. Sotres**, M. Cerrillo, M. Viñas, and A. Bonmatí. *Nitrogen recovery from pig slurry in two chamber bioelectrochemical system (BES)* 3-5 of September (2014), Alcalá de Henares, Madrid (Spain).

1st Manuresource. Oral presentation: M. Cerrillo, **A. Sotres**, M., Viñas and A. Bonmatí. *Improved energy and ammonia recovery from anaerobic digestion and microbial fuel cell integrated systems.* 5-6 of December (2013), Bruges (Belgium).

4th International Microbial Fuel Cell Conference. Oral presentation: **Sotres, A.**, Cerrillo, M., Viñas, M. and Bonmatí, A. *Establishment of nitrifying-denitrifying microbial community on MFC cathode and its feasibility for wastewater treatment.* 1-4 of September (2013), Cairns, Queensland (Australia).

13th IWA congress (World Congress on Anaerobic Digestion). Poster presentation: **A. Sotres**, M. Cerrillo, M. Viñas and A. Bonmatí. *Nitrogen dynamics in a continuous-feed two-chambered microbial fuel cell (MFC).* 25-28 of June (2013), Santiago de Compostela, Galicia (Spain).

1st EU-ISMET (European International Society for Microbial Electrochemical Technologies Meeting). Poster presentation: **A. Sotres**, M. Cerrillo, M. Guivernau, F. Prenafeta-Boldú, A. Magrí, J. Illa, A. Bonmatí and M. Viñas. *Electroactive biofilm adapted to high nitrogen loads and electricity generation in a microbial fuel cell fed with pig slurries.* 27-28 of September (2012), Ghent (Belgium).

3rd International Microbial Fuel Cell. Poster presentation: **A. Sotres**, J. Díaz, A. Burniol, A. Bonmatí and M. Viñas. *Microbial community dynamics in MFC operating with different ion exchange membranes.* June (2011), Leuwarden (Holland).

9th Meta Conference (Mesa Española de Tratamiento de Aguas). Oral presentation: **A. Sotres**, A. Bonmatí y M. Viñas. *Screening of materials and inocula for Microbial Fuel Cells (MFCs) performance.* 9-11 of December (2010), Bilbao (Spain).

3th Industrial Microbiology and Microbial Biotechnology Conference. Poster presentation: **A. Sotres**, A. Bonmatí, J. Díaz, M. Guivernau and M. Viñas. *Study of different ion exchange membranes in microbial fuel cells: effects on the microbial community and the electrochemical process.* 17-19 of November (2010), Madrid (Spain).

2nd Ecofarm conference (Spanish conference of integrated management of livestock manure). Poster presentation: M.Viñas, **A. Sotres**, M.Guivernau, F.X. Prenafeta, A. Magrí, A. Bonmatí, X.Flótsats and J.Gerritse. *Molecular characterization of microbial populations in a Microbial Fuel Cell (MFC) running with cow manure*. 9-10 of June (2010), Barcelona (Spain).

12th SEM's conference (Microbiology Spanish Society). Poster presentation: **A. Sotres**, C. Méndez, C. Velarde, J.R. Gallego, J.Sánchez and A.I. Peláez. *Biorremediation of contaminated soil with polycyclic aromatic hydrocarbons*. 21-24 of September (2009), Almería (Spain).

14th International Biodeterioration and Biodegradation Symposium. Poster presentation: J.R.Gallego, R.Villa, **A.Sotres**, I. Mori, A.I.Peláez, A.Manteca, and J.Sánchez. *Biotreatability study of a soil affected by PAHs and selection of a suitable bioremediation treatment*. 6-11 of October (2008), Messina (Italy).

Journal papers

A. Sotres, J. Díaz, M. Guivernau, J. Illa, A. Magrí, F.X. Prenafeta-Boldú, A. Bonmatí and M. Viñas (2014). *Microbial community dynamics in two-chambered microbial fuel cells: effect of different ion exchange membranes*. Journal Chemical Technology Biotechnology. DOI 10.1002/jctb.4465.

A.I. Peláez, I. Lores, **A. Sotres**, C. Menéndez-García, C. Fernández-Velarde, J.A. Santos, J.R. Gallego and J. Sanchez (2013). *Design and field-scale implementation of an on-site bioremediation treatment in PAHs polluted soil*. Environmental Pollution. 181, 190-199.

Bonmatí A, **Sotres A**, Mu Y, Rozendal R, Keller J. and Rabaey K (2013). *Oxalate degradation in a bioelectrochemical system: reactor performance and microbial community characterization*. Bioresource Technology. 143, 147-153.

A. Sotres, M. Cerrillo, M. Guivernau, F. Prenafeta-Boldú, A. Magrí, J.Illa, A. Bonmatí and M. Viñas (2012). *Electroactive Biofilm Adapted to High Nitrogen Loads and Electricity Generation in a Microbial Fuel Cell Fed with Pig Slurries*. Communications in Agricultural and Applied Biological Sciences. 77(2), 95. ISSN: 1379-1176.

Sotres, A., Bonmatí, A. and Viñas, M. (2011). Screening de materiales e inóculos para su aplicación en celdas de combustible microbianas (Microbial Fuel Cells-MFC). Aguasresiduales.info.

C. Sierra, J.R. Gallego, J.M. Menéndez-Aguado, **A. Sotres**, A.I. Peláez and J. Sánchez (2009). *Tendencias actuales en la recuperación de terrenos contaminados por hidrocarburos*. Oilgas, petróleo, petroquímica y gas. 487: 34-41. ISSN: 0030-1493.

In preparation

Sotres, A., Cerrillo, M., Viñas, M., Bonmatí, A. “Nitrogen removal in a two-chambered microbial fuel cell – Establishment of a nitrifying-denitrifying microbial community on an intermittent aerated cathode” (Journal, in preparation)

Sotres, A., Cerrillo, M., Viñas, M., Bonmatí, A. “Nitrogen recovery from pig slurry in a two-chambered bioelectrochemical system” (Journal, in preparation)

Sotres, A. Tey, L., Bonmatí, A., Viñas, M. “Microbial community dynamics in continuous microbial fuel cells fed with synthetic wastewater and pig slurry” (Journal, in preparation)

